Helge Niemann

Rates and signatures of methane turnover in sediments of continental margins

Cover image. Violent methane venting at Håkon Mosby Mud Volcano (Barents Sea, 1250 metre water depth). The lower part of the jet consists of methane gas, whereas the upper section (~1 metre above sea floor) comprises methane gas-hydrate flakes. Image source: IFREMER, Brest and Alfred Wegener Institute for Polar and Marine Research, Bremerhaven cruise ARK IXX3b.

Rates and signatures of methane turnover in sediments of continental margins

Dissertation

zur Erlangung des Doktorgrades der Naturwissenschaften

- Dr. rer. nat. -

dem Fachbereich Biologie/Chemie der Universität Bremen vorgelegt von

Helge Niemann

Bremen

Juni 2005

Die vorliegende Doktorarbeit wurde in der Zeit vom Januar 2002 bis Juni 2005 an der Universität Bremen durchgeführt. Die Untersuchungen fanden am Max Planck Institut für Marine Mikrobiologie in Bremen statt.

1. Gutachter: Prof. Dr. Dieter Wolf-Gladrow
2. Gutachterin: Prof. Dr. Antje Boetius

weitere Prüfer:

Prof. Dr. Wilhelm Hagen
Dr. Marcus Elvert

Tag des Promotionskolloquiums: 8. Juli 2005

What we know is a drop. What we don't know is an ocean.

- Isaac Newton

This work is dedicated to Silke

Summary

Methane is an aggressive greenhouse gas and an important component of the global carbon cycle. High amounts of methane are temporarily stored in sediments of the continental margins as free gas, dissolved or frozen as clathrate. At cold seeps, focused flow transports high amounts of methane from deep reservoirs into shallow surface sediments. Locally, methane emission into the water column from seeps can be observed in the form of gas ebullition. Furthermore, large expanses of continental margin sediments contain high amounts of methane. However, the contribution of the oceans to atmospheric methane sources is globally estimated as <3 %. This is because the anaerobic oxidation of methane (AOM) with sulphate as the terminal electron acceptor removes ~80 % of methane in the sediment. AOM is mediated by archaea related to methanogens in consortium with sulphate reducing bacteria. This process produces large amounts of sulphide in marine sediments, and supports thiotrophic communities such as filamentous bacteria, and symbiotic worms and clams. AOM often co-occurs with the precipitation of authigenic carbonates which may build up reef like structures. Another sink for methane in the ocean is the aerobic oxidation of methane (MOx). This process is mediated by bacteria, which may occur as free-living cells or in symbiosis with megafauna organisms. However, marine sediments are barely penetrated by oxygen and will mostly not provide suitable conditions for free living MOx communities. In contrast, motility, sediment dwelling and ventilation activities of the animal hosts to MOx bacteria enlarges the range for the distribution of MOx. Previous work has shown that the process of AOM dominates methane turnover at seeps and consumes 60-100 % of the methane flux.

In this thesis, a variety of different cold seep systems (mud volcanoes and a gas seep) were investigated using a multidisciplinary approach to gain a more systematic understanding of these, methane-driven “biogeosystems”. The main goals were the detection and quantification

of hot spots of methane oxidation as well as an assessment of environmental factors determining the activity and the distribution of methanotrophic communities. Furthermore, key microbial players were identified and the impact of AOM and MOx activity on the surrounding, marine environment was studied. The investigations revealed the following:

1. Submarine mud volcanoes are colonized by specialized microbial communities utilizing the fluxes of reduced substrates such as methane and sulphide as energy source. At the actively methane-seeping Håkon Mosby mud volcano (HMMV, Barents Sea), a distinct spatial zonation of several novel clades of free-living and symbiotic aerobic and anaerobic methanotrophs was found. The main selection mechanism determining vertical and horizontal distribution and dominance of the methanotrophic communities were fluid flow rates controlling access to electron acceptors for methane oxidation.

2. The analysis of archaeal and bacterial specific lipid concentrations and their associated $\delta^{13}C$-values from three seepage areas at HMMV (thermal centre, grey mats and *Beggiatoa* site) showed a distinct distribution of methanotrophic biomass. At the centre, MOx was the primary biomass-generating process in surface sediments as shown by the predominance of bacterial lipids belonging to a type I methanotroph. In patches of reduced sediment, covered by greyish, thiotrophic, microbial mats at the boundary of the centre, a four-fold increase in archaeal lipids specific for anaerobic methanotrophs was found. It was accompanied by a strong depletion in ^{13}C, giving evidence of active microbial communities, which mediate AOM in the upper 20 cm of sediment. Further away from the centre, in the zone covered by *Beggiatoa* mats, anaerobic methanotrophy appeared to be the predominant biomass generating process. Here, sharp, vertical gradients of ^{13}C-depleted archaeal and bacterial lipids indicate that AOM communities were restricted to a narrow surface horizon of no more than 4 cm. A combination of molecular techniques (DAPI, FISH, gene libraries) and

biomarker fingerprints provided evidence that the AOM community was dominated by a novel strain of archaea (termed ANME-3) and SRB of the *Desulfobulbus* cluster.

3. Biogeochemical investigations at HMMV revealed a high upward flow of sulphate-free subsurface fluids in the centre, strongly limiting the penetration of sulphate and oxygen from seawater. Here, MOx was restricted to the top sediment layer with rates of 0.9 mol m^{-2} yr^{-1} and AOM was absent. In the patches of reduced sediments covered with grey mats, a deeper penetration of sulphate was observed, fueling AOM activity down to >12 cm with rates of 12.4 mol m^{-2} yr^{-1}. Adjacent to the centre at the *Beggiatoa* site, decreased upward fluid flow allowed for an AOM zone of ca 4 cm at the sediment surface with rates of 4.5 mol m^{-2} yr^{-1}. At the outer rim of the HMMV, bioventilation of the pogonophoran worms irrigated a much deeper zone with oxygen- and sulphate-rich seawater. MOx activity in the oxygenated surface sediments was comparably low with 0.2 mol m^{-2} yr^{-1}. AOM activity in sulphate-rich sediments just beneath the roots of the worms was high with 7.1 mol m^{-2} yr^{-1}. With respect to the area size of the different habitats at HMMV, microbial consumption reduces the methane efflux of HMMV by ca 7* 10^{-5} Tg yr^{-1}, i.e. 22 to 55 %.

4. The abundant mud volcanoes of the Gulf of Cadiz are currently much less active than the HMMV. Here, thermogenic methane and associated higher hydrocarbons were completely consumed anaerobically in subsurface sediments. AOM and SR rates showed maxima in distinct subsurface sediment horizons between 20 to 200 cm below sea floor. In comparison to other methane dominated environments of the world oceans, AOM activity and diffusive methane fluxes (<0.4 mol m^{-2} yr^{-1}, respectively) were low to mid range. AOM was generally exceeded by SRR, most likely because other hydrocarbons were oxidised anaerobically by SR microbes. Lipid biomarker and 16S rDNA clone library analyses gave evidence that AOM

was mediated by a mixed community of previously described anaerobic methanotrophic archaea (ANME-2 and ANME-1) and associated SRB (Seep-SRB1 group).

5. The Tommeliten gas seep is located in the central North Sea. Here, cracks in a buried marl horizon allow thermogenic methane to migrate into overlying clay-silt sediments. Hydroacoustic sediment echosounding showed several gas flares coinciding with the apex of the marl domes. Here, methane is released into the water column and potentially to the atmosphere during deep mixing situations. Carbonates in the vicinity of the gas seep contained ^{13}C-depleted, archaeal lipids indicating long-term AOM activity. In the sediment, the zone of active methane consumption was restricted to a distinct horizon of no more than 20 cm. Diagnostic, ^{13}C-depleted archaeal and bacterial lipids as well as 16S rDNA clone libraries provided evidence that AOM was mediated by ANME-1b archaea and SRB most likely belonging to the Seep-SRB1 cluster.

The investigations presented in this thesis confirm that AOM is an ubiquitous process in methane bearing, marine sediments. For the first time, the microbial ecology and biogeochemistry of mud volcanoes and a coastal gas seep was investigated systematically. The magnitude of AOM vs. MOx was mainly controlled by gas and fluid transport processes and by the presence of symbiotic fauna. The process of AOM was found to be spatially restricted to hotspots controlled by (1) fluid flow rates, (2) bioirrigation activities, (3) diffusion and thermodynamic limitations and by (4) the sedimentological layering. Despite the horizontal and vertical restriction, AOM represents a major sink for methane at mud volcanoes and coastal gas seeps. AOM and MOx biomass, activity, diagnostic lipid concentrations and their associated δ^{13}C-values showed matching vertical distributions allowing to use a particular profile as a proxy for the other. Furthermore, lipid biomarker

analysis matched very well 16S rDNA-based estimates of the diversity of microbial communities mediating AOM and MOx.

Zusammenfassung

Methan ist ein potentes Treibhausgas. Große Mengen sind hiervon in Sedimenten der Kontinentalränder als freies oder gelöstes Gas, aber auch gefroren in Form von Gashydraten eingelagert. An den sogenannten „Cold Seeps“ werden große Mengen dieses Gases aus tieferliegenden Lagerstätten in oberflächennahe Sedimenthorizonte transportiert. Lokal begrenzt kann an den Cold Seeps auch ein Austritt von Methan aus dem Ozeanboden in die Wassersäule beobachtet werden. Obwohl Methan zusätzlich in weiten Flächen des Meeresbodens an den Kontinentalränden enthalten ist, gehen globale Schätzungen davon aus, dass weniger als 3 % des atmosphärischen Methangehaltes aus den Ozeanen stammt. Dies liegt daran, dass die anaerobe Methanoxidation (engl.: anaerobic oxidation of methane; AOM) mit Sulfat als terminalen Elektronenakzeptor ca. 80 % des aufsteigenden Methans schon im Sediment aufzehrt. Verantwortlich für diesen Prozess sind Archaeen, die in einem Konsortium mit sulfatreduzierenden Bakterien (engl.: sulphate reducing bacteria; SRB) leben. Phylogenetisch sind diese Archaeen mit den Methanogenen verwand. Während der AOM wird Sulfid produziert, das wiederum von thitrophen Lebensgemeinschaften wie filamentösen Bakterien und symbiotischen Würmern und Muscheln aufgenommen wird. Außerdem gibt es wahrscheinlich eine kausale Verbindung zwischen der AOM und der Ausfällung authigener Karbonate. An den oft durch schlammige Sedimente gekennzeichneten Cold Seeps, stellen exponierte Karbonate einen harten Untergrund für die Besiedlung sessiler Organismen dar. Abgesehen von der AOM ist die aerobe Methanoxidation (MOx) eine weitere Senke für Methan im Ozean. Für den Prozess der MOx sind Bakterien verantwortlich, die entweder freilebend oder in Symbiose mit Megafaunaorganismen vorkommen. Die Lebensbedingungen für freilebende MOx Bakterien im Ozeanboden sind eher schlecht, da die Eindringtiefe von Sauerstoff in den Meeresboden sehr begrenzt ist. Im Gegensatz dazu eröffnen Beweglichkeit und/oder Ventilation und Bioturbation der Megafaunawirte den symbiotischen MOx

Bakterien ein größeres Potential an Lebensräumen. Bisherige Publikationen haben allerdings gezeigt, dass die AOM der dominante Modus der Methanoxidation an den Cold Seeps ist. 60 bis 100 % des Methanflusses werden hier durch die AOM gezehrt.

In dieser Doktorarbeit wurden eine Reihe verschiedener Cold Seeps (Schlammvulkane und Gasseeps) mit einem multidisziplinären Ansatz untersucht, um ein systematisches Verständnis dieser „Bio-Geo-Systeme" zu erlangen. Hauptziele waren die Detektion und Quantifikation der sogenannten „Hot Spots", an denen Methanoxidation stattfindet, sowie eine Einschätzung der Umweltfaktoren, die potenziell die Aktivität und Verteilung der methanotrophen Lebensgemeinschaften bestimmen. Zudem wurden die mikrobiellen Schlüsselorganismen identifiziert und der Einfluss von AOM- und MOx-Aktivität auf das umgebende, marine Ökosystem eingeschätzt. Die Untersuchungen haben folgendes ergeben:

1. Unterseeische Schlammvulkane werden von spezialisierten, mikrobiellen Lebensgemeinschaften besiedelt, welche den Fluss von reduzierten Substraten, wie Methan und Sulfid als Energieressource nutzen können. Eine räumlich abgegrenzte Zonierung verschiedener neuentdeckter, freilebender und symbiotischer aerober und anaerober methanotropher Organismen wurde am aktiven Schlammvulkan Håkon Mosby (HMMV) gefunden. Die Fliessgeschwindigkeit des Porenwassers bestimmt hier, wie hoch die Verfügbarkeit von Elektronenakzeptoren ist, und selektiert somit die vertikale und horizontale Verteilung sowie die Dominanz verschiedener methanotropher Organismen.

2. An drei verschiedenen Arealen des HMMVs (Zentrum, graue Matten und *Beggiatoa* Habitat) zeigte die Analyse spezifischer archaealer und bakterieller Lipidkonzentrationen und deren assoziierte $\delta^{13}C$-Werte eine stark abgegrenzte Verteilung methanotropher Biomassen. Am Zentrum des Schlammvulkans ist die MOx der dominante, biomassegenerierende

Prozess. Dies zeigte sich durch eine Dominanz von bakteriellen Lipiden, die Typ I methanotrophen Bakterien zugeordnet werden konnten. In reduzierten Sedimenten der grauen Matten, die am äußeren Rand des Zentrums und in der Nähe von Fluid- und Gasaustrittsstellen kleinere Flecken bedecken, wurde, im Vergleich zum Zentrum, eine vierfach höhere Konzentration von AOM assoziierten Lipiden gefunden. Diese Lipide waren durch eine starke Abreicherung des Isotops ^{13}C gekennzeichnet. Die Konzentrationen und die leichten $\delta^{13}C$-Werte wiesen darauf hin, dass die mikrobielle Gemeinschaft in den oberen 20 cm des Sedimentes das Methan anaerob umsetzt. Das Zentrum ist von einer Zone reduzierter Sedimente umgeben, die mit dichten Matten von *Beggiatoa sp.* bedeckt sind. Hier wurde die AOM als der primäre, biomasseproduzierende Prozess identifiziert. Steile, vertikale Gradienten von ^{13}C-abgereicherten archaealen und bakteriellen Lipiden deuteten darauf hin, dass die AOM Gemeinschaft auf einen schmalen, oberflächennahen Horizont von ca. 4 cm begrenzt ist. Eine Kombination molekularer Analysetechniken (DAPI, FISH und Genbanken) sowie die Biomarkerverteilungen zeigten eine neuartige, dominante AOM-Gemeinschaft. Diese besteht aus Archaeen, welche ANME-3 genannt wurden, und sulfatreduzierenden Bakterien der *Desulfobulbus*-Gruppe.

3. Biogeochemische Untersuchungen am HMMV zeigten eine hohe Flussrate sulfatfreier Fluide. Diese Fluide stammen aus großer Tiefe des Schlammvulkans und werden durch einen Kanal an die Oberfläche des Zentrums transportiert. Im Zentrum beschränkt der Fluss dieser Fluide die Eindringtiefe von Sauerstoff und Sulfat aus dem Bodenwasser auf einen dünnen Oberflächenhorizont des Sedimentes. In diesem Horizont ist die MOx mit 0.9 mol m^{-2} a^{-1} dominant. AOM konnte hingegen nicht nachgewiesen werden. In Sedimenten, die mit grauen Matten bedeckt sind, wurde eine große Eindringtiefe von Sulfat in das Sediment beobachtet, was eine hohe AOM-Aktivität in einem ausgedehnten Horizont (>12 cm) mit Methanumsatzraten von 12.4 mol m^{-2} a^{-1} zur Folge hat. Im Vergleich zum Zentrum, hat in

den von *Beggiatoa sp.* bedeckten Sedimenten eine Reduktion im Fluidfluss eine größere Eindringtiefe von Sulfat zur Folge. Die vergleichsweise hohe Verfügbarkeit von Sulfat resultiert in AOM Raten von 4.5 mol m^{-2} a^{-1} in den oberen 4 cm des Sedimentes. Der äußere Rand des Vulkans ist von dichten *Pogonophora sp.* Beständen besiedelt. Die Bioventilation dieser Würmer führt zum Eintrag von sauerstoff- und sulfatreichem Bodenwasser in tiefere Sedimentschichten. In den sauerstoffreichen Oberflächensedimenten ist die MOx Aktivität mit 0.2 mol m^{-2} a^{-1} vergleichsweise gering. Jedoch konnte eine hohe AOM-Aktivität von 7.1 mol m^{-2} a^{-1} in einem Sedimenthorizont direkt unterhalb der Würmer (60 bis 80 cm Sedimenttiefe) gemessen werden. Dies ist ein extrem hoher Methanumsatz für diese Sedimenttiefe. Am HMMV werden insgesamt ca. $7*10^{-5}$ Tg Methan a^{-1} durch mikrobielle Zehrung umgesetzt. Dies ist äquivalent zu einer Reduktion der Methanemissionen um 22 bis 55 %.

4. Der Golf von Cadiz ist durch eine hohe Anzahl von Schlammvulkanen gekennzeichnet, die allerdings weit weniger aktiv als z.B. der HMMV sind. An den Schlammvulkanen im Golf von Cadiz werden Methan und assoziierte, höhere Kohlenwasserstoffe in tieferen Sedimentschichten (20 – 200 cm Sedimenttiefe) aufgezehrt. Dort konnten maximale AOM- und SR-Raten in abgegrenzten Horizonten gemessen werden. Im Vergleich zu anderen, methandominierten, marinen Systemen sind sowohl AOM-Raten wie auch diffuse Methanflüsse (jeweils <0.4 mol m^{-2} a^{-1}) gering bis mittel-hoch. Generell wurden höhere SR- als AOM-Raten gemessen, weil auch die höheren Kohlenwasserstoffe, wahrscheinlich anaerob mit Sulfat, in dem gleichen Horizont wie Methan oxidiert werden. Lipidbiomarker und 16S rDNA-Klonbanken zeigten, dass eine gemischte Gemeinschaft, bestehend aus ANME-1 und ANME-2 Archaeen, assoziiert zu Sulfatreduzierern der Seep-SRB1 Gruppe, Methan anaerob oxidieren.

5. An den Tommeliten Gasseeps in der zentralen Nord See steigt thermogenes Methan durch Risse eines verschütteten Mergelhorizontes in aufliegende Silt-Ton-Sedimente. Hydroakustische Messungen zeigten, dass tiefere Horizonte (wahrscheinlich Mergel) an verschiedenen Stellen kuppelförmige Schwellungen aufweisen. Mehrere Stellen, an denen Methan aus dem Meeresboden in die Wassersäule und damit potenziell in die Atmosphäre entweicht, fallen räumlich mit den Scheitelpunkten dieser Kuppeln zusammen. In der Nähe der Gasaustrittsstellen wurden Karbonate gefunden. Biomarkeranalysen zeigten, dass diese Karbonate ^{13}C-abgereicherte, archaeale und bakterielle Lipide enthalten. Dies deutet auf lange Zeitperioden hin, die durch AOM- und damit Seep-Aktivität gekennzeichnet waren. Die Zone, in der Methan im Sediment gezehrt wird, ist begrenzt auf einen Horizont von <20 cm. Diagnostische archaeale und bakterielle Lipide und 16S rDNA-Genbanken legen nahe, dass Methan von ANME-1b Archaeen und Sulfatreduzierern der Seep-SRB1 Gruppe anaerob oxidiert wird.

Die Untersuchungen im Rahmen dieser Doktorarbeit bestätigen, dass AOM ein ubiquitärer Prozess in methanreichen, marinen Sedimenten ist. Zum ersten Mal ist es gelungen, die mikrobielle Ökologie und Biogeochemie an Schlammvulkanen und küstennahen Cold Seeps, systematisch zu untersuchen. Die AOM- und MOx-Aktivität wird hauptsächlich von Fluid-Transportprozessen sowie durch das Vorhandensein symbiotischer Fauna kontrolliert. Es wurde nachgewiesen, dass der Prozess der AOM räumlich auf einen Hot Spot begrenzt ist, dessen vertikale Position und Ausdehnung von (1) Fluid Flüssen, (2) Bioirrigation, (3) Diffusion und thermodynamischen Limitierungen sowie (4) der Sedimentabfolge bestimmt wird. Obwohl die Ausdehnung des AOM Horizontes begrenzt ist, repräsentiert die AOM die Hauptsenke für Methan an Schlammvulkanen und küstennahen Gasseeps. Die Biomasse der AOM- und MOx- Gemeinschaften, deren Aktivität sowie diagnostische Lipide und deren assoziierte δ^{13}C-Werte zeigten eine sich deckende vertikale Verteilung. Dadurch kann in

zukünftigen Studien einer dieser Parameter als qualitatives Maß für die anderen genutzt werden. Zusätzlich konnte gezeigt werden, dass 16S rDNA und Lipiddaten übereinstimmen und für eine Einschätzung der mikrobiellen Diversität von AOM- und MOx-Organismen geeignet sind.

Index of contents

Introduction

The following sections outline the nature and global significance of methane turnover and thus the relevance of this dissertation in the field of biogeochemistry and geomicrobiology. The first two parts will give an overview about the current knowledge on the chemical and physical characteristics of methane as well as the processes forming and consuming methane. Also, budgets for- and fluxes between the major compartments of the global methane cycle are presented. In the third part of the introduction, methane-rich habitats of the oceans are presented and current analytical tools for determining microbial key players and metabolic activities in methane turnover are provided. The fourth part outlines the main objectives of this work. The final part of the introduction gives an overview on the chapters containing the five manuscripts prepared in the framework of the thesis, and specifies my contributions to each of them.

1. CHEMICAL AND PHYSICAL PROPERTIES OF METHANE

Methane is the most reduced form of carbon and belongs to the compound class of hydrocarbons, which also comprise for instance ethane, propane and butane. Methane is the simplest molecule of all organic compounds consisting of a central carbon atom covalently bound to four hydrogen atoms in a tetrahedron (Fig. 1). The molecular weight of methane is 16.04 atomic mass units on average. Under

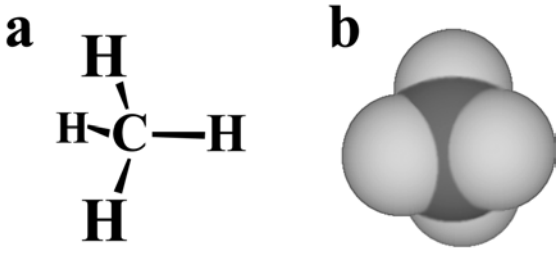

Figure 1. Two models of methane: (a) rod, (b) space filling.

standard conditions (273 K, 0.1 MPa), methane is a colourless, odourless gas and its melting and boiling points are –183 and –164°C, respectively. Three isotopes of methane are commonly encountered in nature: the stable isotopes ^{12}C and ^{13}C and the radioactive β^- radiator ^{14}C, which has a half life of 5730 yrs. ^{12}C is the most abundant isotope in nature, however, certain chemical and biological processes discriminate against the heavy isotope ^{13}C leading to a significant enrichment of ^{12}C in the reaction products. The stable isotope composition of carbon is usually reported in the standard δ-notation ($\delta^{13}C$) expressed as per mill (‰) deviation from the Pee Dee Belemnite standard (PDB):

$$\delta^{13}C = \left[\frac{\left(^{13}C/^{12}C\right)_{Sample}}{\left(^{13}C/^{12}C\right)_{Standard}} - 1\right] 10^3 \qquad (1)$$

By definition, PDB has a $\delta^{13}C$ -value of 0‰. Thus, negative $\delta^{13}C$-values indicate depletion in ^{13}C (or an enrichment in ^{12}C) relative to PDB.

At atmospheric pressure, methane is poorly soluble in water (~1.5 mM). Salinity as well as temperature have a negative effect on solubility (Yamamoto et al., 1976). According to

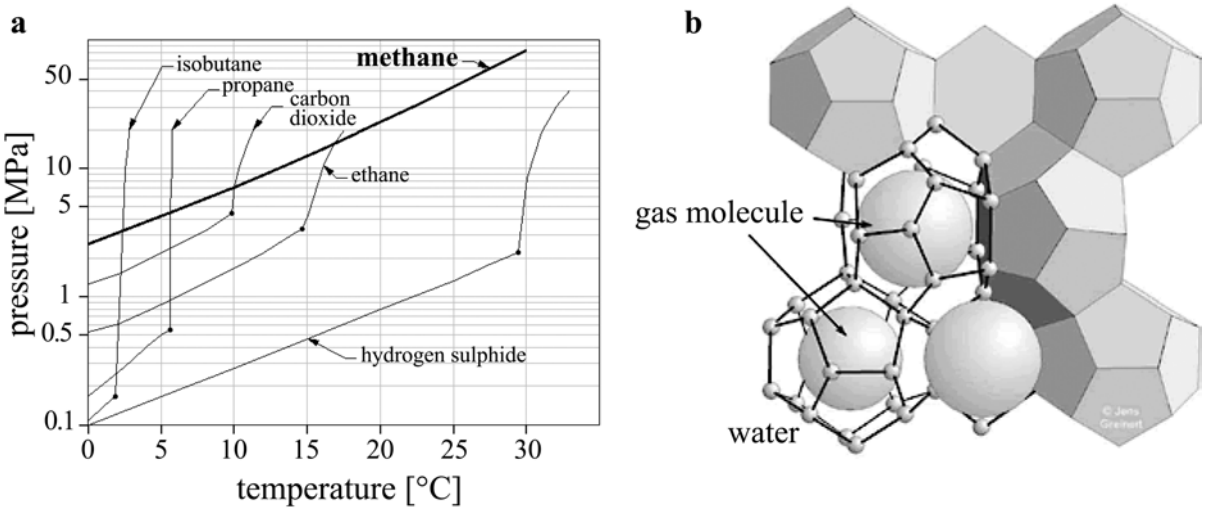

Figure 2. (a) Phase diagram of selected molecules. Lines mark the PT conditions of hydrate stability (modified after Carroll, 2002). (b) Model of structure I hydrates (modified after Greinert, 1998)

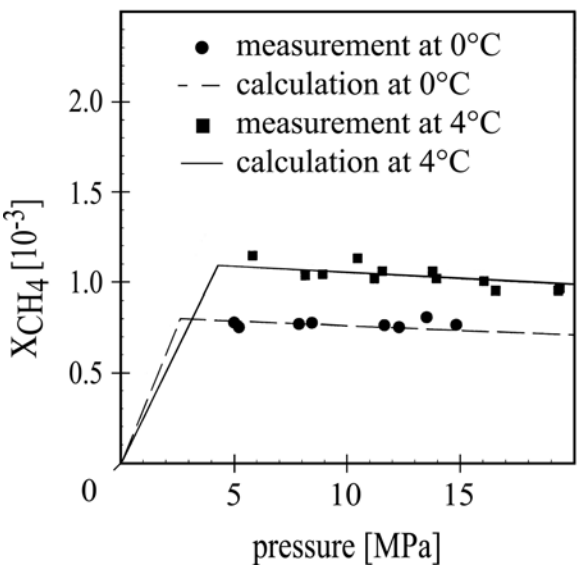

Figure 3. Measured and calculated molar mixing ratio (X) of methane at various PT conditions (modified after Yang et al., 2002)

Henry's Law, solubility increases with increasing hydrostatic pressure, however, this changes at about 400 m depth in waters of temperate and tropical (non-polar) latitudes. At these PT-conditions (4°C, 4 MPa), methane and water form a hydrate structure, which is a crystalline, ice-like, non-stoichiometric compound of methane molecules encaged by water (Kvenvolden 1993, Fig. 2b). In a two-phase system containing such gas hydrates and aqueous methane, Yang and co-workers (2001) showed that the solubility of methane decreases with increasing pressure (Fig. 3). Moreover, at PT-conditions where gas hydrate is stable, elevations in temperature and salinity increase the solubility of methane. Gas hydrates are also called clathrates (lat.: clatratus = cage) and may be formed with molecules other than methane such as higher hydrocarbons (up to butane), carbon dioxide and hydrogen sulphide as well. So far, three crystalline clathrate structures are known (I, II and H). Whereas structure I (Fig. 2b) is mostly formed with methane as the central molecule, the formation of structure II and H includes larger gas molecules such as ethane, propane or butane.

Among other constituents of the earth atmosphere such as water vapour, carbon dioxide, and nitrous oxide, methane has the ability to absorb and re-emit infrared radiation, which has major implications for the energy budget of the atmosphere (Campbell, 1986). Gases with this ability are also termed greenhouse gases. Most of the incoming solar radiation is absorbed by the earth surface and heats it up. Thereby, infrared radiation is emitted to the lower strata of

the atmosphere where the greenhouse gases absorb most of it. Such absorption heats the atmosphere, stimulating it to emit more infrared radiation, which is again absorbed by the greenhouse gases. This phenomenon is also known as the greenhouse effect and the balance between the absorbed solar radiation and the infrared radiation re-emitted to space determines the net radiative forcing on the climate. A positive radiative forcing is beneficial to some extend as it keeps the earth surface in its present habitual temperature conditions. However, an increase in the concentrations of greenhouse gases increases the radiative forcing and most probably contributes to global climate changes (Wuebbles and Hayhoe, 2002). The cause of climatic changes in Earth's history is commonly attributed to an increase of greenhouse gases in the paleo-atmosphere. Analysis of the Vostok ice core (Fig. 4a) gives evidence for a positive coupling between concentrations of atmospheric CO_2, CH_4 and temperature (Falkowski et al., 2000; Petit et al., 1999). Although the ice-core record shows that there were periods with atmospheric temperatures that may have increased without extensive changes in concentrations of greenhouse gases, the reverse was not observed (Smith et al., 1999). Furthermore, it specifically has to be considered that the global warming potential of methane is 21 to 56-fold higher compared to CO_2. The emissions of methane have more than doubled

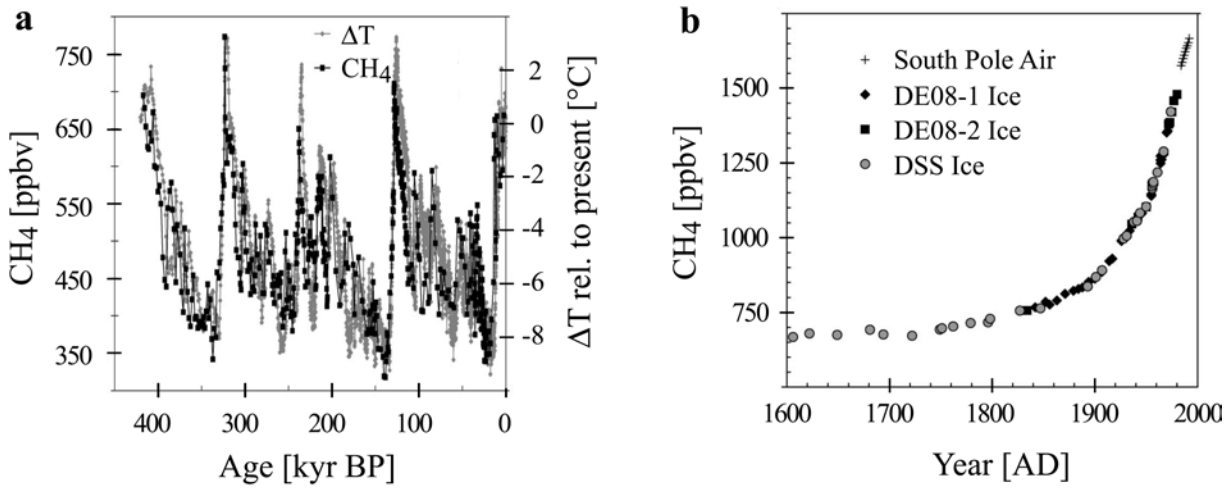

Figure 4. Vostok ice core records of methane concentrations and atmospheric temperature changes over the last 420 kyr (a) and atmospheric methane concentrations from the 17th century to 1998 (b). Modified after Wuebbles and Hayhoe 2002

since the industrialisation leading to an increase in the atmosphere by 2- to 3-fold (Fig. 4b). The increasing methane concentrations might have contributed to about 20% to the total change in radiative forcing since the mid 1700's which makes methane a very important greenhouse gas (Manne and Richels, 2001; Wuebbles and Hayhoe, 2002). Increasing research effort has therefore been dedicated to elucidate sources and sinks of methane, especially with regard to the ocean and its methane reservoirs.

2. ORIGINS, SOURCES AND SINKS OF METHANE

2.1 Methane Production

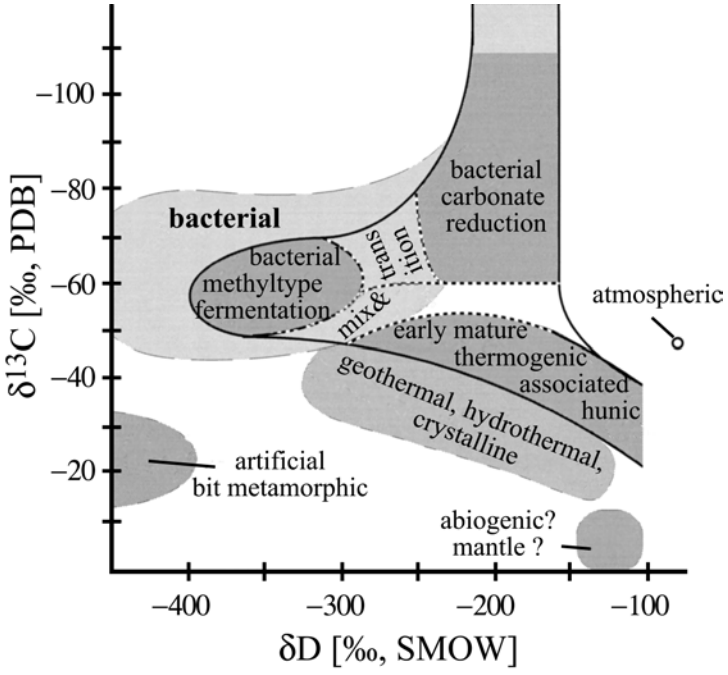

Figure 5. CD-diagram of methane (modified after Whiticar et al., 1999)

Methane originates from three different processes in nature: abiogenic, thermogenic, and microbial. Methane of either source is characterised by a specific range of $\delta^{13}C$ and δD-values as well as by the proportion of co-occurring higher hydrocarbons (C_{2+}) and their stable carbon isotope composition (Fig. 5, Lollar et al., 2002; Whiticar, 1999). Both,

abiogenic and thermogenic methane are produced under high temperature and pressure conditions. Abiogenic methane is produced from carbonate reduction during magma cooling and serpentinisation of exposed peridotite rocks whereas thermogenic methane is formed during the thermal degradation of buried organic matter (Charlou and Donval, 1993; Horita and Berndt, 1999; Kelley, 1996; Lollar et al., 2002; Whiticar, 1999). Accordingly, thermogenic methane is also termed fossil methane. Abiogenic methane is most enriched in ^{13}C with values ranging between 0 to -42‰ and δD-values of –100‰ to -450‰ (Horita and Berndt, 1999; Kelley and Fruh-Green, 1999; Lollar et al., 2002; Whiticar, 1999). The formation of abiogenic methane can be catalysed by a nickel-iron alloy leading to the lower range of the observed $\delta^{13}C$-values (Horita and Berndt, 1999). Thermogenic methane is usually more depleted in ^{13}C with values between –15 to -55‰ (Whiticar, 1999). Besides temperature conditions during formation and the state of maturity, the isotope variations of thermogenic methane depend on the precursor molecules which are ultimately originated from photosynthesis and thus already depleted in ^{13}C (Whiticar, 1999). Abiogenic and thermogenic methane formation are accompanied by the formation of C_{2+}-compounds. While thermogenic C_{2+}-molecules show a progressive enrichment in ^{13}C with higher carbon numbers, $\delta^{13}C$-values of abiogenic C_{2+}-molecules were not found to show this trend (Lollar et al., 2002).

Anaerobic, microbial degradation of organic matter ultimately leads to methane formation, mediated by methanogenic archaea at redox levels <-200 mV (Madigan et al., 2000). The mode of methanogenesis can be classified with respect to the carbon precursor: (1) hydrogenotrophic (2) acetotrophic and (3) methylotrophic (Whiticar, 1999 and references therein). Furthermore, methanogenesis is associated with a significant kinetic isotope effect (KIE) leading to a ^{13}C-depletion of produced methane relative to the residual carbon precursor (Fig. 5, Whiticar, 1999). That is, the carbon substrate molecules with the lower isotopic mass (i.e, containing ^{12}C) diffuse and react faster than the heavier species (i.e., containing ^{13}C).

KIEs decrease with higher amounts of carbon atoms of the reactants, thus leading to lower $\delta^{13}C$-values of methane originated from C_1-precoursors compared to that of C_2 or C_3-precursors (Whiticar, 1999). Depending on the environmental conditions, i.e. fresh water vs. marine, other microbial metabolisms compete with methanogenesis for the same substrates. In marine environments, aerobic respiration is predominant in the top horizon of the sedimentary sequence followed by nitrate, iron and manganese reduction. Below these sediment layers sulphate reduction (SR) is predominant. Sulphate reducing bacteria (SRB) out-compete methanogens for labile carbon compounds (e.g. acetate) and hydrogen. However, once sulphate is exhausted, methanogenesis becomes a dominant microbial process (Whiticar, 1999). Because volatile carbon substrates like acetate are often already depleted by the SRB in marine environments, carbonate reduction, i.e. hydrogenotrophy, prevails:

$$HCO_3^-{}_{(aq)} + 9H^+{}_{(aq)} + 8e^-{}_{(aq)} \rightarrow CH_4{}_{(aq)} + 3H_2O_{(l)},\ \Delta G^0 = -159\ kJ\ mol^{-1} \quad (2)$$

In fresh water systems, in contrast, methanogenesis proceeds uninhibited once oxygen is depleted because sulphate concentrations are low and sulphate reduction is thus of minor importance. In these environments, acetoclastic methanogenesis (acetotrophy) is the dominating methane-generating process (up to 70%; Whiticar et al., 1999 and references therein):

$$CH_3COO^-{}_{(aq)} + H^+{}_{(aq)} + OH^-{}_{(aq)} \rightarrow CH_4{}_{(aq)} + HCO_3^-{}_{(aq)},\ \Delta G^0 = -95\ kJ\ mol^{-1} \quad (3)$$

The utilisation of bicarbonate and methylated substrates was suggested to account for the remaining 30% of methane production.

The different origins of methane observed on Earth fuel scientific discussion about the nature of methane on other planets, and whether methane can be used as a biomarker gas for extraterrestrial life (Schindler and Kasting, 2000). It is believed that methane on the gas giants Jupiter, Saturn, Uranus and Neptune as well as on smaller objects such as Titan, one of Saturn's moons, is abiogenic. However, the discovery of methane in the Martian atmosphere by ESAs space probe "Mars Express" is discussed controversially (Formisano et al., 2004; Krashnopolsky et al., 2004). Methane has a lifetime <400 yr in the Martian atmosphere compelling a relatively constant formation of methane. Because tectonic activities on Mars are believed to have ceased 10 million years ago, Krashnapolsky and co-workers (2004) proposed the possibility of a subsurface, microbial source of the methane.

2.2 Methane Consumption

On Earth, methane is consumed by microbial and chemical pathways. The latter include the combustion of methane with oxygen. An even more important chemical sink is the reaction with hydroxyl radicals in the tropo- and stratosphere. Here, hydroxyl radicals are formed as a result of the photochemical degradation of ozone and a subsequent reaction with water prior to the reaction with methane (Lelieveld et al., 1998; Levy, 1971):

$$O_3 + h\nu \rightarrow O_2 + O^* \quad (4)$$

$$O^* + H_2O \rightarrow 2HO^* \quad (5)$$

$$HO^* + CH_4 \rightarrow H_2O + CH3^* \quad (6)$$

Through a reaction cascade involving oxygen and nitrogen monooxide, the CH_3 radicals are then transformed into formaldehyde (Grosjean, 1995).

In the biosphere, bacteria and archaea mediate the biological consumption of methane under aerobic and anaerobic conditions, respectively. The reaction of aerobic methanotrophy (MOx) is according to the following equation:

$$CH_{4\,(aq)} + 2O_{2\,(aq)} \rightarrow CO_{2\,(aq)} + 2H_2O_{\,(l)},\ \Delta G^0 = -842\ kJ\ mol^{-1} \qquad (7)$$

The first MOx bacterium was isolated in 1906 by Söhngen. The basis for the present phylogenetic classification into biochemically distinct groups was established in the early 70's (Whittenbury et al., 1970). Organisms involved in aerobic methanotrophy were found among the α, β and γ subdivision of the *Proteobacteria* and have been reported as free-living cells from a variety of terrestrial, limnic and marine environments (Hanson and Hanson, 1996). Methanotrophs are also found as intracellular symbionts in invertebrates (Fisher, 1990; Hanson et al., 1993; Larock et al., 1994; Le Mer and Roger, 2001). The catalyst of MOx is a group of enzymes termed methane monooxygenases, which is the defining characteristic of all aerobic methanotrophs. MOx bacteria can be further classified into type I, II and X according to the enzymatic pathway of formaldehyde assimilation during methane metabolism. Type I methanotrophs utilise the ribulose monophosphate (RuMP) pathway, whereas type II utilise the serine pathway (Hanson and Hanson, 1996). Type X methanotrophs utilise both, the RuMP and the serine pathway. Furthermore, a variety of MOx bacteria can also use carbon substrates other than methane such as chlorinated hydrocarbons, especially trichloroethylene, which raised biotechnical interest in these microbes (Hanson and Hanson, 1996; Wilson and Wilson, 1985).

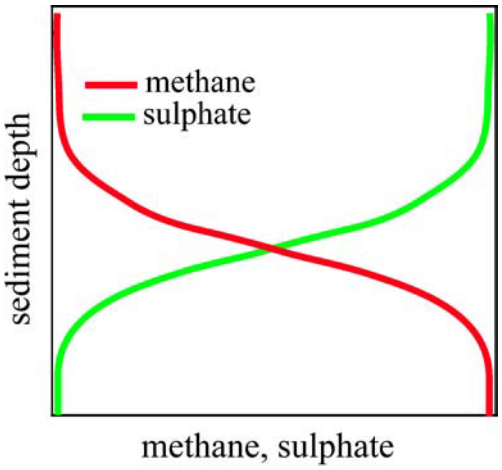

Figure 6. Pore water sulphate and methane profiles in anoxic marine sediments.

Evidence for the anaerobic oxidation of methane (AOM) has been first found in organic rich, anoxic marine sediments. Martens and Berner (1974) detected that methane was not accumulating before sulphate was consumed (Fig. 6). To explain the methane decrease in the sulphate reducing zone, it was proposed that methane is oxidised with sulphate as an electron acceptor (Barnes and Goldberg, 1976; Iversen and Jørgensen, 1985; Martens and Berner, 1974):

$$CH_{4\,(aq)} + SO_4^{2-}{}_{(aq)} \rightarrow HCO_3^{-}{}_{(aq)} + HS^{-}{}_{(aq)} + H_2O_{\,(l)},\ \Delta G^0 = -33\ kJ\ mol^{-1} \quad (8)$$

The necessity of sulphate as an electron acceptor limits AOM to marine and probably -although not yet found - to a few sulphate rich, limnic environments. So far, attempts to isolate anaerobic methanotrophs have failed. However, combinations of DNA and lipid biomarker analyses (section 3.2) of environmental samples provided evidence that two distinct lineages of archaea mediate AOM, both of which are closely related to the methanogenic *Methanosarcinales*. They are commonly found in consortium with SRB of the *Desulfosarcina/Desulfococcus* cluster which were termed Seep-SRB1 (Boetius et al., 2000;

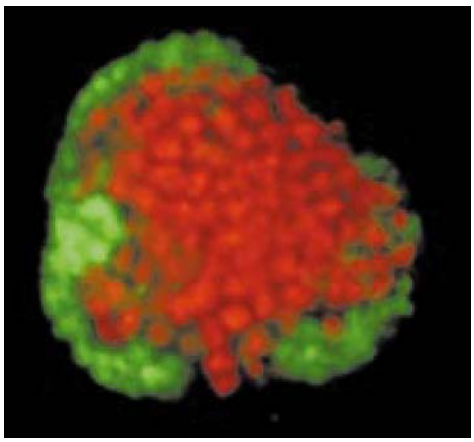

Figure 7. Microbial consortium of methane oxidising archaea (ANME II, stained red) and sulphate reducing bacteria (Seep SRB 1, stained green (Boetius et al., 2000)

Hinrichs et al., 1999; Knittel et al., 2003; Michaelis et al., 2002; Orphan et al., 2001). With respect to the ability to mediate AOM, the two phylogenetic groups of anaerobic methane oxidisers were termed ANME-1 and ANME-2. For the first time, these consortia could be visualised by fluorescence *in situ* hybridisation (section 1.3.2) in sediments above gas hydrates at Hydrate Ridge, Oregon (Boetius et al., 2000; Fig. 7). The biochemical functioning of AOM has not been elucidated yet, but increasing evidence suggest that the process is a reversal of methanogenesis (Hallam et al., 2004; Hoehler et al., 1994; Krüger et al., 2003; Valentine and Reeburgh, 2000). The role of the SRB involved in AOM is probably the removal of an up to now unknown intermediate via SR, maintaining favourable thermodynamic conditions for AOM according to reaction (8). The stoichiometry of this reaction has been validated by means of *ex situ* and *in vitro* rate measurements for environments where ANME-1 and/or ANME-2 prevail (Nauhaus et al., 2002; Nauhaus et al., 2005; Treude et al., 2003).

2.3 Global Budget

An assessment of production and consumption of methane on a global scale is difficult, because the spatial dimensions and fluxes from several types of methane producing and consuming environments have not been well constrained. Especially the estimates for polar environments and the ocean are preliminary and will most likely be adjusted in the future. However, the identification of major sources and sinks and agreeable estimates of methane production and consumption allowed for tentative, global budget calculations (Judd et al., 2002; Lelieveld et al., 1998; Reeburgh 1996). The largest sink of atmospheric methane is

within the atmosphere itself where methane is oxidised by hydroxyl radicals according to reaction (6). Besides this major sink, a variety of other sources and sinks were identified (Fig. 8a, b). The majority of recent methane production is of a biogenic, i.e. thermogenic or microbial origin whereas abiogenic methane appears to be of lesser importance (Lollar et al., 2002; Whiticar, 1999). However, recent findings of novel off-axis hydrothermal vents emitting abiogenically formed methane suggest a possible underestimation of abiogenic production of methane (Früh-Green et al., 2005; Kelley et al., 2001; Kelley et al., 2005).

2.3.1 Anthropogenic Sources and Sinks

The highest emission of methane to the atmosphere at present is from anthropogenic sources (Fig. 8a, Judd et al., 2002; Reeburgh, 1996). These can be divided into microbially mediated fermentation and chemical processes. Methane production as a terminal process of fermentation occurs where large amounts of organic matter accumulate in aqueous systems,

a

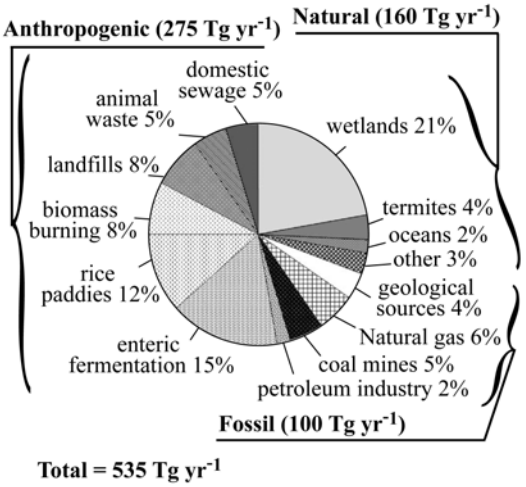

b

Source / Sink	Global Production	Global Consuption	Net Emission
Animals	80	0	80
Rice Production	577	477	100
Biomass Burning	55	0	55
Landfills	62	22	40
Coal Production	35	0	35
Gas Production	58	18	40
Wetlands	142	27	115
Termites	44	24	20
Hydrates	10	5	5
Oceans & Freshwater	85	75	10
Soil consumption	0	10	-10
Photochemical Oxidation	0	450	-450
Global Budget	1148	1108	40

Figure 8. (a) Sources of atmospheric methane (modified after Judd et al., 2002). (b) Global budget of methane production and consumption in Tg yr^{-1} (modified after Reeburgh 1996). Discrepancies within and between both estimates are due to uncertainties of particular budgets. Note that the global budget of panel a does not encompass photochemical degradation.

i.e. in flooded rice paddies, waste dumps (landfills) as well as manure and sewage storages. However, methane is not only produced but also consumed in those systems. For instance, the rice plants pump oxygen into the soil via their roots (arenchyma) fostering high rates of MOx (Conrad, 1993; Krüger et al., 2001; Wang et al., 1997). At the same time, the ventilation also amplifies methane emissions because the major fraction of methane leaves the soil via the arenchyma (e.g. Wang et al., 1997 and references therein). Furthermore, MOx was found to consume a substantial fraction of methane which is produced in biofilms covering sewage outlets (Damgaard et al., 2001).

Another major contribution of anthropogenic methane to the atmosphere is due to the enteric fermentation in the intestines of ruminants. Ruminants lack enzymes for the break down of polymeric substances such as cellulose, pectin and other ß-linked carbohydrates. They therefore host a diverse microbial community, which decomposes these polymers, transforms the hydrolytic products into volatile fatty acids and builds up microbial protein, which can be resorbed by the host. The role of the methanogens in this community is to scavenge hydrogen in order to maintain energetically favourable conditions for the carbohydrate decomposing, bacterial symbionts resulting in a production of ~83 kg methane cow^{-1} yr^{-1} (Benchaar et al., 1998). Methane oxidizers do not occur in the cow intestines and the methane is directly released via the esophagus into the atmosphere.

Biomass burning represents a chemical formation pathway of methane. In this process, methane is produced when organic matter is combusted incompletely. Besides other gases and smoke, methane is directly released into the atmosphere. Deforestation and fuel-wood use in tropical areas account for 85% of this methane source (Hao and Ward, 1993).

40% of fossil methane emissions to the atmosphere are caused by human explorations of fossil energy resources (Judd et al., 2002). Methane co-occurs with oil and coal and in the process of coal mining, gas and oil production methane may escape to the atmosphere as a result of outgassing and leakage. The co-occurrence of methane and coal is known since the first underground coal mines. Accordingly, the methane in mines was a termed “mine gas” or “firedamp” and caused numerous explosions and fatalities in the history of mining.

2.3.2 Natural Sources and Sinks

60% of the fossil methane emissions to the atmosphere comprise natural leakages of both, marine and terrestrial oil and gas reservoirs (Fig. 8a). A prominent example of a natural system releasing fossil methane to the atmosphere is the terrestrial mud volcano Lokbatan, Azerbaijan (Aliyev et al., 2002; Kholodov, 2002). About 900 mud volcanoes occur terrestrially. Their abundance as well as that of other seep types in the ocean is unknown. Hence, the estimate for natural sources of fossil methane is poorly constrained.

The highest fraction of natural emissions of recent methane to the atmosphere is contributed by wetlands. These encompass the tundra, bogs, moors, swamps, alluvial and marshes. For centuries, methane from wetlands is known as “marsh” or “swamp gas”. These systems are similar to rice paddies accumulating high contents of organic matter, which is fermented leading to methanogenesis. By diffusion and advective transport, methane enters the upper, oxic horizons of wetlands where it is partly oxidised by MOx bacteria.

Termites contribute another significant, natural source of methane to the atmosphere. The process of methane formation in these animals is similar to that in ruminants. Termites also

lack an enzymatic system for the breakdown of polymers, which are their main diet (i.e., wood). This type of methane emission is also unregulated.

Soils are a significant sink of atmospheric methane. However, the regulation of methane consumption in soils by aerobic methanotrophs is a poorly understood process. Its magnitude may vary with respect to oxygen ventilation, water content and land usage (King, 1992; Mosier et al., 1997). Recent finding describe methanotrophs which can utilize atmospheric methane and hence must have extremely efficient enzymes (Bull et al., 2000; Henckel et al., 2000; Holmes et al., 1999)

70% of the Earth is covered by oceans. Here, anoxic conditions prevail in deeper sediment strata providing good conditions for microbial methanogenesis. Indeed, stable carbon isotope ratios confirmed that methane in marine sediments is to a large extend of a microbial origin (Claypool and Kvenvolden, 1983). Furthermore, the majority of gas hydrate, the largest methane reservoir on earth, is located in the marine environment (Kvenvolden, 1988). Calculations of reservoir sizes are highly speculative, however, estimates of gas hydrate deposits range between 500 and 24000 Gt carbon, which strongly exceed the reservoir size of conventional gas deposits (140 Gt; Falkowski et al., 2000). It is thus surprising that the marine methane production and the emission to the atmosphere appear to be comparably small (Fig. 8a, b). There are three major reasons for this phenomenon: (1) the sequestration of methane in the seabed, (2) localised maxima of organic matter fluxes and (3) most important, the high capacity for AOM in marine systems.

(1) An oversaturation of methane reaching PT conditions of hydrate stability lead to gas hydrate formation. The majority of gas hydrates within the hydrate stability zone is relatively “safely” locked within the sediments and will remain there unless temperature

and pressure conditions will change (Judd et al., 2002). Submarine earthquakes and local gas hydrate dissociation can trigger sub marine landslides which can lead to a subsequent, large-scale release of seabed gas hydrates into the water column and consequently to the dissociation of the upward floating hydrates. This scenario, also known as the "clathrate smoking gun" hypothesis, might have altered Earth climate 55 million years ago leading to a rise of atmospheric temperatures which allowed modern mammals to propagate globally (Kennett et al., 2000; Kerr, 1999).

(2) The bulk of methane is produced in continental shelf areas which comprise only ~3.5% of the total area covered by the oceans (Reeburgh, 1996). High rates of primary production in the largely euphotic water column of the shelf seas is fostered by nutrient inputs from rivers, upwelling and a fast recycling of organic matter in the seabed that releases nutrients back into the water column (Fig. 9a; Lohrenz et. al, 1997; Graf et al., 1992; Graf et al., 1983; Field et al., 1998; Johnson et al., 1999). In contrast, only 1-5% of surface primary production reaches the sea floor of the abyssal and bathyal ocean as a result of biodegradation of detritus particles during sedimentation.

(3) The bulk of methane oxidation in marine sediments is mediated anaerobically consuming >80% of uprising methane in the sediments (Reeburgh, 1996). The high capacity for AOM in the oceans is supported by the high availability of the electron acceptor sulphate exceeding oxygen concentrations by 100-fold in sea water. This makes sulphate an ample electron acceptor in marine sediments. In contrast, the penetration depth of oxygen into the sediment is very limited as a result of oxygen consuming process other than MOx. One may assume that AOM rates in the sediment reflect the flux of organic matter, however, according to the limited amount of currently available data, this link appears to be relatively weak (Hinrichs and Boetius, 2002). Hinrichs and Boetius (2002) extrapolated

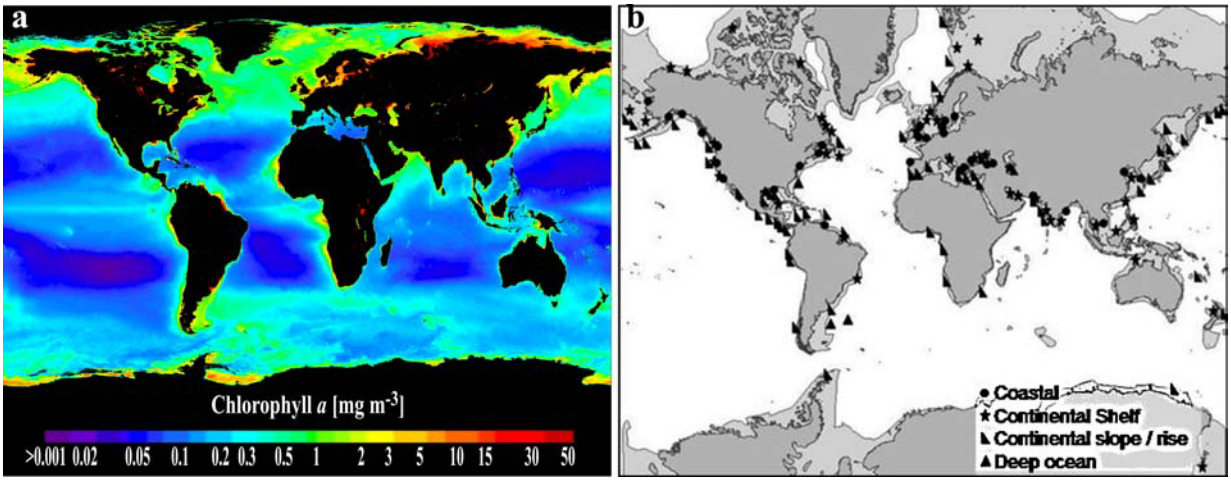

Figure 9. (a) Average, aquatic Chlorophyll *a* concentrations (Oct. 1997 – Apr. 2002, image by SeaWiFS, NASA . (b) Global distribution of methane seepages (after Judd, 2003). Note that hydrothermal vents on the oceanic ridges are not included in panel b.

from literature data that ocean margin sediments characterised by diffusive methane fluxes, support AOM in the order of 300 Tg yr^{-1}. This is nearly four times higher than the previous estimate by Reeburgh (1996). In seepage areas, predominantly found at the continental margins (Fig. 9b), the rates of AOM can be more than one order of magnitude higher compared to non-seep sediments. Consequently, the global methane production in the ocean is probably strongly underestimated as well (Hinrichs and Boetius, 2002). Furthermore, knowledge on the number of methane seeps, magnitudes of AOM activity, identities of methanotrophic organisms and processes that control methane seepage is limited. Hence, further studies filling these gaps are important to understand the role and fate of methane in the ocean.

3. METHANE-RICH HABITATS

Various types of methane-rich sedimentary habitats were discovered in marine environments. These habitats might be fuelled with microbial methane from *in situ* methanogenesis or with fossil methane from deeper reservoirs. Nothing is known on sediments hosting abiogenic methane. In general, methane-rich habitats can be ranked according to the amount of methane transported into near-surface sediment horizons and/or methane discharge into the hydrosphere. Among the most active systems are the so-called cold seeps, which can be defined as an environment where gas and/or fluids are transported by advective processes from ocean sediments into the hydrosphere, often in the form of ebullition of free gas. Apart from their potential role in the global methane cycle, these systems are spectacular oases of life formed by chemosynthetic communities. Similar to the hot vents, various cold seep environments were found to support enormous amounts of microbial and invertebrate biomass either directly fuelled by methane or indirectly by the AOM end product sulphide (Boetius and Suess, 2004 and references therein). Furthermore, cold seeps are often associated with authigenic carbonates forming crusts, chimneys or reef-like structures (Hovland and Judd, 1988). Besides the cold seeps, a variety of less active and less spectacular but with respect to the global budget more important methane-rich sediments are wide spread on the continental shelf (Hinrichs and Boetius, 2002; Judd et al., 2002).

With an emphasis to the habitats studied in this thesis, the following section (3.1.) describes common properties of methane-rich habitats in the marine environment. The differentiation between methane-rich geo-bio-systems is based on more or less long-lived features such as size, shape and venting activity. Hence, some definitions overlap. At the end of this section

(3.2), an overview of analytical tools for the determination of microbial key players and metabolic turnover rates of methane is provided.

3.1 Habitats

Mud volcanoes – These structures were previously identified as an important escape pathway of methane and higher hydrocarbons and were reported from terrestrial and oceanic settings (Dimitrov, 2002; Dimitrov, 2003; Judd et al., 2002; Kopf et al., 2001). Mud volcanism is caused by various geological processes such as tectonic accretion and faulting, rapid burial of sediments, slope failures or fluid emissions from mineral dehydration. These processes can lead to an abnormally high pore fluid pressure and the extrusion of mud and fluids through a central conduit to the sea floor which is often accompanied by the expulsion of methane and higher hydrocarbons (Charlou et al., 2003; Kopf, 2002; Milkov, 2000; Somoza et al., 2003). Methane from mud volcanoes can be of thermogenic and/or microbial origin, depending on the oceanographic and tectonic setting. The shape of these structures is diverse, ranging from amorphous mud pies to conical structures from a few meters to kilometres in size. While there is a reliable number of ~900 known terrestrial mud volcanoes, estimates for deep water mud volcanoes, mainly situated along the continental margins, range between 800 and 100000 (Dimitrov, 2002; Dimitrov, 2003; Milkov, 2000; Milkov et al., 2003). This makes budget calculations very preliminary. However, global estimates suggest that terrestrial and shallow water mud volcanoes contribute between 2.2 and 6.0 Tg yr^{-1} of methane to the atmosphere and that 27 Tg yr^{-1} of methane may escape from deep water mud volcanoes (Dimitrov, 2003; Milkov et al., 2003). Mud volcanism is therefore a key process in the global methane cycle.

Mud volcanoes may erupt violently in regular or irregular time intervals or emit mud, fluid and gases continuously. Three types of mud volcanoes are distinguished (Dimitrov, 2003 and references therein):

(1) Lokbatan-type: This type of mud volcanisms was named after the Lokbatan mud volcano, Azerbaijan. Lokbatan type mud volcanoes are characterised by violent outbreaks and long phases of dormancy.

(2) Chikishlyar-type: Calm, relatively weak and continuous venting of gas, water and mud are typical for this type of mud volcano.

(3) Shugin-type: This type of mud volcanism is transitional between the other types, characterised by long periods of weak activity interrupted by eruptive events. Dimitrov (2003) suggests that this type of mud volcanism is the most common.

Mud volcanoes can become inactive when the source of gas expansion and fluid flow stops (Planke et al., 2003). Most oceanic mud volcanoes were discovered and investigated in the last decade, when the appropriate high-resolution geophysical tools and submersibles became available to science. In many cases it is therefore unknown what activity-type a particular mud volcano may represent as eruptive events could be separated by extremely long periods (>100 yr) of dormancy.

Mud volcanoes were found to support a wide range of seep-related biomass. Authigenic carbonates and other seepage features maybe present or absent, depending on the history and activity of the mud volcano. The Håkon Mosby Mud Volcano, which is the focus of the chapters 2 to 4 of this thesis, might be a comparably active Chikishlyar- or Shugin-type,

whereas those mud volcanoes studied in the Gulf of Cadiz (chapter 5) appear to be either weak Chikishlyar- or Lokbatan-types.

Gas seeps – Gas seep systems are generally characterized by high rates of AOM and associated biomass (Boetius et al., 2000; Boetius and Suess, 2004; Elvert et al., 1999; Joye et al., 2004; Michaelis et al., 2002; Orphan et al., 2004; Treude et al., 2003). Gas seeps are associated with gas leakages from ancient gas reservoirs, gas hydrate dissociation and gas escape from shallow gas accumulations. Gas seepage may co-occur with fluid seepage. Gas seeps provide a permanently high supply of methane to surface sediment and methane is discharged via gas ebullition into the hydrosphere. Prominent examples of hydrate driven gas seeps are Hydrate Ridge, Oregon (Boetius and Suess, 2004; Suess et al., 1999) and cold seeps in the Gulf of Mexico (Joye et al., 2004). High amounts of seep related biota and carbonates were reported from these systems (Sibuet and Olu, 1998). The gas seep studied in this work (Tommeliten, North Sea, chapter 6) is fed by thermogenic methane escaping from a deep reservoir through a central conduit. The Tommeliten seep area also comprises small pockmark-like depressions of a few meters in size which were probably formed due to gas escape (Hovland and Judd, 1988).

Pockmarks - Pockmarks are an ubiquitous phenomenon which have been reported from various oceanographic and geological settings and can be formed by multiple processes (Hovland and Judd, 1988; Judd, 2003; Whiticar and Werner, 1981; Zuhlsdorff and Spiess, 2004). These may or may not be associated to recent gas venting.

(1) One type of pockmarks forms when gases and/or fluids are trapped in shallow reservoirs below impermeable sediments. Here, increasing pressure leads to a dome-like swelling of subsurface- and subsequently of surface sediments. Once an escape

path to the sea floor is established, the pressure drop results in an outburst of gas/fluids and mobilised sediments (Judd et al., 1994; Woolsey et al., 1975). After the initial outburst, these pockmarks may either become inactive if the sub surface reservoir of gas/fluid is depleted or undergo cycles of activity that are interrupted by phases of dormancy where the shallow reservoir is recharged and no or little seepage occurs (Çifçi et al., 2003; Hovland and Judd, 1988). This type of pockmarks is therefore similar to mud volcanoes as described above with the exception that pockmarks do not emit large amounts of solid matter (mud) over longer time scales.

(2) A second process of pockmark formation is suggested to occur when sub-surface gas hydrates destabilise. This mode of formation might have been common on continental shelves covered by seabed ice during the last glacial maximum. Melting of this ice would have caused a catastrophic release of potential sub-surface gas hydrate (Judd et al., 2002).

(3) Pockmarks may also be formed by processes which are not related to gas emissions but to focused fluid flow leading to failures in the sediments and thus to the observed pockmark structure. This type of pockmark was for instance found in Eckernförde Bay (Whiticar, 2002).

Similar to mud volcanoes, the contribution to atmospheric methane from pockmarks is difficult to estimate. With respect to vent activity, pockmarks may be encrusted with authigenic carbonates and support seep related biomass.

Hydrothermal vents - Along the mid-ocean spreading zones, the interaction between hot basaltic material and cold seawater drives hydrothermal flow. Reduced chemical compounds are formed by rock-water interactions and ions dissolve in the heated seawater. Once the water is ejected and mixed with the cold surrounding seawater, the solutes precipitate and form large chimneys (e.g., black smokers). These systems support enormous amounts of biomass based on free-living and endosymbiotic, thiotrophic bacteria which utilise sulphur compounds that are expelled (Canganella, 2001; Corliss et al., 1979). Not much is known on the occurrence of AOM in hydrothermal systems, but some evidence points to the existence of thermophilic ANME groups (Kelley et al., 2005; Teske et al., 2002).

Permanently anoxic waters – The lower part of the Black Sea is the most prominent anoxic, marine water body covering numerous mud volcanoes, pockmarks, gas seepage, gassy sediments and diffusive systems. Here, the anoxic conditions allow AOM communities to form reef structures purely consisting of microbial biomass and methane related carbonates (Michaelis et al., 2002; Pimenov et al., 1997). Furthermore, biomarker evidence suggest that AOM also occurs within the euxenic water column (Schouten et al., 2001).

Gassy coastal sediments – *In situ* methanogenesis is usually the source of methane in these systems. High production rates lead to supersaturation and consequently to the formation of methane gas bubbles (Martens et al., 1986; Whiticar, 2002). The sulphate methane transition zone (SMT) is usually found within the upper few metres of the sediment, however, occurrences of gas ebullition from these sediments were also reported (Garcia-Gil et al., 2002). Gassy sediments are likely to occur in estuaries, rias (drowned valleys) and bays characterised by high deposition rates of organic matter.

Diffusive systems – Molecular diffusion is the sole transport mechanism in these sediments whereas advective processes accelerating fluids and gas transport are absent (Judd et al., 2002). Similar to gassy sediments, microbial *in situ* production is commonly the source of methane which is then consumed by AOM in overlying, sulphate rich sediment horizons (Hensen et al., 2003; Iversen and Jørgensen, 1985; Niewöhner et al., 1998). As a general rule, the SMT is located some meters below sea floor. Consequently, methane does not escape to the hydrosphere. Although gassy sediments and diffusive systems are characterised by comparably low methane production and consumption rates, their areal extension make them highly important with respect to the global methane budget (Hinrichs and Boetius, 2002).

3.2 Detection of methanotrophic organisms and assessment of metabolic rates

3.2.1 Lipid biomarker

As described in section 2.2, MOx is mediated by methanotrophic bacteria, and AOM by archaea in consortium with SRB. The analyses of lipid membrane structures is a useful criteria for differentiating archaea from bacteria (or eukaryotes) and to determine the community structure of microbial assemblages as well as to link these to dominant biogeochemical processes (Boschker et al., 1998; Madigan et al., 2000). In general, bacterial membranes consist of phospholipid bilayers built from fatty acids which are bound via an ester bond to the glycerol backbone (Fig. 10). The fatty acids may contain double bonds, methyl branching or C_3 ring structures. Higher organisms (eukaryotes) also synthesise fatty acids, however, the suite of fatty acids commonly found in eukaryotes differs from those

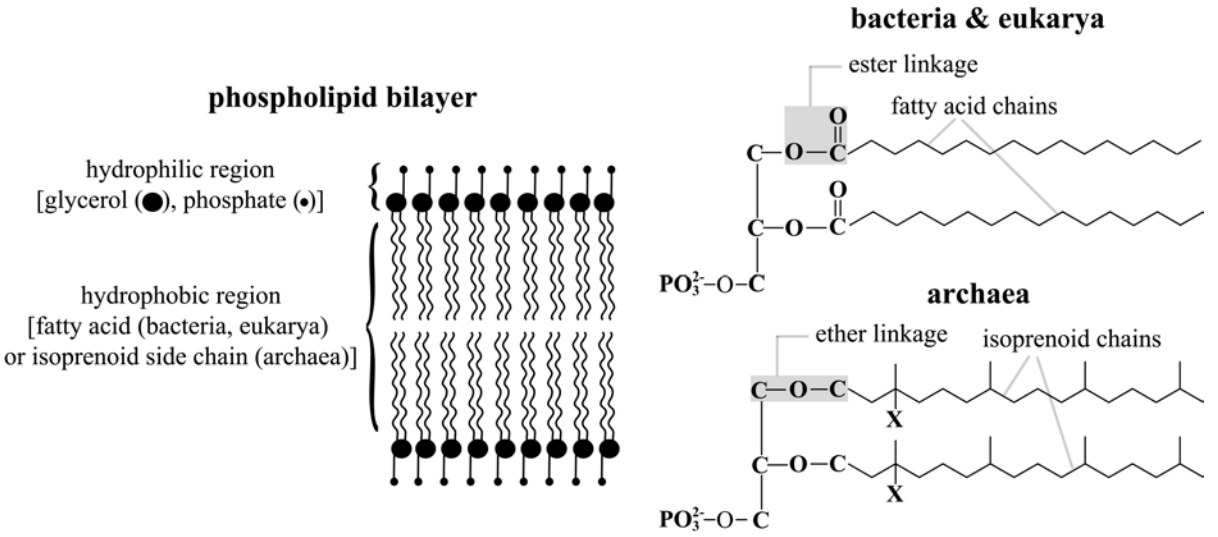

Figure 10. Chemical bonds and lipid structures in the phospholipid bilayers of bacteria, eukarya and archaea. X denotes a hydroxyl group or a hydrogen atom, respectively (modified after Elvert, 1999).

found in bacteria. In contrast, archaeal membranes comprise branched isoprenoidal alcohols, which are ether-linked to the glycerol backbone. Besides the diethers shown in figure 10, archaea may also contain glycerol tetraethers forming a membrane monolayer instead of a bilayer (De Rosa and Gambacorta, 1988; Koga et al., 1993). The presence of specific lipid compounds as well as their relative abundance thus indicates particular groups of archaea or bacteria. Furthermore, methane consuming microorganisms discriminate against the heavy isotope ^{13}C leading to a significant ^{13}C-depletion of their lipid biomass compared to the source methane (Elvert et al., 1999; Hinrichs et al., 1999; Jahnke et al., 1999). The presence of isotopically depleted crocetane, a tail-to-tail inked isoprenoidal hydrocarbon, in subsurface sediments of the Kattegat provided the first evidence for the archaeal identity of AOM communities (Bian, 1994; Bian et al., 2001). Further evidence for the involvement of archaea belonging to the *Methanosarcinales* was provided by findings of such isotopically depleted isoprenoidal hydrocarbons (crocetane and pentamethylicosane) and di-ethers (archaeol and *sn2*-hydroxyarchaeol) in sediments of cold seeps in the NW Pacific (Elvert et al., 1999;

Hinrichs et al., 1999). Similarly, $\delta^{13}C$-depleted fatty acids with 16 or 18 carbon atoms and double bonds at the ω-8 position ($C_{16:1\omega8}$, $C_{18:1\omega8}$, respectively) are a diagnostic marker for MOx-bacteria (Hanson and Hanson, 1996).

16S rDNA - A second way to detect methanotrophic communities is the analysis of 16S rDNA sequences. This method dates back on the pioneer work of Woese and Fox (1977) on ribosomal DNA as an appropriate molecular marker for phylogenetic relationships. It takes advantage of the very low mutation rate of the genes encoding the nucleotide sequence of the ribosomes. Furthermore, it is thought that lateral gene transfer does not affect these genes. Hence, the nucleotide sequences encoding these genes slowly change with time and the degree of similarity constantly increases at lower taxonomical levels. The rapidly increasing size of the global nucleotide data bases (e.g. Entrez Nucleotides database, www.ncbi.nlm.nih.gov), that contains roughly 40 billion bases (status 2004), and developments of software tools for phylogentic tree calculations (e.g., ARB, Ludwig et al., 2004) allow to match unknown environmental sequences against sequences of cultured and uncultured relatives for taxonomical identification. Using this method, the current phylogentic classification of methanotrophic bacteria and archaea as well as sulphate reducing bacteria that are putatively involved in AOM has been established (e.g., Hanson and Hanson, 1996; Knittel et al., 2003; Knittel et al., 2005; Orphan et al., 2001).

FISH - Direct visualisation and quantification of microbes in environmental samples became possible by means of fluorescence *in situ* hybridisation (FISH; Amann et al., 1990). Similar to 16S rDNA analysis, this method takes advantage of the conserved structure of ribosomes. Here, a fluorescence dye is conjugated to a short oligonucleotide sequence (probe) complementary designed to unique regions of the ribosomal RNA. Consequently, intact cells carrying fluorescently labelled probes, positively bound by base pairing to the ribosomes,

light up at specific wavelengths and can be quantified by fluorescence microscopy. With this method, spherical ANME-2/DSS consortia from Hydrate Ridge were the first AOM communities that could be visualised (Boetius et al., 2000). Subsequent discoveries found ANME-2 and/or ANME-1 in consortium with SRB at many cold seep systems (Michaelis et al., 2002; Orphan et al., 2002; Treude, 2003).

AOM and SR rates – Anaerobic oxidation of methane coupled to sulphate reduction is the key process consuming methane in the world oceans (see section 2.3). Estimates for AOM and SR rates can be gained by measuring metabolic activities directly after sediment retrieval (*ex situ*) under simulated *in situ* conditions (usually temperature). This technique is based on the work of Iversen and Jørgensen (1985). Here, sediment is incubated with trace amounts of $^{14}CH_4$ and $^{35}SO_4^{2-}$, which is metabolised with almost the same velocity as the non-radioactive substrate. The concentrations of methane and sulphate as well as the ratios of the radioactive products relative to the radioactive reactants determine the magnitude of the *ex situ* rates. This technique revealed that a substantial fraction of uprising methane is consumed within the sediment and that the metabolic activity of AOM communities can be very high (>4 mol m^2 yr^{-1}) at cold seep systems (Boetius et al., 2000; Joye et al., 2004; Nauhaus et al., 2002; Treude et al., 2003). Aerobic oxidation of methane can be measured with the same technique. Besides this technique, concentration gradients of methane and sulphate dissolved in porewater can be used as a proxy for rates of AOM and SR. This method is limited to diffusive systems without further model fits. According to Fick's first law of diffusion, the fluxes can be calculated by determining the concentration gradients and the diffusion coefficients of methane and sulphate. This approach has been used successfully to infer AOM rates at non-seep environments (Hensen et al., 2003; Niewöhner et al., 1998) where rates are often at the detection limit of tracer-incubation techniques (i.e., <55 mmol m^{-2} yr^{-1} on average)

4. OBJECTIVES OF THIS PHD THESIS

In this thesis I used a combination of different analytical tools to acquire an understanding of the spatial distribution of methane turnover and the responsible microorganisms in different geo-bio-systems. Several systems with various degrees of activity in methane turnover were explored during this thesis. These systems were barely known with respect to biogeochemical and microbiological processes. The Håkon Mosby Mud Volcano has been discovered during geophysical surveys, and the concentric distribution of different biocoenoses has been described, but the biogeochemical and microbiological causes for this zonation were not known. The Gulf of Cadiz mud volcanoes and the Tommeliten gas seeps have not been investigated before in terms of biogeochemistry and microbial ecology. For each habitat studied, the following questions were of particular interest:

- What microbial key players are present?
- How abundant are they?
- What are the dominant pathways of methane consumption?
- What is the magnitude of methane consumption?
- What is the relation between lipid signatures, DNA profiles, cell counts and activities?
- What are the dominant factors controlling the environment?
- Is there a contribution of methane to the hydrosphere?

The central aim of this thesis was a systematic study of the microbial ecology and biogeochemistry of these novel systems. Collaborations with scientists from other scientific disciplines allowed comparing biological, biogeochemical and physical data sets and to determine the mechanisms controlling vent activity and the distribution of seep related biota.

In combination with biogeochemical data, direct sea floor observations, facilitated by sledge cameras or remotely operated vehicles (ROV), allowed to estimate if methane escapes to the hydrosphere.

5. CHAPTERS AND PUBLICATIONS OUTLINE

This work includes the first version of five manuscripts (chapters 2-6). All manuscripts will be submitted within the next months, depending on the comments by the co-authors. The final discussion is a synthesis of the work presented in the articles (chapters 2-6), which appear in the order as described in the following. All articles were written by myself, with the exception of the manuscript presented in chapter 2 which was jointly written with Antje Boetius. Both Antje Boetius and Marcus Elvert advised me in the writing process of each article.

Chapter 2. Microbial colonization of a submarine mud volcano: how subsurface fluid flow structures methanotrophic communities

(to be submitted to Nature)

Helge Niemann, Tina Lösekann, Dirk de Beer, Marcus Elvert, Katrin Knittel, Rudolph I. Amann, Eberhard Sauter, Michael Schlüter, Michael Klages, Jean P. Foucher, Antje Boetius

Geological features such as turbidity flows, slope failures and mud volcanoes are known to deposit large amounts of sub-surface mud to the sea floor. These newly formed habitats are

colonised by microbial communities shaping the benthic environment. This article describes a multidisciplinary approach to study the identities and environmental factors determining the development and selection of microbial communities in such newly created habitats at the arctic Håkon Mosby Mud Volcano (HMMV, 72° N, 14°.44' E, 1250 m water depth). HMMV was visited twice during joint international research cruises with R/V Atalante and R/V Polarstern. Most of the sampling was facilitated with ROV Victor 6000. A combination of lipid biomarker, 16S rDNA and FISH analyses identified multiple groups of methanotrophs and provided evidence that the high methane flow at HMMV supports all known methanotrophic guilds, i.e. MOx bacteria (type I methanotroph, *Methylococcus sp.*), a novel AOM community (ANME-III / *Desulfobulbus sp.* aggregate) and symbiotic MOx bacteria (associated with the pogonophoran worm *Oligobrachia haakonmosbiensis*). The methanotrophic communities were respectively found to prevail in distinct, concentrically arranged habitats. Decisive factors determining about the success of the methanotrophic guilds were identified as a combination of pore water flow, bio ventilation and growth rate.

Field work organisation and sampling for lipid biomarker, 16S rDNA FISH analysis as well as for methane, sulphate, porosity AOM and SR rate measurements were performed by myself. Parts of the sulphate data were acquired by Eberhard Sauter and Michael Schlüter. Dirk deBeer performed microsensor measurements. Lipid biomarker analysis was accomplished by myself. Methane, sulphate, AOM and SR rate measurements were accomplished by myself with help by project technicians of Antje Boetius. Tina Lösekann carried out FISH and DNA analysis.

Chapter 3. Lipid signatures and distribution of methanotrophic microbial communities at Håkon Mosby Mud Volcano, Barents Sea

(to be submitted to Geobiology)

Helge Niemann, Marcus Elvert, Tina Lösekann, Jakob Jakob, Thierry Nadalig, Antje Boetius

This study provides a detailed analysis of lipid biomarkers in sediments of HMMV. The lipid analysis shown here provides evidence that methane oxidation is the base of the food web at HMMV. Diagnostic molecules of the newly discovered ANME-3 / *Desulfobulbus sp.* community and the type I methanotroph are presented. Furthermore, a phylogentic tree of the ANME-3 archaea and a correlation between concentrations of specific lipids and aggregate counts is provided.

Sampling for lipid, 16S rDNA and FISH analysis were accomplished by Antje Boetius, Tina Lösekann, Thierry Nadalig and myself. Lipid analysis was carried out by myself under the supervision of Marcus Elvert. During that time I instructed Jakob Jakob for a lab rotation analysing a fraction of the biomarker samples. Tina Lösekann performed DNA analysis whereas Thierry Nadalig carried out the FISH analysis.

Chapter 4. Aerobic and anaerobic oxidation of methane in sediments of Håkon Mosby Mud Volcano, Barents Sea

(to be submitted to Limnology and Oceanography)

Helge Niemann, Eberhard Sauter, Martin Krüger, Friederike Heinrich, Tina Lösekann, Marcus Elvert, Antje Boetius

This article provides a detailed analysis of methane oxidation and SR rates in sediments of HMMV. The predominant modes of methane oxidation, i.e. MOx and AOM, as well as their magnitudes are shown and an overview of the variability of methane oxidation and SR within this habitat is provided. With the aid of chloride and bromide concentration profiles, fluid flow is pointed out as one factor determining the mode of methane oxidation. Moreover, physiological parameters of ANME-3 such as temperature optimum, response to substrate concentration and the stoichiometry of AOM were analysed.

Together with Friederike Heinrich, Antje Boetius and myself carried out sediment sampling for the *in vitro* experiments, AOM and SR rate, methane and sulphate concentration and porosity measurements. Subsampling for sulphate concentrations as well as sulphate concentration measurements were carried out by Eberhard Sauter and myself. Eberhard Sauter also acquired the sediment samples for bromide and chloride and measured these concentrations. AOM and SR rate, methane and sulphate concentration as well as porosity measurements were carried out by myself with help by project technicians of Antje Boetius. Friederike Heinrich and Martin Krüger performed the *in vitro* experiments.

Chapter 5. Microbial methane turnover at mud volcanoes of the Gulf of Cadiz

(to be submitted to Geochimica et Cosmochimica Acta)

Helge Niemann, Joana Duarte, Christian Hensen, Enoma Omoregie, Vito. H. Magalhães, Marcus Elvert, Luis Pinheiro, Achim Kopf, Antje Boetius.

The Gulf of Cadiz (GoC) is an area characterised by numerous mud volcanoes, diapirs and pockmarks. However, the activity of mud volcanism as well as the identity of potential methane oxidisers is unknown from this region. This article provides an overview of vent activity and associated microorganisms of several mud volcanoes in the Gulf of Cadiz, which were sampled during the GAP (Gibraltar Arc Processes) cruise with R/V Sonne. Prior to sampling, most mud volcanoes were investigated with a video sledge to identify potential locations of increased vent activity. However, these observations could not reveal any sign of recent fluid or gas venting. Using a multidisciplinary approach, sediment samples were analysed for pore water constituents, AOM and SR rates, lipid biomarker contents and 16S rDNA signatures. This revealed a complete reduction of thermogenic methane and associated higher hydrocarbons mediated by multiple AOM communities in defined sub-surface horizons of the studied mud volcanoes.

This study was carried out by myself and is part of a Portuguese-German collaboration between the University of Aveiro, the University of Bremen and the Max Planck Institute for Marine Microbiology. All of the sampling as well as the laboratory analyses were performed by myself with the exception of sulphate and sulphide concentration measurements and diffusive flux calculations, which were carried out by Christian Hensen. During that time I introduced lipid analyses as well as AOM and SR rate measurements to Joana Duarte, who I instructed in her master thesis. She analysed parts of the lipids, AOM, SR rate and porosity of

the samples. Vito. H. Magalhães and L. Pinheiro provided seismic sections and areal maps. Enoma Omoregie performed the 16S rDNA analyses.

Chapter 6. Methane emission and consumption at a North Sea gas seep (Tommeliten area)

(to be submitted to Biogeosciences)

H. Niemann, M. Elvert, M. Hovland, B. Orcutt, A. Judd, I. Suck, J. Gutt, S. Joye, E. Damm, K. Finster, A. Boetius

Most studies on methane rich habitats were conducted in highly active seep environments at the continental slopes. This article deals with a seep system located in the Tommeliten area, central North Sea, at 75 m water depth. During two cruises with R/V Heinke, video imaging and hydroacoustic profiling showed recent seepage from small point sources. Similar to highly active seeps, the methane at Tommeliten is consumed in a defined sediment horizon where methane related, authigenic carbonates were found. The identities of methane oxidising communities as well as the community size was analysed by lipid biomarker, 16S rDNA and FISH analyses. Slabs of methane related carbonates outcropping the sea floor were found to provide a hard substrate, on the sandy seafloor. These carbonates were densely colonised by sessile invertebrates showing that methane seepage and related processes effectively shape the environment.

Sampling and onboard work was organised by Antje Boetius and myself. Lipid biomarker, 16S rDNA and FISH analysis as well as AOM and SR rate, sulphate and sulphide concentration and the *in vitro* experiment were accomplished by myself. Beth Orcutt performed the methane concentration measurements, Inken Suck and Julian Gutt carried out video imaging and Jens Wunderlich and Gerd Wendt performed the hydroacoustic measurements.

Chapter 7. Final Discussion and conclusion

Helge Niemann

In this chapter, the data acquired during this PhD work are summarised and discussed in a global context. Environmental factors determining the magnitude of AOM as well as the hot spots of methane oxidation in the environment are presented. An overview on the key microbial players as well as diagnostic lipid patterns typifying methanotrophic communities is provided as well. Also, the impacts of methane turnover on the adjacent marine environments at cold seeps are highlighted. Finally, an outlook on potential future research on methane turnover in marine sediments is given.

References

Aliyev A. A., Guliyev I. S., and Belov I. S. (2002) *Catalogue of recorded eruption of mud volcanoes of Azerbaijan (for period of years 1810-2001)*. Nafta Press, Baker.

Amann R. I., Krumholz L., and Stahl D. A. (1990) Fluorescent-oligonucleotide probing of whole cells for determinative, phylogenetic, and evironmental studies in microbiology. *Journal of Bacteriology* **172**, 762-770.

Barnes R. O. and Goldberg E. D. (1976) Methane Production and Consumption in Anoxic Marine-Sediments. *Geology* **4**(5), 297-300.

Benchaar C., Rivest J., Pomar C., and Chiquette J. (1998) Prediction of methane production from dairy cows using existing mechanistic models and regression equations. *Journal of Animal Science* **76**(2), 617-627.

Bian L. Q. (1994) Isotopic biogeochemistry of individual compounds in a modern coastal marine sediment (Kattegat, Denmark and Sweden). Master thesis, Indiana University.

Bian L. Q., Hinrichs K. U., Xie T. M., Brassell S. C., Iversen H., Fossing H., Jorgensen B. B., and Hayes J. M. (2001) Algal and archaeal polyisoprenoids in a recent marine sediment: Molecular isotopic evidence for anaerobic oxidation of methane. *Geochemistry Geophysics Geosystems* **2**, U1-U22.

Boetius A., Ravenschlag K., Schubert C., Rickert D., Widdel F., Gieseke A., Amann R., Jørgensen B. B., Witte U., and Pfannkuche O. (2000) A marine microbial consortium apparently mediating anaerobic methane of oxidation. *Nature* **407**, 623-626.

Boetius A. and Suess E. (2004) Hydrate Ridge: a natural laboratory for the study of microbial life fueled by methane from near-surface gas hydrates. *Chemical Geology* **205**(3-4), 291-310.

Boschker H. T. S., Nold S. C., Wellsbury P., Bos D., de Graaf W., Pel R., Parkes R. J., and Cappenberg T. E. (1998) Direct linking of microbial populations to specific biogeochemical processes by ^{13}C-labelling of biomarkers. *Nature* **392**, 801-805.

Bull I. D., Parekh N. R., Hall G. H., Ineson P., and Evershed R. P. (2000) Detection and classification of atmospheric methane oxidizing bacteria in soil. *Nature* **405**, 175-178.

Campbell I. M. (1986) *Energy and the atmosphere: A physical-chemical approach*. John Wiley & Son Ltd.

Canganella F. (2001) Hydrothermal vent ecosystems and representative hyperthermophilic microorganisms. *Annals of Microbiology* **51**(1), 11-27.

Carroll J. J. (2002) *Natural Gas Hydrates: A Guide for Engineers*. Gulf Professional Publishers.

Charlou J.-L. and Donval J.-P. (1993) Hydrothermal methane venting between 12 N and 26 N along the Mid-Atlantic Ridge. *Journal of Geophysical Research* **98**, 9625-9642.

Charlou J. L., Donval J. P., Zitter T., Roy N., Jean-Baptiste P., Foucher J. P., and Woodside J. (2003) Evidence of methane venting and geochemistry of brines on mud volcanoes of the eastern Mediterranean Sea. *Deep-Sea Research Part I-Oceanographic Research Papers* **50**(8), 941-958.

Çifçi G., Dondurur D., and Ergün M. (2003) Deep and shallow structures of large pockmarks in the Turkish shelf, Eastern Black Sea. *Geo-Marine Letters* **23**(3-4), 311-322.

Claypool G. E. and Kvenvolden K. A. (1983) Methane and Other Hydrocarbon Gases in Marine Sediment. *Annual Review of Earth and Planetary Sciences* **11**, 299-327.

Conrad R. (1993) Mechanisms controlling methane emissions from rice fields. In *The biogeochemistry of global change: radiative trace gases* (ed. R. S. Oremland), pp. 317-335. Chapman & Hall.

Corliss J. B., Dymond J., Gordon L. I., Edmond J. M., Herzen R. P. V., Ballard R. D., Green K., Williams D., Bainbridge A., Crane K., and Vanandel T. H. (1979) Submarine Thermal Springs on the Galapagos Rift. *Science* **203**(4385), 1073-1083.

Damgaard L. R., Nielsen L. P., and Revsbech N. P. (2001) Methane microprofiles in a sewage biofilm determined with a microscale biosensor. *Water Research* **35**(6), 1379-1386.

De Rosa M. and Gambacorta A. (1988) The lipids of archaebacteria. *Progress in Lipid Research* **27**, 153-175.

Dimitrov L. I. (2002) Mud volcanoes - the most important pathway for degassing deeply buried sediments. *Earth-Science Reviews* **59**(1-4), 49-76.

Dimitrov L. I. (2003) Mud volcanoes - a significant source of atmospheric methane. *Geo-Marine Letters* **23**(3-4), 155-161.

Elvert M. (1999) Microbial biomarkers in anaerobic marine environments dominated by methane. Ph.D. thesis, Chrsitian-Albrechts-University of Kiel, Germany.

Elvert M., Suess E., and Whiticar M. J. (1999) Anaerobic methane oxidation associated with marine gas hydrates: superlight C-isotopes from saturated and unsaturated C_{20} and C_{25} irregular isoprenoids. *Naturwissenschaften* **86**(6), 295-300.

Falkowski P., Scholes R. J., Boyle E., Canadell J., Canfield D., Elser J., Gruber N., Hibbard K., Hogberg P., Linder S., Mackenzie F. T., Moore B., Pedersen T., Rosenthal Y., Seitzinger S., Smetacek V., and Steffen W. (2000) The global carbon cycle: A test of our knowledge of earth as a system. *Science* **290**(5490), 291-296.

Fisher C. R. (1990) Chemoautotrophic and Methanotrophic Symbioses in Marine-Invertebrates. *Reviews in Aquatic Sciences* **2**(3-4), 399-436.

Formisano V., Atreya S., Encrenaz T., Ignatiev N., and Giuranna M. (2004) Detection of methane in the atmosphere of Mars. *Science* **306**(5702), 1758-1761.

Früh-Green G., Kelley D. S., Bernasconi S. M., Karson J. A., Ludwig K. A., Butterfield D. A., Boshi C., and Proskurowski G. (2005) 30,000 Years of Hydrothermal Activity at the Lost City Vent Field. *Science* **301**, 495-498.

Garcia-Gil S., Vilas F., and Garcia-Garcia A. (2002) Shallow gas features in incised-valley fills (Ria de Vigo, NW Spain): a case study. *Continental Shelf Research* **22**(16), 2303-2315.

Grosjean D. (1995) Atmospheric Chemistry of Biogenic Hydrocarbons - Relevance to the Amazon. *Quimica Nova* **18**(2), 184-201.

Hallam S. J., Putnam N., Preston C. M., Detter J. C., Rokhsar D., Richardson P. M., and DeLong E. F. (2004) Reverse methanogenesis: Testing the hypothesis with environmental genomics. *Science* **305**(5689), 1457-1462.

Hanson R. S., Bratina B. J., and Brusseau G. A. (1993) Phylogeny and ecology of methylotrophic bacteria. In *Microbial Growth on C_1 Compounds* (ed. J. C. Murrell and D. P. Kelly), pp. 285-302. Intercept Limited.

Hanson R. S. and Hanson T. E. (1996) Methanotrophic bacteria. *Microbiological Reviews* **60**(2), 439-&.

Hao W. M. and Ward D. E. (1993) Methane Production from Global Biomass Burning. *Journal of Geophysical Research-Atmospheres* **98**(D11), 20657-20661.

Henckel T., Jackel U., Schnell S., and Conrad R. (2000) Molecular Analyses of Novel Methanotrophic Communities in Forest Soil That Oxidize Atmospheric Methane. *Appl. Environ. Microbiol.* **66**(5), 1801-1808.

Hensen C., Zabel M., Pfeifer K., Schwenk T., Kasten S., Riedinger N., Schulz H. D., and Boettius A. (2003) Control of sulfate pore-water profiles by sedimentary events and the significance of anaerobic oxidation of methane for the burial of sulfur in marine sediments. *Geochimica Et Cosmochimica Acta* **67**(14), 2631-2647.

Hinrichs K.-U. and Boetius A. (2002) The anaerobic oxidation of methane: New insights in microbial ecology and biogeochemistry. In *Ocean Margin Systems* (ed. G. Wefer, D. Billett, and D. Hebbeln), pp. 457-477. Springer-Verlag, Berlin.

Hinrichs K.-U., Hayes J. M., Sylva S. P., Brewer P. G., and DeLong E. F. (1999) Methane-consuming archaebacteria in marine sediments. *Nature* **398**, 802-805.

Hoehler T. M., Alperin M. J., Albert D. B., and Martens C. S. (1994) Field and laboratory studies of methane oxidation in an anoxic marine sediment: Evidence for a methanogenic-sulfate reducer consortium. *Global Biogeochemical Cycles* **8**(4), 451-463.

Holmes A. J., Roslev P., McDonald I. R., Iversen N., Henriksen K., and Murrell J. C. (1999) Characterization of methanotrophic bacterial populations in soils showing atmospheric methane uptake. *Applied and Environmental Microbiology* **65**(8), 3312-3318.

Horita J. and Berndt M. E. (1999) Abiogenic methane formation and isotopic fractionation under hydrothermal conditions. *Science* **285**(5430), 1055-1057.

Hovland M. and Judd A. G. (1988) *Seabed Pockmarks and Seepages: Impact on Geology, Biology and the Marine Environment*. Graham & Trotman.

Iversen N. and Jørgensen B. B. (1985) Anaerobic methane oxidation rates at the sulfate-methane transition in marine sediments from Kattegat and Skagerrak (Denmark). *Limnology and Oceanography* **30**(5), 944-955.

Jahnke L. L., Summons R. E., Hope J. M., and Des Marais D. J. (1999) Carbon isotopic fractionation in lipids from methanotrophic bacteria II: The effects of physiology and environmental parameters on the biosynthesis and isotopic signatures of biomarkers. *Geochimica et Cosmochimica Acta* **63**(1), 79-93.

Joye S. B., Boetius A., Orcutt B. N., Montoya J. P., Schulz H. N., Erickson M. J., and Lugo S. K. (2004) The anaerobic oxidation of methane and sulfate reduction in sediments from Gulf of Mexico cold seeps. *Chemical Geology* **205**(3-4), 219-238.

Judd A. G. (2003) The global importance and context of methane escape from the seabed. *Geo-Marine Letters* **23**(3-4), 147-154.

Judd A. G., Hovland M., Dimitrov L. I., Gil S. G., and Jukes V. (2002) The geological methane budget at Continental Margins and its influence on climate change. *Geofluids* **2**(2), 109-126.

Judd A. G., Long D., and M. S. (1994) Pockmark formation and activity, U.K. Block 15/25, North Sea. *Bulletin Geological Society of Denmark* **14**, 34-49.

Kelley D. S. (1996) Methane-rich fluids in the oceanic crust. *Journal of Geophysical Research-Solid Earth* **101**(B2), 2943-2962.

Kelley D. S. and Fruh-Green G. L. (1999) Abiogenic methane in deep-seated mid-ocean ridge environments: Insights from stable isotope analyses. *Journal of Geophysical Research-Solid Earth* **104**(B5), 10439-10460.

Kelley D. S., Karson J. A., Blackman D. K., Fruh-Green G. L., Butterfield D. A., Lilley M. D., Olson E. J., Schrenk M. O., Roe K. K., Lebon G. T., Rivizzigno P., and the AT3-60 Shipboard Party. (2001) An off-axis hydrothermal vent field near the Mid-Atlantic Ridge at 30[deg] N. *Nature* **412**(6843), 145-149.

Kelley D. S., Karson J. A., Früh-Green G., and Yoerger D. R. (2005) A Serpentinite-Hosted Ecosystem: The Lost City Hydrothermal Field. *Science* **307**, 1428-1434.

Kennett J. P., Cannariato K. G., Hendy I. L., and Behl R. J. (2000) Carbon isotopic evidence for methane hydrate instability during quaternary interstadials. *Science* **288**(5463), 128-133.

Kerr R. A. (1999) CLIMATE CHANGE:A Smoking Gun for an Ancient Methane Discharge. *Science* **286**(5444), 1465-.

Kholodov V. N. (2002) Mud Volcanoes: Distribution Regularities and Genesis (Communication 2. Geological–Geochemical Peculiarities and Formation Model). *Lithology and Mineral Resources* **37**(4), 293-310.

King G. M. (1992) Ecological aspects of methane oxidation, a key determinant of global methane dynamics. In *Advances in Microbial Ecology*, Vol. 12 (ed. K. C. Marshall), pp. 431-468. Plenum Press.

Knittel K., Boetius A., Lemke A., Eilers H., Lochte K., Pfannkuche O., Linke P., and Amann R. (2003) Activity, distribution, and diversity of sulfate reducers and other bacteria in sediments above gas hydrate (Cascadia margin, Oregon). *Geomicrobiology Journal* **20**(4), 269-294.

Koga Y., Nishihara M., Morii H., and Akagawa-Matsushita M. (1993) Ether polar lipids of methanogenic bacteria: Structures, comparative aspects, and biosyntheses. *Microbiological Reviews* **57**(1), 164-182.

Kopf A., Klaeschen D., and Mascle J. (2001) Extreme efficiency of mud volcanism in dewatering accretionary prisms. *Earth and Planetary Science Letters* **189**(3-4), 295-313.

Kopf A. J. (2002) Significance of mud volcanism. *Reviews of Geophysics* **40**(2).

Krashnopolsky V. A., Maillard J. P., and Owen T. C. (2004) Detection of methane in the martian atmosphere: evidence for life? *Icarus* **172**(2), 537-547.

Krüger M., Frenzel P., and Conrad R. (2001) Microbial processes influencing methane emission from rice fields. *Global Change Biology* **7**(1), 49-63.

Krüger M., Meyerdierks A., Glockner F. O., Amann R., Widdel F., Kube M., Reinhardt R., Kahnt R., Bocher R., Thauer R. K., and Shima S. (2003) A conspicuous nickel protein in microbial mats that oxidize methane anaerobically. *Nature* **426**(6968), 878-881.

Kvenvolden K. A. (1988) Methane hydrate - a major reservoir of carbon in the shallow geosphere? *Chemical Geology* **71**, 41-51.

Kvenvolden K. A. (1993) A primer on gas hydrates. *U.S. Geological Survey Professional Paper* **1570**, 279-291.

Larock P. A., Hyun J. H., and Bennison B. W. (1994) Bacterioplankton Growth and Production at the Louisiana Hydrocarbon Seeps. *Geo-Marine Letters* **14**(2-3), 104-109.

Le Mer J. and Roger P. (2001) Production, oxidation, emission and consumption of methane by soils: A review. *European Journal of Soil Biology* **37**(1), 25-50.

Lelieveld J., Crutzen P. J., and Dentener F. J. (1998) Changing concentration, lifetime and climate forcing of atmospheric methane. *Tellus Series B-Chemical and Physical Meteorology* **50**(2), 128-150.

Levy H. (1971) Normal Atmosphere - Large Radical and Formaldehyde Concentrations Predicted. *Science* **173**(3992), 141-&.

Lollar B. S., Westgate T. D., Ward J. A., Slater G. F., and Lacrampe-Couloume G. (2002) Abiogenic formation of alkanes in the Earth's crust as a minor source for global hydrocarbon reservoirs. *Nature* **416**(6880), 522-524.

Ludwig W., Strunk O., Westram R., Richter L., Meier H., Yadhukumar, Buchner A., Lai T., Steppi S., Jobb G., Forster W., Brettske I., Gerber S., Ginhart A. W., Gross O., Grumann S., Hermann S., Jost R., Konig A., Liss T., Lussmann R., May M., Nonhoff B., Reichel B., Strehlow R., Stamatakis A., Stuckmann N., Vilbig A., Lenke M., Ludwig T., Bode A., and Schleifer K.-H. (2004) ARB: a software environment for sequence data. *Nucl. Acids Res.* **32**(4), 1363-1371.

Madigan M. T., Martinko J. M., and Parker J. (2000) *Brock Biology of Microorganisms*. Prentice-Hall, Inc.

Manne A. S. and Richels R. G. (2001) An alternative approach to establishing trade-offs among greenhouse gases. *Nature* **410**(6829), 675-677.

Martens C. S. and Berner R. A. (1974) Methane Production in Interstitial Waters of Sulfate-Depleted Marine Sediments. *Science* **185**(4157), 1167-1169.

Martens C. S., Blair N. E., Green C. D., and Des Marais D. J. (1986) Seasonal variations in the stable carbon isotopic signature of biogenic methane in a coastal sediment. *Science* **233**, 1300-1303.

Michaelis W., Seifert R., Nauhaus K., Treude T., Thiel V., Blumenberg M., Knittel K., Gieseke A., Peterknecht K., Pape T., Boetius A., Amann R., Jorgensen B. B., Widdel F., Peckmann J. R., Pimenov N. V., and Gulin M. B. (2002) Microbial reefs in the Black Sea fueled by anaerobic oxidation of methane. *Science* **297**(5583), 1013-1015.

Milkov A. V. (2000) Worldwide distribution of submarine mud volcanoes and associated gas hydrates. *Marine Geology* **167**(1-2), 29-42.

Milkov A. V., Sassen R., Apanasovich T. V., and Dadashev F. G. (2003) Global gas flux from mud volcanoes: A significant source of fossil methane in the atmosphere and the ocean. *Geophysical Research Letters* **30**(2).

Mosier A. R., Delgado J. A., Cochran V. L., Valentine D. W., and Parton W. J. (1997) Impact of agriculture on soil consumption of atmospheric CH4 and a comparison of CH4 and N2O flux in subarctic, temperate and tropical grasslands. *Nutrient Cycling in Agroecosystems* **49**(1-3), 71-83.

Nauhaus K., Boetius A., Kruger M., and Widdel F. (2002) In vitro demonstration of anaerobic oxidation of methane coupled to sulphate reduction in sediment from a marine gas hydrate area. *Environmental Microbiology* **4**(5), 296-305.

Nauhaus K., Treude T., Boetius A., and Kruger M. (2005) Environmental regulation of the anaerobic oxidation of methane: a comparison of ANME-I and ANME-II communities. *Environmental Microbiology* **7**(1), 98-106.

Niewöhner C., Hensen C., Kasten S., Zabel M., and Schulz H. D. (1998) Deep sulfate reduction completely mediated by anaerobic methane oxidation in sediments of the upwelling area off Namibia. *Geochimica et Cosmochimica Acta* **62**(3), 455-464.

Orphan V. J., House C. H., Hinrichs K. U., McKeegan K. D., and DeLong E. F. (2001) Methane-consuming archaea revealed by directly coupled isotopic and phylogenetic analysis. *Science* **293**(5529), 484-487.

Orphan V. J., House C. H., Hinrichs K. U., McKeegan K. D., and DeLong E. F. (2002) Multiple archaeal groups mediate methane oxidation in anoxic cold seep sediments. *Proceedings of the National Academy of Sciences of the United States of America* **99**(11), 7663-7668.

Orphan V. J., Ussler W., Naehr T. H., House C. H., Hinrichs K. U., and Paull C. K. (2004) Geological, geochemical, and microbiological heterogeneity of the seafloor around methane vents in the Eel River Basin, offshore California. *Chemical Geology* **205**(3-4), 265-289.

Petit J. R., Jouzel J., Raynaud D., Barkov N. I., Barnola J. M., Basile I., Bender M., Chappellaz J., Davis M., Delaygue G., Delmotte M., Kotlyakov V. M., Legrand M., Lipenkov V. Y., Lorius C., Pepin L., Ritz C., Saltzman E., and Stievenard M. (1999) Climate and atmospheric history of the past 420,000 years from the Vostok ice core, Antarctica. *Nature* **399**(6735), 429-436.

Pimenov N. V., Rusanov I. I., Poglazova M. N., Mityushina L. L., Sorokin D. Y., Khmelenina V. N., and Trotsenko Y. A. (1997) Bacterial mats on coral-like structures at methane seeps in the Black Sea. *Microbiology* **66**(3), 354-360.

Planke S., Svensen H., Hovland M., Banks D. A., and Jamtveit B. (2003) Mud and fluid migration in active mud volcanoes in Azerbaijan. *Geo-Marine Letters* **23**(3-4), 258-268.

Reeburgh W. S. (1996) "Soft spots" in the global methane budget. In *Microbial Growth on C_1 Compounds* (ed. M. E. Lidstrom and F. R. Tabita), pp. 334-342. Kluwer Academic Publishers.

Schindler T. L. and Kasting J. F. (2000) Synthetic spectra of simulated terrestrial atmospheres containing possible biomarker gases. *Icarus* **145**(1), 262-271.

Schouten S., Wakeham S. G., and Damste J. S. S. (2001) Evidence for anaerobic methane oxidation by archaea in euxinic waters of the Black Sea. *Organic Geochemistry* **32**(10), 1277-1281.

Sibuet M. and Olu K. (1998) Biogeography, biodiversity and fluid dependence of deep-sea cold-seep communities at active and passive margins. *Deep-Sea Research II* **45**(1-3), 517-567.

Smith H. J., Fischer H., Wahlen M., Mastroianni D., and Deck B. (1999) Dual modes of the carbon cycle since the Last Glacial Maximum. *Nature* **400**(6741), 248-250.

Somoza L., Diaz-del-Rio V., Leon R., Ivanov M., Fernandez-Puga M. C., Gardner J. M., Hernandez-Molina F. J., Pinheiro L. M., Rodero J., Lobato A., Maestro A., Vazquez J. T., Medialdea T., and Fernandez-Salas L. M. (2003) Seabed morphology and hydrocarbon seepage in the Gulf of Cadiz mud volcano area: Acoustic imagery, multibeam and ultra-high resolution seismic data. *Marine Geology* **195**(1-4), 153-176.

Suess E., Torres M. E., Bohrmann G., Collier R. W., Greinert J., Linke P., Rehder G., Trehu A., Wallmann K., Winckler G., and Zuleger E. (1999) Gas hydrate destabilization: enhanced dewatering, benthic material turnover and large methane plumes at the Cascadia convergent margin. *Earth and Planetary Science Letters* **170**(1-2), 1-15.

Teske A., Hinrichs K. U., Edgcomb V., Gomez A. D., Kysela D., Sylva S. P., Sogin M. L., and Jannasch H. W. (2002) Microbial diversity of hydrothermal sediments in the Guaymas Basin: Evidence for anaerobic methanotrophic communities. *Applied and Environmental Microbiology* **68**(4), 1994-2007.

Treude T. (2003) The anaerobic oxidation of methane in marine sediments, Unversity of Bremen.

Treude T., Boetius A., Knittel K., Wallmann K., and Jorgensen B. B. (2003) Anaerobic oxidation of methane above gas hydrates at Hydrate Ridge, NE Pacific Ocean. *Marine Ecology-Progress Series* **264**, 1-14.

Valentine D. L. and Reeburgh W. S. (2000) New perspectives on anaerobic methane oxidation. *Environmental Microbiology* **2**(5), 477-484.

Wang Z. P., Zeng D., and Patrick W. H. (1997) Characteristics of methane oxidation in a flooded rice soil profile. *Nutrient Cycling in Agroecosystems* **49**(1-3), 97-103.

Whiticar M. J. (1999) Carbon and hydrogen isotope systematics of bacterial formation and oxidation of methane. *Chemical Geology* **161**(1-3), 291-314.

Whiticar M. J. (2002) Diagenetic relationships of methanogenesis, nutrients, acoustic turbidity, pockmarks and freshwater seepages in Eckernforde Bay. *Marine Geology* **182**(1-2), 29-53.

Whiticar M. J. and Werner F. (1981) Pockmarks: Submarine vents of natural gas or freshwater seeps? *Geo-Marine Letters* **1**(3-4), 193-199.

Whittenbury R., Phillips K. C., and Wilkinso.Jf. (1970) Enrichment, Isolation and Some Properties of Methane-Utilizing Bacteria. *Journal of General Microbiology* **61**, 205-&.

Wilson J. T. and Wilson B. H. (1985) Biotransformation of Trichloroethylene in Soil. *Applied and Environmental Microbiology* **49**(1), 242-243.

Woolsey T. S., McCallum M. e., and Schumm S. A. (1975) Modelling of diatreme emplacement by fluidization. *Physics and Chemistry of the Earth* **9**, 24-42.

Wuebbles D. J. and Hayhoe K. (2002) Atmospheric methane and global change. *Earth-Science Reviews* **57**(3-4), 177-210.

Yamamoto S., Alcauskas J. B., and Crozier T. E. (1976) Solubility of Methane in Distilled Water and Seawater. *Journal of Chemical and Engineering Data* **21**(1), 78-80.

Yang S. O., Cho S. H., Lee H., and Lee C. S. (2001) Measurement and prediction of phase equilibria for water plus methane in hydrate forming conditions. *Fluid Phase Equilibria* **185**(1-2), 53-63.

Zuhlsdorff L. and Spiess V. (2004) Three-dimensional seismic characterization of a venting site reveals compelling indications of natural hydraulic fracturing. *Geology* **32**(2), 101-104.

Microbial colonisation of a submarine mud volcano: how subsurface fluid flow structures methanotrophic communities

Niemann H.[1,2], Lösekann T.[1], deBeer D.[1], Elvert M.[1,*], Knittel K.[1], Amann R.[1], Sauter E.[2], Schlüter M.[2], Klages M.[2], Foucher JP.[3], Boetius A.[1,4]

[1]Max Planck Institute for Marine Microbiology Bremen, Celsiusstr.1, 28359 Bremen, Germany

[2]Alfred Wegener Institute for Polar and Marine Research, Am Handelshafen 12, 27515 Bremerhaven, Germany

[3]IFREMER Centre de Brest, BP 70, 29280 Plouzane, France

[4]International University Bremen, Campusring, 28759 Bremen, Germany

[*]Present address: Research Center Ocean Margins, University of Bremen, Leobener Str., 28359 Bremen

Author to whom correspondence should be addressed:

Helge Niemann
Max Planck Institute for Marine Microbiology, Celsiusstr. 1, 28359 Bremen, Germany
email: hniemann@mpi-bremen.de, phone +49-421-2028653

Submarine mud volcanoes are mesoscale seafloor structures caused by episodic eruption of gases, fluids and muds from the deep subsurface. If such mud volcanoes remain active and continue to emit gas to the ocean, cold seep ecosystems may establish to utilize the focused energy source. As a first step, fluid flow impacted sediments are colonized by specialized microbial communities utilizing the rising methane or other hydrocarbons. If anaerobic methanotrophic communities establish, the sulphide production from their anaerobic oxidation of methane with sulphate invites other free-living and symbiotic microbial organisms. The methano- and thiotrophic microbial communities represent the primary producers in cold seep ecosystems, forming fascinatingly rich ocean biotopes. To analyse which factors determine colonisation patterns of chemosynthetic primary producers at cold seeps, we investigated the methane-seeping Håkon Mosby mud volcano (Barents Sea) with high-resolution *in situ* methods. We found a distinct spatial zonation of several novel clades of free-living and symbiotic aerobic and anaerobic methanotrophs. The main selection mechanism determining vertical and horizontal distribution and dominance of different methanotrophic communities were fluid flow rates controlling access to electron acceptors for methane oxidation. The winner in the competition for deep energy delivered via rising fluids appeared to be symbiotic pogonophoran tube worms, which are optimally adapted to exploit the gradient between electron donor and acceptor.

Just as hydrothermal vents, cold seep ecosystems represent highly productive islands of chemoautotrophic life on the vast ocean floor. Both types of chemosynthetic ecosystems were discovered at the end of the 70ies and have ever since fascinated scientists and the public alike for their diverse accumulation of alien symbiotic and extremophilic organisms (Kennicutt et al., 1985; Spiess et al., 1980; Suess et al., 1985). Despite the substantial biogeographical variation, key morphologies of hot vents and cold seeps include dense colonies of microbial mats, tubeworms, bivalves, as well as a variety of mineral and metal precipitates sometimes forming large and distinct structures on the seafloor. Another typical characteristic of these ecosystems is their composition of highly fractured and variable microenvironments in space and time, which makes their quantitative investigation extremely difficult (Boetius and Suess, 2004). It is generally assumed that the main habitat-structuring factor for chemosynthetic microbes and microbe-invertebrate symbioses is the access to electron donors (methane, sulphide, reduced iron, hydrogen) and electron acceptors (oxygen, nitrate, iron, sulphate). Unfortunately, relating temporal and spatial patterns in fluxes of these compounds to the community structure at vents and seeps is still very difficult because of the lack of *in situ* measurements and long term observation. *Ex situ* measurements generally suffer from many uncertainties and artefacts, because retrieved samples are cut off from fluid and gas flow, and because subsequent depressurisation and temperature change during sample recovery kills or impacts most fauna. Here we report for the first time *in situ* biogeochemical analyses of element fluxes in relationship to community patterns at a deep water cold seep system, the highly active arctic Håkon Mosby Mud Volcano (HMMV) on the Barents Sea margin (72°N, 14°44'E; 1250 m water depth). This cold seep is known for its highly gas charged sediments and distinct habitat zonation (Milkov et al., 2004). The HMMV is a circular structure of 1 km diameter and <10 m elevation above bottom (Hjelstuen et al., 1999; Vogt et al., 1997a; Vogt et al., 1991) (Fig. 1). It is fuelled by a deep gas reservoir (-3 km bsf)

expelling fluids, gases and muds to the ocean floor (Fig. 2-1). The fluid upwelling can be detected as rather steep temperature anomaly reaching >20°C at 10 meter sediment depth below the ice-cold bottom waters (-1°C) (Damm and Budeus, 2003; Ginsburg et al., 1999). At single spots in the centre of the mud volcano, the warm fluids reached the seafloor. Furthermore, in the Northern part of the centre emission of free and frozen gas from holes in the seafloor were observed visually, forming a large gas flare above the HMMV (Fig. 2-2)(Damm and Budeus, 2003; Klages et al., 2004; Sauter et al., submitted). A transition from very recent mud-flows to stabilized sediment deposits can be identified visually along radial transects across the circular structure. The apparently barren centre (Fig. 2-3) is enclosed by thiotrophic bacterial mats (Fig. 2-4, -5) followed by large fields of pogonophoran tubeworm

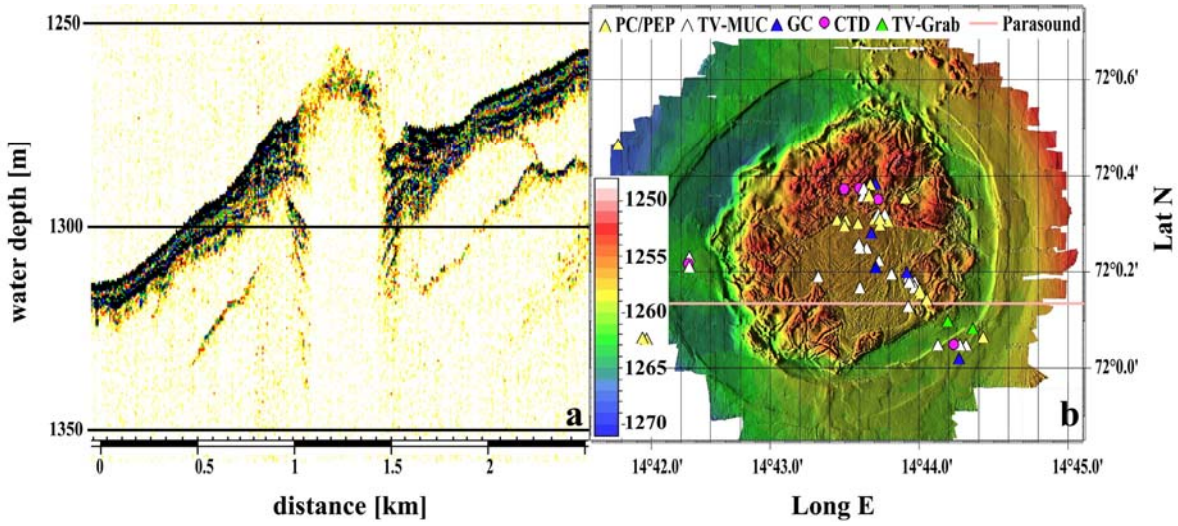

Figure 1. The Håkon Mosby Mud Volcano. The left panel is a PARASOUND sediment echosounder image of a transect through the mud volcano. It displays a 2.5 km long profile crossing the Mud Volcano from south to north. In the centre, almost no signal penetration is due to the high gas content of the sediments leading to a blanking of the signal. North and south of the central part, the signal penetration rises to around 30 m and a stack of sedimentary layers is displayed which is partially formed by sediments emerging as mud flows from the volcano. The right panel is a high resolution bathymetric map of the HMMV showing all sampling stations during the POLARSTERN expedition ARK XIX3b with ROV VICTOR 6000 (Reson SeaBat 8125 and EM2000 with Posidonia positioning). The IFREMER software CARAIBES was used to process the microbathymetry data acquired by the multibeam echosounder mounted on ROV VICTOR.

colonies (Fig. 2-6). The morphology and geology of the HMMV and the composition of its benthic communities were described in detail recently (Milkov et al., 1999; Milkov et al., 2004; Pimenov et al., 1999; Shilov et al., 1999; Vogt et al., 1997a; Vogt et al., 1997b). Observation and sampling took place during two cruises with R/V Atalante/ROV VICTOR 6000 (2001) and R/V Polarstern/ROV VICTOR 6000 (2003) as part of a French/German research initiative (Klages et al., 2002; Klages et al., 2004). Subsurface and surface sediments were collected with gravity corers and ROV pushcores, respectively, along a radial transect from the centre to the east of the mud volcano (Fig. 1). *In situ* microsensor profiles of temperature, oxygen, pH and sulphide were obtained at the same sites via positioning of the instruments with the ROV (Fig. 3).

The central area of the HMMV showed signs of recent mud depositions and gas eruptions like chaotic sediment mounds, furrows, trenches and holes. The most recent mud flow is directed down-slope, towards the South-East. Gravity core samples of the upper 4 m of centre mud consisted of uniformly mixed, greyish highly gassy clays. These contained very low amounts of lipid biomarker (< 0.1 micro gram per gram dry weight, µg g-dw^{-1}) and extremely low cell numbers (<10^7 cells cm^{-3}) typical for deep biosphere sediments from >100 m sediment depth according to the global correlation established by Parkes et al. (2000). Archaeal 16S rDNA clone sequences indicate a dominance of *Crenarchaeota* (67 of 67 clones) which were previously detected in deep biosphere sediments(Knittel et al., 2005). No euryarchaeotal or ∂-proteobacterial (sulphate reducer) sequences were retrieved from the central muds, and rates of anaerobic oxidation of methane (AOM) and sulphate reduction (SR) were at detection limit. Sediments from the surface of the seafloor were retrieved by push coring with the ROV and were dominated by sequences of aerobic methanotrophic bacteria. Fluorescence *in situ* hybridisation (FISH) of these samples revealed that a population of *Methylobacter* sp., a

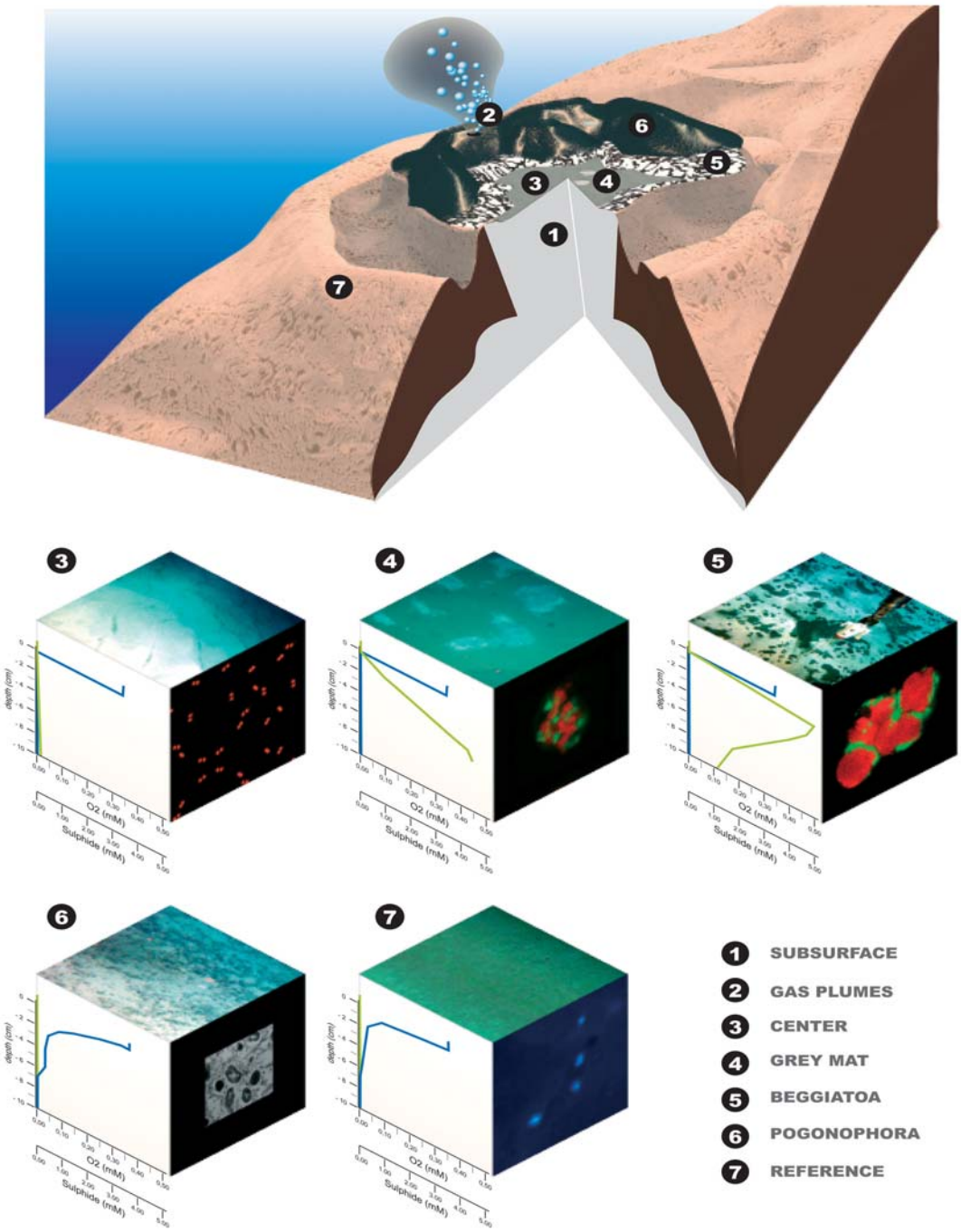

Figure 2. A schematic diagram of the different microbial habitats at HMMV. (1) Subsurface muds rising from a deep reservoir; (2) Gas and fluid channels in the northern region of the volcano where free methane gas immediately forms gas hydrate flakes in the water column. The squares (3-7) show underwater-photographies of the seafloor on the top panel, idealized concentration gradients of oxygen and sulphide on the left panel and the dominating microbial organisms on the right panel. (3) Central sediments colonised by aerobic methanotrophic bacteria (type I affiliated to *Methylobacter* sp.); (4) Patches of reduced sediments covered by a grey biofilm harbouring diverse methano- and thiotrophic communities; (5) *Beggiatoa* mats covering sediments dominated by an ANME-3/DBB population; (6) Colonies of *Pogonophora* tubeworms harbouring symbiotic MOx bacteria, above a subsurface AOM horizon >60 cm bsf; (7) a reference station at the flank of the volcano (1270 m water depth).

type I methanotroph, accounted for 46% of all DAPI stained cells in the top 5 mm ($26^{*}10^{8}$ cells cm^{-3}, Fig. 3a3). The second most abundant bacterial group populating the surface of the centre is affiliated with methylotrophic *Methylophaga* species. Accordingly, ^{13}C-depleted FA were the most abundant biomarker fraction with a dominance of the type I methanotroph specific FA C16:1ω8c in the top surface cm (Fig. 2a4). Aerobic oxidation of methane (MOx) measured *ex situ* (at ca 1.5 mM methane concentration) was 0.1 µmol cm^{-3} d^{-1} (Fig. 3a2), i.e. 0.9 mol m^{-2} yr^{-1}. The diffusive O_2 influx in this area was 3.8 mol m^{-2} yr^{-1} as calculated from *in situ* microsensor profiles (Fig. 3a1) (de Beer et al., submitted). The microsensor profiles showed a depletion of oxygen within the first few millimetres of the gassy centre muds. The limited penetration of oxygen explains why MOx as well as the methane-oxidizing bacteria are restricted to the top surface sediment. *In situ* oxygen penetration at a nearby reference site outside of the mud volcano (Fig. 2-7, 50 km East of the centre) was >3 cm, indicating that processes connected to fluid flow are responsible for oxygen limitation. First, methane consumption reduces oxygen rapidly. Secondly, the relatively high velocity of upward flow of oxygen-free fluids hinder oxygen diffusion from the bottom water into the sediments (de Beer et al., submitted). The difference between in- and *ex situ* O_2 profiles at the same sampling site indicate a flow velocity of approximately 0.4 µm s^{-1}, equivalent to 13 m yr^{-1} which is among the high end of fluid flow velocities measured in cold seep settings (Wallmann et al., 1997). At this flow velocity, neither oxygen, nor other electron acceptors such as nitrate and sulphate (Fig. 3a2) can penetrate into the sediment via diffusion according to an integrated local mass balance.

The chemistry of the porewater in the centre indicates a depletion of sulphate (<0.5 mM) in the rising fluids as well as an anomaly in the chloride concentration (415 mM at 18 cm sediment depth compared to the seawater concentration of 610 mM). The lack of sulphate

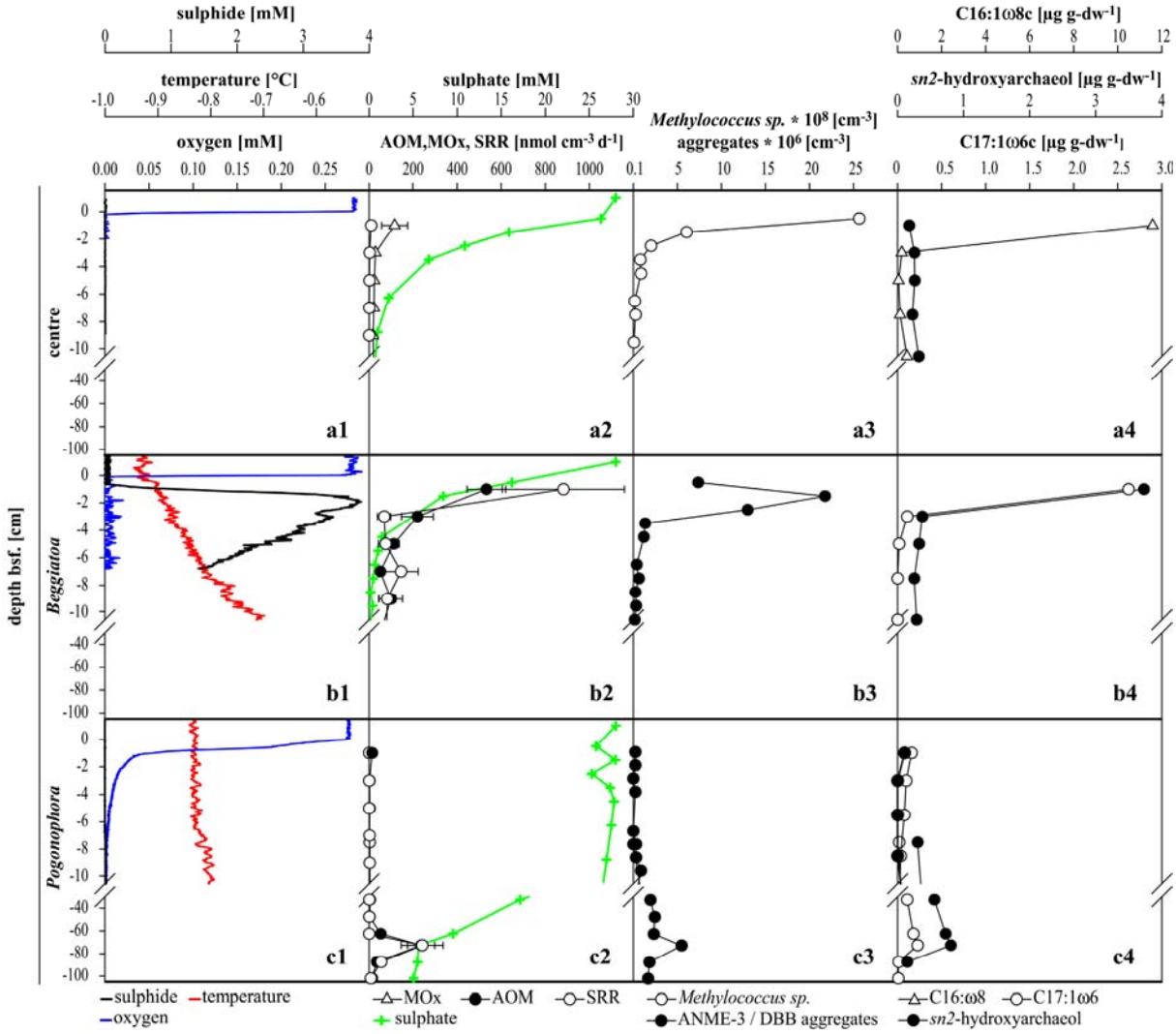

Figure 3. Vertical profiles of oxygen, sulphide and temperature (a1-c1); sulphate, *ex situ* methane and sulphate turnover (a2-c2), bacteria and aggregate counts (a3-c3) and selected lipid biomarker (a4-c4) from the centre (a), *Beggiatoa*-covered sediments (b) and the *Pogonophora* field (c). Oxygen, sulphide and temperature were measured *in situ* with microsensors mounted on a deep-sea profiling unit. AOM, SR, sulphate, cell and aggregate counts as well as lipid biomarker contents were determined *ex situ* from sediments recovered by ROV push coring.

throughout the upper 4 m of sediment in the centre explains the absence of anaerobic methanotrophs despite the high methane availability. No sulphide production from the anaerobic oxidation of methane (AOM) with sulphate was measured in the centre (Fig. 3a1) and only minor amounts of ^{13}C-depleted archaeal lipids (Fig. 3a4) were found in the centre muds. Using specific FISH probes for Archaea and Bacteria as well as for anaerobic

methanotrophs (AMNE) (Knittel et al., 2005), we did not find any positive signals of ANME-related archaea or archaeal-bacterial consortia in the centre muds (0-25 cm sediment depth).

Close to gas ebullition sites (Fig. 2-2) and in the transition from the inner center to the periphery of the mud flows (Fig. 2-3), circular patches of reduced, gassy sediments of 10-100 cm diameter were found, covered by a greyish-whitish biofilm (Fig 2-4,). *In situ* microsensor profiles showed a sulphide production zone below 2 cm sediment depth and an overlap of oxygen and sulphide in the surface sediments. Modelling of the *ex situ* sulphide profiles indicated diffusive sulphide fluxes of up to 2.4 mol m^{-2} yr^{-1} (data points of *in situ* profiles were too scattered to allow for modelling). AOM rates were rather variable between replicate push core samples, ranging from 0,1 to 0,55 µmol cm^{-3} d^{-1} (12.4 mol m^{-2} yr^{-1} on average) accounting for 85% of sulphate reduction. Archaeal lipids typical for ANME communities were retrieved reaching concentrations of 1.2 µg cm^{-3}. These were strongly depleted in ^{13}C (-99 ‰ for *sn2*-hydroxyarchaeol, -117‰ for pentamethylicosene with four double bonds (PMI:4), -97‰ for crocetene with two double bonds). Microscopy of FISH-targeted cells showed the presence of members of two distinct phylogenetic clusters of ANME, namely ANME-2 and a novel phylogenetic group. The greyish-whitish biofilm covering the sediments harbour a considerable diversity of giant sulphide oxidizing bacteria, including various types of filamentous bacteria and globular giant cells, which morphologically resemble *Thiomargarita* (de Beer et al., submitted). The high rate of AOM-based sulphide production within these patches supports the growth of thiotrophic bacterial mats at the sediment surface (Fig. 1-4). It remains unknown which geological processes cause the formation of these fragmented habitats for AOM communities in the centre of the HMMV. Taking the slow growth rate of the AOM populations into account (Girguis et al., 2003;

Nauhaus et al., 2002; Nauhaus et al., 2005), a relatively stable supply of methane and sulphate is available at these sites.

The most striking transition in microbial habitats occurs from the central mudflows to the more stabilized seabed about 250 m away from the geographical centre of HMMV. An area of highly sulphidic sediments covered to 40-80 % by white bacterial mats, encloses the mud volcano (Fig. 2-5). The white mats consist of a population of filamentous *Beggiatoa* with a cell diameter of 10 µm. *In situ* microsensor profiles indicate a high sulphide production, reaching its maximum directly beneath the seafloor (Fig. 2b1). Total sulphide production was calculated from the *in situ* microsensor profiles with 8 mol m^{-2} y^{-1}. Integrated AOM and SRR rates (Fig. 2b2) were equivalent to 5.5 mol m^{-2} $yr^{-1}$of methane consumption and sulphide production, respectively, at ca 1.5 mM methane and 5 mM sulphate concentration. The active methanotrophic zone in the Beggiatoa covered sediments was restricted to a distinct zone of ca. 3 cm below the seafloor. Within this horizon, the high-resolution profiles of sulphide concentration (Fig. 3b1) and aggregate counts (Fig. 3b3) showed a distinct peak at 1.5 cm sediment depth, coinciding with the maximum in AOM and SR rates (Fig. 3b2) as well as archaeal and bacterial lipid concentrations (Fig. 3b4). The concentration of the AOM biomass and activity within this narrow zone is likely a consequence of the optimal positioning between the maximal upward flux in methane and the maximal downward flux in sulphate, by diffusion and possibly also by transport with the gliding *Beggiatoa* filaments. 16S rDNA, FISH, and lipid biomarker analysis revealed that AOM is mediated in this zone by a novel cluster of archaea, most closely related to *Methanosarcinaceae,* but forming a distinct phylogenetic branch (ANME-3). Similar sequences were previously retrieved from other cold seeps like the Eel River Basin and Hydrate Ridge (Knittel et al., 2005; Orphan et al., 2001). However, this is the first finding of a habitat dominated by this phylogenetic group. The

average number of ANME-3 aggregates at 1.5 cm was $22*10^6$ aggregates cm^{-3} (Fig. 3b3). The lipid pattern of ANME-3 is dominated by the diethers *sn2*-hydroxyarchaeol and archaeol followed by PMI:5 and PMI:4 all of which are strongly depleted in ^{13}C with values <-98‰ in the surface horizon. No PMIs with higher degrees of saturation or crocetane could be detected which is in contrast to biomarker patterns of ANME-1 and ANME-2 communities (Blumenberg et al., 2004; Elvert et al., 1999; Hinrichs et al., 1999; Michaelis et al., 2002). The ANME-3 population at HMMV forms dense shell-type aggregates with a novel type of SRB partner, phylogenetically different from those usually associated with AOM (Fig. 2-5) (Knittel et al., 2005). 16S rDNA sequence analyses and FISH with targeted probes showed that the SRB partner in the HMMV ANME-3 consortia is closely related to *Desulfobulbus* sp. (DBB). Accordingly, the most depleted bacterial FAs (-70‰) found below *Beggiatoa* mats are C16:1ω5c and C17:1ω6c both of which have been described from isolates of this bacterium. The ANME-3/DBB population clearly dominated microbial biomass in the sediments around the centre of HMMV. However, similar to the MOx populations dominating the centre surface sediments, they were limited in their downward extension in the seafloor, despite the high availability of methane. This can be explained with the lack of the AOM electron acceptor sulphate in subsurface sediments. Compared to the centre, the penetration of sulphate via diffusion from bottom water reaches a few cm deeper, due to the reduced velocity of upward fluid flow of ca. 0.1 μm s^{-1} (4 m yr^{-1}) according to de Beer et al. (submitted). The authors used *in situ* oxygen and sulphide gradients to calculate fluid flow and diffusion depth, showing that the maximum availability of sulphate is found between 0-3 cm sediment depth at this site, matching exactly the peak in AOM and ANME-3 biomass.

The next major transition in HMMV habitats occurs about 400m from its geographical centre, where the sulphide oxidizer mats are completely replaced by dense tubeworm colonies

stretching over hundreds of square meters around the HMMV (Fig. 2-6). Gravity cores from *Pogonophora* fields showed the presence of cm-thick layers of gas hydrate below 100 cm sediment depth. As a prerequisite for gas hydrate formation in these sediments, this indicates the absence of a strong geothermal gradient, i.e. low fluid flow rates. Two Pogonophoran species, *Oligobrachia haakonmosbiensis* and *Sclerolinum contortum* (Smirnov, 2000) populate this area of the HMMV with biomasses of ca 2 kg m^{-2} wet weight. *Oligobrachia,* an extremely long, thin tubeworm (ca 60 cm body length, 3 mm diameter) harbours MOx bacteria in its trophosome, which provide the worm's main carbon source as indicated by similar $\delta^{13}C$ values (-70 ‰) of worm- and bacteria-derived lipids. A comparison of *in situ* microsensor profiles in the tubeworm field and a nearby reference site shows that the tubeworms actively pump oxygen and sulphate into the sediments (Fig. 2-6, -7; 3c1, 3c2). Likely, the presence of oxygen in surface sediments displaces the anaerobic AOM communities to deeper anoxic layers. Elevated AOM rates (Fig. 3c2) were found just at the base of the worm tubes (-70 cm bsf) and match a subsurface peak of ANME-3 aggregates and specific archaeal lipid concentrations (Fig. 3c3-4). Here, sulphate concentrations reach 5 mM (Fig. 3c2), whereas both the centre and the Beggiatoa mat habitats are almost sulphate-free at these sediment depths. Unfortunately we were not able to measure methane oxidation by the tubeworm colonies, as the worms were not retrieved alive. The areal AOM and SR of free-living methanotrophs was 0.2 mol m^{-2} yr^{-1} in the upper 20 cm sediment depth and 7.1 mol m^{-2} yr^{-1} including the deep AOM zone. *In situ* oxygen consumption calculated from microsensor profiles (excluding worm respiration) in this zone was estimated with 0.7 mol m^{-2} yr^{-1}. In comparison, at the reference site, which was not impacted by fluid flow and did not contain methane in the top meter of sediments, oxygen consumption driven by marine organic matter diagenesis was ca. 0.3 mol m^{-2} yr^{-1}.

In conclusion, methane is the main energy source in all different habitat zones of HMMV and its availability clearly selects for methanotrophic organisms. Depending on the fluid flow velocity and hence access to electron acceptors, populations of free-living aerobic or anaerobic methanotrophs or methanotrophic bacteria-worm symbioses dominated the total microbial biomass in the habitat (reaching >60% of total microbial biomass in all zones). At the centre of the mud volcano, the high fluid flow rates formed a barrier against the diffusion of electron acceptors into the gassy sediments, selecting for aerobic methanotrophs in the top surface layer (<5 mm). In this zone of active mud volcanism, the repeated mixing of sediments may also favour the faster growing aerobic methanotrophs over the slow growing anaerobic methanotrophs (doubling time >>3 month; Nauhaus et al., 2005). Sulphate concentrations in seawater are two orders of magnitude higher than oxygen. Nevertheless, the replenishment of sulphate via diffusion from the bottom water is a very slow process. The vertical expansion of anaerobic methanotrophs in the Beggiatoa covered sediments was limited to the top 3-5 cm of surface sediments at the relatively high flow rates still present in this area of the HMMV. Regarding vertical (60 cm) and lateral (area of 0.4 km^2 compared to 0.2 km^2 in Beggiatoa and centre sediments, respectively) expansion as well as total biomass, the symbiotic association of methanotrophs with *Pogonophoran* tubeworms appears to be the winner at HMMV. The advantage of methanotrophic microbe-invertebrate symbioses of cold seep ecosystems is the increased access to both electron donor as well as acceptor provided by adaptations in the internal circulatory system as well as by motility (bivalves such as *Acharax*, *Calyptogena* and *Bathymodiolus*) (Cordes et al., 2005; Sahling et al., 2002; Treude et al., 2003) or body shape (tube worms). This first *in situ* investigation of an active mud volcano shows that the efficiency of the microbial filter against the greenhouse gas methane is controlled by fluid flow, which may inhibit the complete breakdown of the gas at high velocities, hence exerting a negative feedback mechanism. Quantitative *in situ* measurements

of gas fluxes and fluid flow are necessary to constrain the relevance of greenhouse gas emission from these and other fluid-flow impacted geosystems.

METHODS

Sulphate Reduction and Methane Oxidation Rates

Microbial rates of methane oxidation and sulphate reduction in sediments were determined *ex situ* from the turnover of radio labelled $^{14}CH_4$ and $^{35}SO_4^{2-}$ tracers as described previously(Treude et al., 2003). Directly after retrieval, gravity cores were sliced open and sediment subsamples were transferred into 6 ml glass tubes, sealed with butyl rubber stoppers and transferred to a cold room (2 °C) where $^{35}SO_4^{2-}$ and $^{14}CH_4$ was injected. ROV push cores were processed as described previously (Treude et al., 2003). Glass tubes and cores were incubated for 24h at *in situ* temperature before the reaction was stopped by mixing the sediment with respectively 20% $ZnCl_2$ and 5% NaOH solution. Separation of radioactive species and rate calculations were performed as described previously (Boetius et al., 2000; Michaelis et al., 2002; Treude et al., 2003). Aerobic and anaerobic methane oxidation was distinguished according to the presence or absence of oxygen during the tracer incubations.

Lipid Analysis

Lipid biomarker were extracted from frozen sediment samples and *Pogonophora sp.* tissue by successive sonication in solvent mixtures of decreasing polarity and derivated as described previously (Elvert et al., 2003; Michaelis et al., 2002) before injection onto a 50 m HP5 fused silica capillary column (0.32 mm i.d., 0.17 µm film thickness). Chromatographic conditions

for lipid analysis were the same as described previously (Elvert et al., 2003) with slight modifications of the temperature gradient for the analysis of the neutral fraction. Column temperature was programmed from 60 to 150 °C at a rate of 10 °C min^{-1} and then at a rate of 4 °C min^{-1} to 310 °C (45 min isothermal). Compounds were identified on a Finnigan Trace MS. Stable carbon isotope composition of single compounds were determined with a Finnigan Delta Plus isotope mass spectrometer. Reported $\delta^{13}C$-values are corrected for the introduction of additional carbon atoms during derivatisation. $\delta^{13}C$-values have an analytical error of ±1‰

Fluorescence *In Situ* Hybridisation

Cells of *Methylobacter sp.* and ANME-3/DBB aggregates were quantified by fluorescence *in situ* hybridization with horseradish peroxidase (HRP)-labelled oligonucleotide probes and tyramide signal amplification (CARD-FISH) according to previously described methods (Pernthaler et al., 2002). New oligonucleotide probes used in this study were MetI-444 (*Methylobacter* sp.; 5'-CCTGCCTGTTTTCCTCCC-3'), probe 660 (*Desulfobulbus* sp.; 5'-GAATTCCACTTTCCCCTCTG-3') and ANME3-1249 (ANME-3 archaea; 5'-TCGGAGTAGGGACCCATT-3'), purchased from biomers.net GmbH, Ulm, Germany. Sediments were treated prior to FISH staining as described previously (Boetius et al., 2000; Snaidr et al., 1997)**.**

Sulphate and Sulphide Concentrations

Sulphate concentrations were determined from 5ml sediment fixed in 50 ml corning vials with 25 ml zinc acetate solution (20%, w/v). An aliquot of the supernatant was injected into a Waters HPLC system (Waters 512 HPLC pump, I.C.-Pak anion-column (Waters; WAT007355) 4.6 x 50 mm, Waters 730 conductivity detector). Isophtalic acid (1mM) was used as a solvent at a constant flow rate of 1ml min^{-1}. Sulphate concentrations were corrected for porosity which was determined according to a previously described method (Treude et al., 2003). Total sulphide concentrations were determined *in situ* using microsensors for H_2S and pH measurements mounted to a free falling lander system or directly deployed by the ROV.

Microsensor Measurements

Microsensors for Oxygen, H_2S and pH were manufactured and used as described previously (de Beer et al., 2005). Tip diameters were ca. 20 µm and the response time (t_{90}) <3 sec. The temperature sensor (Pt100, UST Umweltsensortechnik GmbH, Thüringen, Germany) had a tip diameter of 3 mm and a response time of ca. 5 sec. The sensors were calibrated after mounting on a deep sea profiling unit as described previously (Wenzhofer and Glud, 2002). Total sulphide concentrations were calculated from H_2S and pH. The profiler was pre-programmed to measure profiles with a spatial resolution of 0.025 cm. The effect of pore water upflow on the sulphate concentration profile was estimated from the local mass balance v*C=D*dC/dx. Integrated over depth $C_x = C_0 \, e^{-\frac{v}{D}}$ where C_x is the sulphate concentration at depth x, C_0 the surface sulphate concentration, D the diffusion coefficient for sulphate in the sediment ($Dsed_{,sulfate}$= 0.18e-9 m^2s^{-1}).

References

Blumenberg M., Seifert R., Reitner J., Pape T., and Michaelis W. (2004) Membrane lipid patterns typify distinct anaerobic methanotrophic consortia. *Proceedings of the National Academy of Sciences of the United States of America* **101**(30).

Boetius A., Ravenschlag K., Schubert C., Rickert D., Widdel F., Gieseke A., Amann R., Jørgensen B. B., Witte U., and Pfannkuche O. (2000) A marine microbial consortium apparently mediating anaerobic methane of oxidation. *Nature* **407**, 623-626.

Boetius A. and Suess E. (2004) Hydrate Ridge: a natural laboratory for the study of microbial life fueled by methane from near-surface gas hydrates. *Chemical Geology* **205**(3-4), 291-310.

Cordes E. E., Arthur M. A., Shea K., Arvidson R. S., and Fisher C. R. (2005) Modeling the mutualistic interactions between tubeworms and microbial consortia. *Plos Biology* **3**(3), 497-506.

Damm E. and Budeus G. (2003) Fate of vent-derived methane in seawater above the Hakon Mosby mud volcano (Norwegian Sea). *Marine Chemistry* **82**(1-2), 1-11.

de Beer D., Sauter E., Niemann H., Witte U., and Boetius A. (submitted) In situ fluxes and zonation of microbial activity in surface sediments of the Håkon Mosby Mud Volcano. *Limnology and Oceanography*.

de Beer D., Wenzhofer F., Ferdelman T. G., Boehme S. E., Huettel M., van Beusekom J. E. E., Bottcher M. E., Musat N., and Dubilier N. (2005) Transport and mineralization rates in North Sea sandy intertidal sediments, Sylt-Romo Basin, Wadden Sea. *Limnology and Oceanography* **50**(1), 113-127.

Elvert M., Boetius A., Knittel K., and Jorgensen B. B. (2003) Characterization of specific membrane fatty acids as chemotaxonomic markers for sulfate-reducing bacteria involved in anaerobic oxidation of methane. *Geomicrobiology Journal* **20**(4), 403-419.

Elvert M., Suess E., and Whiticar M. J. (1999) Anaerobic methane oxidation associated with marine gas hydrates: superlight C-isotopes from saturated and unsaturated C_{20} and C_{25} irregular isoprenoids. *Naturwissenschaften* **86**(6), 295-300.

Ginsburg G. D., Milkov A. V., Soloviev V. A., Egorov A. V., Cherkashev G. A., Vogt P. R., Crane K., Lorenson T. D., and Khutorskoy M. D. (1999) Gas hydrate accumulation at the Hakon Mosby Mud Volcano. *Geo-Marine Letters* **19**(1-2), 57-67.

Girguis P. R., Orphan V. J., Hallam S. J., and DeLong E. F. (2003) Growth and methane oxidation rates of anaerobic methanotrophic archaea in a continuous-flow bioreactor. *Applied and Environmental Microbiology* **69**(9), 5472-5482.

Hinrichs K.-U., Hayes J. M., Sylva S. P., Brewer P. G., and DeLong E. F. (1999) Methane-consuming archaebacteria in marine sediments. *Nature* **398**, 802-805.

Hjelstuen B. O., Eldholm O., Faleide J. I., and Vogt P. R. (1999) Regional setting of Hakon Mosby Mud Volcano, SW Barents Sea margin. *Geo-Marine Letters* **19**(1-2), 22-28.

Kennicutt M. C., Brooks J. M., Bidigare R. R., Fay R. R., Wade T. L., and MacDonald T. J. (1985) Vent-type taxa in a hydrocarbon seep region on the Louisiana slope. *Nature* **317**, 351-353.

Klages M., Mesnil B., Soldtwedel T., and Christophe A. (2002) L' expédition "AWI" sur NO L'Atalante en 2001. [The Expedition "AWI" on RV L'Atalante in 2001]. Alfred-Wegener-Institute for Polar and Marine Research.

Klages M., Thiede J., and Foucher J. P. (2004) The Expedition ARKTIS XIX/3 of the Research Vessel POLARSTERN in 2003 Reports of legs 3a, 3b and 3c, pp. 355. Alfred-Wegener-Institute for Polar and Marine Research.

Knittel K., Losekann T., Boetius A., Kort R., and Amann R. (2005) Diversity and distribution of methanotrophic archaea at cold seeps. *Applied and Environmental Microbiology* **71**(1), 467-479.

Michaelis W., Seifert R., Nauhaus K., Treude T., Thiel V., Blumenberg M., Knittel K., Gieseke A., Peterknecht K., Pape T., Boetius A., Amann R., Jorgensen B. B., Widdel F., Peckmann J. R., Pimenov N. V., and Gulin M. B. (2002) Microbial reefs in the Black Sea fueled by anaerobic oxidation of methane. *Science* **297**(5583), 1013-1015.

Milkov A., Vogt P., Cherkashev G., Ginsburg G., Chernova N., and Andriashev A. (1999) Sea-floor terrains of Hakon Mosby Mud Volcano as surveyed by deep-tow video and still photography. *Geo-Marine Letters* **19**(1-2), 38-47.

Milkov A. V., Vogt P. R., Crane K., Lein A. Y., Sassen R., and Cherkashev G. A. (2004) Geological, geochemical, and microbial processes at the hydrate-bearing Hakon Mosby mud volcano: a review. *Chemical Geology* **205**(3-4), 347-366.

Nauhaus K., Boetius A., Kruger M., and Widdel F. (2002) In vitro demonstration of anaerobic oxidation of methane coupled to sulphate reduction in sediment from a marine gas hydrate area. *Environmental Microbiology* **4**(5), 296-305.

Nauhaus K., Treude T., Boetius A., and Kruger M. (2005) Environmental regulation of the anaerobic oxidation of methane: a comparison of ANME-I and ANME-II communities. *Environmental Microbiology* **7**(1), 98-106.

Orphan V. J., Hinrichs K. U., Ussler W., Paull C. K., Taylor L. T., Sylva S. P., Hayes J. M., and Delong E. F. (2001) Comparative analysis of methane-oxidizing archaea and sulfate- reducing bacteria in anoxic marine sediments. *Applied and Environmental Microbiology* **67**(4), 1922-1934.

Parkes R. J., Cragg B. A., and Wellsbury P. (2000) Recent studies on bacterial populations and processes in subseafloor sediments: A review. *Hydrogeology Journal* **8**(1), 11-28.

Pernthaler A., Preston C. M., Pernthaler J., DeLong E. F., and Amann R. (2002) Comparison of fluorescently labeled oligonucleotide and polynucleotide probes for the detection of pelagic marine bacteria and archaea. *Applied and Environmental Microbiology* **68**(2), 661-667.

Pimenov N., Savvichev A., Rusanov I., Lein A., Egorov A., Gebruk A., Moskalev L., and Vogt P. (1999) Microbial processes of carbon cycle as the base of food chain of Håkon Mosby mud volcano benthic community. *Geo-Marine Letters* **19**, 89-96.

Sahling H., Rickert D., Lee R. W., Linke P., and Suess E. (2002) Macrofaunal community structure and sulfide flux at gas hydrate deposits from the Cascadia convergent margin, NE Pacific. *Marine Ecology-Progress Series* **231**, 121-138.

Sauter E., Muyakshin J., Charlou J., Schlüter M., Boetius A., Jerosch K., Damm E., Foucher J. P., and Klages M. (submitted) Methane discharge from a deep-sea submarine mud volcano into the upper water column by gas hydrate-coated methane bubbles. *Earth and Planetary Science Letters*.

Shilov V. V., Druzhinina N. I., Vasilenko L. V., and Krupskaya V. V. (1999) Stratigraphy of sediments from the Hakon Mosby Mud Volcano Area. *Geo-Marine Letters* **19**(1-2), 48-56.

Smirnov R. V. (2000) Two new species of Pogonophora from the arctic mud volcano off northwestern Norway. *Sarsia* **85**(2), 141-150.

Snaidr J., Amann R., Huber I., Ludwig W., and Schleifer K. H. (1997) Phylogenetic analysis and in situ identification of bacteria in activated sludge. *Applied and Environmental Microbiology* **63**(7), 2884-2896.

Spiess F. N., Macdonald K. C., Atwater T., Ballard R., Carranza A., Cordoba D., Cox C., Diazgarcia V. M., Francheteau J., Guerrero J., Hawkins J., Haymon R., Hessler R., Juteau T., Kastner M., Larson R., Luyendyk B., Macdougall J. D., Miller S., Normark

W., Orcutt J., and Rangin C. (1980) East Pacific Rise - Hot Springs and Geophysical Experiments. *Science* **207**(4438), 1421-1433.

Suess E., Carson B., Ritger S. D., Moore J. C., Jones M. L., Kulm L. D., and Cochrane G. R. (1985) Biological communities at vent sites along the subduction zone off Oregon. *Biological Society of the Washington Bulletin* **6**, 475-484.

Treude T., Boetius A., Knittel K., Wallmann K., and Jorgensen B. B. (2003) Anaerobic oxidation of methane above gas hydrates at Hydrate Ridge, NE Pacific Ocean. *Marine Ecology-Progress Series* **264**, 1-14.

Vogt P. R., Cherkashev A., Ginsburg G. D., Ivanov G. I., Crane K., Lein A. Y., Sundvor E., Pimenov N. V., and Egorov A. (1997a) Haakon Mosby mud volcano: A warm methane seep with seafloor hydrates and chemosynthesis-based Ecosystem in late Quantemary Slide Valley, Bear Island Fan, Barents Sea passive margin. *EOS Transactions of the American Geophysical Union Supplement* **78**(17), 187-189.

Vogt P. R., Cherkashev G., Ginsburg G., Ivanov G. I., Milkov A., Crane K., Lein A., Sundvor E., Pimenov N. V., and Egorov A. (1997b) Haakon Mosby Mud Volcano Provides Unusual Example of Venting. *EOS Transactions of the American Geophysical Union Supplement* **78**(48), 549, 556-557.

Vogt P. R., Crane K., Pfirman S., Sundvor E., Cherkis N., Fleming H., Nishimura C., and Shor A. (1991) SeaMARC II sidescan sonar imagery and swath bathymetry in the Nordic Basin. *EOS* **72**(486).

Wallmann K., Linke P., Suess E., Bohrmann G., Sahling H., Schlüter M., Dählmann A., Lammers S., Greinert J., and von Mirbach N. (1997) Quantifying fluid flow, solute mixing, and biogeochemical turnover at cold vents of the eastern Aleutian subduction zone. *Geochimica et Cosmochimica Acta* **61**(24), 5209-5219.

Wenzhofer F. and Glud R. N. (2002) Benthic carbon mineralization in the Atlantic: a synthesis based on in situ data from the last decade. *Deep-Sea Research Part I-Oceanographic Research Papers* **49**(7), 1255-1279.

Lipid signatures and distribution of methanotrophic microbial communities at Håkon Mosby Mud Volcano, Barents Sea

Helge Niemann[1,2], Marcus Elvert[1,*], Tina Lösekann[1], Jakob Jakob[1], Thierry Nadalig[3,#], Antje Boetius[1,2]

[1]Max Planck Institute for Marine Microbiology Bremen, Celsiusstr.1, 28359 Bremen, Germany

[2]Alfred Wegener Institute for Polar and Marine Research, Am Handelshafen 12, 27515 Bremerhaven, Germany

[3]IFREMER Centre de Brest, BP 70, 29280 Plouzane, France

[*]Present address: Research Center Ocean Margins, University of Bremen, Loebener Str., 28359 Bremen

#Present address: Dynamique, Evolution, et Expression des Genomes de Microorganismes, FRE 2326 Université Louis Pasteur, 67083 Strasbourg, France

Author to whom correspondence should be addressed:

Helge Niemann
Max Planck Institute for Marine Microbiology, Celsiusstr. 1, 28359 Bremen, Germany
email: hniemann@mpi-bremen.de, phone +49-421-2028653

ABSTRACT

The Håkon Mosby Mud Volcano (HMMV) is an active methane seeping mud volcano at 1250 m water depth on the Norwegian margin of the Barents Sea. Sediment samples from three distinct zones of the mud volcano (central crater, grey microbial mats and *Beggiatoa* fields) were investigated for archaeal and bacterial lipid signatures and their associated $\delta^{13}C$-values. Measurements obtained in 2 cm sections over a vertical profile down to 20 cm sediment depth revealed a distinct horizontal and vertical distribution of aerobic and anaerobic methanotrophic guilds. In the central area, aerobic methanotrophy (MOx) is the primary biomass-generating process. Here, the predominant bacterial fatty acids $C_{16:1\omega8}$ and $C_{16:2}$ with $\delta^{13}C$ values <-80‰ belong to a type I methanotroph. This MOx horizon is restricted to the sediment surface. Below, only traces of anaerobic methanotrophs are present, indicated by low amounts of the ^{13}C-depleted, archaeal lipids archaeol and *sn2*-hydroxyarchaeol. In patches of reduced sediment, covered by greyish, thiotrophic microbial mats at the boundary of the centre, a four-fold increase in archaeal lipids specific for anaerobic methanotrophs was observed. It was accompanied by a strong depletion in ^{13}C with values down to -118‰, giving evidence of active microbial communities, which mediate anaerobic oxidation of methane (AOM) in the upper 20 cm of the sediment. Further away from the centre, in the zone covered by *Beggiatoa* mats, anaerobic methanotrophy appeared to be the predominant biomass generating process in the surface sediments. Consortia of methanotrophic archaea and sulphate reducing bacteria were most abundant down to 4 cm sediment depth as indicated by sharp, vertical gradients of archaeal and bacterial lipids with $\delta^{13}C$-values down to -109‰. These gradients correlated with a surface peak of $22*10^6$ microbial aggregates cm^{-3}. Diagnostic, archaeal lipids found in the uppermost sediment horizon were dominated by *sn2*-hydroxyarchaeol and pentamethylicosane (PMI) with 5 double bounds followed by archaeol and PMI:4. Diagnostic bacterial fatty acids were dominated by $C_{16:1\omega5}$ followed by ai-$C_{15:0}$, i-

$C_{15:0}$ and $C_{17:1\omega6}$. A combination of molecular techniques (DAPI, FISH, 16S rDNA clone libraries) and biomarker fingerprints of ^{13}C-depleted archaeal and bacterial lipids provide evidence that the AOM community was dominated by a novel cluster of methanotrophic archaea (termed ANME-3) and sulphate reducing bacteria (SRB) of the *Desulfobulbus* cluster. HMMV can be considered as a natural laboratory where different types of methanotrophic communities are selected by the geological and hydrodynamical structure of the mud volcano.

1. INTRODUCTION

Methane is an aggressive greenhouse gas with a 21 to 56 fold higher global warming potential than carbon dioxide (Manne and Richels, 2001). The atmospheric concentration of methane has reached 1740 ppb and is further increasing, most probably contributing to global climate change (Wuebbles and Hayhoe, 2002). High amounts of methane are temporarily stored at continental margins as free gas, dissolved or as solid clathrate. Increasing research effort has therefore been dedicated to elucidate sources and sinks of methane. Actively gas-emitting mud volcanoes have been recognized as an important natural source of methane and were reported from terrestrial and oceanic settings (Dimitrov, 2002; Dimitrov, 2003; Judd et al., 2002; Kopf et al., 2001). Mud volcanism is caused by various geological processes, such as tectonic accretion and faulting, rapid burial of sediments, slope failures or fluid emissions from mineral dehydration. These processes can lead to an abnormally high pore fluid pressure and the extrusion of mud and fluids through a central conduit to the sea floor, which is often accompanied by the expulsion of methane and higher hydrocarbons (Charlou et al., 2003; Kopf, 2002; Milkov, 2000; Somoza et al., 2003). Methane from mud volcanoes can be of thermogenic and/or microbial origin, depending on the oceanographic and tectonic setting. The shape of these structures is diverse, ranging from amorphous mud pies to conical structures and from a few meters to kilometres in size. While there is a reliable number of ~900 known terrestrial mud volcanoes, estimates for deep water mud volcanoes, mainly situated along the continental margins, range between 800 and 100000 (Dimitrov, 2002; Dimitrov, 2003; Milkov, 2000; Milkov et al., 2003). This makes budget calculations very preliminary. However, global estimates suggest that terrestrial and shallow water mud volcanoes contribute between 2.2 and 6 Tg yr^{-1} of methane to the atmosphere and that 27 Tg

yr^{-1} of methane may escape from deep water mud volcanoes (Dimitrov, 2003; Milkov et al., 2003). Mud volcanism is therefore a key process in the global methane cycle.

At sites of active gas emission, communities of microbial organisms develop that can utilise methane as en energy source (Hanson et al., 1993; Sibuet and Olu, 1998). The microbial oxidation of methane is a significant sink term in the global methane budget (Reeburgh, 1996; Whiticar, 1999). Methane oxidation can be mediated aerobically by bacteria using oxygen as electron acceptor, or anaerobically by archaea and SRB, using sulphate as the terminal electron acceptor. Organisms involved in MOx belong to the α, β and γ subdivision of the *Proteobacteria* and have been reported from oxygenated wetlands, soils and the marine water column (Hanson et al., 1993; Le Mer and Roger, 2001). However, marine sediments have a very limited oxygen penetration depth and will mostly not provide suitable conditions for MOx communities. Due to the higher availability of sulphate in seawater, AOM is the main sink for methane in marine sediments (Hinrichs and Boetius, 2002). AOM is mediated by archaea phylogenetically related to the methanogens. So far, the known anaerobic methane oxidisers (ANME-1 and ANME-2) have been detected in consortium with SRB of one cluster in the *Desulfosarcina/Desulfococcus* branch (Seep-SRB1; Knittel et al. 2003). This was determined using combinations of lipid analyses and 16S rDNA methods in various methane seep environments (Aloisi et al., 2002; Boetius et al., 2000; Elvert et al., 1999; Hinrichs et al., 1999; Knittel et al., 2003; Knittel et al., 2005; Michaelis et al., 2002; Orphan et al., 2001a; Orphan et al., 2001b).

Generally, both aerobic and anaerobic methanotrophy are accompanied by a discrimination against the heavy stable carbon isotope ^{13}C, leading to a substantial ^{12}C-enrichment of metabolites and microbial biomass (Elvert et al., 1999; Hinrichs et al., 1999; Orphan et al., 2001b; Summons et al., 1994; Thiel et al., 1999; Whiticar, 1999). Moreover, AOM and MOx

derived carbon can fuel higher trophic levels in the benthic food web (Levin and Michener, 2002; Werne et al., 2002), and provide energy to symbiotic invertebrates hosting methanotrophic or thiotrophic symbionts (Fisher and Childress, 1992). Although increasing knowledge is available on the structure and distribution of cold seep communities at continental margins, the factors selecting for free-living versus invertebrate-associated methanotrophs, or aerobic versus anaerobic microbial communities at submarine methane seeps remain so far unknown.

To study the composition and distribution of methanotrophic communities at an active submarine mud volcano, we investigated HMMV with the research vessel R/V Atalante and the ROV VICTOR 6000 in 2001 and with R/V Polarstern and ROV VICTOR 6000 in 2003 (Klages et al., 2002; Klages et al., 2004). The HMMV is a glacial deposit of 3 km thickness (Shilov et al., 1999) located at 72° 00,25'N and 14° 43.50'E in 1250 m water depth in the SW Barents Sea (Shilov et al., 1999; Vogt et al., 1997a; Vogt et al., 1997b). It has a circular shape and is 1 km in diameter with a relief of 10 m (Hjelstuen et al., 1999). Thermal gradients in the centre are high with values >1000 mK m^{-1} where methane-rich sediments are expelled through a central conduit (Eldholm et al., 1999; Vogt et al., 1997b). Source methane at HMMV is of a mixed microbial-thermogenic origin with $\delta^{13}C$ values of –60 ±5 ‰ (Lein et al., 1999). Previous studies revealed three main habitats: (1) bare greyish sediments in the central crater; (2) a concentric zone of strongly reduced sediments that are densely covered by white, microbial mats consisting of the filamentous, sulphide oxidising bacteria *Beggiatoa sp.* adjacent to the centre; (3) an outer rim which is densely colonised by two species of pogonophoran worms, *Oligobrachia haakonmosbiensis* and *Sclerolinum contortum* (Milkov et al., 1999; Milkov et al., 2004; Smirnov, 2000). During our ROV dives we discovered another type of habitat, i.e. patches of reduced sediments, which were covered with greyish, putatively thiotrophic, microbial mats in the transition zones between the central area and

Beggiatoa covered sediments. The main focus of this study was the quantitative investigation of the diversity and distribution of methanotrophic organisms in sediments of the central area, grey mat and *Beggiatoa* habitat of HMMV, applying cultivation-independent molecular techniques (biomarker and 16S rDNA-based).

2. MATERIALS AND METHODS

2.1 Sample Collection and Storage

Sediment samples were recovered with the remotely operated vehicle (ROV) Victor 6000 by push coring during two cruise with R/V L'Atalante (IFREMER) in 2001 and R/V Polarstern in 2003 from four different stations (thermal centre, core 25a; grey mat, core 377-13; *Beggiatoa*-covered, core 19; reference station, core 28). Upon recovery, sediment cores were sliced in 1 cm and 2 cm sections for microbiological and lipid analysis, respectively. Sediment sections for lipid and DNA analysis were transferred into pre-cleaned glass vials and stored at –25°C until extraction. Sediments for microbiological analysis were stored at *in situ* temperature until cell fixation.

2.2 Biomarker Analysis

2.2.1 Extraction of Sediment Samples and Preparation of Derivates

Extraction procedure and the preparation of fatty acid methyl esters (FAMES) was carried out according to Elvert and co-workers (2003). Briefly, total lipid extracts (TLE) were obtained from 10-12 g of wet sediment. The TLE was extracted with the aid of ultrasonication in solvents of decreasing polarity. Internal standards of known concentration and carbon isotopic compositions were added prior to extraction. Ester bonded fatty acids (FAs) in glyco- and phospholipids were cleaved by a saponification reaction with KOH-solution. After extraction

of the neutral lipid fraction from this mixture, FAs were extracted subsequently to acidification, and methylated for analysis using BF_3 in methanol yielding FAMES.

Neutral lipids were further separated into hydrocarbons, ketones and alcohols over a SPE silica glass cartridge (0.5 g). Prior to separation, the column was cleaned three times with 5 ml *n*-hexane/dichloromethane (95:5, v/v). After the neutral fraction was applied to the column, solvent mixtures of increasing polarity were subsequently added: (I) 5 ml *n*-hexane/dichloromethane (95:5, v/v), (II) 5 ml *n*-hexane/dichloromethane (2:1, v/v) and (III) 5 ml dichloromethane/acetone (9:1, v/v). Neutral lipid fractions (hydrocarbons (I), ketones (II) and alcohols (III), respectively) were collected in tipped flasks and excess solvent was evaporated down to 100 µl and stored at –20°C until further processing and analysis. Alcohols were analysed as their trimethylsilyl (TMS) ethers. Shortly before analysis (<1 week), excess solvent of selected alcohol fractions was evaporated close to dryness. 100 µl pyridine and 50 µl bis(trimethylsilyl)triflouracetamid were added and the reaction was carried out at 70°C for 1 h. After cooling, excess solvent was evaporated and the remaining TMS adducts were re-suspended in 50 µl of *n*-hexane. TMS-adducts were stored at –20°C until GC, GC-MS and GC-IRMS analysis.

2.2.2 Preparation of Dimethyl Disulphide (DMDS) Adducts

Double bond position of monoenoic FAs were determined by analysis as their DMDS adducts according to previous publications (Moss and Lambert-Fair, 1989; Nichols et al., 1986). Briefly, an aliquot of a selected sample (dissolved in 50µl *n*-hexane) was treated with DMDS (100µl) and iodine-diethyl ether solution (20 µl, 6% w/v). Formation of DMDS adducts was carried out at 50°C for 48 h. After cooling, 0.5 ml *n*-hexane were added and excess iodine was

reduced with 0.5 ml sodium thiosulphate solution (5% w/v in water). The organic phase was removed and the aqueous phase was again extracted twice with 0.5 ml *n*-hexane. All organic phases were combined and excess solvent was evaporates close to dryness under a stream of nitrogen and stored at –20°C.

2.2.3 Gas Chromatography (GC), Gas Chromatography-Mass Spectrometry (GC-MS), Gas Chromatography-Isotope Ratio Mass Spectrometry (GC-IRMS)

Concentration, identity and stable carbon isotope ratios of individual lipid compounds were determined by GC, GC-MS and GC-IRMS analysis, respectively. Instrument specifications and operation modes of the GC, GC-MS and GC-IRMS units were set according to Elvert and co-workers (2003). The temperature programs used for analysis of FA, alcohols and hydrocarbons are shown in Table 1. Concentrations were calculated against internal standards. Identities of acquired mass spectra were compared to known standards and published data. Stable isotope ratios are given in the δ-notation against Pee Dee Belemnite (PDB). δ^{13}C-values of FAs and alcohols were corrected for the introduction of additional carbon atoms during derivatisation. Internal standards were used to monitor precision and reproducibility during measurements. Reported δ^{13}C-values have an analytical error of ± 1‰.

Table 1. Temperature programs used for GC, GC-MS, and GC-IRMS analyses, respectively. (Alc = alcohols, CxHy = hydrocarbons).

	rate [°C min^{-1}]	final temp [°C]	hold time [min]
FAMES			
Initial		60	1
Ramp I	10	150	0
Ramp II	2	230	0
Ramp III	5	310	20
Alc, CxHy			
Initial		60	1
Ramp I	10	150	0
Ramp II	4	310	50

2.3 Analysis of Microbial Consortia

2.3.1 Fluorescence In Situ Hybridisation

Aggregates of archaeal cells were quantified by fluorescence *in situ* hybridisation (FISH) according to the method and instrument specifications of Knittel and co-workers (2003, 2005). Briefly, sediments of the centre and below *Beggiatoa* mats were fixed with 2% formaldehyde (final concentration), washed twice with 1xPBS (10 mM sodium phosphate, 130 mM NaCl) and finally stored in 1xPBS/EtOH (1:1) at –20°C. Fixed samples were diluted 1:10, treated by mild sonication and filtered on 0.2 µm GTTP polycarbonate filters. Hybridisation with Cy3-labeled Arch915 and staining of cells with 4´,6´-diamidino-2-phenylindole (DAPI) was performed as described previously (Amann et al., 1990; Snaidr et al., 1997). Samples were examined with an epifluorescence microscope (Axiophot II microscope; Carl Zeiss, Jena, Germany).

2.3.2 DNA Extraction and Clone Library Construction

Total community DNA in sediments below Beggiatoa mats was directly extracted from 2 g of wet surface sediments (0-2 cm) according to Zhou et al. (1996). Crude DNA was purified with the Wizard DNA Clean-Up Kit (Promega, Madison, WI). Almost full-length archaeal 16S rRNA genes from the extracted chromosomal DNAs were amplified using primers 20f (Massana et al., 1997) and Uni1392R (Lane et al., 1985). PCRs were performed with a Mastercycler Gradient (Eppendorf, Hamburg, Germany) as described previously (Ravenschlag et al., 1999), except that the annealing temperature was 58°C. PCR products of

several reactions were combined and purified with the QiaQuick PCR Purification Kit (Qiagen, Hilden, Germany). DNA was ligated in the pGEM T-Easy vector (Promega, Madison, WI) or the pCR4 TOPO vector (Invitrogen, Carlsbad, CA) and transformed into *E. coli* TOP10 cells (Invitrogen, Carlsbad, CA) according to the manufacturer's recommendations. Sequencing was performed by *Taq* cycle sequencing with a model ABI1377 sequencer (Applied Biosystems) with insert-specific and vector primers. The absence of chimeric sequences in the clone library was verified with the CHIMERA_CHECK program of the Ribosomal Database Project II (http://rdp.cme.msu.edu/html/analyses.html). Sequence data were analysed with the ARB software package (Strunk et al., 1998). Phylogenetic trees were calculated by parsimony, neighbour-joining, and maximum-likelihood analysis with different sets of filters that consider only 50% conserved regions of the 16S rDNA of Archaea. For tree calculation, only full-length sequences (>1315 bp) were considered. Partial sequences were inserted into the reconstructed tree by parsimony criteria with global/local optimisation without allowing changes in the overall tree topology. The sequence data reported here will appear in the EMBL, GenBank, and DDBJ nucleotide sequence databases under the accession no. AJ704631, AJ704650-AJ704653.

3. RESULTS

3.1 Lipid Biomarker

3.1.1 Centre

Fatty acids were found to be the dominant membrane lipids in sediments of the centre (Fig. 1b, Tab. 2a). FAs at the centre of HMMV were concentrated in a narrow subsurface horizon (0-2 cm bsf) and sharply decreased with increasing sediment depth (Fig. 1b). Specific FAs include i-$C_{15:0}$, ai-$C_{15:0}$, $C_{16:1\omega9c}$, $C_{16:1\omega8c}$, $C_{16:1\omega7c}$ and $C_{16:2}$. These FAs were strongly depleted in ^{13}C and of higher abundance than other bacterial FAs. $\delta^{13}C$-values of FAs showed highest ^{13}C-depletions in the top horizon with very low values ranging between –67‰ (i-$C_{15:0}$) to –89‰ ($C_{16:1\omega7c}$). High amounts and a strong $\delta^{13}C$-depletion of FA $C_{16:1\omega8c}$ directly indicates the presence of methanotrophic bacteria in the surface sediments (Hanson and Hanson, 1996). At 7.5 cm bsf, $\delta^{13}C$-values of $C_{16:1\omega8c}$ and $C_{16:1\omega7c}$ showed a second minimum with –47‰ and –69‰, respectively, but increased to –32‰ in the bottom horizon. Hence, the isotopic signature of specific FAs showed the strongest depletion in the zone with the highest concentration of the lipids. Below this zone, only minor amounts of archaeol and *sn2*-hydroxyarchaeol were found in the centre sediments. Both compounds were moderately depleted in ^{13}C but showed an offset in $\delta^{13}C$ of about 25‰ with a heavier signature of archaeol compared to *sn2*-hydroxyarchaeol (Fig. 1a). Other specific biomarkers of archaeal origin include trace amounts of PMI:4 and PMI:5 for which carbon isotopic values could not be measured due to their low abundance.

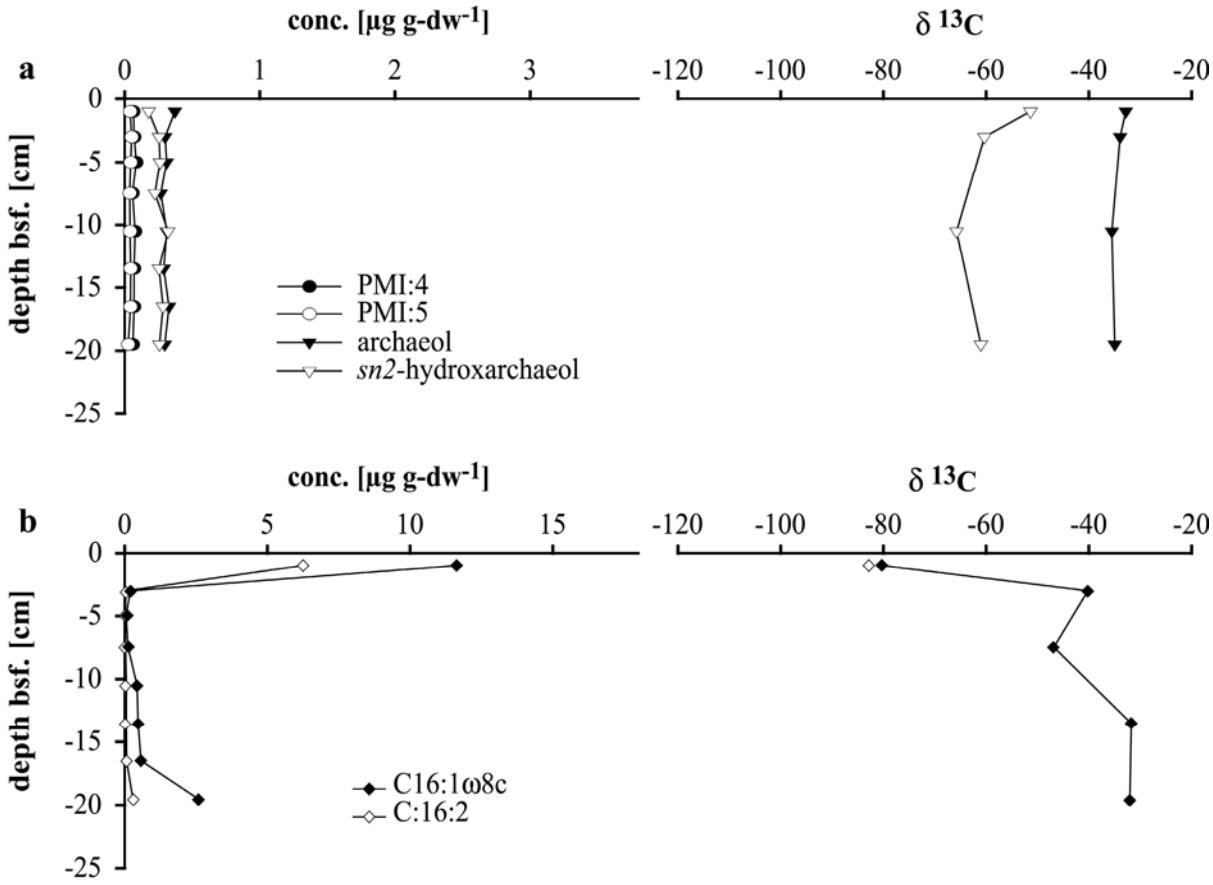

Figure 1. Biomarker concentrations and associated $\delta^{13}C$-values of representative (a) archaeal and (b) bacterial lipids in sediments of the centre.

3.1.2 Grey mats

Patches of greyish thiotrophic mats of ca. 1 m in diameter were sampled at the northern border of the central plain. Archaeal lipids showed highest concentrations in a surface horizon between 2 and 7.5 cm bsf and declined with depth (Fig. 2a). *sn2*-hydroxyarchaeol was the most abundant archaeal lipid in the sediments below grey mats showing a 4-fold higher concentration compared to central sediments. Moderate amounts of crocetene (2,6,11,15-tetramethylhexadecane) with 2 double bonds (CR:2), lower amounts with one double bound (CR:1), and trace amounts of PMI:2 and PMI:3 were also found (Tab. 3). PMI:4 and PMI:5

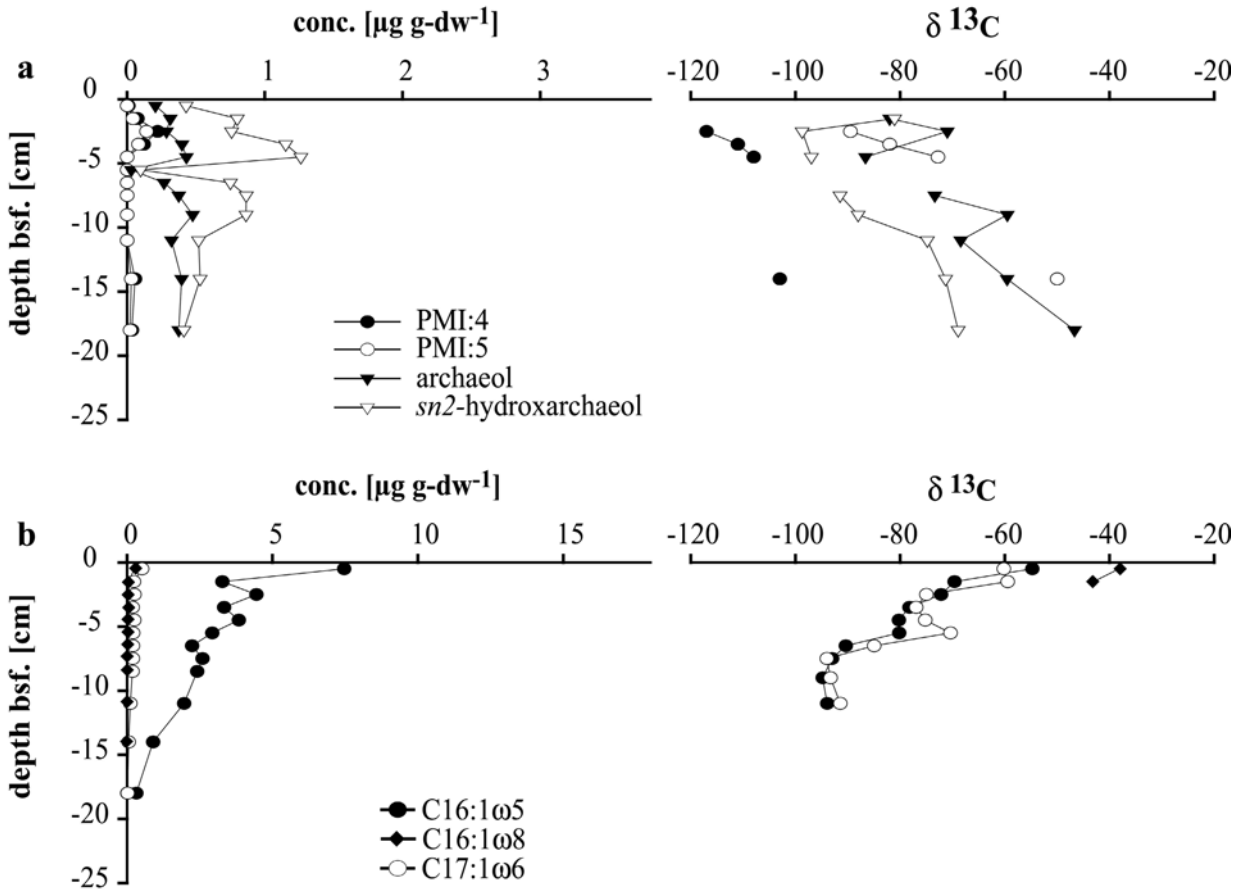

Figure 2. Biomarker concentrations and associated $\delta^{13}C$-values of diagnostic archaeal (a) and bacterial lipids (b) in sediments covered by grey mats.

showed a subsurface maximum at about 3 cm (Fig. 2a) and concentrations of crocetenes, PMI:2 and PMI:3 were similarly distributed (data not shown). All archaeal biomarkers were strongly depleted in ^{13}C in surface sediments with $\delta^{13}C$ values ranging between –71‰ (archaeol) to –118‰ (PMI:4) and showed an increase in $\delta^{13}C$-values with decreasing concentration and with sediment depth (Fig. 2a). Concentrations of bacterial FAs were highest in the uppermost horizon also declining with depth (Fig. 2b, Tab. 2b). The most dominant FAs in the top horizons included $C_{16:1\omega7c}$ and $C_{16:1\omega5c}$. In contrast to central sediments, the concentration of $C_{16:1\omega8c}$ in surface sediments of the grey mat site was very low. Other specific FAs such as $cyC_{17:0\omega5,6}$, a marker for *Desulfosarcina/Desulfococcus* species detected in

Table 2. FA concentrations and δ^{13}C-values obtained from sediments of the centre (a), below grey (b) and *Beggiatoa* mats (c) and from the reference station (d). Note that Concentrations and δ^{13}C-values for sediment strata below 4 cm bsf were pooled whereas down core profiles of specific lipid biomarkers show a resolution of 2-4 cm (Fig. 1-3). Unreliable δ^{13}C-values caused by low concentrations and/or a high background were excluded from the table.

a

Centre	0-2 cm		2-4 cm		4-10 cm		10-20 cm	
i-C14:0	0.2	-57					tr	
C14:0	1.0	-49	0.2	-29	0.2	-31	0.8	-28
i-C15:0	0.3	-67	0.1	-31	tr		0.1	-30
ai-C15:0	0.4	-73	tr	-33	tr		0.1	-30
C15:0	0.3	-47	0.1		0.1	-31	0.4	-31
C16:1ω9	5.2	-69						
C16:1ω8	11.6	-80	0.2	-40	0.1	-47	0.9	-32
C16:1ω7	4.7	-89	0.1	-44	0.1	-69	0.5	-38
C16:2	6.2	-83	0.1		tr		0.1	
C16:1ω5							tr	
C16:0	3.4	-56	0.7	-29	0.5	-29	2.2	-29
c17:1ω6	0.1							
cyC17:0ω5,6								
C18:3								
C18:2	3.9	-32	0.9	-30	0.7	-33	5.5	-29
C18:1ω9	2.3	-35	0.7	-29	0.4	-31	2.9	-30
C18:1ω7	1.0	-53	0.1		0.1		0.6	-36
C18:0	1.1	-41	0.4	-29	0.3	-29	1.2	-32
Sum	41.5		3.7		2.6		15.3	

b

Grey mat	0-2 cm		2-4 cm		4-10 cm		10-20 cm	
i-C14:0	1.3	-25	0.2		0.1	-53	tr	
C14:0	1.7	-34	0.4	-59	0.2	-66	0.1	
i-C15:0	0.5	-41	0.2	-70	0.1	-73	tr	
ai-C15:0	0.6	-48	0.4	-70	0.3	-73	0.1	
C15:0	0.2	-44	0.1	-66	0.1	-62	tr	
C16:1ω9								
C16:1ω8	0.2	-45	tr		0.1	-51	tr	
C16:1ω7	19.9	-49	3.7	-54	1.4	-59	0.2	
C16:2								
C16:1ω5	5.4	-59	3.9	-75	2.8	-86	1.1	
C16:0	3.4	-36	0.8	-55	0.5	-51	0.2	
c17:1ω6	0.4	-60	0.2	-76	0.2	-83	0.1	
cyC17:0ω5,6			tr		0.2	-97	0.1	
C18:3	2.4	-50	0.2	-51	0.2		0.1	
C18:2								
C18:1ω9	2.7	-38	0.8	-46	0.5	-64	0.1	
C18:1ω7	2.3	-36	0.1		tr		tr	
C18:0	0.3	-29	0.2	-41	0.3	-27	0.1	
Sum	41.3		11.2		7.0		2.0	

c

Beggiatoa	0-2 cm		2-4 cm		4-10 cm		10-20 cm	
i-C14:0	0.5	-32	tr					
C14:0	4.2	-50	0.3	-41	0.1	-30	0.1	-29
i-C15:0	2.3	-65	0.1	-58	tr		tr	
ai-C15:0	3.0	-62	0.1	-58	tr		tr	
C15:0	0.9		0.1	-37	tr		0.1	-30
C16:1ω9	2.7		0.4		0.1		0.1	
C16:1ω8								
C16:1ω7	74.7	-53	0.8	-54	0.3	-39	1.4	-36
C16:2								
C16:1ω5	16.3	-71	0.9	-68	0.2	-47	0.1	-49
C16:0	2.9	-52	0.8	-35	0.5	-29	0.5	-27
c17:1ω6	2.6	-69	0.1	-70	tr		tr	
cyC17:0ω5,6								
C18:3								
C18:2	1.2		0.4	-26	0.1	-26	0.1	-26
C18:1ω9	0.7		0.5	-30	0.2	-28	0.3	-28
C18:1ω7	18.3	-53	0.3	-51	0.2	-36	0.2	-33
C18:0	1.8	-30	0.2	-28	0.2	-28	0.2	-27
Sum	137.3		5.1		1.9		3.0	

d

Reference	0-2 cm		2-4 cm		4-10 cm		10-20 cm	
i-C14:0	0.2		0.1					
C14:0	0.7	-27	0.4	-26	0.3	-30	0.4	-28
i-C15:0	0.5	-23	0.4	-24	0.2	-27	0.1	-28
ai-C15:0	0.7	-24	0.5	-24	0.2	-27	0.1	-30
C15:0	0.2	-30	0.1	-27	0.1	-31	0.1	-28
C16:1ω9	0.4		0.2		0.1	-26	0.1	-22
C16:1ω8								
C16:1ω7	2.1	-23	1.1	-23	0.5	-24	0.2	-22
C16:2								
C16:1ω5	0.6	-26	0.4	-26	0.2	-26	0.1	
C16:0	2.1	-27	1.2	-27	1.0	-29	1.2	-27
c17:1ω6	0.3	-30	0.2	-40	0.1			
cyC17:0ω5,6								
C18:3								
C18:2					0.1	-28	1.6	-28
C18:1ω9	0.7	-24	0.5	-26	0.2	-27	0.9	-29
C18:1ω7	1.7	-25	0.9	-26	0.3	-25	0.2	-34
C18:0	0.6	-28	0.4	-28	0.4	-28	0.8	-28
Sum	10.8		6.4		3.7		5.8	

Table 3: Concentrations and δ^{13}C-values of putatively ANME-2 specific lipids obtained from sediments covered by grey mats.

Grey mat	0-2 cm		2-4 cm		10-20 cm	
Cr:1	0.1	-89	0.2	-100	0.1	-84
Cr:2	0.2	-91	0.6	-102	0.1	-97
PMI:2	tr		tr		tr	
PMI:3	tr		tr		tr	

ANME-2 dominated AOM settings (Elvert et al., 2003), were only present in deeper sediment layers (<3.5 cm, Tab. 2b). In contrast to isotope signatures of the other FAs, δ^{13}C-values of cy$C_{17:0\omega5,6}$ decreased with depth and reached values comparable to archaeal lipids (Fig. 2a, b).

3.1.3 Beggiatoa-Covered Sediments

Concentration measurements of single lipid compounds revealed that most of the lipids specific for archaea and bacteria are concentrated in a narrow surface horizon of not more than 4 cm (Fig. 3a, b, Tab. 2c). Stable carbon isotope analyses revealed highest ^{13}C-depletion with δ^{13}C-values ranging from –109 (PMI:5) to –98‰ (archaeol) for archaeal lipids and from –71‰ ($C_{16:1\omega5c}$) to –52‰ (ai-$C_{15:0}$) for bacterial lipids. Below 3 cm sediment depth, archaeal and bacterial biomarker concentrations decreased sharply to concentrations <1 µg g-dw^{-1}. Hence, concentrations of archaeal lipids in deeper sediment layers at the *Beggiatoa* site are similar to those encountered at the centre. However, archaeol, *sn2*-hydroxyarchaeol and $C_{16:1\omega7c}$ had a second maximum at 16.5 cm bsf. (Fig. 3a,b). Stable carbon isotope signatures of archaeal and bacterial lipids showed higher values with increasing sediment depth (Fig. 3a, b, Tab 2c). Similar to centre sediments, δ^{13}C-values of archaeol were heavier than *sn2*-hydroxyarchaeol by ca. 25 ‰ at depths below 4 cm (Fig. 3a). Archaeal lipids found in the uppermost sediment horizon were dominated by *sn2*-hydroxyarchaeol and PMI:5 followed by archaeol and PMI:4. In contrast to the grey mats, higher saturated PMI's and the C_{20} isoprenoid crocetane and its unsaturated counterparts were not found. Specific bacterial FA in sediments below *Beggiatoa* mats included, i-$C_{15:0}$, ai-$C_{15:0}$, $C_{16:1\omega5c}$ and $C_{17:1\omega6c}$ (Tab. 2c).

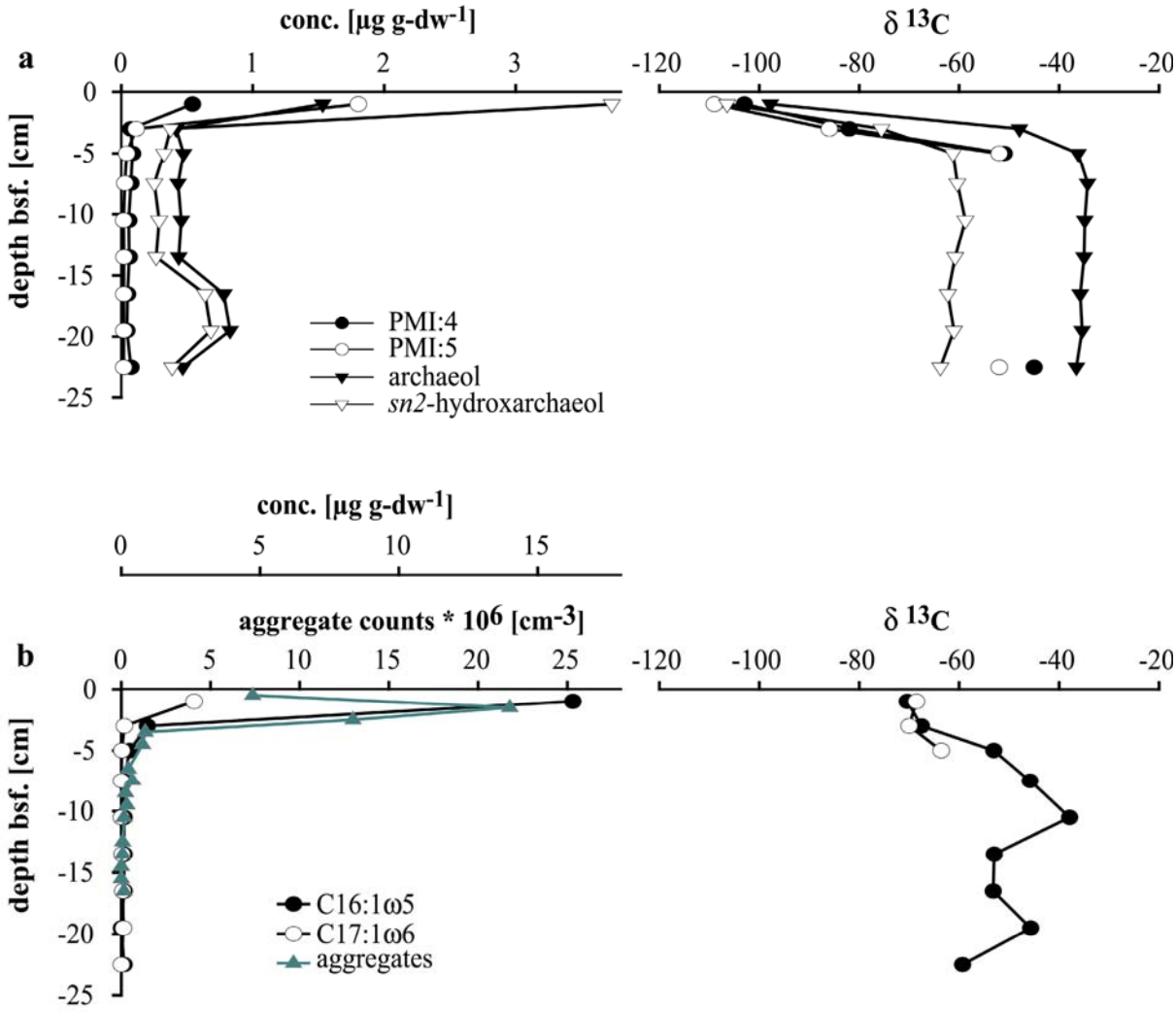

Figure 3. Biomarker concentrations and associated $\delta^{13}C$-values of representative (a) archaeal and (b) bacterial lipids and microbial aggregate counts in *Beggiatoa* covered sediments.

3.1.3 Reference

A reference site outside of the fluid-flow impacted area of the HMMV was sampled at ca. 1 km east to the crater. Archaeal biomarkers were below detection limit at the reference station and FA concentrations were lower than those at all stations of the HMMV (Tab. 2d). Total FA concentrations at the surface were roughly 13-fold and 4-fold lower compared to *Beggiatoa*-

covered and centre sediments, respectively. In contrast to methane dominated sediments of HMMV, $C_{16:1\omega7}$, $C_{16:0}$ and $C_{18:1\omega7}$ were the most abundant FAs showing comparably heavy $\delta^{13}C$-values in the first subsurface horizon (≥27‰, Tab. 2d), indicating a main contribution of phytoplankton-derived biomass as the carbon source. FA decreased steadily with depth but showed a second small concentration increment at 15.5 cm bsf.

3.2 Microbial Aggregates in *Beggiatoa*-Covered Sediments

In sediments below *Beggiatoa* mats, abundant microbial aggregates containing archaea and bacterial cells were detected (Fig. 3b, 4a, b). Direct counts of these microbial consortia revealed highest numbers of $22*10^6$ aggregates cm^{-3} sediment in the shallow surface horizon (1 – 2 cm sediment depth) reflecting the peak in specific archaeal and bacterial biomarkers (Fig. 3a, b). Aggregate sizes increased with increasing sediment depth. In contrast to the *Beggiatoa* site, such aggregates were not found at the centre and the reference station.

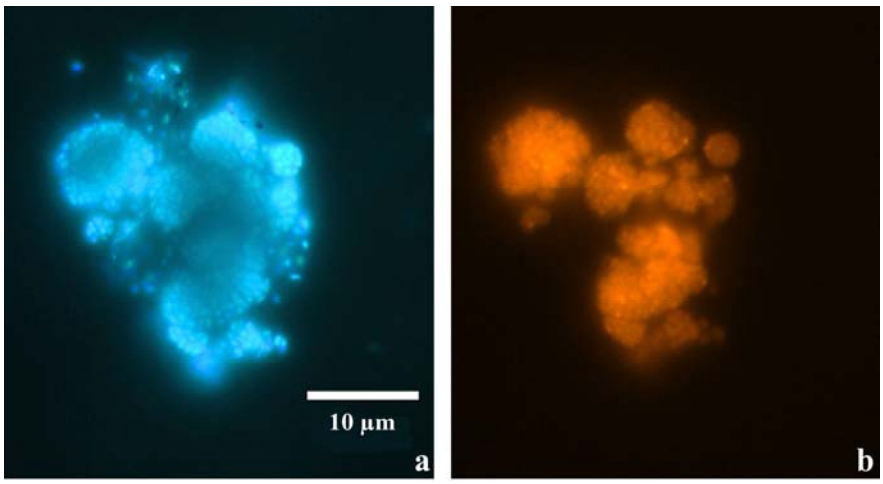

Figure 4. Microbial aggregates in near surface sediments covered by *Beggiatoa* mats. Whole aggregates are visualized by DAPI (a) and archaeal cells with the oligonucleotide probe ARCH 915 (b).

DNA was extracted from 0-2 cm sediment depth beneath the *Beggiatoa* mat to construct a 16S rDNA clone library. A total of 67 archaeal

clones were obtained. All archaeal HMMV sequences could be grouped in a new, distinct cluster within the order Methanosarcinales, together with two sequences from Hydrate Ridge and the Eel River Basin (Fig. 5). This cluster, termed ANME-3, has a distinct phylogenetic position, but is relatively closely related to ANME-2 and ANME-1 (Knittel et al., 2005; Orphan et al., 2001a). Sequence similarity within the ANME-3 group is 97 – 99%. It shares a similarity of 95 – 96% with its next cultivated relative, *Methanococcoides methylutens*.

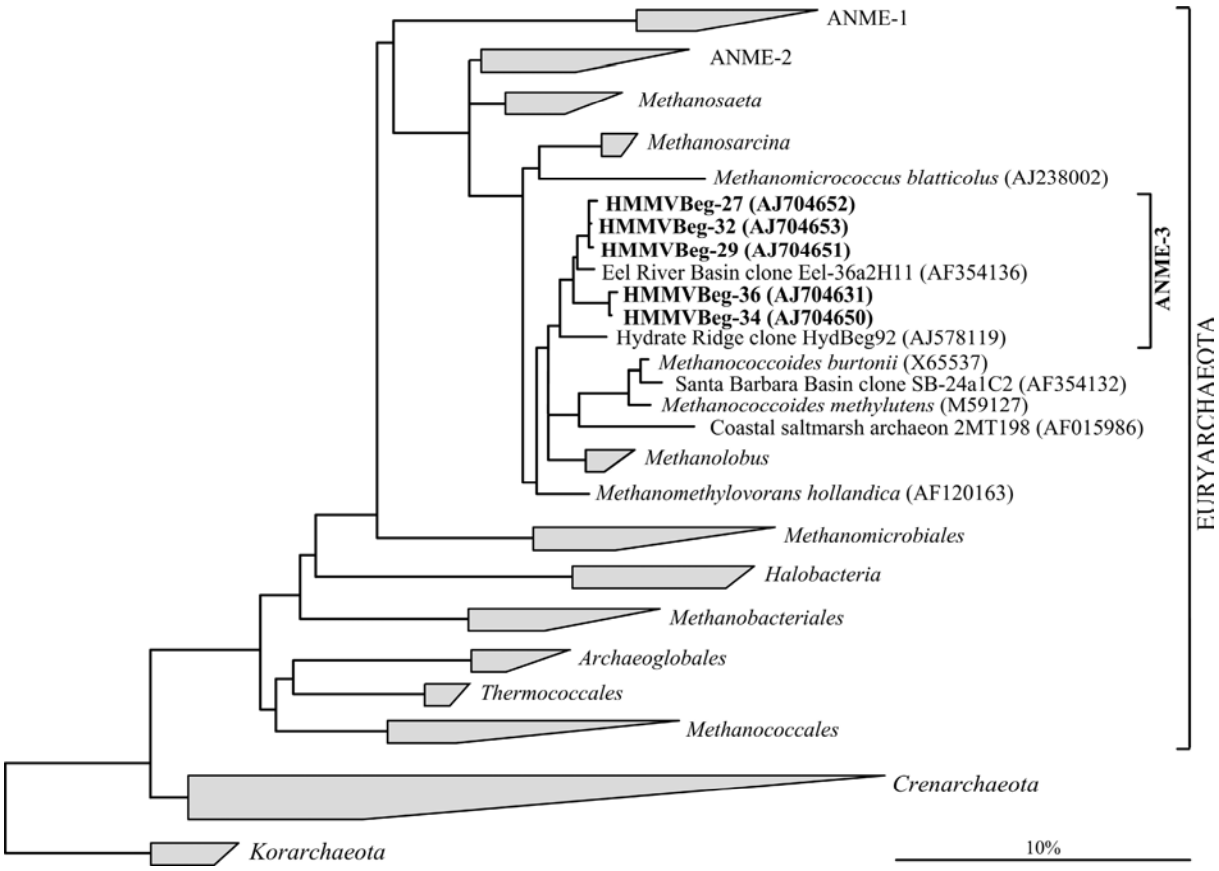

Figure 5. Phylogenetic tree showing the affiliations of HMMV 16S rDNA clone sequences (bold face type) from *Beggiatoa* covered sediments to selected sequences of the domain Archaea. Branching orders that are not supported by all calculation methods are shown as multifurcations. The bar represents 10 % estimated phylogenetic divergence. All euryarchaeal clone sequences obtained from surface sediments below *Beggiatoa* mats group in a distinct cluster, termed ANME-3.

4. DISCUSSION

4.1 Identity of Methanotrophic Communities in *Beggiatoa*-Covered Sediments

Elevated concentrations of specific archaeal and bacterial biomarkers and their highly depleted $\delta^{13}C$-values indicate the presence of anaerobic methanotrophic microorganisms in *Beggiatoa*-covered sediments. Our data show a ^{13}C-fractionation in diagnostic archaeal lipids and bacterial FAs as high as -55‰ and -15‰, respectively, compared to the source methane (-60 ±5‰, Lein et al., 1999). These values are in good agreement with AOM settings described elsewhere (Elvert et al., 2000; Elvert et al., 1999; Orphan et al., 2001a). Nevertheless, the composition of archaeal isoprenoid hydrocarbons differ substantially from the pattern of known archaeal strains capable of AOM, i.e. ANME-1 and ANME-2. Microbial mats dominated by ANME-1 contain PMI:0 and abundant concentrations of its unsaturated analogues with one to five double-bonds as well as predominant amounts of archaeol compared to *sn2*-hydroxyarchaeol (Blumenberg et al., 2004; Michaelis et al., 2002; Thiel et al., 2001). In contrast, sediments and microbial mats with high abundances of ANME-2 comprise saturated and unsaturated PMI's, crocetane and its unsaturated analogues as well as a high *sn2*-hydroxyarchaeol to archaeol ratio (Blumenberg et al., 2004; Boetius et al., 2000; Elvert et al., 2001; Elvert et al., 1999; Teske et al., 2002). To our knowledge, no AOM setting has been found with methanotrophic archaea lacking crocetane and possessing only PMI's with 4 and 5 double bonds while all other higher saturated PMI homologues are completely missing. Hence, the exclusive presence of ^{13}C-depleted PMI:5 and PMI:4 together with dominant amounts of *sn2*-hydroxyarchaeol relative to archaeol indicates the presence of a novel community of archaea involved in AOM. This line of evidence is well corroborated by the retrieval of novel archaeal 16S rDNA sequences forming a deeply branching cluster with

other sequences, called the ANME-3 group (Fig. 5). Taking into account that no other euryarchaeal sequences were found in the top sediment horizon, it appears likely that ANME-3 is the predominant archaeal group in sediments below *Beggiatoa* mats.

A striking finding is the fractionation offset by ca. 25‰ between *sn2*-hydroxyarchaeol and archaeol throughout the 20 cm of sediment below the *Beggiatoa* mat. An offset in $\delta^{13}C$ could point to the presence of two different organisms, but the parallel concentration profiles suggest a single organism (Freeman et al., 1994). A possible source for the observed archaeal biomarker pattern could be the presence of methanogenic archaea in subsurface sediments of HMMV. Previous studies demonstrated that methanogenesis occurs at HMMV (Pimenov et al., 1999). Furthermore, the archaeol carries an isotope signature typical for methanogens (Hayes et al., 1987; Hinrichs et al., 2003). However, no DNA sequences of methanogenic archaea were detected in the clone library. Possibly, one organism is producing archaeol and *sn2*-hydroxyarchaeol via different metabolic pathways. However, this seems unlikely for such structurally similar biomolecules. Therefore, it might also be possible that the archaeal guilds in the deeper sediment strata of HMMV operate in a mixed AOM – methanogenic mode probably due to temporal or spatial differences in energy availability.

The unique presence and elevated concentrations of specific FAs in methane-dominated sediments below *Beggiatoa* mats (Fig. 6, Tab. 2a, c) give evidence for a bacterial community that is distinct from a typical, deep-sea community of the Barents Sea as present in the sediments of the reference site. Non-seep sediments in Arctic oceans would be fueled by a planktonic carbon source, dominated by high amounts of $C16_{:1\omega7}$ and $C_{18:1\omega7}$ with $\delta^{13}C$-values ranging from –20 to –30‰ (Birgel et al., 2004; Rau et al., 1989). This is similar to the lipid pattern of the reference station (Tab. 2d). In contrast, the sediments below *Beggiatoa* mats contain high amounts of the significantly ^{13}C-depleted, unusual FAs $C_{16:1\omega5}$ and $C_{17:1\omega6}$ (Tab.

2b, Fig. 6). In comparison to other AOM settings where ANME-1 and ANME-2 are associated to SRBs of the Seep-SRB1 cluster, our samples are lacking predominant amounts of ai-$C_{15:0}$ and cy$C_{17:0\omega5,6}$, respectively (Blumenberg et al., 2004; Elvert et al., 2003; Elvert et al., submitted). In contrast, our samples contain elevated concentrations of the FA $C_{17:1\omega6c}$, which has been described as an indicator for *Desulfobulbus sp*. in cultures of this genus (Lien et al., 1998; Sass et al., 2002; Taylor and Parkes, 1983). $C_{17:1\omega6c}$ has also been detected in SRB species other than *Desulfobulbus sp.* such as *Desulforhabdus*, *Desulfomicrobium* as well as *Desulforhopalus* species (Knoblauch et al., 1999; Rutters et al., 2002; Rütters et al., 2001). However, comparative FA patterns of *Desulforhopalus, Desulfomicrobium* and *Desulforhabdus* species substantially deviate from *Desulfobulbus sp*. (Elvert et al., 2003 and

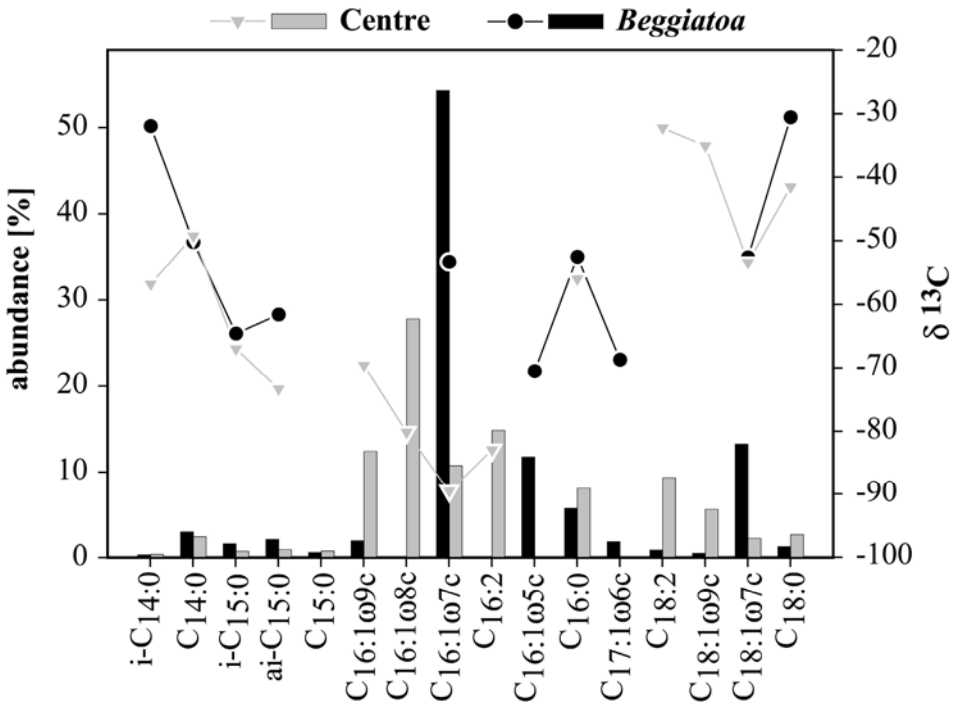

Figure 6. Fatty acid fingerprint pattern: relative abundance (columns) and carbon isotopic composition (circles, triangles) of FAs found in the uppermost horizon of *Beggiatoa* covered and centre sediments. Specific ^{13}C-depleted FAs show a pattern indicative for *Desulfobulbus sp.* (*Beggiatoa* covered) and aerobic type I methanotrophic bacteria (Centre).

references therein) and the FA fingerprint presented in this work. This suggests that the microbial consortia at HMMV are composed of ANME-3 and a SRB most likely affiliated to *Desulfobulbus sp*. which is different from other known AOM settings (Boetius et al., 2000; Michaelis et al., 2002; Orphan et al., 2001a).

This community is restricted to a narrow, subsurface horizon of not more than 4 cm where AOM appears to be the dominant, biomass generating process. In contrast, deeper sediment strata below the Beggiatoa mats are characterised by diminished microbial biomass as indicated by strongly reduced contents of biomarkers and AOM-aggregates (Fig. 3a, b). Here, heavier $\delta^{13}C$ values of archaeal and bacterial biomarkers have been detected.

4.2 Identity of Aerobic Methanotrophs in Sediments of the Centre

In contrast to the *Beggiatoa* site, the centre is dominated by aerobic methanotrophy, however, restricted to an even narrower surface horizon. In the surface sediments of the centre, specific FAs carrying depleted $\delta^{13}C$-signatures are predominant, concentrations of archaeal biomarkers are low and microbial consortia were not observed microscopically. Type I and II methanotrophic bacteria are known to synthesise either $C_{16:1}$ or $C_{18:1}$ fatty acids, respectively, with double bond positions dominating the ω8-position (Bowman et al., 1991; Bowman et al., 1993; Fang et al., 2000; Roslev et al., 1998). Hence, the predominance of ^{13}C-depleted $C_{16:1}$ FA, especially $C_{16:1\omega8c}$ (Fig. 6) points to a microbial community dominated by a type I methanotroph. Isotope fractionations with $\Delta\delta^{13}C$-values as high as -35‰ compared to the source methane are in the upper range of the RuMP pathway, which is used by type I methanotrophs for methane oxidation (Jahnke et al., 1999). Such high carbon isotope fractionations are quite possible considering the cold growth temperatures at HMMV

(T = -1°C, Ginsburg et al., 1999), whereas higher temperatures lead to a lower fractionation (Jahnke et al., 1999). A comparison of the FA fingerprint obtained from surface sediments of the centre (Fig. 6) with published FA signatures of type I methanotrophs indicates a bacterium of the genus *Methylomonas* (Bowman et al., 1991; Bowman et al., 1993; Hanson and Hanson, 1996; Summons et al., 1994). However, the high abundance of $C_{16:1\omega9c}$ and $C_{16:2}$ and the lack of $C_{16:1\omega5c,t}$ might also point to another, still unknown methanotroph because these two compounds were not found in the previous studies. Other FA patterns of known methanotrophic bacteria do not match the observed lipid fingerprint. Bacteria of the genus *Methylococcus* and *Methylobacter*, which are both close relatives of *Methylomonas*, for instance lack $C_{16:1\omega8c}$ but comprise dominant contents of $C_{16:0}$ and $C_{16:1\omega7c}$ and also vital amounts of $C_{16:1\omega5c,t}$ (Bowman et al., 1993; Hanson and Hanson, 1996). More surprisingly, only trace amounts of free hopanoids were found in sediments of the centre even though Rohmer et al. (1984) found hopanol (after degradation reactions) in almost all methanotrophs. Thus, if hopanoids are present in our samples it is most likely that these occur in the biological form as polyols.

Similar to the subsurface sediments covered by *Beggiatoa* mats, deeper sediment strata at the centre likely harbour a low number of archaea as indicated by low contents of moderately depleted archaeol and *sn2*-hydroxyarchaeol (Fig. 1a). Similar to deeper strata at the *Beggiatoa* site, the isotopic offset of these molecules remains unclear.

4.3 Methanotrophic Guilds Below Grey Mats

Homologous to *Beggiatoa* covered sediments, elevated concentrations and associated low $\delta^{13}C$-values of archaeal biomarkers (Fig. 2a) give evidence that AOM is an important biomass

generating process in sediments below the greyish thiotrophic, microbial mats. Compared to *Beggiatoa* covered sediments, concentrations of archaeal lipids are lower (Fig. 2a). Small but detectable amounts of FA $C_{16:1\omega8}$, give evidence that the sediment surface still harbours minor biomass of aerobic type I methanotrophs. In contrast, MOx-specific FAs have not been detected in AOM-dominated *Beggiatoa* covered sediments. Most of the patchy grey mats occur in the transition between centre and Beggiatoa mats and around gas vents. It is hence possible that they represent an early stage in the development of AOM communities.

The vertical distribution of archaeal lipid concentrations (Fig. 2a) gives evidence that the AOM community is dispersed over a greater sediment interval as observed at the Beggiatoa mat. Furthermore, the composition of specific archaeal lipids deviates from *Beggiatoa* covered sediments by the presence of comparably high amounts ^{13}C-depleted CR:1, CR:2 and trace amounts of PMI:2 and PMI:3 (Tab. 3) all of which were previously identified in ANME-2 bearing sediments and microbial mats (Blumenberg et al., 2004; Elvert et al., 2001; Orphan et al., 2001a). None of these compounds were detected in the ANME-3 dominated sediments below the *Beggiatoa* mats, hence ANME-3 can be excluded as a source of these compounds. We suggest that ANME-3 as well as ANME-2 co-occur in sediments below grey mats, both contributing to the lipid biomass content. Moreover, elevated concentrations of several ^{13}C-depleted FAs give evidence that a higher diversity of SRB are involved in AOM in this habitat compared to the *Beggiato*a mats. The presence of the ^{13}C-depleted FA $C_{17:1\omega6}$ indicates that SRB related to *Desulfobulbus sp.* could be the main partner in AOM in near surface sediments of the grey mat habitats. At depth below 3.5 cm, increasing concentrations of ^{13}C-depleted $cyC_{17:0\omega5.6}$ (Tab. 2b), indicate that SRB related to the Seep-SRB1 cluster (*Desulfosarcina/Desulfococcus*, Elvert et al., 2003; Knittel et al., 2003) are also involved in AOM. This higher diversity of methanotrophic bacteria and archaea could also be an

indication that the grey mats are a transient community, and that the much more abundant *Beggiatoa* mats at HMMV represent the climax stage in AOM-community development.

4.4 Correlation Between Biomarker Concentrations and Biomass

The predominance of unsaturated archaeal and bacterial lipids over their saturated counterparts in sediments of HMMV indicates that these membrane components very likely originate from living biomass. Unsaturated FAs have been shown to be very labile in marine sediments (Parker et al., 65). Incubation experiments with radioactive labelled palmitic ($C_{16:0}$) and oleic ($C_{18:1}$) acid provided evidence that more than 90% of the label was lost within the first 20 days of incubation (Sun et al., 1997). Moreover, the decay of the unsaturated FA was two fold faster under anoxic conditions. Archaea from living mat system-cultures and enrichments contain only little or no saturated PMIs (Michaelis et al., 2002; Schouten et al., 1997). The diagenetically stable and saturated form PMI:0 that is prevailing in carbonates of methanotrophic origin could be a result of the hydrogenation of PMI's from decaying biomass under reduced conditions (Peckmann et al., 2002; Peckmann et al., 1999; Thiel et al., 2001).

At the surface (0-4 cm) where the aggregate abundance was highest, the average aggregate size was 60 μm^3 and each aggregate contained ca. 80 archaeal cells. In deeper sediment horizons, the number of aggregates decreased substantially, but the average size increased to 145 μm^3 and each aggregate contained ca. 200 archaeal cells (Lösekann et al. unpubl.). Concentrations of the diagnostic archaeal biomarkers archaeol, *sn2*-hydroxyarchaeol, PMI:4 and PMI:5 were positively correlated with the abundance of archaeal cells (data not shown). The linear correlation of *sn2*-hydroxyarchaeol, PMI:4 and PMI:5 with the archaeal cell number showed high R^2-values (>0.7) but was lower for archaeol (0.62). With respect to the

abundance of archaeal cells, the cell specific lipid contents of the diagnostic archaeal biomarkers archaeol, *sn2*-hydroxyarchaeol, PMI:4 and PMI:5 where 3.6 (±1.9 S_E) , 2.6 (±1.1 S_E), 0.6 (±0.2 S_E)and 0.4 (±0.4 S_E) fg $cell^{-1}$ on average. In contrast, ANME-2 at Hydrate Ridge was found to contain 0.23 and 0.9 fg $cell^{-1}$ of archaeol and *sn2*-hydroxyarchaeol, respectively (Elvert et al., submitted)

4.5 Distribution of Habitats and Methanotrophic Guilds at HMMV

The investigated mud volcano is an active methane seep at 1250 m water depth of about 0.8 km^2 (Milkov et al. 2004). We found that it hosts a variety of methanotrophic communities, which inhabit distinct areas structured concentrically around the active centre. Fluid and methane migration through the volcanoes central conduit leads to mud diapirism that fuels the central area with fresh, methane rich mud (Eldholm et al., 1999; Vogt et al., 1997b). Here, overlapping gradients of methane and oxygen provide suitable conditions for aerobic microbes. Compared to sulphate concentrations in seawater, 100-fold lower oxygen concentration and the slow diffusive oxygen transport into deeper sediment layers are probably the cause for the observed restriction of the MOx community to a narrow surface horizon. AOM communities develop probably later than MOx communities in oxygen-depleted sediments in the presence of methane and sulphate. The slow growth rates with doubling times of several months (Nauhaus et al., 2005) are possibly one reason for this phenomenon. Sea floor observations and the biomarker patterns found in the transition zone from centre to *Beggiatoa* mats indicate that the AOM zone could spread from small patches of reduced sediments. Here, both MOx and AOM communities were detected, and the AOM communities comprised both ANME-2 / Seep-SRB1 and ANME-3 / *Desulfobulbus*. Previous work showed that methane oxidation rates are highest in sediments below *Beggiatoa* mats

(Milkov et al., 2004; Pimenov et al., 1999), controlling methane emission very efficiently. Efflux of methane was found to be very low in this area of the HMMV with an up to 100-fold lower bottom water concentrations of methane compared to the thinly colonized mud volcano centre (Damm and Budeus, 2003; Sauter et al., submitted; Sauter et al., 2002). This provides evidence that AOM at the *Beggiatoa* site is an efficient filter for uprising methane.

CONCLUSION

Methane oxidation is the predominant, microbial biomass generating process in sediments of Håkon Mosby Mud Volcano. Biomarker analysis give evidence for a dominant, aerobic type I methanotrophic community prevailing in sediments of the central area, restricted to a thin surface layer of <1 cm in vertical extension. In the transition zone between the centre and the surrounding *Beggiatoa* habitat, small patches of reduced sediments are colonized by different methanotrophic guilds. Finally, a novel type of anaerobic methanotroph colonizes a <5 cm thick zone of the surface sediments, fuelling extensive *Beggiatoa* mats. Biomarker analyses, isotopic patterns and 16S rDNA identification were highly correlated. Maxima in microbial biomass were reflected in most depleted isotope signatures, indicating a strong selection of individual methanotrophic populations by the different habitats.

Acknowledgements

We thank the officers, crew and shipboard scientific party for support during the R/V Atalante and R/V Polarstern cruise in 2001 and 2003, respectively. We are especially indebted to the ROV Victor 6000 team for excellent technical operation and sample retrieval. Imke Busse, Viola Beyer and Friderike Heinrich are thanked for their support during sampling. Gabriele Klockether is acknowledged for support in the biomarker laboratory. This study was part of the MUMM (Mikrobielle Umsatzraten von Methan in Gashydrathaltigen Sedimenten, FN 03G0554A) supported by the Bundesministerium für Bildung und Forschung (BMBF, Germany). Further support was provided by the Max Planck Gesellschaft (Germany).

References

Aloisi G., Bouloubassi I., Heijs S. K., Pancost R. D., Pierre C., Damste J. S. S., Gottschal J. C., Forney L. J., and Rouchy J. M. (2002) CH4-consuming microorganisms and the formation of carbonate crusts at cold seeps. *Earth and Planetary Science Letters* **203**(1), 195-203.

Amann R. I., Krumholz L., and Stahl D. A. (1990) Fluorescent-oligonucleotide probing of whole cells for determinative, phylogenetic, and evironmental studies in microbiology. *Journal of Bacteriology* **172**, 762-770.

Birgel D., Stein R., and Hefter J. (2004) Aliphatic lipids in recent sediments of the Fram Strait/Yermak Plateau (Arctic Ocean): composition, sources and transport processes (revised version February 19th, 2004). *Marine Chemistry* **88**(3-4), 127-160.

Blumenberg M., Seifert R., Reitner J., Pape T., and Michaelis W. (2004) Membrane lipid patterns typify distinct anaerobic methanotrophic consortia. *Proceedings of the National Academy of Sciences of the United States of America* **101**(30).

Boetius A., Ravenschlag K., Schubert C., Rickert D., Widdel F., Gieseke A., Amann R., Jørgensen B. B., Witte U., and Pfannkuche O. (2000) A marine microbial consortium apparently mediating anaerobic methane of oxidation. *Nature* **407**, 623-626.

Bowman J. P., Skerratt J. H., Nichols P. D., and Sly L. I. (1991) Phospholipid Fatty-Acid and Lipopolysaccharide Fatty-Acid Signature Lipids in Methane-Utilizing Bacteria. *Fems Microbiology Ecology* **85**(1), 15-22.

Bowman J. P., Sly L. I., Nichols P. D., and Hayward A. C. (1993) Revised taxonomy of the methanotrophs: Description of *Methylobacter* gen. nov., emendation of *Methylococcus*, validation of *Methylosinus* and *Methylocystis* species, and a proposal that the family *Methylococcaceae* includes only the group I methanotrophs. *International Journal of Systematic Bacteriology* **43**(4), 735-753.

Charlou J. L., Donval J. P., Zitter T., Roy N., Jean-Baptiste P., Foucher J. P., and Woodside J. (2003) Evidence of methane venting and geochemistry of brines on mud volcanoes of the eastern Mediterranean Sea. *Deep-Sea Research Part I-Oceanographic Research Papers* **50**(8), 941-958.

Damm E. and Budeus G. (2003) Fate of vent-derived methane in seawater above the Hakon Mosby mud volcano (Norwegian Sea). *Marine Chemistry* **82**(1-2), 1-11.

Dimitrov L. I. (2002) Mud volcanoes - the most important pathway for degassing deeply buried sediments. *Earth-Science Reviews* **59**(1-4), 49-76.

Dimitrov L. I. (2003) Mud volcanoes - a significant source of atmospheric methane. *Geo-Marine Letters* **23**(3-4), 155-161.

Eldholm O., Sundvor E., Vogt P. R., Hjelstuen B. O., Crane K., Nilsen A. K., and Gladczenko T. P. (1999) SW Barents Sea continental margin heat flow and Hakon Mosby Mud Volcano. *Geo-Marine Letters* **19**(1-2), 29-37.

Elvert M., Boetius A., Knittel K., and Jorgensen B. B. (2003) Characterization of specific membrane fatty acids as chemotaxonomic markers for sulfate-reducing bacteria involved in anaerobic oxidation of methane. *Geomicrobiology Journal* **20**(4), 403-419.

Elvert M., Greinert J., Suess E., and Whiticar M. J. (2000) Archaea mediating anaerobic methane oxidation in deep-sea sediments at cold seeps of the eastern Aleutian subduction zone. *Organic Geochemistry* **31**(11), 1175-1187.

Elvert M., Greinert J., Suess E., and Whiticar M. J. (2001) Carbon isotopes of biomarkers derived from methane-oxidizing microbes at Hydrate Ridge, Cascadia convergent margin. In *Natural gas hydrates: Occurrence, distribution, and dynamics*, Vol. 124 (ed. C. K. Paull and W. P. Dillon), pp. 115-129. American Geophysical Union.

Elvert M., Hopmans E. C., Boetius A., and Hinrichs K.-U. (submitted) Spatial variatons of archaeal-bacterial assambladges in gas hydrate bearing sediments at a cold seep: Implications from a high resolution molecular and isotopic approach.

Elvert M., Suess E., and Whiticar M. J. (1999) Anaerobic methane oxidation associated with marine gas hydrates: superlight C-isotopes from saturated and unsaturated C_{20} and C_{25} irregular isoprenoids. *Naturwissenschaften* **86**(6), 295-300.

Fang J. S., Barcelona M. J., and Semrau J. D. (2000) Characterization of methanotrophic bacteria on the basis of intact phospholipid profiles. *Fems Microbiology Letters* **189**(1), 67-72.

Fisher C. R. and Childress J. J. (1992) Organic-Carbon Transfer from Methanotrophic Symbionts to the Host Hydrocarbon-Seep Mussel. *Symbiosis* **12**(3), 221-235.

Freeman K. H., Wakeham S. G., and Hayes J. M. (1994) Predictive isotopic biogeochemistry: Hydrocarbons from anoxic marine basins. *Organic Geochemistry* **21**(6/7), 629-644.

Hanson R. S., Bratina B. J., and Brusseau G. A. (1993) Phylogeny and ecology of methylotrophic bacteria. In *Microbial Growth on C_1 Compounds* (ed. J. C. Murrell and D. P. Kelly), pp. 285-302. Intercept Limited.

Hanson R. S. and Hanson T. E. (1996) Methanotrophic bacteria. *Microbiological Reviews* **60**(2), 439-&.

Hayes J. M., Takigiku R., Ocampo R., Callot H. J., and Albrecht P. (1987) Isotopic compositions and probable origins of organic molecules in the Eocene Messel shale. *Nature* **329**, 48-51.

Hinrichs K.-U. and Boetius A. (2002) The anaerobic oxidation of methane: New insights in microbial ecology and biogeochemistry. In *Ocean Margin Systems* (ed. G. Wefer, D. Billett, and D. Hebbeln), pp. 457-477. Springer-Verlag, Berlin.

Hinrichs K.-U., Hayes J. M., Sylva S. P., Brewer P. G., and DeLong E. F. (1999) Methane-consuming archaebacteria in marine sediments. *Nature* **398**, 802-805.

Hinrichs K.-U., Hmelo L. R., and Sylva S. P. (2003) Molecular Fossil Record of Elevated Methane Levels in Late Pleistocene Coastal Waters. *Science* **299**(5610), 1214-1217.

Hjelstuen B. O., Eldholm O., Faleide J. I., and Vogt P. R. (1999) Regional setting of Hakon Mosby Mud Volcano, SW Barents Sea margin. *Geo-Marine Letters* **19**(1-2), 22-28.

Jahnke L. L., Summons R. E., Hope J. M., and Des Marais D. J. (1999) Carbon isotopic fractionation in lipids from methanotrophic bacteria II: The effects of physiology and environmental parameters on the biosynthesis and isotopic signatures of biomarkers. *Geochimica et Cosmochimica Acta* **63**(1), 79-93.

Judd A. G., Hovland M., Dimitrov L. I., Gil S. G., and Jukes V. (2002) The geological methane budget at Continental Margins and its influence on climate change. *Geofluids* **2**(2), 109-126.

Klages M., Mesnil B., Soldtwedel T., and Christophe A. (2002) L' expédition "AWI" sur NO L'Atalante en 2001. [The Expedition "AWI" on RV L'Atalante in 2001]. Alfred-Wegener-Institute for Polar and Marine Research.

Klages M., Thiede J., and Foucher J. P. (2004) The Expedition ARKTIS XIX/3 of the Research Vessel POLARSTERN in 2003 Reports of legs 3a, 3b and 3c, pp. 355. Alfred-Wegener-Institute for Polar and Marine Research.

Knittel K., Boetius A., Lemke A., Eilers H., Lochte K., Pfannkuche O., Linke P., and Amann R. (2003) Activity, distribution, and diversity of sulfate reducers and other bacteria in sediments above gas hydrate (Cascadia margin, Oregon). *Geomicrobiology Journal* **20**(4), 269-294.

Knittel K., Losekann T., Boetius A., Kort R., and Amann R. (2005) Diversity and distribution of methanotrophic archaea at cold seeps. *Applied and Environmental Microbiology* **71**(1), 467-479.

Knoblauch C., Sahm K., and Jørgensen B. B. (1999) Psychrophilic sulfate-reducing bacteria isolated from permanently cold arctic marine sediments: description of *Desulfofrigus oceanense* gen. nov., sp. nov., *Desulfofrigus fragile* sp. nov., *Desulfofaba gelida* gen. nov., sp. nov., *Desulfotalea psychrophila* gen. nov., sp. nov. and *Desulfotalea arctica* sp. nov. *International Journal of Systematic Bacteriology* **49**, 1631-1643.

Kopf A., Klaeschen D., and Mascle J. (2001) Extreme efficiency of mud volcanism in dewatering accretionary prisms. *Earth and Planetary Science Letters* **189**(3-4), 295-313.

Kopf A. J. (2002) Significance of mud volcanism. *Reviews of Geophysics* **40**(2).

Lane D. J., Pace B., Olsen G. J., Stahl D. A., Sogin M. L., and Pace N. R. (1985) Rapid-Determination of 16s Ribosomal-Rna Sequences for Phylogenetic Analyses. *Proceedings of the National Academy of Sciences of the United States of America* **82**(20), 6955-6959.

Le Mer J. and Roger P. (2001) Production, oxidation, emission and consumption of methane by soils: A review. *European Journal of Soil Biology* **37**(1), 25-50.

Lein A., Vogt P., Crane K., Egorov A., and Ivanov M. (1999) Chemical and isotopic evidence for the nature of the fluid in CH4-containing sediments of the Hakon Mosby Mud Volcano. *Geo-Marine Letters* **19**(1-2), 76-83.

Levin L. A. and Michener R. H. (2002) Isotopic evidence for chemosynthesis-based nutrition of macrobenthos: The lightness of being at Pacific methane seeps. *Limnology and Oceanography* **47**(5), 1336-1345.

Lien T., Madsen M., Steen I. H., and Gjerdevik K. (1998) Desulfobulbus rhabdoformis sp. nov., a sulfate reducer from a water-oil separation system. *International Journal of Systematic Bacteriology* **48**, 469-474.

Manne A. S. and Richels R. G. (2001) An alternative approach to establishing trade-offs among greenhouse gases. *Nature* **410**(6829), 675-677.

Massana R., Murray A. E., Preston C. M., and DeLong E. F. (1997) Vertical distribution and phylogenetic characterization of marine planktonic Archaea in the Santa Barbara Channel. *Applied and Environmental Microbiology* **63**(1), 50-56.

Michaelis W., Seifert R., Nauhaus K., Treude T., Thiel V., Blumenberg M., Knittel K., Gieseke A., Peterknecht K., Pape T., Boetius A., Amann R., Jorgensen B. B., Widdel F., Peckmann J. R., Pimenov N. V., and Gulin M. B. (2002) Microbial reefs in the Black Sea fueled by anaerobic oxidation of methane. *Science* **297**(5583), 1013-1015.

Milkov A., Vogt P., Cherkashev G., Ginsburg G., Chernova N., and Andriashev A. (1999) Sea-floor terrains of Hakon Mosby Mud Volcano as surveyed by deep-tow video and still photography. *Geo-Marine Letters* **19**(1-2), 38-47.

Milkov A. V. (2000) Worldwide distribution of submarine mud volcanoes and associated gas hydrates. *Marine Geology* **167**(1-2), 29-42.

Milkov A. V., Sassen R., Apanasovich T. V., and Dadashev F. G. (2003) Global gas flux from mud volcanoes: A significant source of fossil methane in the atmosphere and the ocean. *Geophysical Research Letters* **30**(2).

Milkov A. V., Vogt P. R., Crane K., Lein A. Y., Sassen R., and Cherkashev G. A. (2004) Geological, geochemical, and microbial processes at the hydrate-bearing Hakon Mosby mud volcano: a review. *Chemical Geology* **205**(3-4), 347-366.

Moss C. W. and Lambert-Fair M. A. (1989) Location of Double Bonds in Monounsaturated Fatty Acids of Campylobacter cryaerophila with Dimethyl Disulfide Derivatives and Combined Gas Chromatography-Mass Spectrometry. *JOURNAL OF CLINICAL MICROBIOLOGY* **27**(7), 1467-1470.

Nauhaus K., Treude T., Boetius A., and Kruger M. (2005) Environmental regulation of the anaerobic oxidation of methane: a comparison of ANME-I and ANME-II communities. *Environmental Microbiology* **7**(1), 98-106.

Nichols P. D., Guckert J. B., and White D. C. (1986) Determination of monounsaturated fatty acid double-bond position and geometry for microbial monocultures and complex consortia by capillary GC-MS of their dimethyl disulphide adducts. *Journal of Microbiological Methods* **5**, 49-55.

Orphan V. J., Hinrichs K. U., Ussler W., Paull C. K., Taylor L. T., Sylva S. P., Hayes J. M., and Delong E. F. (2001a) Comparative analysis of methane-oxidizing archaea and sulfate- reducing bacteria in anoxic marine sediments. *Applied and Environmental Microbiology* **67**(4), 1922-1934.

Orphan V. J., House C. H., Hinrichs K. U., McKeegan K. D., and DeLong E. F. (2001b) Methane-consuming archaea revealed by directly coupled isotopic and phylogenetic analysis. *Science* **293**(5529), 484-487.

Peckmann J., Goedert J. L., Thiel V., Michaelis W., and Reitner J. (2002) A comprehensive approach to the study of methane-seep deposits from the Lincoln Creek Formation, western Washington State, USA. *Sedimentology* **49**(4), 855-873.

Peckmann J., Thiel V., Michaelis W., Clari P., Gaillard C., Martire L., and Reitner J. (1999) Cold seep deposits of Beauvoisin (Oxfordian; southeastern France) and Marmorito (Miocene; northern Italy): microbially induced authigenic carbonates. *International Journal of Earth Sciences* **88**(1), 60-75.

Pimenov N., Savvichev A., Rusanov I., Lein A., Egorov A., Gebruk A., Moskalev L., and Vogt P. (1999) Microbial processes of carbon cycle as the base of food chain of Håkon Mosby mud volcano benthic community. *Geo-Marine Letters* **19**, 89-96.

Rau G. H., Takahashi T., and Marais D. J. D. (1989) Latitudinal Variations in Plankton Delta-C-13 - Implications for Co2 and Productivity in Past Oceans. *Nature* **341**(6242), 516-518.

Ravenschlag K., Sahm K., Pernthaler J., and Amann R. (1999) High bacterial diversity in permanently cold marine sediments. *Applied and Environmental Microbiology* **65**(9), 3982-3989.

Reeburgh W. S. (1996) "Soft spots" in the global methane budget. In *Microbial Growth on C_1 Compounds* (ed. M. E. Lidstrom and F. R. Tabita), pp. 334-342. Kluwer Academic Publishers.

Rohmer M., Bouvier-Nave P., and Ourisson G. (1984) Distribution of hopanoid triterpenes in prokaryotes. *Journal of General Microbiology* **130**, 1137-1150.

Roslev P., Iversen N., and Henriksen K. (1998) Direct fingerprinting of metabolically active bacteria in environmental samples by substrate specific radiolabelling and lipid analysis. *Journal of Microbiological Methods* **31**(3), 99-111.

Rutters H., Sass H., Cypionka H., and Rullkotter J. (2002) Phospholipid analysis as a tool to study complex microbial communities in marine sediments. *Journal of Microbiological Methods* **48**(2-3), 149-160.

Rütters H., Sass H., Cypionka H., and Rullkötter J. (2001) Monoalkylether phospholipids in the sulfate-reducing bacteria *Desulfosarcina variabilis* and *Desulforhabdus amnigenus*. *Archives of Microbiology* **176**(6), 435-442.

Sass A., Rutters H., Cypionka H., and Sass H. (2002) Desulfobulbus mediterraneus sp nov., a sulfate-reducing bacterium growing on mono- and disaccharides. *Archives of Microbiology* **177**(6), 468-474.

Sauter E., Muyakshin J., Charlou J., Schlüter M., Boetius A., Jerosch K., Damm E., Foucher J. P., and Klages M. (submitted) Methane discharge from a deep-sea submarine mud volcano into the upper water column by gas hydrate-coated methane bubbles. *Earth and Planetary Science Letters*.

Sauter E., Schlüter M., Boetius A., and Baumann L. (2002) Geochemistry of Hakon Mosby Mud Vulcano (HMMV) bottom water and sediments, Report on Polar and Marine Research, pp. 47-53. Alfred-Wegener-Institut für Polar- und Meeresforschung (AWI).

Schouten S., van der Maarel M. J. E. C., Huber R., and Sinninghe Damsté J. S. (1997) 2,6,10,15,19-pentamethylicosenes in *Methanolobus bombayensis*, a marine methanogenic archaeon, and in *Methanosarcina mazei*. *Organic Geochemistry* **26**(5/6), 409-414.

Shilov V. V., Druzhinina N. I., Vasilenko L. V., and Krupskaya V. V. (1999) Stratigraphy of sediments from the Hakon Mosby Mud Volcano Area. *Geo-Marine Letters* **19**(1-2), 48-56.

Sibuet M. and Olu K. (1998) Biogeography, biodiversity and fluid dependence of deep-sea cold-seep communities at active and passive margins. *Deep-Sea Research Part Ii-Topical Studies in Oceanography* **45**(1-3), 517-+.

Smirnov R. V. (2000) Two new species of Pogonophora from the arctic mud volcano off northwestern Norway. *Sarsia* **85**(2), 141-150.

Snaidr J., Amann R., Huber I., Ludwig W., and Schleifer K. H. (1997) Phylogenetic analysis and in situ identification of bacteria in activated sludge. *Applied and Environmental Microbiology* **63**(7), 2884-2896.

Somoza L., Diaz-del-Rio V., Leon R., Ivanov M., Fernandez-Puga M. C., Gardner J. M., Hernandez-Molina F. J., Pinheiro L. M., Rodero J., Lobato A., Maestro A., Vazquez J. T., Medialdea T., and Fernandez-Salas L. M. (2003) Seabed morphology and hydrocarbon seepage in the Gulf of Cadiz mud volcano area: Acoustic imagery, multibeam and ultra-high resolution seismic data. *Marine Geology* **195**(1-4), 153-176.

Strunk O., Gross O., Reichel B., May M., Hermann S., Stuckman N., Nonhoff B., Lenke M., Ginhart A., Vilbig A., Ludwig T., Bode A., Schleifer K.-H., and Ludwig W. (1998) ARB: a software environment for sequence data. www.mikro.biologie.tu-muenchen.de. Department of Microbiology Technische Universität München, Munich, Germany.

Summons R. E., Jahnke L. L., and Roksandic Z. (1994) Carbon isotopic fractionation in lipids from methanotrophic bacteria: Relevance for interpretation of the geochemical record of biomarkers. *Geochimica Et Cosmochimica Acta* **58**(13), 2853-2863.

Sun M. Y., Wakeham S. G., and Lee C. (1997) Rates and mechanisms of fatty acid degradation in oxic and anoxic coastal marine sediments of Long Island Sound, New York, USA. *Geochimica Et Cosmochimica Acta* **61**(2), 341-355.

Taylor J. and Parkes R. J. (1983) The cellular fatty acids of the sulphate-reducing bacteria, *Desulfobacter* sp., *Desulfobulbus* sp. and *Desulfovibrio desulfuricans*. *Journal of General Microbiology* **129**, 3303-3309.

Teske A., Hinrichs K. U., Edgcomb V., Gomez A. D., Kysela D., Sylva S. P., Sogin M. L., and Jannasch H. W. (2002) Microbial diversity of hydrothermal sediments in the Guaymas Basin: Evidence for anaerobic methanotrophic communities. *Applied and Environmental Microbiology* **68**(4), 1994-2007.

Thiel V., Peckmann J., Richnow H. H., Luth U., Reitner J., and Michaelis W. (2001) Molecular signals for anaerobic methane oxidation in Black Sea seep carbonates and a microbial mat. *Marine Chemistry* **73**(2), 97-112.

Thiel V., Peckmann J., Seifert R., Wehrung P., Reitner J., and Michaelis W. (1999) Highly isotopically depleted isoprenoids: molecular markers for ancient methane venting. *Geochimica et Cosmochimica Acta* **63**(23/24), 3959-3966.

Vogt P. R., Cherkashev A., Ginsburg G. D., Ivanov G. I., Crane K., Lein A. Y., Sundvor E., Pimenov N. V., and Egorov A. (1997a) Haakon Mosby mud volcano: A warm methane seep with seafloor hydrates and chemosynthesis-based Ecosystem in late Quantemary Slide Valley, Bear Island Fan, Barents Sea passive margin. *EOS Transactions of the American Geophysical Union Supplement* **78**(17), 187-189.

Vogt P. R., Cherkashev G., Ginsburg G., Ivanov G. I., Milkov A., Crane K., Lein A., Sundvor E., Pimenov N. V., and Egorov A. (1997b) Haakon Mosby Mud Volcano Provides

Unusual Example of Venting. *EOS Transactions of the American Geophysical Union Supplement* **78**(48), 549, 556-557.

Werne J. P., Baas M., and Damste J. S. S. (2002) Molecular isotopic tracing of carbon flow and trophic relationships in a methane-supported benthic microbial community. *Limnology and Oceanography* **47**(6), 1694-1701.

Whiticar M. J. (1999) Carbon and hydrogen isotope systematics of bacterial formation and oxidation of methane. *Chemical Geology* **161**(1-3), 291-314.

Wuebbles D. J. and Hayhoe K. (2002) Atmospheric methane and global change. *Earth-Science Reviews* **57**(3-4), 177-210.

Aerobic and anaerobic oxidation of methane in sediments of Håkon Mosby Mud Volcano, Barents Sea

Helge Niemann[1,2], Eberhard Sauter[2], Martin Krüger[1+], Friederike Heinrich[1*], Tina Lösekann[1], Marcus Elvert[1×], Antje Boetius[1,2, 3]

[1]Max Planck Institute for Marine Microbiology Bremen, Celsiusstr.1, 28359 Bremen, Germany

[2]Alfred Wegener Institute for Polar and Marine Research, Am Handelshafen 12, 27515 Bremerhaven, Germany

[3]International University Bremen, Campusring, 28759 Bremen, Germany

Present addresses:

[+]Bundesanstalt für Geowissenschaften und Rohstoffe, Stille Weg 2, 30655 Hannover

[*]Institute for Palaeontology, Erlangen University, Loewenichstr. 28, 91054 Erlangen

[x]Research Center Ocean Margins, University of Bremen, Leobener Str., 28359 Bremen

Author to whom correspondence should be addressed:

Helge Niemann
Max Planck Institute for Marine Microbiology, Celsiusstr. 1, 28359 Bremen, Germany
email: hniemann@mpi-bremen.de, phone +49-421-2028653

ABSTRACT

The Håkon Mosby Mud Volcano (HMMV) is an active methane seeping mud volcano of ca. 1 km in diameter at 1250 m water depth on the Norwegian margin of the Barents Sea (72°00'N, 14°45' E). Previous (Milkov et al., 2004) and recent videographic mapping of the seafloor indicates three distinct habitats: (1) a central area covered by greyish muds; concentrically enclosed by (2) a belt of blackish, highly reduced sediments covered with white mats of the thiotrophic bacterium *Beggiatoa sp.*; (3) and an outer rim of brownish sediments, which are densely populated by pogonophoran worms. During dives with the remotely operated vehicle (ROV) Victor 6000 of IFREMER in 2003, another more fractured type of habitat was discovered at the boundary of the centre. Here, and in the vicinity of gas ebullition sites, patches of reduced sediments covered with greyish microbial mats were found. These four habitats were sampled with ROV push cores, a video-guided multiple corer and gravity cores for *ex situ* measurements of aerobic and anaerobic methane oxidation as well as sulphate reduction rates. Aerobic or anaerobic oxidation of methane dominates biogeochemical processes in the HMMV sediments and is carried out by different microbial communities in distinct zones of the mud volcano. Chloride and bromide concentration profiles provide evidence that differences in advective flow of pore water is a main factor determining this zonation. In the centre, a high upward flow of sulphate-free subsurface fluids strongly limits the penetration depth of sulphate and oxygen. Here, aerobic oxidation of methane (MOx) is restricted to the top cm sediment layer with rates of 0.9 mol m^{-2} yr^{-1} and anaerobic oxidation of methane (AOM) is absent. In the patches of reduced sediments covered with grey mats, a deeper penetration of sulphate from seawater was observed, fueling AOM activity down to >12 cm with rates of 12.4 mol m^{-2} yr^{-1}. Adjacent to the centre at the *Beggiatoa* site, decreased upward fluid flow and the activity of the Beggiatoa filaments allows for an AOM zone of ca 5 cm at the sediment surface with rates of 4.5 mol m^{-2} yr^{-1}. The

stoichiometry of anaerobic oxidation of methane with sulphate was 1:1. Furthermore, *in vitro* incubations of surface sediments from the centre and the *Beggiatoa* site revealed the adaptation of aerobic and anaerobic oxidation of methane to the ice-cold temperatures of -1°C at the seafloor. At the outer rim of the HMMV, bioventilation of the pogonophoran worms irrigates a much deeper zone with oxygen- and sulphate-rich seawater. MOx activity of the free-living methanotrophic community in the oxygenated surface sediments was comparably low with 0.2 mol m^{-2} yr^{-1}. A defined methane-sulphate transition zone was found just beneath the roots of the tubeworms at 67 to 77 cm sediment depth. Here, AOM activity was high with 7.1 mol m^{-2} yr^{-1}. With respect to the area size of the different habitats at HMMV, microbial consumption reduces the methane efflux of HMMV by ca 7* 10^{-5} Tg yr^{-1}, i.e. 22 to 55%.

1. INTRODUCTION

Methane is an aggressive greenhouse gas with a high global warming potential (Manne and Richels, 2001). Variation in methane fluxes to the atmosphere have contributed significantly to global climate changes throughout the history of the earth (Kasting and Siefert, 2002; Petit et al., 1999; Wuebbles and Hayhoe, 2002). Increasing research effort has therefore been dedicated to elucidate sources and sinks of methane on earth. One important source of atmospheric methane are mud volcanoes occurring in terrestrial and marine environments (Dimitrov, 2003; Kopf, 2002; Milkov et al., 2003). Marine mud volcanoes represent a special type of cold seep ecosystems expelling deep subsurface muds together with fluids and gases to the sea floor (Charlou et al., 2003; Kopf, 2002; Somoza et al., 2003). Estimates of marine mud volcanoes range between 800 and 100000 worldwide. (Dimitrov and Woodside, 2003; Dimitrov, 2002; Dimitrov, 2003; Kopf, 2002; Milkov, 2000; Milkov et al., 2003). However, it is currently not known how many of these structures are actively emitting gases to the hydrosphere.

Microbial consumption mediated aerobically by bacteria or anaerobically by archaea are the main biological sinks of methane (Hinrichs and Boetius, 2002; Lelieveld et al., 1998; Reeburgh, 1996; Whiticar, 1999). Bacteria involved in MOx have been reported from oxygenated wetlands, soils, freshwater, marine waters and as symbionts in invertebrates (Fisher, 1990; Hanson et al., 1993; Larock et al., 1994; Le Mer and Roger, 2001). Not much is known about the relevance of MOx in marine sediments. However, due to the very limited oxygen penetration depth in aquatic sediments, MOx communities are most likely restricted to very narrow zones of surface sediments whereas methane rich sediments are mostly found deeper in anoxic sediments. Hence, the main sink for methane in the ocean is AOM coupled to sulphate reduction (SR) according to the following net equation:

$$CH_4 + SO_4^{2-} = HCO_3^- + HS^- + H_2O \quad (1)$$

(Hinrichs and Boetius, 2002; Iversen and Jørgensen, 1985). This stoichiometry has been validated by *ex situ* and *in vitro* rate measurements with environmental sediment samples hosting AOM communities (Nauhaus et al., 2002; Nauhaus et al., 2005; Treude et al., 2003). Two distinct lineages of archaea, ANME-1 and ANME-2 are known to mediate AOM in consortium with sulphate reducing bacteria (SRB) of the Desulfosarcina/Desulfococcus cluster (Seep-SRB1; Boetius et al., 2000 ; Hinrichs et al., 1999; Knittel et al. 2003; Knittel et al., 2005 ; Michaelis et al., 2002 ; Orphan et al., 2001). The biochemical functioning of AOM has not been elucidated yet, but increasing evidence suggests that the process is a reversal of methanogenesis (Hallam et al., 2004; Krüger et al., 2003; Valentine and Reeburgh, 2000). The role of SRB could be the rapid removal of an unknown intermediate via SR, thus maintaining thermodynamic conditions favouring AOM.

AOM is of particular importance at deep-water cold seeps where advective fluid flow supplies surface sediments with high amounts of methane (Boetius and Suess, 2004). To date, methane seeps at the Cascadia convergent margin (Hydrate Ridge), in the Gulf of Mexico and on the Crimean Shelf were extensively studied with respect to AOM processes and the responsible microbial communities (Joye et al., 2004; Nauhaus et al., 2002; Nauhaus et al., 2005; Treude et al., 2003). Only very few investigations of methane turnover processes at mud volcanoes have been carried out (Haese et al., 2003; Pimenov et al., 1999). One aim of this study was to quantify methane oxidation rates in different zones of the HMMV, and to compare the relevance of aerobic and anaerobic processes. A second goal was to validate the stoichiometry of AOM at HMMV and to investigate the effect of temperature and methane concentrations *in vitro*. Finally, a preliminary budget for methane consumption versus methane emission at the

HMMV is presented to highlight the relevance of focused methane sources on continental margins.

2. MATERIAL AND METHODS

2.1 Sampling Location

The HMMV is a glacial deposit of 3 km thickness (Shilov et al., 1999) located at 72° 00,25'N and 14° 43.50'E in 1250 m water depth in the SW Barents Sea (Vogt et al., 1997a; Vogt et al., 1997b). A review of previous geological and biological research at HMMV is given by Milkov et al. (2004). Briefly, the HMMV has a circular shape with 1 km in diameter (0.8 km^2), a relief of up to 10 m above sea floor and it is surrounded by a circular, ca. 200 m wide depression (Hjelstuen et al., 1999; Vogt et al., 1997a). Thermal gradients in the centre are high with values of 10°C m^{-1} where methane-rich sediments are expelled through a central conduit (Eldholm et al., 1999; Ginsburg et al., 1999; Vogt et al., 1997b). Source methane at HMMV is of a mixed microbial-thermogenic origin (Lein et al., 1999).

HMMV was visited during two cruises with R/V L'Atalante together with ROV "Victor 6000" (IFREMER, Brest) in 2001 and R/V Polarstern (Alfred Wegener Institut for Polar and Marine Research; ARK XIX 3b) together with ROV Victor 6000 (IFREMER, Brest) in 2003 (Klages et al., 2002; Klages et al., 2004).

2.2 Sample Collection and Storage

Sediment samples were obtained from distinct habitats ("central area", "grey mat", "*Beggiatoa* mats", "*Pogonophora* zones", "reference site") by ROV push coring, video

Table 1. Station data of habitats investigated during two cruises with R/V Atalante (ATL) and Polarstern (ARK XIX3b) in 2001 and 2003, respectively. Sediment cores were recovered with the remote operated vehicle (ROV) Victor 6000, a video guided multiple corer (MUC) and a gravity corer (GC). Applied analytical tools were: AOM, SR = *ex situ* rate measurements of anaerobic oxidation of methane and sulphate reduction; CH_4, SO_4^{2-} = concentration measurements of methane and sulphate; IV = *in vitro* incubation experiments; Cl^-, Br^- = concentration measurements of chloride and bromide. Note that the applied technique to measure methane oxidation does not discriminate between the aerobic and anaerobic oxidation mode, respectively, but that we assumed zones for MOx and AOM according to the porewater geochemistry (see methods).

Habitat	Cruise	Device (cores)	Applied methods
Centre	ARK XIX3b	MUC (312-7, 314-3)	AOM, SR, CH_4 SO_4^{2-}, IV
	ATL	ROV (25-PC24, 25-PC27)	SO_4^{2-}, Cl^-, Br^-
gr. mat	ARK XIX3b	ROV (347, 377)	AOM, SR, CH_4 SO_4^{2-}
Beggiatoa	ARK XIX3b	ROV (317-1, 317-2)	AOM, SR, CH_4 SO_4^{2-}, IV
		MUC (322)	AOM, SR, CH_4 SO_4^{2-}, IV
	ATL	ROV(19-PC3, 25PC-17, 25PC8)	SO_4^{2-}, Cl^-, Br^-, IV
		MUC (12)	SO_4^{2-}, Cl^-, Br^-
Pogonophora	ARKXIX3b	ROV (326)	AOM, SR, CH_4 SO_4^{2-}, IV
		GC (341, 336)	AOM, SR, CH_4 SO_4^{2-}
	ATL	ROV (25-PC8')	SO_4^{2-}, Cl^-, Br^-, IV
		MUC (18, 22)	SO_4^{2-}, Cl^-, Br^-, IV
Reference	ARKXIX3b	MUC (362-1)	AOM, SR, CH_4 SO_4^{2-}, IV
	ATL	MUC (28)	SO_4^{2-}, Cl^-, Br^-

guided multiple-coring and gravity coring (Tab. 1). Upon recovery, push core and multiple corer (MUC) core samples were immediately transferred into a cold room. Gravity cores where sectioned on deck into 1 m pieces, cut in half, and immediately subsampled. Sediments obtained during the Atalante cruise in 2001 were mainly analysed for concentrations of pore water constituents (sulphate, chloride, bromide). Methane analyses were problematic due to the rapid degassing upon retrieval in samples from central, Beggiatoa, and grey mat sites. During the Polarstern cruise in 2003 we concentrated on *ex situ* concentrations and turnover rates of methane and sulphate (Tab. 1). During the Atalante cruise in 2001, ROV push and

MUC cores were sliced into 1 cm sections and pore water was extracted by pressure filtration (5 bars) through Teflon squeezers provided with 0.2 µm cellulose acetate filters. Aliquots of pore water for sulphate concentration measurements were fixed in aqueous zinc-acetate solution (20%, w/v) whereas samples for chloride and bromide concentration measurements were stored at –20°C until chromatography analysis. ROV push and MUC cores obtained during the Polarstern cruise in 2003 were subsampled vertically with small push cores (acrylic core liners, 26 mm diameter) according to a previous publication (Treude et al., 2003). The gravity cores were subsampled horizontally with glass tubes (60 mm length, 10 mm diameter). The small push cores and the glass tubes were sealed immediately after subsampling with butyl rubber stoppers to prevent gas exchange. Sediments for *in vitro* incubation experiments were pooled from replicate ROV push and MUC cores and stored aerobically or anaerobically at *in situ* temperature until further treatment (Tab. 1).

2.3 Field Measurements

2.3.1 Ex-situ AOM, MOx and SR Rate Measurements

Sediment for turnover rate measurements were incubated on board according to previously described methods (Treude et al., 2003). Briefly, 25µl $^{14}CH_4$ (dissolved in water, 2.5 kBq) and 5 µl $^{35}SO_4^{2-}$ tracer (dissolved in water, 50 kBq) were injected in 2 cm intervals into the small push cores (whole core injection) or into the butyl rubber sealed glass tubes. Incubations were carried out for 24 h (pushcores) or for 36 h (gravity cores) at *in situ* temperature in the dark. Subsequently, incubated AOM and SR rate samples were fixed in 25 ml NaOH (2.5%, w/v) and 25 ml zinc acetate solution (20%, w/v), respectively. Further processing of AOM and SR

rate samples was performed according to Treude et al (2003) and references therein. Turnover rates were calculated according to the following formulas:

$$\mathrm{AOM} = \frac{{}^{14}\mathrm{CO_2}}{{}^{14}\mathrm{CH_4} + {}^{14}\mathrm{CO_2}} \times \frac{\mathrm{conc.\,CH_4}}{\mathrm{incubat.\,Time}} \quad (2)$$

$$\mathrm{SRR} = \frac{\mathrm{TRI}^{35}\mathrm{S}}{{}^{35}\mathrm{SO_4}^{2-} + \mathrm{TRI}^{35}\mathrm{S}} \times \frac{\mathrm{conc.\,SO_4}^{2-}}{\mathrm{incubat.\,Time}} \quad (3)$$

Here, $^{14}CO_2$, $^{35}SO_4^{2-}$ and $TRI^{35}S$ are the activities (Bq) of carbon dioxide, sulphate and total reduced sulphur species, respectively, whereas conc. CH_4 and conc. SO_4^{2-} are the concentrations of methane and sulphate at the beginning of the incubation. MOx activity was determined in the same way as AOM. In both processes the oxidized ^{14}C-methane is trapped as $^{14}CO_2$. The availability of either oxygen or sulphate determines which process occurs. Here, we distinguished between MOx and AOM zones by (1) *ex situ* oxygen and sulphide measurements (de Beer et al., submitted) and (2) absence or presence of sulphate reduction rates (SRR). *In situ* MOx zones were defined as the top most sediment horizon at the centre (0-2 cm), 0-9 cm at the *Pogonophora* site and 0-4 cm at the reference site. Due to the high sulphide concentrations and the AOM to SR stoichiometry in the *Beggiatoa* and grey mat sediments as well as in deeper strata of the *Pogonophora* site, we assumed an absence of MOx at these sites.

Ex situ measurements of gassy deep-water sediments are problematic because concentrations of methane and sulphate after core retrieval will deviate from methane and sulphate concentrations *in situ*, especially at sites of high advective fluid flow. In the highly gassy sediments of the HMMV from 1250 m water depth, there is most likely substantially more methane but less sulphate and oxygen available *in situ* compared to *ex situ*. Hence, our rate

measurements are likely to underestimate aerobic and anaerobic methane oxidation and the figures for areal methane consumption could be substantially higher.

2.3.2 Methane and Sulphate Concentrations

Core samples were sliced in 2 cm sections and sediments for methane or sulphate concentration measurements were fixed with 25 ml NaOH (2.5%, w/v) in a diffusion tight glass vial or with 25 ml zinc acetate solution (20%, w/v) in a 50 ml corning vial, respectively. Shortly after the cruise, methane concentrations were determined according to the "headspace" method using a gas chromatograph as described elsewhere (Treude et al., 2003). Methane concentration measurements were calibrated for a concentration range of 0.001 to 5 mM methane (final concentration in the sediment). For sulphate concentration measurements, the sediment particles were separated from the aqueous phase by centrifugation and filtration. Sulphate concentrations were determined from an aliquot of the aqueous supernatant using a Waters HPLC system (Waters 512 HPLC pump, I.C.-Pak anion-column (Waters; WAT007355) 4.6 x 50 mm, Waters 730 conductivity detector). Isophtalic acid (1 mM) was used as a solvent at a constant flow rate of 1ml min^{-1}. The system was calibrated using standard solutions in the sulphate specific concentration range. Total sulphate concentrations were corrected for porosity which was determined according to a previously described method (Treude et al., 2003).

2.3.3 Chloride and Bromide Concentrations

Anions were analysed by ion chromatography. A Metrohm^{TM} 761 Compact IC with chemical suppression and conductivity detector was used, equipped with a 250 x 4 mm ultra high capacity column of the type Metrosep^{TM} A Supp 5. Combined with a variable amplification of the conductivity signal, this column allows simultaneous measures of major and minor anions. A carbonate buffer solvent (3.2 mM Na_2CO_3 / 1 mM $NaHCO_3$) was used at a flow of 0.7 ml min^{-1}. Pore water samples were diluted 1:40 with the solvent and in-line filtered by a Metrohm^{TM} 788 IC auto sampler right before 20 µl were injected into the chromatography system. The system was calibrated using Merck CertiPUR^{TM} standard solutions in the ion-specific concentration range.

2.3.4 In Vitro Incubations

2.3.4.1 Sediment slurry preparations - Sediment samples were split on board into two sets for subsequent aerobic and anaerobic manipulations, respectively. Aerobic manipulations were carried out at atmospheric oxygen concentrations. For the aerobic experiments, oxygenated artificial seawater medium with 28 mM sulphate concentration was used (Widdel and Bak, 1992). Sediment samples were diluted 1:1 with this medium prior to transfer into Hungate tubes (20 ml) and incubation as specified previously (Nauhaus et al., 2002). 3 ml of these slurries were then mixed with 9 ml of oxygenated seawater medium yielding the final slurries for *in vitro* incubations. The remaining headspace was filled with an O_2-CH_4 mixture (1:1, v/v). Anaerobic experiments were conducted at strictly anoxic conditions under a nitrogen atmosphere (glove box). For the anaerobic experiments, sediment slurries were prepared as for aerobic manipulations except that anaerobic artificial seawater media with 0.5 mM

sulphide concentration was used (Widdel and Bak, 1992). Furthermore, the headspace was filled with pure methane yielding a concentration of ca. 1.5 mM methane in the aqueous medium (Yamamoto et al., 1976),.

2.3.4.2 In vitro MOx, AOM and SR rate measurements – In contrast to *ex situ* rates, *in vitro* rates represent conditions where the microbial community in the sediment is supplied with known concentrations of substrate (oxygen, methane at atmospheric saturation). In the present experiment, we used sediments which were pre-incubated for ~0.5 yr under methane which might have lead to higher numbers of methane oxidising and sulphate reducing microbes. To measure the potentials of MOx, AOM and SR at the four major habitats at HMMV (centre, grey mat, *Beggiatoa*, *Pogonophora*) and a reference site, sediment slurries from the surface (0-3 cm) and a deeper horizon (3-10 cm) were incubated in a vertical position to facilitate gas diffusion at 4°C for 1 wk. As a control, the same slurries were incubated with pure N_2 instead of CH_4 in the headspace. Aliquots of the headspace and the medium were extracted in balance with nitrogen daily and analysed for concentrations of methane and sulphide, respectively, according to Nauhaus et al. (2002). Turnover rates were determined from the change in methane and sulphide concentrations, respectively.

The temperature optimum and the stoichiometry of AOM and SR as well as the response of AOM activity to changing methane concentrations were determined from sediment slurries of the *Beggiatoa* site (0-3 cm). The response of MOx activity to temperature and changing methane concentrations was determined from sediment slurries of the centre site (0-3 cm). The temperature optimum for AOM at HMMV was determined from slurry incubations at temperatures of 1, 4, 8, 16 and 20°C, respectively. For MOx, 4 different temperatures (4, 12, 20 and 28°C) were chosen to investigate the response to temperature. These incubations were

carried out for 1 wk. To investigate the stoichiometry of AOM, methane utilisation and sulphide production were investigated at 4°C over a time period of 144 days. Furthermore, the effect of increasing methane concentrations on AOM activity was examined in incubations (1 wk) of sediment slurries with methane concentrations of 1.75, 15.4 and 40 mM by applying methane partial pressures of 0.1, 1.1 and 2.9 MPa, respectively. The response of MOx activity to changing methane concentrations was investigated at methane concentrations of 3.3 mM (0.24 MPa) and 8.3 mM (0.6 MPa). Pressure incubations were carried out according to the specifications provided by Nauhaus et al. (2002).

3. RESULTS

3.1 Field Measurements

3.1.1 Centre

As a result of the strong pressure change during recovery (1250 m water depth), sediment cores from the centre were subjected to gas ebullition. Methane concentrations were thus close to the saturation level of 1.5 mM at the ambient pressure on board (1 bar) over the entire vertical profile (data not shown). Sulphate concentrations showed a substantial decline with depth in all cores (n = 3, Fig. 1a). The *ex situ* sulphate penetration depth varied from 8 to 22 cm bsf between replicate cores. Similarly, chloride concentrations declined with depth from concentrations typical for sea water (610 mM) at the sediment surface to values as low as 415 mM at the bottom of the core (Fig. 1b). Bromide showed an increase from seawater values (0.84 mM) to values ~1.8 mM at 17.5 cm bsf (Fig. 1c). MOx rates were between 0.04 and 0.29 μmol cm^{-3} d^{-1} in the uppermost (0-2 cm) sediment horizon in all replicates (Fig.1a). Integrated over this horizon, methane oxidation (n = 4) was 0.9 (±0.4 standard error, S_E) mol m^{-2} yr^{-1} (Fig. 3). Despite the sharp sulphate gradients, SR was low in all replicates over the entire vertical profile down to 19 cm (on average 0.002 μmol cm^{-3} d^{-1}) (Fig. 2b). Integrated over depth (0-12 cm) SR (n = 4) was 0.11 (±0.05 S_E) mol m^{-2} yr^{-1} on average (Fig. 3). SR and methane oxidation rates were insignificant (<0.001 μmol cm^{-3} d^{-1}) in deeper sediment layers sampled by gravity coring (data not shown).

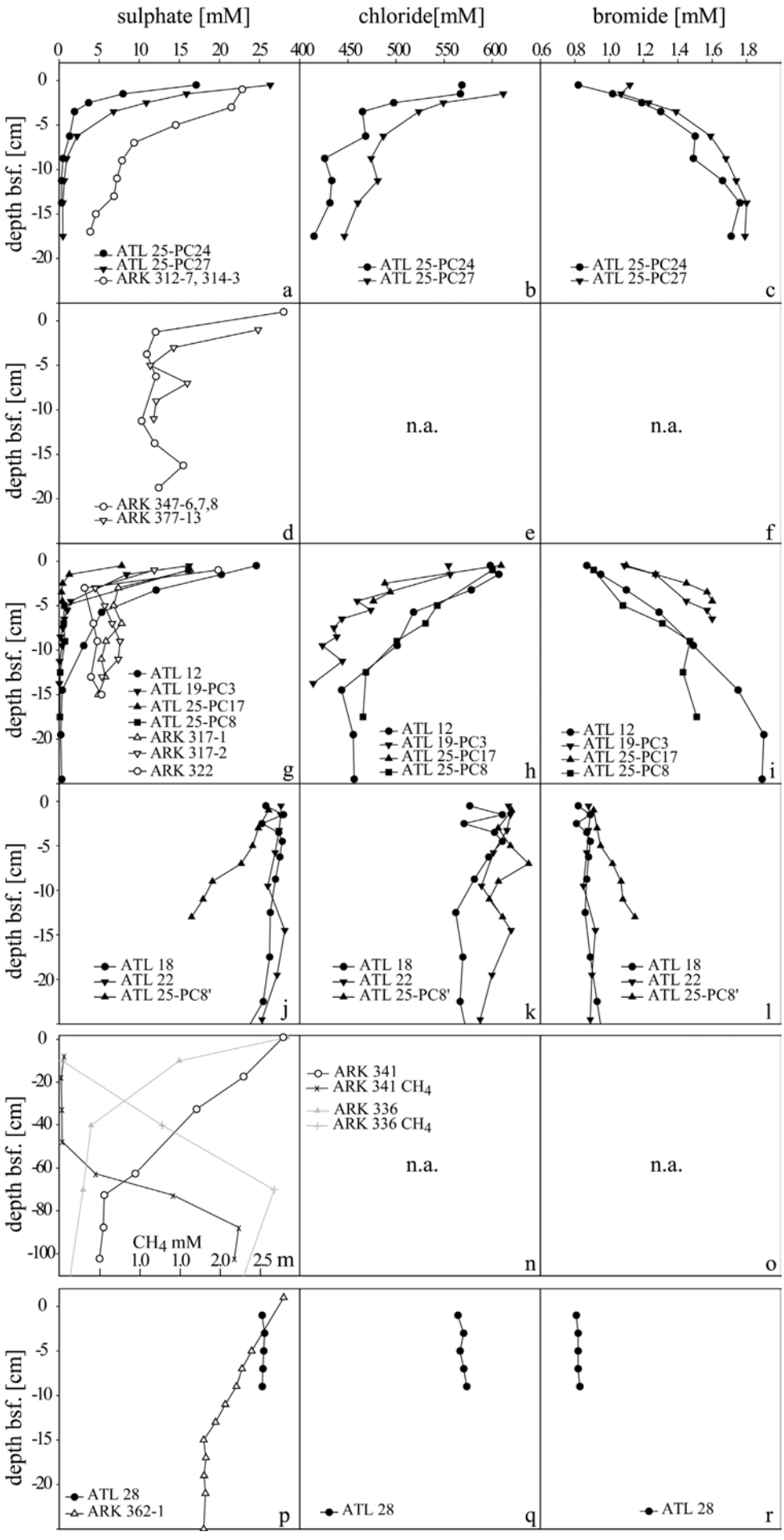
sulphate [mM]
chloride[mM]
bromide [mM]
depth bsf. [cm]
ATL 25-PC24
ATL 25-PC27
ARK 312-7, 314-3
a
b
c
ARK 347-6,7,8
ARK 377-13
d
n.a.
e
f
ATL 12
ATL 19-PC3
ATL 25-PC17
ATL 25-PC8
ARK 317-1
ARK 317-2
ARK 322
g
h
i
ATL 18
ATL 22
ATL 25-PC8'
j
k
l
ARK 341
ARK 341 CH4
ARK 336
ARK 336 CH4
CH4 mM
m
n
o
ATL 28
ARK 362-1
p
q
r

Figure 1. Pore water concentrations of sulphate (left panels), chloride (central panels) and bromide (right panels) at the centre (a,-c), grey mat (d), *Beggiatoa* (g-i), *Pogonophora* (j-m) and reference site (p-r). Methane concentrations are presented for the *Pogonophora* site (m). Note that the figure legend of panel (m) is in panel (n). Methane concentrations were at saturation level (~1.5 mM) for the on board conditions in retrieved cores of the centre, grey mat and *Beggiatoa* site and <0.01 mM at the reference site. n.a. = not available. ARK and ATL indicate samples taken during the R/V Polarstern and R/V Atalante cruise, respectively.

3.1.2 Grey Mats

Similar to the centre site, sediments recovered from the grey mats were subjected to gas ebullition. Consequently, methane concentrations were at ca. 1.5 mM over the entire vertical profile (data not shown). Sulphate concentrations showed an initial decline with depth but remained relatively constant at approximately 11 mM below 5 cm bsf (Fig. 1d). Chloride and Bromide were not measured in sediments below grey mats. AOM and SR rates showed a high variability between stations (different patches of grey mats) and replicates (Fig. 2c,d). At station ARK XIX3b 377, AOM and SR rates were comparably low with values ranging from 0.01 to 0.1 (n = 2) and from 0.01to 0.12 μmol cm^{-3} d^{-1} (n = 3), respectively, without showing any specific trend with sediment depth. AOM and SR rates at station ARK XIX3b 347 were higher with values ranging from 0.04 to 0.76 (n = 3) and from 0.01 to 2.24 μmol cm^{-3} d^{-1} (n = 3), respectively. Despite the high variability between replicates, AOM and SR rates were generally highest in the upper 5 cm of the sediment core. Notably, one replicate of SRR measurements was one order of magnitude higher than the other replicates of station ARK XIX3b 347. At the grey mat site, AOM (n = 5) and SR (n = 6), integrated over 0-12 cm sediment depth, showed comparable mean values of 12.4 (±3.1 S_E) and 14.6 (±11.7 S_E) mol m^{-2} yr^{-1}, respectively (Fig. 3).

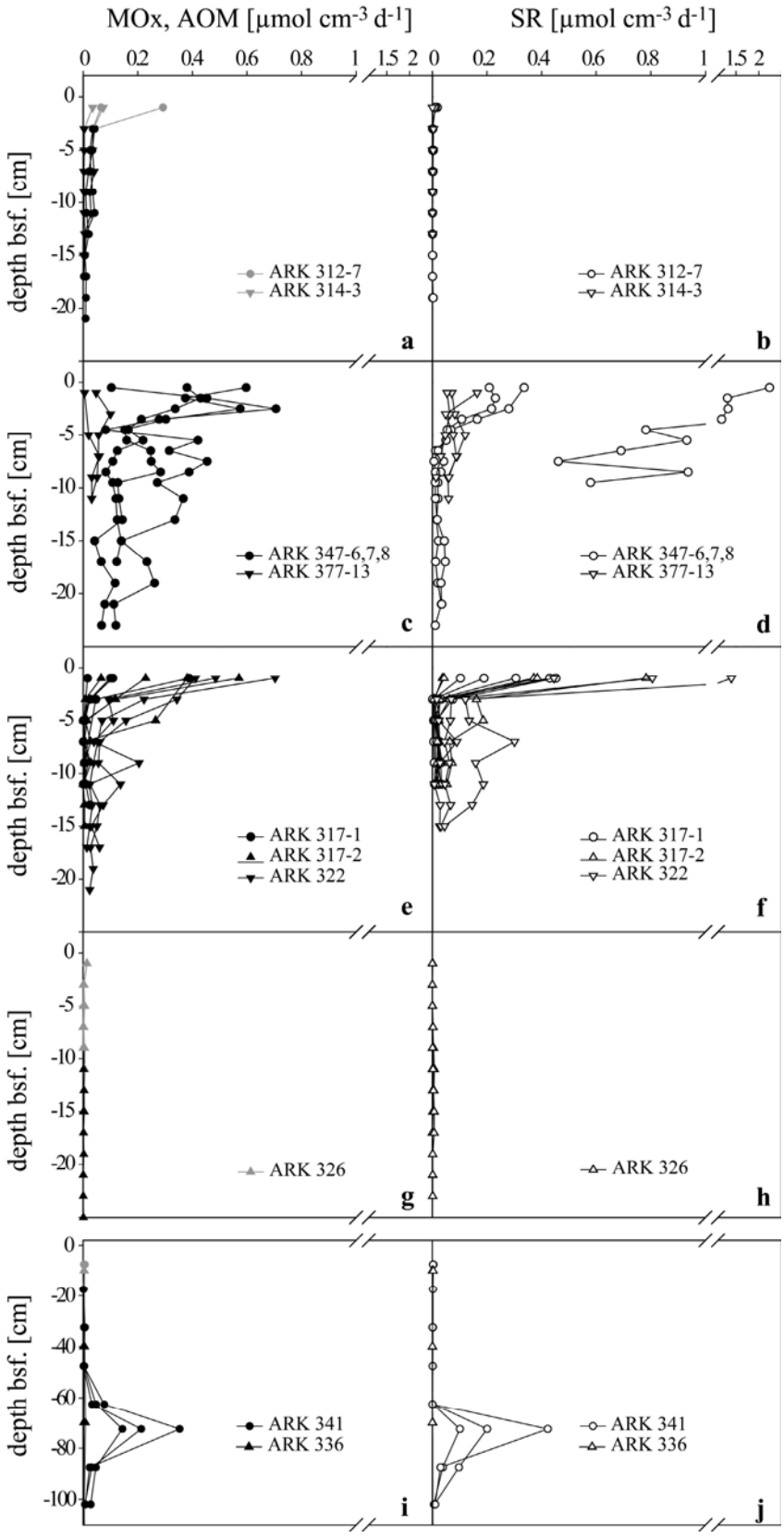
MOx, AOM [µmol cm-3 d-1]
SR [µmol cm-3 d-1]
depth bsf. [cm]
ARK 312-7
ARK 314-3
a
b
ARK 347-6,7,8
ARK 377-13
c
d
ARK 317-1
ARK 317-2
ARK 322
e
f
ARK 326
g
h
ARK 341
ARK 336
i
j

Figure 2. Aerobic (highlighted in grey) and anaerobic oxidation of methane (highlighted in black) (left panels) and sulphate reduction rates (highlighted in white, right panels) at the centre (a,b), grey mat (c,d), *Beggiatoa* (e,f) and *Pogonophora* site (g-j). Note that methane turnover in sediment sections below 2 cm bsf of the centre could not be attributed to either MOx or AOM activity (see method section). Note the difference in depth scale in panels (i) and (j). Replicates of one station are represented with the same symbol. ARK indicates samples taken during the R/V Polarstern cruise.

3.1.3 Beggiatoa

Similar to the centre and grey mat site, sediments recovered from *Beggiatoa* mats were subjected to gas ebullition. Hence, methane concentrations were at ca. 1.5 mM over the entire vertical profile (data not shown). Sulphate concentrations decreased substantially with depth at all stations (n = 7, Fig. 1g). At 3 stations sulphate declined to trace amounts within the upper 5 cm of the sediment. 4 stations had relatively constant sulphate concentrations between 3 and 7 mM below 3 cm sediment depth. Compared to the centre, the decrease of chloride and increase of bromide with depth was less steep in all replicates (n = 4) (Fig. 1h,i). In sediments below *Beggiatoa* mats, AOM and SR rates were highest in the uppermost sediment horizon but also varied considerably in magnitude between replicates and stations with values ranging from 0.02 to 0.70 and from 0.04 to 1.40 µmol cm^{-3} d^{-1}, respectively (Fig. 2e,f). All replicates showed a sharp decline of AOM and SR rates to values <0.20 and <0.30 µmol cm^{-3} d^{-1}, respectively, with depth below 5 cm. AOM and SR rates were insignificant (<0.001 µmol cm^{-3} d^{-1}) in deeper sediment layers sampled by gravity coring (data not shown). Integrated over depth (0-12 cm), AOM (n = 11) and SR (n = 13) showed mean values of 4.5 (±1.5 S_E) and 5.5 (±2.0 S_E) mol m^{-2} yr^{-1}, respectively (Fig. 3).

3.1.4 Pogonophora

A distinct methane sulphate transition zone (SMT) was observed in subsurface sediments at the *Pogonophora* site (Fig. 1m). In core 336, the SMT was between 20-40 cm and in core 341 between 60-80 cm bsf, (Fig. 1m). Methane concentrations in surface sediments were comparably low with values <0.05 mM whereas a strong increase was observed at depth of 20 and 60 cm bsf in cores 336 and 341, respectively. Gas hydrates were observed at 110 cm bsf in core 341 and at 350 cm bsf in core 336. The decrease of sulphate in near surface sediments was moderate in comparison to *Beggiatoa* covered sediments but variable between stations (n = 4, Fig. 1j). At depths below 70 cm bsf, sulphate declined to concentrations of approximately 3 mM in core 336 and 5 mM in core 341. Just as sulphate, chloride and bromide concentrations (n = 3) also showed a less steep decrease in comparison to the centre and *Beggiatoa* site (Fig. 1k,l). At the sediment surface, MOx rates were slightly elevated with values around 0.01 µmol cm^{-3} d^{-1} (n = 3) (Fig. 2g). Between 9 and 47.5 cm bsf, methane turnover was

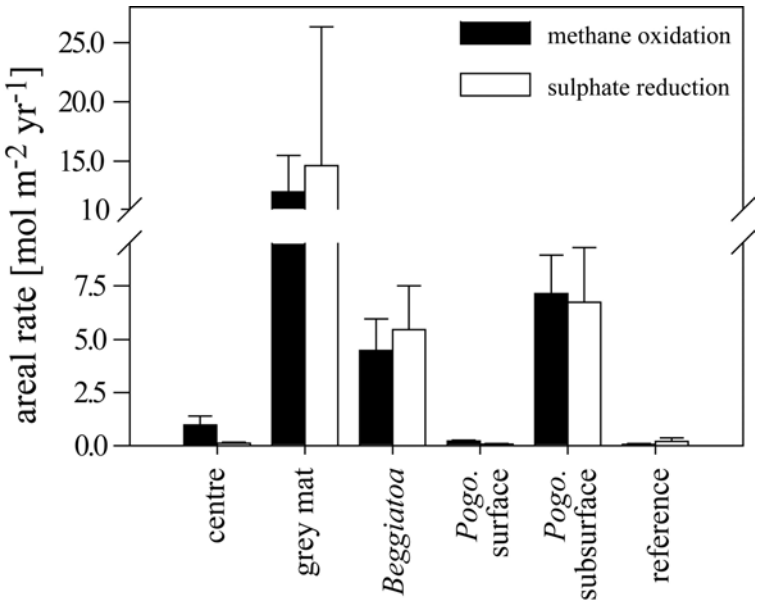

Figure 3. Methane oxidation and sulphate reduction rates integrated over depth at the centre, grey mat, *Beggiatoa*, *Pogonophora* (*Pogo.* surface) and reference site. Methane turnover at the centre was integrated over the top most horizon (0-2 cm). Sulphate reduction rates at the centre as well as sulphate reduction and methane oxidation rates at the other sites were integrated over 0-12 cm. For the *Pogonophora* site, methane oxidation and sulphate reduction rates were also integrated over 9 to 105 cm (*Pogo.* subsurface). Error bars are standard errors.

<0.005 µmol cm^{-3} d^{-1}. SRR was very low with values <0.005 µmol cm^{-3} d^{-1} (n = 3) from the sea floor down to 47.5 cm bsf. Box core and gravity core samples showed that tubes of the pogonophoran worm *O. haakonmosbiensis* extend to a depth of approximately 60 cm bsf. Below this depth at the SMT (60-80 cm bsf, core 341), AOM and SR rates peaked in with values ranging from 0.14 to 0.35 (n = 3) and from 0.10 to 0.42 (n = 3) µmol cm^{-3} d^{-1}, respectively (Fig. 2j). However, AOM and SR rates remained generally low (<0.005 µmol cm^{-3} d^{-1}) in core 336 (Fig. 2j). On average, AOM and SR rates were 7.1 (±1.8 S_E) and 6.7 (±2.6 S_E) mol m^{-2} yr^{-1} over a depth interval of 9-105 cm. In contrast, MOx at the surface was 0.22 (±0.04 S_E) and SR was 0.07 (±0.03 S_E) mol m^{-2} yr^{-1} over 0-12 cm (Fig. 3).

3.1.5 Reference

As a reference site we chose two stations ca. 1 km to the east of the centre of the HMMV. Methane concentrations were very low in the upper 10 cm with values of about 0.002 mM increasing to about 0.01 mM below this depth (data not shown). At one station (core 362-1), sulphate (n = 2) showed a very weak decrease with depth (Fig. 1p). The concentrations of chloride and bromide (n = 1, core 28) were constant over depth (Fig. 1q-r). Methane oxidation and SR rates were comparably low at the reference station (core 362-1). At the sediment surface, MOx rates were 0.006 (±0.006 S_E, n = 3) µmol cm^{-3} d^{-1} decreasing with depth to detection limit (<0.001 µmol cm^{-3} d^{-1}, data not shown). SRR were elevated at 11 cm bsf with values of 0.008 (±0.008 S_E, n = 3) µmol cm^{-3} d^{-1} but low above and below this depth with values <0.002 µmol cm^{-3} d^{-1} (data not shown). Integrated over depth (0-12 cm), mean methane oxidation and SR were 0.06 (±0.04 S_E) and 0.19 (±0.17 S_E) mol m^{-2} yr^{-1}, respectively (Fig. 3).

3.2 *In Vitro* Experiments

Replicate incubations (n = 5) at temperatures of 1, 4, 8, 12, 16 and 20°C showed with values of up to 0.72 µmol cm^{-3} d^{-1} 1.7-fold higher AOM rates at 8°C compared to 1°C and 4°C, and 2.4 fold higher rates in comparison to 12°C (Fig. 4a). AOM rates were very low at 16°C and below detection limit at 20°C. MOx was highest at 4°C with 8.5 (±0.6 S_E) µmol cm^{-3} d^{-1} (n = 5) and decreased to 6.3 (±0.3 S_E) µmol cm^{-3} d^{-1} (n = 5) at 12°C (data not shown). No MOx activity was measured at 20 and 28°C, respectively. Temperatures lower than 4°C were not investigated in this experiment.

Simultaneous measurements of methane consumption and sulphide production (n = 5) showed a high correlation with a molar ratio of AOM to sulphide production of 1:0.94 (Fig. 4b). This indicates a close coupling of AOM and SR at HMMV. Increasing methane concentrations from 1.7 to 40 mM had a positive effect on AOM rates, increasing them from 0.3 to 1.1 µmol cm^{-3} d^{-1} (n = 5, Fig. 4c). Under the experimental conditions, a methane concentration

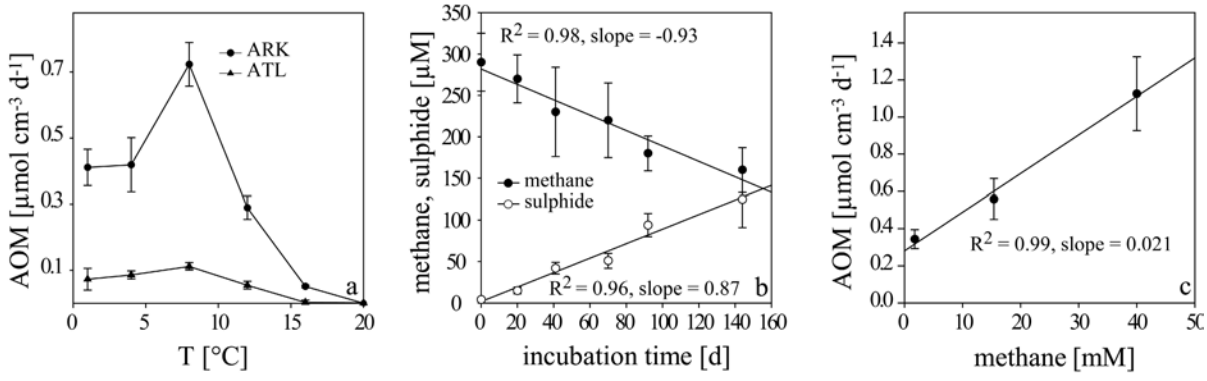

Figure 4. *In vitro* incubations of surface sediments (0 to 3 cm) from the *Beggiatoa* site under strictly anoxic conditions: AOM rates at various temperatures (a), decrease of methane and increase of sulphide concentrations in a long term incubation (b) and AOM rates at various methane concentrations. Errors are given as standard errors. Rates of anaerobic oxidation of methane are relative to sediment volume. ARK and ATL indicate samples taken during the R/V Polarstern and R/V Atalante cruise, respectively.

increment of 1 mM lead to an average increment in AOM of 0.021 µmol cm^{-3} d^{-1}. Similar to AOM, MOx activity was elevated at the higher methane concentrations. Under the experimental conditions, MOx was 0.85 µmol cm^{-3} d^{-1} in sediment slurries with 3.3 mM methane concentrations and 2.4 µmol cm^{-3} d^{-1} in slurries with 8.3 mM methane concentrations (data not shown).

Potential rates (n = 7, respectively) were substantially higher than rates measured *ex situ* but they showed similar vertical trends in comparison to *ex situ* measurements at similar methane concentrations (~1.5 mM) but higher sulphate concentrations (*in vitro*: ~28 mM, *ex situ*: <<25 mM) (Tab. 2). MOx rates were highest in central sediments but also relatively high in all near surface sediments in the presence of oxygen. Highest AOM rates were measured in the near surface sediments from *Beggiatoa* covered areas followed by the deeper horizon of this area. Lower AOM rates were found in the deeper horizon of the centre. The control incubations without methane yielded overall low SRR, indicating that methane is the main electron donor for SR.

Table 2. Potential rates of anaerobic oxidation of methane, sulphate reduction in methane free sediments and aerobic oxidation of methane. Rates are relative to sediment volume. Potential rates were determined by *in vitro* incubation experiments at 4°C with surface (0-3 cm) and deeper (3-10 cm) sediments from different habitats of Håkon Mosby Mud Volcano. Errors are given as standard errors. nd = no detection.

	Activity [µmol cm^{-3} d^{-1}]		
Habitat	AOM	SR w/o CH_4	MOx
Centre 0-3	nd	0.04 ±0.01	1.12 ±0.07
Centre 3-10	0.15 ±0.02	0.05 <0.01	0.44 ±0.01
Beggiatoa 0-3	1.03 ±0.12	0.09 ±0.02	0.7 ±0.07
Beggiatoa 3-10	0.6 ±0.06	0.08 <0.01	0.18 ±0.05
Pogonophora 0-3	nd	nd	0.72 ±0.09
Pogonophora 3-10	nd	nd	0.11 ±0.05
Reference 0-3	nd	nd	0.25 ±0.05
Reference 3-10	nd	nd	0.1 ±0.02

4. DISCUSSION

4.1 Geochemical Zonation of HMMV

The HMMV is an active, methane and fluid seeping, deep-water mud volcano at the Norwegian margin of the Barents Sea. Its roughly circular shape is 1 km in diameter covering an area of about 0.8 km^2 and the relief is <10 m (Hjelstuen et al., 1999; Klages et al., 2004; Milkov et al., 2004; Vogt et al., 1997a; Vogt et al., 1997b). The habitats can be divided into approximately concentric areas enclosing the central crater. (1) The central plain is covered by greyish muds and has a diameter of ca. 500 m (0.2 km^2). The centre is surrounded by a ca. 100 m wide belt (0.2 km^2) of reduced sediments, covered with thiotrophic, filamentous bacteria *(Beggiatoa sp.)*. The hummocky rim is ca. 150 m wide (0.4 km^2) and colonised by pogonophoran worms. Furthermore, during the dives with the ROV Victor 6000, we observed violent gas and fluid emissions at the northern edge of the centre. Small patches (<1m^2) of reduced sediments covered with whitish-greyish filamentous bacteria were observed in close proximity to fluid escape and at the boundary of the centre. Quantification of the area covered by grey mats was not possible due to their patchiness. However, we assume that they cover a total area of less than 0.001 km^2 at HMMV.

A deep origin of methane-rich fluids transported upwards by advective flow is indicated by the anomalies of chloride and bromide concentrations, which are most prominent in the centre. Our observations are in good agreement with previous findings showing high bromide and low chloride concentrations in surface sediments of the centre (Lein et al., 1999). Several different causes are known to affect bromide and chloride concentrations in marine sediments. Amongst them are salt diapirism, degradation of organic matter, release of fresh water from

ground water seepage and sediment compression or gas hydrate dissociation. High bromide concentrations may result from sea water evaporation and from the degradation of marine, organic matter (Egeberg and Barth, 1998; Pedersen and Price, 1980; Price and Calvert, 1977). Salt diapirism is absent at HMMV (Vogt et al., 1999), but there is good evidence for bromide originating from subsurface degradation of organic matter. The isotopic signature of methane points to a mixed microbial-thermogenic origin, and the bromide could be transported together with the methane from depth (Lein et al., 1999). Decreasing chloride concentrations are most likely a result of fresh water influx from mineral dehydration under high pressure at great depth which has been proposed for HMMV and is typical for clay-rich mud volcanoes (Kopf, 2002; Lein et al., 1999). Other freshwater sources such as gas hydrate dissociation are unlikely because gas hydrates were not found at the centre due to the relatively high geothermal temperature gradient of about 10°C repressing hydrate formation (Eldholm et al., 1999; Ginsburg et al., 1999; Vogt et al., 1997b).

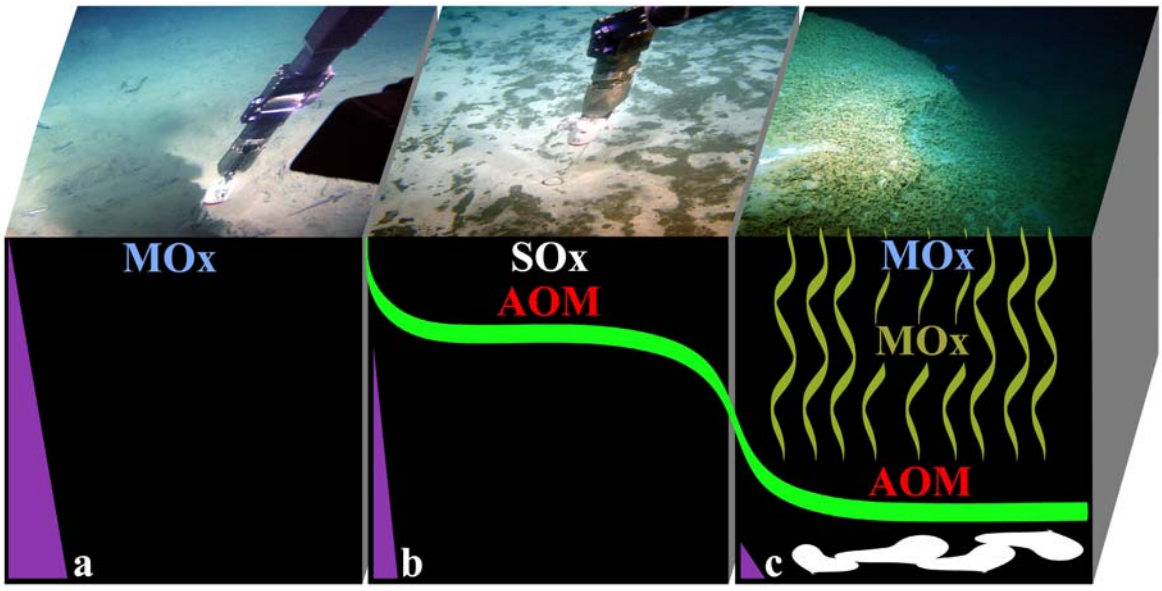

Figure 5. Sea floor terrains and dominating biogeochemical processes at the centre (a) *Beggiatoa* (b) and *Pogonophora* site (c). Purple triangles denote the magnitude of fluid flow. MOx mediated by free living and endosymbiotic bacteria is indicated in blue and brown, respectively. Undulated brown lines indicate pogonophoran worms. The green line denotes the sulphate penetration depth. White patches in panel (c) indicate gas hydrates. Note that the grey mat site is not included.

The decrease of the chloride and bromide gradients with distance to the centre give evidence for a decreasing velocity of fluid seepage away from the central conduit at HMMV (Fig. 5, Eldholm et al., 1999). Unfortunately, an estimate of the magnitude of pore water flow based on the chloride and bromide gradients is not possible. These gradients were altered due to gas ebullition and consequent seawater inflow during sediment retrieval. Based on microsensor measurements, de Beer et al. (submitted) estimated a flow velocity of 0.4 μm s^{-1} at the centre and a reduced velocity of 0.1 μm s^{-1} in the surrounding *Beggiatoa*-covered sediments. As a consequence, the penetration depth of sulphate and probably other seawater solutes such as oxygen is very limited at the centre in comparison to *Beggiatoa* covered sediments (Fig. 5a, b). This also explains the steep sulphate gradients in spite of an insignificant SR at the centre (Fig. 1a, 2b). Such effects of high advective flow of sulphate-depleted subsurface fluids have previously been observed at cold seeps off Costa Rica (Hensen et al., 2004).

Accordingly, MOx and AOM at HMMV were horizontally and vertically restricted at the different sites. Gas ebullition during sediment retrieval provides evidence that *in situ* methane concentrations are high in surface sediments of the centre, *Beggiatoa* and grey mat site. Hence, the availability of the electron acceptor could be the limiting factor in methane oxidation. *In situ* measurements show that diffusion of oxygen and sulphate from bottom waters into the sediments of the centre are restricted to the top few millimetres (de Beer et al., submitted). Here, the presence of oxygen most likely represses the development of AOM communities in this narrow horizon. At slightly lower fluid flow rates at the *Beggiatoa* site, a deeper penetration of sulphate of down to 5 cm into the sediment supports an active AOM zone. The high rates of sulphide production by this process and rapid re-oxidation by thiotrophic bacteria could exclude MOx communities. Sediments below grey mats represent a special situation as sulphate concentrations were elevated over a larger depth interval despite the proximity to central and *Beggiatoa* covered sediments. The reasons for the deeper

sulphate penetration in these sediment patches are currently unknown. The *Pogonophora*-populated outer rim of the volcano is less influenced by advective flow as indicated by weak chloride and bromide concentration gradients, and much lower geothermal gradients (Klages et al. 2004). Previous work and our data show that the environmental conditions allow for gas hydrate formation below ca. 50 cm in this region (Ginsburg et al., 1999). The pogonophoran worms appear perfectly adapted to such a situation of deep methane and sulphide maxima with their body length of >50 cm and their ability to transport oxygen, methane and potentially also sulphide to their symbionts by blood circulation.

4.2 Anaerobic Oxidation of Methane

AOM is the predominant mode of methane oxidation in near surface sediments at the *Beggiatoa* and grey mat site as well as in subsurface sediments at the *Pogonophora* site (Fig. 5b, c). Our AOM measurements at the *Beggiatoa* site (on average 0.314 µmol cm^{-3} d^{-1}, 0-2 cm bsf) strongly exceed previous estimates of methane oxidation rates provided by Pimenov et al. (1999). Below *Beggiatoa* mats, these authors detected highest rates of 9.94 µg carbon dm^{-3} d^{-1}, ($0.83*10^{-3}$ µmol methane cm^{-3} d^{-1}) at 20 – 30 cm bsf but did not find an AOM peak at the surface. With respect to fluid flow, which limits the sulphate penetration to the top few cm of the sediment, an active AOM community in subsurface sediments (>>5 cm bsf) appears unlikely. One reason for the findings of Pimenov et al. (1999) might be that these authors used a box corer for sediment sampling, which most probably lead to a loss of the surface sediments during core recovery.

AOM was almost in a 1:1 ratio with SR at all sites both in *ex situ* as well as *in vitro* experiments (Fig. 3, 4), indicating that methane is the main electron donor for SR.

Accordingly, SR at the reference site was negligible with only 0.19 mol m^{-2} yr^{-1}, i.e. <5% of the SR at the *Beggiatoa* site. Similarly, SRR in methane-free *in vitro* incubations of surface sediments from the *Beggiatoa* site were 0.09 µmol cm^{-3} d^{-1} which accounts for <10% of the SRR in methane saturated incubations of the same sediment type (1.03 µmol cm^{-3} d^{-1}, Tab. 2). The optimal temperature for AOM was with 8°C somewhat higher than the ambient temperatures of -1°C, but lower than the optimal temperature of AOM communities retrieved from temperate continental margins of the NW Pacific and the Black Sea (Nauhaus et al. 2004).

The areal rates of AOM were 4.5 mol m^2 yr^{-1} at the Beggiatoa and 12.4 mol m^2 yr^{-1} at the grey mat site. At least for the *Beggiatoa* site, *ex situ* rates appear to be a conservative estimate of the *in situ* rates. *In situ* miocrosensor measurements at the this site showed that sulphide is completely oxidized within the sediment (Fig. 5b) resulting in a flux of 11 mol m^{-2} yr^{-1} (de Beer et al., submitted). This is about 2-fold higher than the *ex situ* measurements of SR and AOM at this site. The AOM activity in sediments of HMMV is comparable to highly active methane seeps such as Hydrate Ridge and the Gulf of Mexico where areal AOM rates were determined with a maximum of 36 and 4 mol m^{-2} yr^{-1}, respectively (Joye et al., 2004; Treude et al., 2003).

The exceptionally high AOM and SR rates below the roots of pogonophoran tubeworms are most likely related to enhanced sulphate supply due to the bioirrigation activities of the worms (Fig. 5c). Diffusive processes cannot explain the measured AOM and SR in core 341. Assuming that the methane and sulphate gradients (ca. 0.1, ca. -0.4 µmol cm^{-4}, respectively) were a result of diffusive transport, the flux of methane and sulphate would account for <5% of the measured *ex situ* AOM and SR, respectively, according to Fick's law of diffusion (porosity = ~50%). The AOM activity at the *Pogonophora* site (7.1 mol m^2 yr^{-1}) is to our

knowledge the ever highest measured in subsurface sediments, pointing to the relevance of bioirrigation by chemosynthetic symbiosis at seeps (Cordes et al., 2005). AOM rates at non-irrigated methane-sulphate transition zones in subsurface sediments are usually <0.06 µmol m^{-2} yr^{-1} (Hensen et al., 2003; Jørgensen et al., 2001; Niewöhner et al., 1998; Whiticar, 2002). Nevertheless, the estimated areal methane turnover at the *Pogonophora* site is most likely a low estimate. The pogonophoran worms live in a symbiosis with aerobic methanotrophs (Gebruk et al., 2003; Smirnov, 2000) and contribute themselves to methane oxidation. Unfortunately, *ex situ* incubation methods cannot account for this, and the filter capacity of *Pogonophora* at cold seeps is so far unknown.

An extrapolation of the areal AOM rates allows for a conservative estimate of the total amount of methane consumed in the grey mat, *Beggiatoa* and *Pogonophora* habitats. With respect to the areal extensions of these habitats, AOM consumes a total of $0.1*0^5$, $8.5*10^5$, and $28.4*10^5$ mol methane yr^{-1}, respectively. Previous findings showed a 100-fold decrease in bottom water methane concentrations from the centre to *Beggiatoa* covered areas and almost background values above the outer rim of HMMV (Bogdanov et al., 1999; Damm and Budeus, 2003; Milkov et al., 2004; Sauter and Schlüter, 2004). Hence, AOM appears to be an efficient filter system against methane emission at HMMV.

4.3 Aerobic Methane Oxidation

MOx is the predominant mode of methane oxidation in surface sediments at the centre, the *Pogonophora* and the reference site (Fig. 5a, c). This is confirmed by *in vitro* incubations showing elevated MOx rates in these sediments whereas AOM could not be detected. In surface sediments of the centre, the *ex situ* MOx rates were 0.9 mol m^{-2} yr^{-1}. These rates are to

our knowledge among the highest ever measured in marine sediments and are just 5-fold lower than the AOM rates at the *Beggiatoa* site. In oxygenated surface sediments of a methane seep in the Baltic Sea (Jensen et al., 1992) and in low-flux seep sediments at Hydrate Ridge which are populated by the ventilating bivalve *Acharax* (Treude et al., 2003), MOx was 1.5-fold lower in comparison to HMMV's centre, although the penetration depth of oxygen into the sediment was limited to a few millimetres at HMMV's centre (de Beer et al., submitted).

The aerobic methanotrophs appear well adapted to the ice-cold *in situ* temperatures at HMMV. *In vitro* incubations provide evidence that the optimum temperature for methane oxidation at the centre is <<12°C. Most isolated strains of psychrophilic methanotrophs show highest methane oxidation rates at temperatures ≥10°C and were found to grow at temperatures between 3.5 and 20°C (Hanson and Hanson, 1996; Trotsenko and Khmelenina, 2002).

Similar to AOM, *ex situ* MOx rates are problematic because the oxygen penetration depth was higher during *ex situ* incubations leading to an overestimation of the aerobic methane turnover, whereas lower *ex situ* methane concentrations would underestimate *in situ* MOx as shown by *in vitro* incubations at different methane concentrations. However, the diffusive influx of oxygen at the centre site was estimated with 3.7 (*in situ*) and 0.5 mol m^{-2} and yr^{-1} (*ex situ*) (de Beer et al., submitted). The measured *ex situ* MOx rates (0.9 mol m^{-2} d^{-1}) are within this range, indicating that MOx consumes most of the available oxygen in the top surface layer. With respect to the areal extension of the centre site, a total of $3.3*10^5$ mol methane yr^{-1} is oxidised in this environment. However, comparably high bottom water concentrations of methane above the centre with values as high as 0.27 mM (Bogdanov et al., 1999; Milkov et al., 2004) provide evidence that a substantial fraction of uprising methane escapes the benthic

microbial filter system. This is most probably a result of the high upward flow of methane-rich fluids and the limited availability of electron acceptors. The relevance of MOx is thus comparably small at HMMV. MOx at the centre and in surface sediments of the Pogonophora site amounts to $3.4*10^5$ mol yr^{-1} which is about 10-fold lower in comparison to AOM at the grey mat, *Beggiatoa* and *Pogonophora* site.

In conclusion, aerobic and anaerobic methane turnover are very important processes reducing a substantial fraction of methane efflux at HMMV. Several point sources of mud, fluid, gas and gas hydrate escape have been detected in the centre of the HMMV (Damm and Budeus, 2003; Sauter et al., submitted). Furthermore, emission of methane via diffusive methane fluxes from the centre make the HMMV a substantial source of methane (Sauter et al., submitted). The total amount of methane emitted from HMMV to the hydrosphere was preliminarily estimated with ~$68*10^5$ mol yr^{-1} ($1.5*10^5$ m^3 yr^{-1}, Milkov et al., 2004) and $35*10^5$ to $148*10^5$ mol yr^{-1} (Sauter et al., submitted). These are in the same order of magnitude of methane turnover in the sediment ($40*10^5$ mol yr^{-1}, $7*10^{-5}$ Tg yr^{-1}). Hence, at least 22 to 55% of the total methane efflux at HMMV is reduced by methanotrophic organisms. However, this figure is a conservative estimate and potentially higher due to a most likely elevated *in situ* methane turnover. Previous estimates of methane turnover at other active seeps also found that the methanotrophic communities are representing efficient filters for the greenhouse gas methane, consuming 60-100% of this gas transported with uprising fluids (Treude et al., 2003). At HMMV, we observed that the chemical composition and velocity of the fluid flow probably control microbial activity by limiting access to electron acceptors.

Acknowledgements

We thank the officers, crew and shipboard scientific party for support during the R/V Atalante and R/V Polarstern cruise in 2001 and 2003, respectively. We are especially indebted to the ROV Victor 6000 team for excellent technical operation and sample retrieval. Viola Beyer, Imke Busse, and Friderike Heinrich are thanked for their support during sampling. This study was part of the MUMM (Mikrobielle Umsatzraten von Methan in Gashydrathaltigen Sedimenten, FN 03G0554A) supported by the Bundesministerium für Bildung und Forschung (BMBF, Germany). Further Support was provided by the Max Planck Gesellschaft (Germany).

References

Boetius A., Ravenschlag K., Schubert C., Rickert D., Widdel F., Gieseke A., Amann R., Jørgensen B. B., Witte U., and Pfannkuche O. (2000) A marine microbial consortium apparently mediating anaerobic methane of oxidation. *Nature* **407**, 623-626.

Boetius A. and Suess E. (2004) Hydrate Ridge: a natural laboratory for the study of microbial life fueled by methane from near-surface gas hydrates. *Chemical Geology* **205**(3-4), 291-310.

Bogdanov Y. A., Sagalevitch A. M., Vogt P. R., Mienert Y., Sundvor E., Krane K., Lein A. Y., Egorov A. V., Pepesypkin V. I., Cherkashev G. A., Gebruk A. V., Ginsburg G. D., and Voitov D. T. (1999) The Haakon Mosby mud volcano in the Norwegian Sea: Results of comprehensive investigations with submersibles. *Okeanologiya* **39**(3), 412-419.

Charlou J. L., Donval J. P., Zitter T., Roy N., Jean-Baptiste P., Foucher J. P., and Woodside J. (2003) Evidence of methane venting and geochemistry of brines on mud volcanoes of the eastern Mediterranean Sea. *Deep-Sea Research Part I-Oceanographic Research Papers* **50**(8), 941-958.

Cordes E. E., Arthur M. A., Shea K., Arvidson R. S., and Fisher C. R. (2005) Modeling the mutualistic interactions between tubeworms and microbial consortia. *Plos Biology* **3**(3), 497-506.

Damm E. and Budeus G. (2003) Fate of vent-derived methane in seawater above the Hakon Mosby mud volcano (Norwegian Sea). *Marine Chemistry* **82**(1-2), 1-11.

de Beer D., Sauter E., Niemann H., Witte U., and Boetius A. (submitted) In situ fluxes and zonation of microbial activity in surface sediments of the Håkon Mosby Mud Volcano. *Limnology and Oceanography*.

Dimitrov L. and Woodside J. (2003) Deep sea pockmark environments in the eastern Mediterranean. *Marine Geology* **195**(1-4), 263-276.

Dimitrov L. I. (2002) Mud volcanoes - the most important pathway for degassing deeply buried sediments. *Earth-Science Reviews* **59**(1-4), 49-76.

Dimitrov L. I. (2003) Mud volcanoes - a significant source of atmospheric methane. *Geo-Marine Letters* **23**(3-4), 155-161.

Egeberg P. K. and Barth T. (1998) Contribution of dissolved organic species to the carbon and energy budgets of hydrate bearing deep sea sediments (Ocean Drilling Program Site 997 Blake Ridge). *Chemical Geology* **149**(1-2), 25-35.

Eldholm O., Sundvor E., Vogt P. R., Hjelstuen B. O., Crane K., Nilsen A. K., and Gladczenko T. P. (1999) SW Barents Sea continental margin heat flow and Hakon Mosby Mud Volcano. *Geo-Marine Letters* **19**(1-2), 29-37.

Fisher C. R. (1990) Chemoautotrophic and Methanotrophic Symbioses in Marine-Invertebrates. *Reviews in Aquatic Sciences* **2**(3-4), 399-436.

Gebruk A. V., Krylova E. M., Lein A. Y., Vinogradov G. M., Anderson E., Pimenov N. V., Cherkashev G. A., and Crane K. (2003) Methane seep community of the Hakon Mosby mud volcano (the Norwegian Sea): composition and trophic aspects. *Sarsia* **88**(6), 394-403.

Ginsburg G. D., Milkov A. V., Soloviev V. A., Egorov A. V., Cherkashev G. A., Vogt P. R., Crane K., Lorenson T. D., and Khutorskoy M. D. (1999) Gas hydrate accumulation at the Hakon Mosby Mud Volcano. *Geo-Marine Letters* **19**(1-2), 57-67.

Haese R. R., Meile C., Van Cappellen P., and De Lange G. J. (2003) Carbon geochemistry of cold seeps: Methane fluxes and transformation in sediments from Kazan mud volcano, eastern Mediterranean Sea. *Earth and Planetary Science Letters* **212**(3-4), 361-375.

Hallam S. J., Putnam N., Preston C. M., Detter J. C., Rokhsar D., Richardson P. M., and DeLong E. F. (2004) Reverse methanogenesis: Testing the hypothesis with environmental genomics. *Science* **305**(5689), 1457-1462.

Hanson R. S., Bratina B. J., and Brusseau G. A. (1993) Phylogeny and ecology of methylotrophic bacteria. In *Microbial Growth on C_1 Compounds* (ed. J. C. Murrell and D. P. Kelly), pp. 285-302. Intercept Limited.

Hanson R. S. and Hanson T. E. (1996) Methanotrophic bacteria. *Microbiological Reviews* **60**(2), 439-&.

Hensen C., Wallmann K., Schmidt M., Ranero C. R., and Suess E. (2004) Fluid expulsion related to mud extrusion off Costa Rica - A window to the subducting slab. *Geology* **32**(3), 201-204.

Hensen C., Zabel M., Pfeifer K., Schwenk T., Kasten S., Riedinger N., Schulz H. D., and Boettius A. (2003) Control of sulfate pore-water profiles by sedimentary events and the significance of anaerobic oxidation of methane for the burial of sulfur in marine sediments. *Geochimica Et Cosmochimica Acta* **67**(14), 2631-2647.

Hinrichs K.-U. and Boetius A. (2002) The anaerobic oxidation of methane: New insights in microbial ecology and biogeochemistry. In *Ocean Margin Systems* (ed. G. Wefer, D. Billett, and D. Hebbeln), pp. 457-477. Springer-Verlag, Berlin.

Hjelstuen B. O., Eldholm O., Faleide J. I., and Vogt P. R. (1999) Regional setting of Hakon Mosby Mud Volcano, SW Barents Sea margin. *Geo-Marine Letters* **19**(1-2), 22-28.

Iversen N. and Jørgensen B. B. (1985) Anaerobic methane oxidation rates at the sulfate-methane transition in marine sediments from Kattegat and Skagerrak (Denmark). *Limnology and Oceanography* **30**(5), 944-955.

Jensen P., Aagaard I., Burke R. A., Dando P. R., Jorgensen N. O., Kuijpers A., Laier T., Ohara S. C. M., and Schmaljohann R. (1992) Bubbling Reefs in the Kattegat - Submarine Landscapes of Carbonate-Cemented Rocks Support a Diverse Ecosystem at Methane Seeps. *Marine Ecology-Progress Series* **83**(2-3), 103-112.

Jørgensen B. B., Weber A., and Zopfi J. (2001) Sulfate reduction and anaerobic methane oxidation in Black Sea sediments. *Deep-Sea Research Part I-Oceanographic Research Papers* **48**(9), 2097-2120.

Joye S. B., Boetius A., Orcutt B. N., Montoya J. P., Schulz H. N., Erickson M. J., and Lugo S. K. (2004) The anaerobic oxidation of methane and sulfate reduction in sediments from Gulf of Mexico cold seeps. *Chemical Geology* **205**(3-4), 219-238.

Kasting J. F. and Siefert J. L. (2002) Life and the evolution of Earth's atmosphere. *Science* **296**(5570), 1066-1068.

Klages M., Mesnil B., Soldtwedel T., and Christophe A. (2002) L' expédition "AWI" sur NO L'Atalante en 2001. [The Expedition "AWI" on RV L'Atalante in 2001]. Alfred-Wegener-Institute for Polar and Marine Research.

Klages M., Thiede J., and Foucher J. P. (2004) The Expedition ARKTIS XIX/3 of the Research Vessel POLARSTERN in 2003 Reports of legs 3a, 3b and 3c, pp. 355. Alfred-Wegener-Institute for Polar and Marine Research.

Knittel K., Boetius A., Lemke A., Eilers H., Lochte K., Pfannkuche O., Linke P., and Amann R. (2003) Activity, distribution, and diversity of sulfate reducers and other bacteria in sediments above gas hydrate (Cascadia margin, Oregon). *Geomicrobiology Journal* **20**(4), 269-294.

Knittel K., Losekann T., Boetius A., Kort R., and Amann R. (2005) Diversity and distribution of methanotrophic archaea at cold seeps. *Applied and Environmental Microbiology* **71**(1), 467-479.

Kopf A. J. (2002) Significance of mud volcanism. *Reviews of Geophysics* **40**(2).

Krüger M., Meyerdierks A., Glockner F. O., Amann R., Widdel F., Kube M., Reinhardt R., Kahnt R., Bocher R., Thauer R. K., and Shima S. (2003) A conspicuous nickel protein in microbial mats that oxidize methane anaerobically. *Nature* **426**(6968), 878-881.

Larock P. A., Hyun J. H., and Bennison B. W. (1994) Bacterioplankton Growth and Production at the Louisiana Hydrocarbon Seeps. *Geo-Marine Letters* **14**(2-3), 104-109.

Le Mer J. and Roger P. (2001) Production, oxidation, emission and consumption of methane by soils: A review. *European Journal of Soil Biology* **37**(1), 25-50.

Lein A., Vogt P., Crane K., Egorov A., and Ivanov M. (1999) Chemical and isotopic evidence for the nature of the fluid in CH4-containing sediments of the Hakon Mosby Mud Volcano. *Geo-Marine Letters* **19**(1-2), 76-83.

Lelieveld J., Crutzen P. J., and Dentener F. J. (1998) Changing concentration, lifetime and climate forcing of atmospheric methane. *Tellus Series B-Chemical and Physical Meteorology* **50**(2), 128-150.

Manne A. S. and Richels R. G. (2001) An alternative approach to establishing trade-offs among greenhouse gases. *Nature* **410**(6829), 675-677.

Milkov A. V. (2000) Worldwide distribution of submarine mud volcanoes and associated gas hydrates. *Marine Geology* **167**(1-2), 29-42.

Milkov A. V., Sassen R., Apanasovich T. V., and Dadashev F. G. (2003) Global gas flux from mud volcanoes: A significant source of fossil methane in the atmosphere and the ocean. *Geophysical Research Letters* **30**(2).

Milkov A. V., Vogt P. R., Crane K., Lein A. Y., Sassen R., and Cherkashev G. A. (2004) Geological, geochemical, and microbial processes at the hydrate-bearing Hakon Mosby mud volcano: a review. *Chemical Geology* **205**(3-4), 347-366.

Nauhaus K., Boetius A., Kruger M., and Widdel F. (2002) In vitro demonstration of anaerobic oxidation of methane coupled to sulphate reduction in sediment from a marine gas hydrate area. *Environmental Microbiology* **4**(5), 296-305.

Nauhaus K., Treude T., Boetius A., and Kruger M. (2005) Environmental regulation of the anaerobic oxidation of methane: a comparison of ANME-I and ANME-II communities. *Environmental Microbiology* **7**(1), 98-106.

Niewöhner C., Hensen C., Kasten S., Zabel M., and Schulz H. D. (1998) Deep sulfate reduction completely mediated by anaerobic methane oxidation in sediments of the upwelling area off Namibia. *Geochimica et Cosmochimica Acta* **62**(3), 455-464.

Pedersen T. F. and Price N. B. (1980) The Geochemistry of Iodine and Bromine in Sediments of the Panama Basin. *Journal of Marine Research* **38**(3), 397-411.

Petit J. R., Jouzel J., Raynaud D., Barkov N. I., Barnola J. M., Basile I., Bender M., Chappellaz J., Davis M., Delaygue G., Delmotte M., Kotlyakov V. M., Legrand M., Lipenkov V. Y., Lorius C., Pepin L., Ritz C., Saltzman E., and Stievenard M. (1999) Climate and atmospheric history of the past 420,000 years from the Vostok ice core, Antarctica. *Nature* **399**(6735), 429-436.

Pimenov N., Savvichev A., Rusanov I., Lein A., Egorov A., Gebruk A., Moskalev L., and Vogt P. (1999) Microbial processes of carbon cycle as the base of food chain of Håkon Mosby mud volcano benthic community. *Geo-Marine Letters* **19**, 89-96.

Price N. B. and Calvert S. E. (1977) Contrasting Geochemical Behaviors of Iodine and Bromine in Recent Sediments from Namibian Shelf. *Geochimica Et Cosmochimica Acta* **41**(12), 1769-1775.

Reeburgh W. S. (1996) "Soft spots" in the global methane budget. In *Microbial Growth on C_1 Compounds* (ed. M. E. Lidstrom and F. R. Tabita), pp. 334-342. Kluwer Academic Publishers.

Sauter E., Muyakshin J., Charlou J., Schlüter M., Boetius A., Jerosch K., Damm E., Foucher J. P., and Klages M. (submitted) Methane discharge from a deep-sea submarine mud

volcano into the upper water column by gas hydrate-coated methane bubbles. *Earth and Planetary Science Letters*.

Sauter E. J. and Schlüter M. (2004) GEOCHEMICAL INVESTIGATIONS AT HAAKON MOSBY MUD VOLCANO, WESTERN BARENTS SEA. *European Geosciences Union (EGU) General Assembly*.

Shilov V. V., Druzhinina N. I., Vasilenko L. V., and Krupskaya V. V. (1999) Stratigraphy of sediments from the Hakon Mosby Mud Volcano Area. *Geo-Marine Letters* **19**(1-2), 48-56.

Smirnov R. V. (2000) Two new species of Pogonophora from the arctic mud volcano off northwestern Norway. *Sarsia* **85**(2), 141-150.

Somoza L., Diaz-del-Rio V., Leon R., Ivanov M., Fernandez-Puga M. C., Gardner J. M., Hernandez-Molina F. J., Pinheiro L. M., Rodero J., Lobato A., Maestro A., Vazquez J. T., Medialdea T., and Fernandez-Salas L. M. (2003) Seabed morphology and hydrocarbon seepage in the Gulf of Cadiz mud volcano area: Acoustic imagery, multibeam and ultra-high resolution seismic data. *Marine Geology* **195**(1-4), 153-176.

Treude T., Boetius A., Knittel K., Wallmann K., and Jorgensen B. B. (2003) Anaerobic oxidation of methane above gas hydrates at Hydrate Ridge, NE Pacific Ocean. *Marine Ecology-Progress Series* **264**, 1-14.

Trotsenko Y. A. and Khmelenina V. N. (2002) Biology of extremophilic and extremotolerant methanotrophs. *Archives of Microbiology* **177**(2), 123-131.

Valentine D. L. and Reeburgh W. S. (2000) New perspectives on anaerobic methane oxidation. *Environmental Microbiology* **2**(5), 477-484.

Vogt P. R., Cherkashev A., Ginsburg G. D., Ivanov G. I., Crane K., Lein A. Y., Sundvor E., Pimenov N. V., and Egorov A. (1997a) Haakon Mosby mud volcano: A warm methane seep with seafloor hydrates and chemosynthesis-based Ecosystem in late Quantemary Slide Valley, Bear Island Fan, Barents Sea passive margin. *EOS Transactions of the American Geophysical Union Supplement* **78**(17), 187-189.

Vogt P. R., Cherkashev G., Ginsburg G., Ivanov G. I., Milkov A., Crane K., Lein A., Sundvor E., Pimenov N. V., and Egorov A. (1997b) Haakon Mosby Mud Volcano Provides Unusual Example of Venting. *EOS Transactions of the American Geophysical Union Supplement* **78**(48), 549, 556-557.

Vogt P. R., Gardner J., and Crane K. (1999) The Norwegian-Barents-Svalbard (NBS) continental margin: Introducing a natural laboratory of mass wasting, hydrates, and ascent of sediment, pore water, and methane. *Geo-Marine Letters* **19**(1-2), 2-21.

Whiticar M. J. (1999) Carbon and hydrogen isotope systematics of bacterial formation and oxidation of methane. *Chemical Geology* **161**(1-3), 291-314.

Whiticar M. J. (2002) Diagenetic relationships of methanogenesis, nutrients, acoustic turbidity, pockmarks and freshwater seepages in Eckernforde Bay. *Marine Geology* **182**(1-2), 29-53.

Widdel F. and Bak F. (1992) The gram negative mesophilic sulfate reducing bacteria. In *The prokaryotes* (ed. M. Dworkin). Springer.

Wuebbles D. J. and Hayhoe K. (2002) Atmospheric methane and global change. *Earth-Science Reviews* **57**(3-4), 177-210.

Yamamoto S., Alcauskas J. B., and Crozier T. E. (1976) Solubility of Methane in Distilled Water and Seawater. *Journal of Chemical and Engineering Data* **21**(1), 78-80.

Microbial methane turnover at mud volcanoes of the Gulf of Cadiz

Niemann, H.[1,2]; Duarte, J.[3]; Hensen, C.[4]; Omoregie, E.[1,7]; Magalhães, V.H.[3,5]; Elvert, M.[6]; Pinheiro, L, M.[3]; Kopf, A.[6]; Boetius, A.[1,7]

[1] Max Planck Institute for Marine Microbiology Bremen, Celsiusstr.1, 28359 Bremen, Germany
[2] Alfred Wegener Institute for Polar and Marine Research, 27515 Bremerhaven, Germany
[3] Geosciences Department, University of Aveiro, Campus de Santiago, 3810-193 Aveiro, Portugal
[4] Leibniz Institute of Marine Sciences, IfM-GEOMAR, 24148 Kiel, Germany
[5] Department National Institute of Engineering, Technology and Innovation, Alfragide, 2720-866 Amadora, Portugal
[6] Research Center Ocean Margins, University of Bremen, 28359 Bremen, Germany
[7] International University Bremen, 28759 Bremen, Germany

Author to whom correspondence should be addressed:

Helge Niemann
email: hniemann@mpi-bremen.de, phone +49-421-2028653

ABSTRACT

The Gulf of Cadiz is a tectonically active area of the European continental margin and characterised by a high abundance of mud volcanoes, diapirs, pockmarks and carbonate chimneys. During the R/V SONNE expedition "GAP- Gibraltar Arc Processes (SO175)" in December 2003, several mud volcanoes were explored for gas seepage and associated microbial methane turnover. Pore water analyses and methane oxidation measurements in sediment cores recovered from the centres of the mud volcanoes Captain Arutyunov, Bonjardim, Ginsburg, Gemini and a newly discovered mud volcano like structure called "No Name" show that thermogenic methane and associated higher hydrocarbons rising from deeper sediment strata are completely consumed within the seabed. The presence of a distinct methane-sulphate transition zone (SMT) overlapping with high sulphide concentrations reveal that methane oxidation is mediated under anaerobic conditions with sulphate as the electron acceptor. Anaerobic oxidation of methane (AOM) and sulphate reduction (SR) rates show maxima in distinct subsurface sediment horizons at the SMT. The position of the SMT varied between mud volcanoes at depths from 20 to 200 cm below sea floor. In comparison to other fluid flow impacted environments of the world oceans, AOM activity (<383 mmol m^{-2} yr^{-1}) and diffusive methane fluxes (<321 mmol m^{-2} yr^{-1}) in mud volcano sediments of the Gulf of Cadiz are low to mid range. AOM was generally exceeded by SR, most likely because other hydrocarbons were oxidized anaerobically by sulphate reducing microbes. Corresponding lipid biomarker and 16S rDNA clone library analysis give evidence that AOM is mediated by a mixed community of anaerobic methanotrophic archaea and associated sulphate reducing bacteria (SRB) in the studied mud volcanoes. Little is known about the variability of methane fluxes in this environment but the ^{13}C-depleted lipid imprint in carbonate crusts that litter the sea floor of mud volcanoes in the northern part of the Gulf of Cadiz shows that extensive, methane-related carbonate precipitation once took place. However, actual sea floor video

observations showed only scarce traces of methane emission and associated biological processes at the seafloor. No active fluid or free gas escape was observed visually. In combination wit the observed depletion of methane in subsurface sediments, this indicates that the contribution of methane to the hydrosphere and potentially to the atmosphere is insignificant at present.

1. INTRODUCTION

Methane is an aggressive greenhouse gas with a global warming potential that is 21 to 56-fold higher compared to CO_2 (Manne and Richels, 2001; Wuebbles and Hayhoe, 2002). In recent years, increasing research effort has therefore been dedicated to elucidate sources and sinks of methane. Anthropogenic sources as well as natural emission from wetlands contribute to the global flux of methane to the atmosphere by 74% (396 Tg yr^{-1}) (Judd et al., 2002). Recently, mud volcanism has been identified as an important escape pathway of methane and higher hydrocarbons (Dimitrov, 2002; Dimitrov, 2003; Judd et al., 2002). Mud volcanism is caused by various geological processes at continental margins such as tectonic accretion and faulting, rapid burial of sediments and fluid emissions from mineral dehydration. These processes can lead to an abnormally high pore fluid pressure and the extrusion of mud and fluids to the surface which is often accompanied by the expulsion of methane and higher hydrocarbons (Charlou et al., 2003; Kopf, 2002; Milkov, 2000; Somoza et al., 2003). Mud volcanoes (MVs) are structurally diverse ranging in shape from amorphous mud pies to conical structures and in size from a few meters to kilometres in diameter and height, respectively (Dimitrov, 2002). Global estimates suggest that terrestrial and shallow water mud volcanoes contribute between 2.2 and 6 Tg yr^{-1} of methane to the atmosphere and that 27 Tg yr^{-1} of methane may escape from deep water mud volcanoes (Dimitrov, 2003; Milkov et al., 2003). While there is a reliable number of ~900 known terrestrial mud volcanoes, estimates for marine mud volcanoes range between 800 and 100000, which makes any budget calculations very preliminary (Dimitrov, 2002; Dimitrov, 2003; Milkov, 2000; Milkov et al., 2003). Previous estimates suggested that the contribution of the worlds oceans to atmospheric methane is small with 2-3% at present (Houghton et al., 1996; Judd et al., 2002; Kvenvolden, 2002; Reeburgh, 1996). However, such estimates do not account for locally focused gas seepage from structures like mud volcanoes and other types of cold seeps.

The main sink for methane in the ocean is the anaerobic oxidation of methane with sulphate as electron acceptor (Hinrichs and Boetius, 2002; Iversen and Jørgensen, 1985; Nauhaus et al., 2002; Treude et al., 2003). This process is mediated by archaea, operating most likely in cooperation with sulphate reducing bacteria. So far, two groups of anaerobic methanotrophic archaea (ANME-1, ANME-2) have been identified (Boetius et al., 2000; Elvert et al., 1999; Hinrichs et al., 1999; Michaelis et al., 2002; Orphan et al., 2001b; Pancost et al., 2000; Thiel et al., 1999). They usually occur together with SRB from a distinct, yet uncultivated cluster within the *Desulfosarcina*/*Desulfococcus* group (Seep-SRB1) (Boetius et al., 2000; Elvert et al., 1999; Hinrichs et al., 1999; Knittel et al., 2003; Knittel et al., 2005; Michaelis et al., 2002; Orphan et al., 2001; Pancost et al., 2000; Thiel et al., 1999). Generally, microbial methane oxidation is characterized by a strong discrimination against the heavy, stable carbon isotope ^{13}C, leading to a significant depletion in the ^{13}C-content of metabolites and biomass (Elvert et al., 1999; Orphan et al., 2001b; Summons et al., 1994; Thiel et al., 1999; Whiticar, 1999; Whiticar et al., 1986). Such conspicuous isotope signatures of specific lipid biomarker for the archaeal and bacterial partners in AOM mediating communities has been a main tool in studying the diversity and functioning of cold seep ecosystems (Blumenberg et al., 2004; Elvert et al., 2003; Elvert et al., 2001; Hinrichs et al., 1999; Michaelis et al., 2002; Orphan et al., 2001b).

During the UNESCO program “Training through Research (TTR)”, numerous mud volcanoes hosting methane-hydrate were discovered in the Gulf of Cadiz (Gardner, 2001; Kenyon et al., 2001; Kenyon et al., 2000; Mazurenko et al., 2002; Somoza et al., 2002). However, the occurrence of methane emission to the hydrosphere and the geochemical and microbiological activity of these potential seep structures remained unknown. During the SO-175 expedition “GAP”, we studied several mud volcanoes with the aid of sea-floor video imaging as well as video-guided sampling of sediments and carbonate crusts. The main focus of this

investigation was to find the hot spots of methane turnover, to estimate the magnitude of methane consumption in the sediments of several mud volcanoes using *ex situ* rate measurements and diffusive flux calculations, as well as to identify the key methanotrophs using lipid biomarker and 16S rDNA methods.

2. MATERIALS AND METHODS

2.1 Geological Setting

The Gulf of Cadiz is located west of the Gibraltar Arc, between Iberia and the African plate (Fig. 1). This area has experienced a complex tectonic history with several episodes of extension, strike-slip and compression related to the closure of the Tethys Ocean, the opening of the N-Atlantic, and the African-Eurasian convergence since the Cenozoic (Maldonado et al., 1999). During the Tortonian, a large olistrostome body made of eroded material from the Betic Cordillera (Spain) and Rif Massif (Morocco) was emplaced west of the Straits of Gibraltar (Maldonado and Comas, 1992; Somoza et al., 2003). Due to the ongoing compression, these rapidly deposited sediments dewater intensely and form MVs and fluid escape structures (Diaz-del-Rio et al., 2003). The Gulf of Cadiz has been intensely surveyed with geophysical tools, leading to the discovery of the first MVs, mud diapirs and pockmarks in 1999 (Gardner, 2001; Kenyon et al., 2000; Pinheiro et al., 2003). In addition, an extensive field of mud volcanoes and diapiric structures covered with carbonate chimneys and crusts was discovered along or in close proximity of the main channels of the Mediterranean outflow water (Diaz-del-Rio et al., 2003; Kenyon et al., 2001; Kenyon et al., 2000; Kopf et al., 2004; Somoza et al., 2003).

In the present study, Captain Arutyunov (Capt. Arutyunov), Bonjardim, Ginsburg, Gemini, Hesperides and Faro MV and a newly discovered structure termed “No Name”, were investigated (Fig. 1, Tab. 1). Prior to biogeochemical sampling, the sea floor of selected MVs was monitored with the video-sled OFOS or with a video-guided multiple-corer (MUC, Tab. 1).

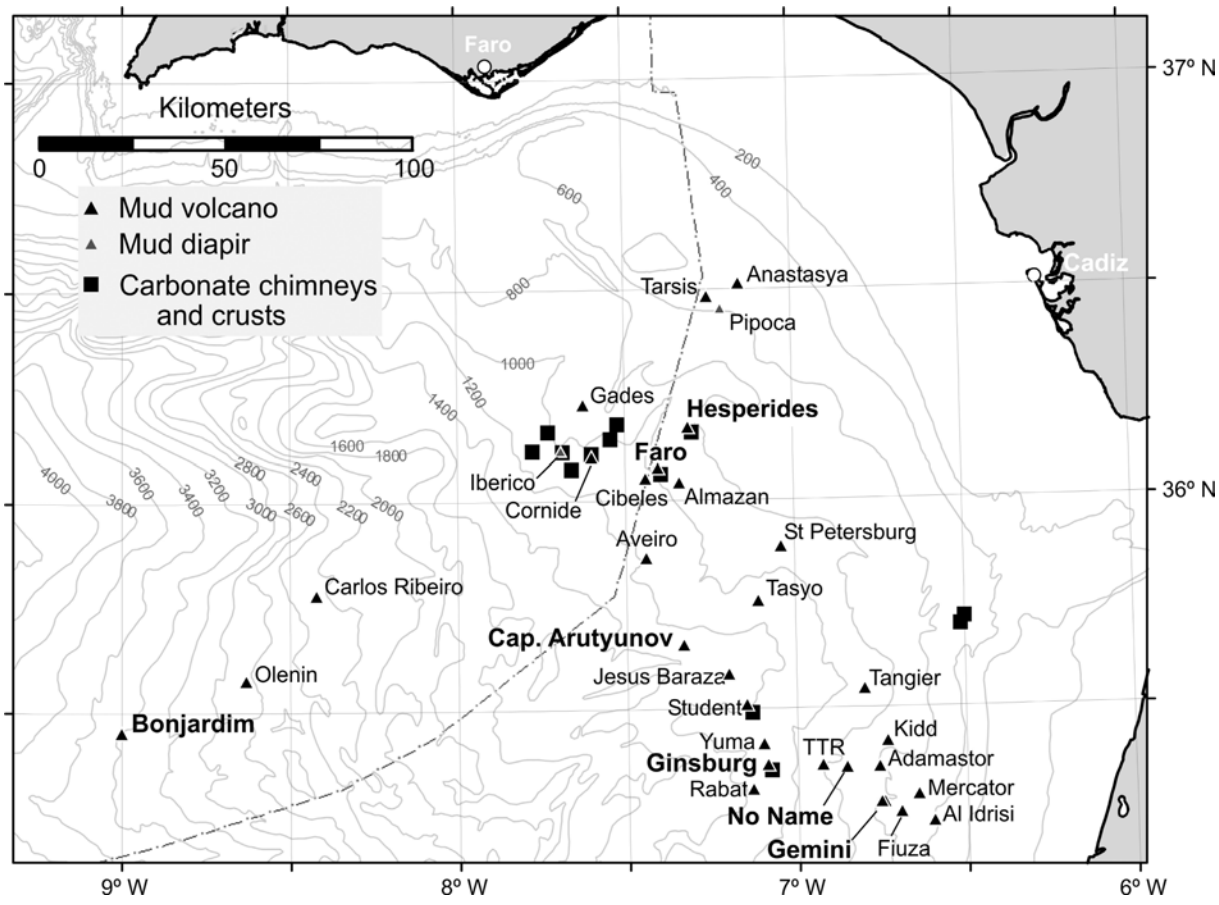

Figure 1. Bathymetric chart of the Gulf of Cadiz showing the locations of known mud volcanoes, diapirs and areas where carbonate chimneys and crusts were discovered. The mud volcanoes studied during the SO-175 expedition are in bold face letters.

2.2 Sample Collection and Storage

Sediments of several mud volcanoes were sampled by gravity coring in the central crater region (Tab. 1, Fig. 2). Additionally, surface sediments of Capt. Arutyunov and Bonjardim MV were obtained with a video-guided MUC because the top decimetres of sediment cover are usually lost during gravity core retrieval. Video-guided MUC sampling enabled the retrieval of undisturbed surface sediments of up to 50 cm sediment depth. Gravity coring retrieved up to 5 m of sediment. To account for an unknown loss of surface sediments during gravity coring, we aligned the depth of gravity cores obtained from Capt. Arutyunov and Bonjardim MV according to the vertical sulphate profiles of MUC-cores recovered from one

site, assuming that sulphate concentrations are mainly a function of depth in proximate cores. According to this procedure, the top sediment horizons of the recovered gravity cores were 40 and 12.5 cm below seafloor at Capt. Arutyunov and Bonjardim MV, respectively. Aligning proximate core sections is an approach to account for a loss of an unknown quantity of surface sediments during gravity coring. However, this approach can be problematic if spatial variability of geochemical gradients is high.

Table 1. Mud volcanoes investigated during the cruise SO-175. The water depth refers to the highest elevation of the mud volcanoes. V = video observations, CH_4 = methane concentration measurements, SO_4^{2-} = sulphate concentration measurements, C_{2+} = concentration measurements of higher hydrocarbons, F = diffusive methane and sulphate flux calculation, R, AOM and SR rate measurements, L = Lipid analyses, D = DNA analysis.

Structure	Relief [m]	Diam. [km]	Water depth [m]	Device	Core/Grab	Lat. N	Long. W	Applied Methods
CAMV	80	2.0	1315	MUC	GeoB 9036-2	35° 39.72'	07° 19.98'	V, CH_4, SO_4^{2-}, C_{2+}, H_2S, F, R, L, D
				GC	GeoB 9041-1	35° 39.70'	07° 19.97'	CH_4, SO_4^{2-}, C_{2+}, H_2S
Bonjardim	100	1.0	3090	MUC	GeoB 9051-1	35° 27.72'	08° 59.98'	V, CH_4, SO_4^{2-}, C_{2+}, H_2S, R, L
				GC	GeoB 9051-2	35° 27.61'	09° 00.03'	CH_4, SO_4^{2-}, C_{2+}, H_2S, F, R, L
Ginsburg	150	4.0	910	GC	GeoB 9061-1	35° 22.42'	07° 05.29'	V, CH_4, SO_4^{2-}, H_2S, F
Gemini	200	4.9	435	GC	GeoB 9067-1	35° 16.92'	06° 45.47'	CH_4, SO_4^{2-}, H_2S, F
No Name	150	3.7	460	GC	GeoB 9063-1	35° 21.99'	06° 51.92'	CH_4, SO_4^{2-}, H_2S, F
Hesperides	160	3.0	690	Grab	GeoB 9023-1	36° 10.73'	07° 18.39'	V, L
Faro	190	2.6	810	Grab	GeoB 9029-3	36° 05.68'	07° 24.12'	V, L

Upon recovery, gravity cores were sectioned into 1 m pieces and vertically cut in halves, prior to sub sampling. All cores were immediately transferred into a cold room and subsampled for concentration measurements of volatile pore water constituents (methane, sulphate, sulphide), AOM and SR rate measurements according to Treude et al (2003, 2005), as well as for lipid biomarker and 16S rDNA analyses (Tab. 1). Sediments for measurements of methane and sulphate concentrations and turnover rate measurements were subsampled vertically with push cores (acrylic core liners, 26 mm diameter, n = 3) from MUC-cores. Gravity cores were

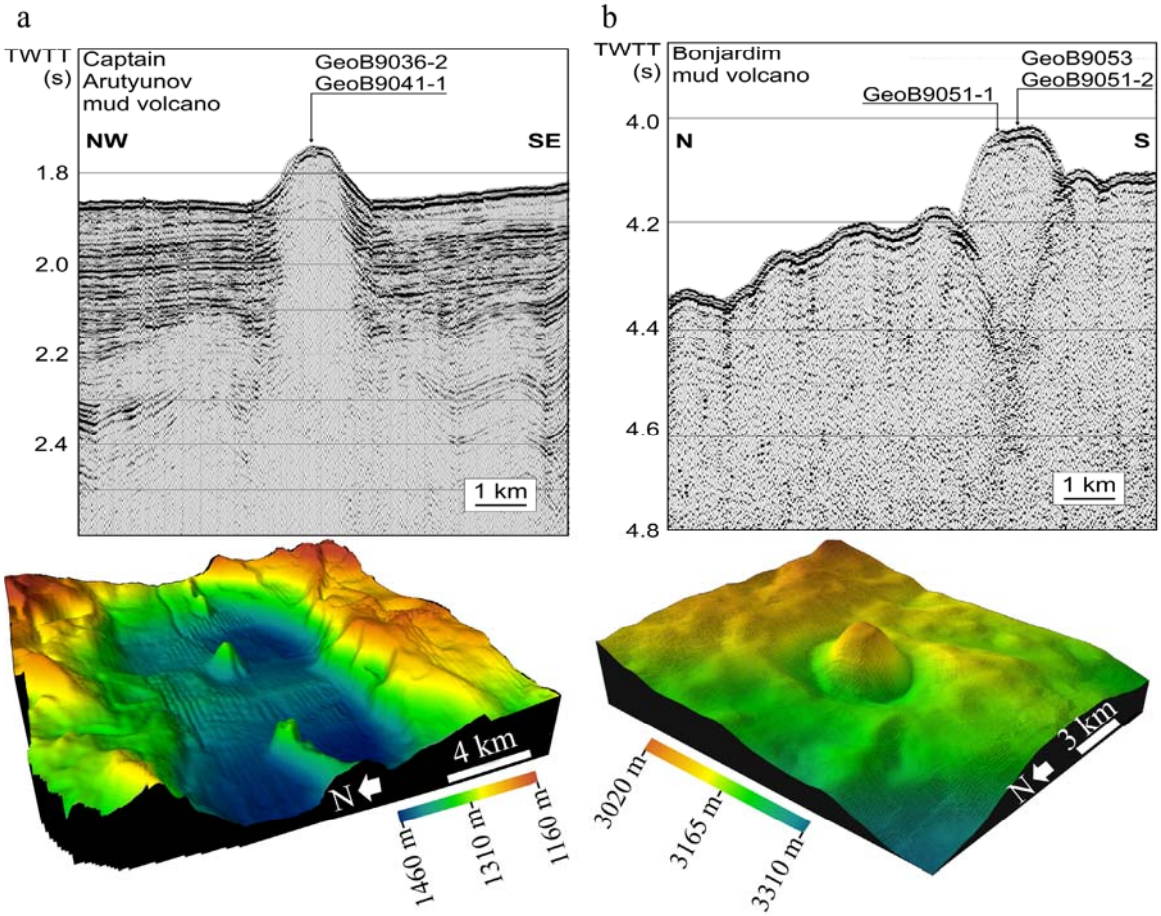

Figure 2. Seismic images and 3D images of multibeam bathymetry of Captain Arutyunov (a) and Bonjardim mud volcano (b). Seismic images show the central conduit below the mud volcanoes and sampling position of the cores recovered during the SO-175 expedition. Captain Arutyunov and Bonjardim MV are conical shaped structures with a relief of 80 and 100 m and a diameter of 2 and 1 km, respectively. Colours denote the bathymetry (m below sea surface). Seismic images were modified after Kenyon et al. (2001) (a) and Pinheiro et al. (2003) (b).

subsampled by plugging glass tubes (60 mm length, 10 mm diameter, n = 5) in selected sediment horizons. The tubes were then sealed with butyl rubber stoppers to allow for an anaerobic incubation of the sediment plug. Sediment samples for pore water extraction, biomarker and 16S rDNA analyses were collected from 2 cm sections of MUC cores and from selected horizons of gravity core sections. Directly after subsampling, pore water from these sediment horizons was extracted by pressure filtration (5 bars) through Teflon squeezers provided with 0.2 µm cellulose acetate filters according to previous works (Hensen et al.,

2003; Niewöhner et al., 1998). Subsequently, the pore water was immediately fixed (see next section). Lipid and DNA samples were stored in cleaned glass vials at –20°C until extraction in the home laboratory. Carbonate crusts from Hesperides and Faro MV were collected with a video guided grab-sampler (Tab.1). Upon recovery, carbonate crusts for lipid biomarker analyses were transferred into plastic bags and stored at –20°C until extraction.

2.3 Methane Concentrations

Methane concentrations in sediments were determined according to the "head space" method from 5 ml sediment fixed with 25 ml NaOH (2.5%, w/v) in a diffusion-tight glass vial as described previously by Treude and co-workers (2003). A vertical resolution of 2 cm was chosen for MUC cores whereas for gravity cores, a vertical resolution of 20-30 cm was chosen. Methane concentrations were determined shortly after the cruise (<2 month) using a gas chromatograph as described elsewhere (Treude et al., 2003). The chromatography system was calibrated for a concentration range of 0.001 to 5 mM methane (final concentration in the sediment). Sediment samples from Capt. Arutyunov and Bonjardim MV were additionally analysed for the concentrations of the higher hydrocarbons (C_{2+}) ethane, propane, isobutene and butane (Σbutane) using the above-described chromatography setting with a temperature gradient. Subsequent to injection at 40°C, the temperature was increased at a rate of 2°C min^{-1} to 200°C and held for 20 min. Identity and concentrations of methane and C_{2+}-compounds were determined with standards of known hydrocarbon compositions.

2.4 Sulphate and Sulphide Concentrations

Standard methods were applied for sulphate and sulphide analyses. Sulphide concentrations were determined immediately after sampling by adding 1 ml of pore water to 50 µl of a zinc acetate gelatine solution. Sulphide was quantitatively removed as ZnS and kept in colloidal solution. After adding a colour reagent the concentration was determined photometrically by measuring the absorbance after 1 hour at 670 nm (see more detailed descriptions at http://www.geomar.de/zd/labs/labore_umwelt/Analytik.html). Sulphate concentrations were determined on 2 ml sub-samples of filtered pore water using a Sykom-S ion chromatography system. Samples were diluted by 1:54 with the eluent (7.5 mM Na_2CO_3-solution).

2.5 Diffusive Flux Calculations

Local fluxes (J) were calculated from the vertical profiles of pore water constituents (methane, sulphate, sulphide) according to Fick's first law of diffusion assuming steady state conditions (e.g. Niewöhner et al., 1998 and references therein),

$$J = -\phi D_s \frac{\delta C}{\delta x} \quad (1)$$

where D_s is the diffusion coefficient in the sediments, ϕ the porosity and $\frac{\delta C}{\delta x}$ the local concentration gradient (in cm^{-4}). D_s was determined from the molecular diffusion coefficient after Boudreau (1997).

$$D_s = \frac{D_0}{1 - \ln(\phi)^2} \quad (2)$$

For each mud volcano, D_0 values were corrected for temperature (3 to 12°C, depending on the actual bottom water temperature), resulting in values ranging between 291 to 392, 178 to 244

and 356 to 434 for methane, sulphate and sulphide, respectively (Boudreau, 1997). ϕ was determined from the weight loss per volume of wet sediment after drying to stable weight at 60°C. In general, ϕ decreased with depth showing values of 57 - 76% in the top sections and 51 - 60% in the bottom sections of the retrieved MUCs and GCs (data shown for the SMT, Tab. 2).

Table 2. Concentrations gradients, diffusive fluxes and *ex situ* AOM and SR rates integrated over depth. A negative flux value indicates downward directed flux, a positive value indicates upward flux. * and ‡ denote gradients and total sulphate fluxes determined from aligning multiple- and gravity cores. Gradients in brackets indicate upward diffusing sulphate and downward diffusing sulphide, respectively.

			Conc. gradient [µmol cm^{-4}]			Diffusive fluxes [mmol m^{-2} yr^{-1}]			Microbial turnover [mmol m^{-2} yr^{-1}]	
Structure	Core GeoB	Porosity [%]	CH_4	SO_4^{2-}	Sulphide	CH_4	ΣSO_4^{2-}	ΣSulphide	AOM	SR
Capt. Arutyunov	9036-2	56	0.40	-1.12	0.63	407	708	702	383	577
Bonjardim	9051-2	58	0.09	-0.76,-1.67*	0.23,0.73* (-0.07)	76	388,867‡	299,795‡	36	690
Ginsburg	9061-1	60	0.05	-0.92 (0.35)	0.32 (-0.15)	55	852	565		
Gemini	9067-1	56	0.02	-0.61	0.12 (-0.09)	21	388	272		
No Name	9063-1	57	0.03	-0.11	0.04 (-0.06)	29	74	108		

2.6 Ex-situ AOM and SR Rate Measurements

Sediment for turnover rate measurements recovered from Capt. Arutyunov and Bonjardim MV were incubated on board according to previously described methods (Treude et al., 2003; Treude et al., 2005). Briefly, 25µl $^{14}CH_4$ (dissolved in water, 2.5 kBq) or 5 µl $^{35}SO_4^{2-}$ tracer (dissolved in water, 50 kBq) were injected into butyl rubber sealed glass tubes from gravity core sub-sampling and in 1 cm intervals into small push cores (whole core injection) used for MUC sub-sampling. Incubation was carried out for 24 h at *in situ* temperature in the dark. Subsequently, incubated AOM and SR rate samples were fixed in 25 ml NaOH (2.5%, w/v)

and 25 ml zinc acetate solution (20%, w/v), respectively. Further processing of AOM and SR rate samples was performed according to Treude et al (2003) and references therein. Turnover rates were calculated according to the following formulas:

$$\mathrm{AOM} = \frac{^{14}\mathrm{CO_2}}{^{14}\mathrm{CH_4} + ^{14}\mathrm{CO_2}} \times \frac{\mathrm{conc.CH_4}}{\mathrm{incubat.Time}} \quad (3)$$

$$\mathrm{SRR} = \frac{\mathrm{TRI}^{35}\mathrm{S}}{^{35}\mathrm{SO_4}^{2-} + \mathrm{TRI}^{35}\mathrm{S}} \times \frac{\mathrm{conc.SO_4}^{2-}}{\mathrm{incubat.Time}} \quad (4)$$

Here, $^{14}CO_2$, $^{35}SO_4^{2-}$ and $TRI^{35}S$ are the activities (Bq) of carbon dioxide, sulphate and total reduced sulphur species, respectively, whereas conc. CH_4 and conc. SO_4^{2-} are the concentrations of methane and sulphate at the beginning of the incubation. To compare *ex situ* microbial rates with the diffusive fluxes of methane and sulphate, AOM and SR rates were integrated over depth in cores 9036-2 and 9051-2, respectively.

2.7 Extraction of Sediment and Carbonate Samples and Preparation of Derivates

Sediments from Capt. Arutyunov and Bonjardim MV as well as carbonate crusts from Hesperides and Faro MV were analysed for lipid biomarker signatures. The extraction procedure and preparation of fatty acid methyl esters (FAMES) was carried out according to Elvert et al. (2003). Briefly, total lipid extracts (TLE) were obtained from ca. 20 g of wet sediment and from authigenic carbonates disintegrated with HCL (2M) prior to extraction. The TLE was extracted by subsequent ultrasonication using organic solvents of decreasing polarity. Internal standards of known concentration and carbon isotopic compositions were added prior to extraction. Fatty acid moieties present in glyco and phospholipids were cleaved by saponification with methanolic KOH-solution. After extraction of the neutral lipid fraction from this mixture, fatty acids (FAs) were methylated with BF_3 in methanol yielding FAMES.

Double bond positions of monoenoic FAs were determined by analysis of dimethyl disulphide adducts according to methods described elsewhere (Moss and Lambert-Fair, 1989; Nichols et al., 1986).

Neutral lipids were further separated into hydrocarbons, ketones and alcohols on a SPE silica glass cartridge (0.5 g packing) with solvents (5 ml each) of increasing polarity (*n*-hexane/dichloromethane (95:5, v/v), *n*-hexane/dichloromethane (2:1, v/v), dichloromethane/acetone (9:1, v/v)). Alcohols were derivatised with bis(trimethylsilyl)triflouracetamid (BSTFA) forming trimethylsilyl (TMS) ethers prior to analyses.

2.8 Gas Chromatography

Concentrations of single lipid compounds were determined by gas chromatography analysis using a Varian 30 m apolar CP-Sil 8 CB fused silica capillary (0.25 mm internal diameter [ID], film thickness 0.25 μm) in a Hewlett Packard 6890 Series gas chromatograph equipped with an on column injector and a flame ionisation detector. Initial Oven temperature was 80°C. Subsequently to injection, the initial temperature was increased to 130°C at a rate of 20°C min^{-1}, then raised to 320°C at a rate of 4°C min and held at 320°C for 30 min. The carrier was helium at a constant flow of 2 ml min^{-1} and the detector temperature was set to 310 °C. Concentrations were calculated relative to internal standards present within the respective lipid fraction.

2.9 Gas Chromatography-Mass Spectrometry (GC-MS), Gas Chromatography-Isotope Ratio Mass Spectrometry (GC-IRMS)

Identity and stable carbon isotope ratios of individual compounds were determined by GC-MS and GC-IRMS analysis, respectively. Instrument specifications and operation modes of the GC-MS and GC-IRMS units were set according to Elvert et al. (2003). Identities of acquired mass spectra were compared to known standards and published data. Stable isotope ratios are given in the δ-notation against Pee Dee Belemite. δ^{13}C-values of FAs and alcohols were corrected for the introduction of additional carbon atoms during derivatisation. Internal standards were used to monitor precision and reproducibility during measurements. Reported δ^{13}C-values have an analytical error of ±1‰.

2.10 DNA Extraction and Clone Library Construction

Total community DNA was extracted from sediments (ca. 1 g) collected from the SMT of Capt. Arutyunov MV (30-40 cm) using the FastDNA spin kit for soil (Q-Biogene, Irvine, California, USA). Samples were bead-beat in a Fastprep machine (Q-Biogene, Irvine, California, USA) at speed 4.5 for 30 seconds. All other steps in the DNA extraction procedure were preformed according to the manufacturer's recommendations. Almost full-length archaeal and bacterial 16S rRNA genes were amplified from sediments samples using the primers 20f (Massana et al., 1997) and Uni1392R (Lane et al., 1985) for archaea and GM3F (Muyzer et al., 1995) and GM4R (Kane et al., 1993) for bacteria. Polymerase chain reactions (PCRs) were performed with TaKaRa Ex Taq (TaKaRa, Otsu Japan), using 2.5 U of enzyme, 1X Buffer, 4 mM of $MgCl_2$, 4 mM of each dNTP, 1 μM of each primer and 2 μl of template in a 50 μl reaction. PCR reactions were preformed in a Mastercycler machine (Eppendorf,

Hamburg, Germany), with the following cycling conditions: 95°C for two minutes, then 30 cycles of 95°C for 30 seconds, 60°C (archaea) or 50°C (bacteria) for 30 seconds and 72°C for 3 minutes, followed by a final incubation step at 72°C for 10 minutes. PCR products were visualized on an agarose gel, and the 16S band excised. PCR products were purified using the QIAquick Gel Extraction Kit (Qiagen, Hilden, Germany). Two microliters of purified DNA were ligated in the pGEM T-Easy vector (Promega, Madison, WI) and transformed into competent E. coli TOP10 cells (Invitrogen, Carlsbad, CA) according to the manufacturer's recommendations. Transformation reactions were plated on LB-agarose plates. Overnight cultures were prepared from individual colonies picked from these plates using the Montage Plasmid Miniprep 96 kit (Millipore, Billerica, USA). Purified plasmids were sequenced in one direction, with either the 958R (archea) or GM1F (bacteria) primers using the BigDye Terminator v3.0 Cycle Sequencing kit (Applied Biosystems, Foster City, USA). Samples were sequenced on an Applied Biosystems 3100 Genetic Analyser (Foster City, USA). A total of 39 archaeal and 47 bacterial clones were partially sequenced (~ 0.5 kb). Using the ARB software package, the sequences were calculated into existing phylogentic trees by parsimony without allowing a change in the tree topology. Representative sequences of each cluster were then fully sequenced (~1.3 kb) and matched against the NCBI data base (http://www.ncbi.nlm.nih.gov/BLAST). Sequences were submitted to the Genbank database (http://www.ncbi.nlm.nih.gov/) and are accessible under the following accession numbers: DQ004661 to DQ004676 and DQ004678 to DQ004680.

3. RESULTS

3.1 Field Observations

A detailed description of sea floor video observations, sedimentology and sampling locations is provided in the report of R/V SONNE cruise SO-175 (Kopf et al., 2004). The mud volcanoes Capt. Arutyunov, Bonjardim, Ginsburg, Gemini, and Faro studied here are cone shaped with a relief of up to 200 m and a maximum diameter of 4.9 km kilometres (Fig. 2a,b; Tab.1). Hesperides MV has comparable dimensions but is composed of 6 single cones. A new structure was discovered east of the TTR MV and termed "No Name" (Fig. 1). Video observations of the mud volcanoes Capt. Arutyunov, Bonjardim, Ginsburg, Hesperides, and Faro could not reveal indications for recent gas, fluid or mud expulsion (2-3 tran-sects with a total bottom observation time of approximately 8 hrs per mud volcano, Kopf et al., 2004). The central craters of Capt. Arutyunov, Bonjardim and Ginsburg MV were covered with

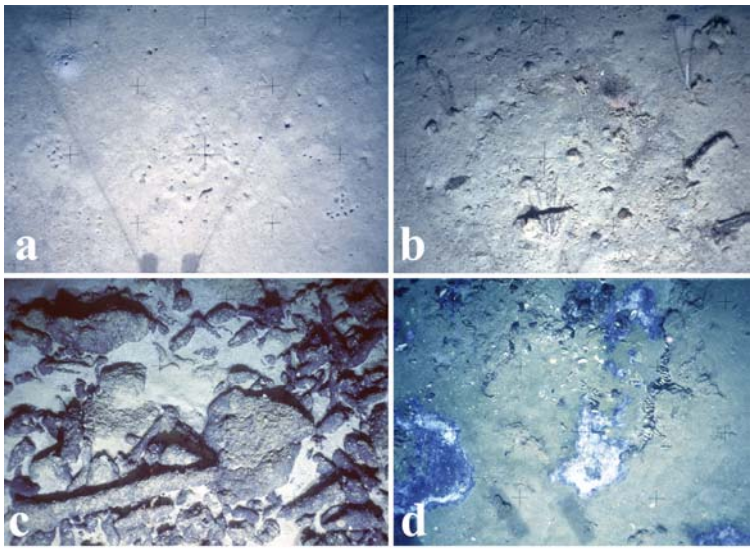

Figure 3. Seafloor images of Capt. Arutyunov (a,b), Hesperides (c) and Faro MV (d). The surface of Capt. Arutyunov, Bonjardim, Ginsburg MV were found to be covered by pelagic sediments as shown in panel a. Some sediment stretches at Capt. Arutyunov MV contained accretions that are interpreted as clasts (b) indicating past mud flows. Hesperides and Faro mud volcano were found littered with carbonate chimneys and crusts as shown for Hesperides MV in panel (c). At Faro mud volcano, also a few dark sediment patches probably covered with giant sulphide oxidizing bacteria were observed (d).

light beige sediments (shown for Capt. Arutyunov MV, Fig. 3a). At Capt. Arutyunov MV, some sediment stretches were scattered with accretions, interpreted as clasts, which may indicate past mud flows (Fig. 3b). At Ginsburg MV, a few small carbonate crusts (<0.5 m) were observed on the seafloor. Beside these observations, no other distinctive sedimentological or biological features indicating gas or fluid seepage were visible on video images at Ginsburg. Surface sediments recovered from Capt. Arutyunov MV contained small tubeworms (diameter <<1 mm), which extended down to 20 cm into the sediment. Tube worms usually harbour methane- or sulphide oxidising symbionts, indicating sulphide and/or methane availability in the sediments (Kimura et al., 2003; Schmaljohann and Flugel, 1987; Sibuet and Olu, 1998; Southward et al., 1986; Southward et al., 1981). The central areas of Hesperides and Faro MV were littered with fragments of carbonate chimneys and carbonate crusts (shown for Hesperides MV, Fig. 3c). Both, chimneys and crusts were ranging in size from several centimetres to meters in length and diameter. At Faro MV, a few, small patches covered with microbial mats possibly consisting of filamentous sulphide oxidising bacteria were observed (Fig. 3d). Moreover, grab samples recovered from this MV also contained a few specimens of the chemosynthetic clam *Acharax sp.* usually harbouring sulphide oxidising bacteria in their gills (Felbeck, 1983; Krueger and Cavanaugh, 1997; Peek et al., 1998; Sibuet and Olu, 1998). Video observations were not carried out at Gemini MV and the "No Name" structure. The MUC-cores retrieved from Capt. Arutyunov and Bonjardim MV contained yellowish, muddy sediments in the top sections at 0-20 and 0-40 cm below sea floor (bsf), respectively. The bottom sections of the MUC-cores contained mud breccia. The gravity cores retrieved from these MVs as well as those retrieved from Ginsburg and Gemini also contained mud breccia. In contrast to the MUC-cores recovered from Capt. Arutyunov and Bonjardim MV, the mud breccia in all of the retrieved gravity cores was only covered by a thin layer (max. 10 cm) of yellowish mud. This directly indicates a loss of the beige surface sediments during sediment sampling and core retrieval. The gravity core recovered from the "No Name"

structure contained a matrix of cold water coral fragments and greyish mud. It has to be further investigated if this structure is a mud volcano or a mud diapir. Grab samples from Hesperides and Faro MV contained carbonate fragments and mud breccia. After recovery, the temperature in the top sediment section (~1 m) at Bonjardim MV was ca. 3°C. In contrast, the temperature was considerably higher at Capt. Arutyunov (12°C), Ginsburg MV, Gemini MV and the "No Name" structure (10°C, respectively) most probably as a result of the warm Mediterranean outflow water, which contributes to the bottom water at these MVs.

3.2 Captain Arutyunov Mud Volcano

3.2.1 Methane, C_{2+}, Sulphate and Sulphide

Methane concentrations in surface sediments (0-20 cm, Fig. 4a) were <0.001 mM indicating a complete consumption of methane rising from deeper sediment strata. A distinct SMT was observed in the lower half of the MUC-core section (25 - 40 cm bsf.). The steepest gradients of methane and sulphate amounted to 0.4 and –1.12 µmol cm^{-4}, respectively (Fig. 4a, Tab. 2). Small gas hydrate chips were found throughout the whole gravity core section from 44 to 235 cm bsf (1941-1). Probably, gas hydrates were also present in the lower section of the MUC-core (9036-2) but dissociated upon core recovery and sediment subsampling. Similar to methane, concentrations of C_{2+}-compounds decreased across the SMT (Fig. 4b). Hydrocarbons in the sediment porewaters comprised methane (> 99%), ethane (<0.4%), propane (<0.07%) with trace amounts of butane and isobutene present. Sulphide concentrations peaked in the SMT with 4.8 mM at 39 cm bsf (Fig. 4d). The steepest sulphide gradient was 0.63 µmol cm^{-4} (Fig. 4d, Tab. 2). A downward sulphide gradient could not be

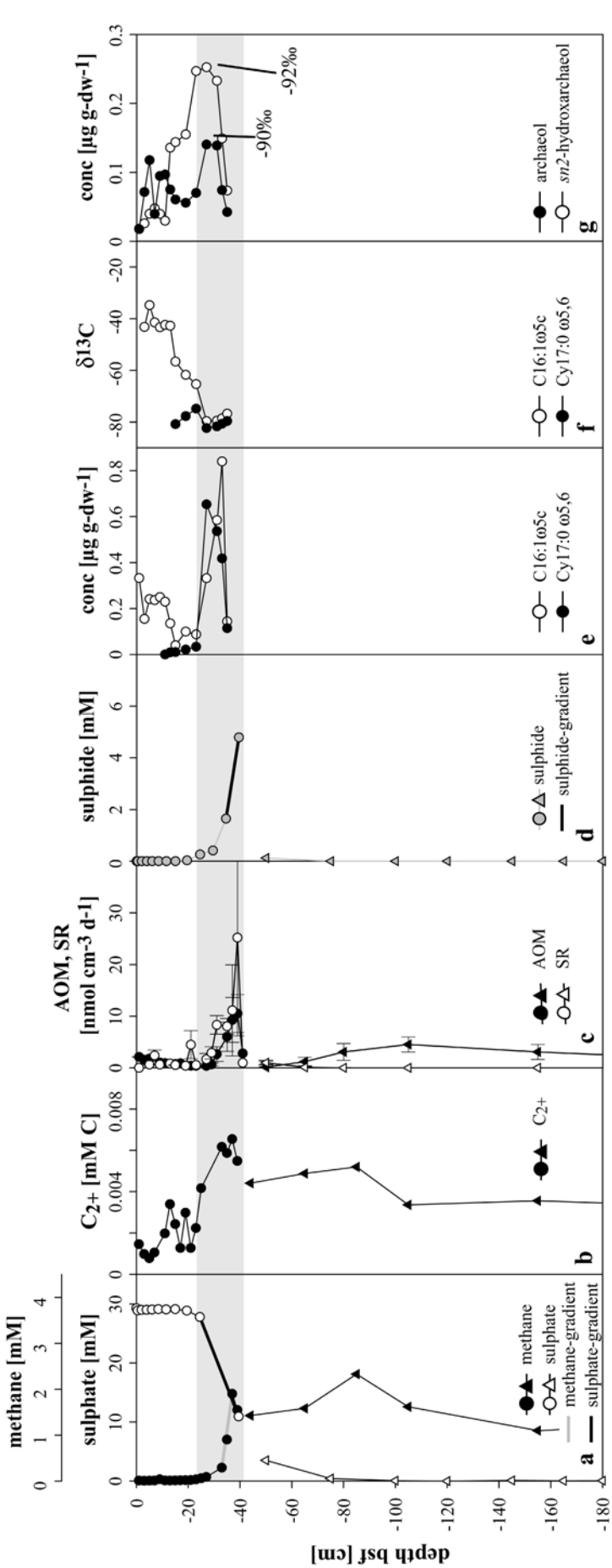

Figure 4. Captain Arutyunov mud volcano. A distinct SMT, highlighted in grey, was found between 25 and 40 cm bsf (a). At this horizon, concentrations of higher hydrocarbons also decline (b). Note that AOM and SR rates (c), sulphide concentrations (d), concentrations (e) and stable carbon isotope values of diagnostic, bacterial fatty acids (f) and concentrations of isoprenoidal diethers (g) all peak at the SMT. Panel (a) and (d) illustrate steepest gradients determined for methane, sulphate and sulphide (bold lines). Circles represent multiple corer and triangles gravity corer samples. Errors are given as standard errors.

determined because highest sulphide concentrations were observed in the lowest sediment horizon of the MUC-core at Capt. Arutyunov MV. Unfortunately, the sulphide profile could not be aligned continuously with the gravity core section.

3.2.2 AOM, SR Rates and Diffusive Fluxes

AOM and SR rates at Capt. Arutyunov MV were highest in the SMT at 39 cm bsf with maximum values of 11 and 25 nmol cm^{-3} d^{-1}, respectively (Fig. 4c). AOM and SR rates sharply decreased above and below this horizon. A 1.8-fold higher areal SR compared to AOM indicates an additional electron donor fuelling sulphate reduction (Tab. 2). The areal AOM and SR rate were in good agreement with diffusive fluxes showing a 1.7-fold higher sulphate flux compared to the methane flux. The sulphide flux to the surface (upward flux) was comparable to the total downward flux of sulphate (Tab. 2).

3.2.3 Lipid Biomarker

Diagnostic archaeal and bacterial lipid concentrations were strongly increased in sediments at the SMT (Fig. 4c,e). At this horizon (-31 cm), stable carbon isotope analysis revealed highest depletion in ^{13}C with minimum values of –92‰ (*sn2*-hydroxyarchaeol) in archaeal specific diether lipids and –82‰ ($cyC_{17:0\omega5,6}$) in bacterial specific FAs (Tab. 3, Fig. 4d,e). The concentration of both archaeal and bacterial lipids decreased just above and below this sediment horizon. At the SMT, the ratio of *sn2*-hydroxyarchaeol relative to archaeol was 1.6:1 (Tab. 3). Other diagnostic, archaeal isoprenoidal hydrocarbons such as 2,6,11,15-tetramethylhexadecane (crocetane) could not be measured due to an unresolved complex

Table 3. Bacterial fatty acids, archaeal diether and isoprenoidal hydrocarbons analysed in sediments at the SMT of Captain Arutyunov and Bonjardim MV as well as in carbonate crusts from Hesperides and Faro MV. Abundances of fatty acids were normalised to i-$C_{15:0}$, archaeal diethers to archaeol and archaeal isoprenoidal hydrocarbons to PMI:0. Specific lipid components are highlighted in grey.

			Sediment		Carbonate	
			Captain Arutyunov	Bonjardim	Hesperides	Faro
Normalised abundance (δ^{13}C-values)	Bacterial fatty acids	$C_{14:0}$	1.3 (-75)	2.0 (-37)	1.1 (-31)	2.3 (-93)
		i-$C_{15:0}$	1.0 (-71)	1.0 (-42)	1.0 (-39)	1.0 (-99)
		ai-$C_{15:0}$	1.3 (-73)	8.4 (-47)	1.5 (-43)	1.9 (-95)
		$C_{15:0}$	0.6 (-73)	1.4 (nd)	0.3 (-45)	0.4 (-96)
		i-$C_{16:0}$	0.2 (-73)	nd	0.2 (nd)	0.2 (-87)
		$C_{16:1\omega9}$	0.7 (-65)	nd	nd	0.1 (-92)
		$C_{16:1\omega7}$	0.8 (-67)	14.6 (-34)	0.6 (-27)	1.8 (-93)
		$C_{16:1\omega5}$	7.7 (-80)	8.4 (-49)	0.1 (-41)	0.7 (-96)
		$C_{16:0}$	2.4 (-67)	7.8 (-21)	4.8 (-27)	1.6 (-77)
		10 $Me_{C16:0}$	0.3 (-67)	nd	nd	1.0 (-94)
		i-$C_{17:0}$	0.3 (-69)	nd	0.3 (-32)	0.3 (-96)
		ai-$C_{17:0}$	0.1 (nd)	1.1	0.5 (-38)	0.3 (-99)
		$C_{17:1\omega7}$	0.9 (-68)	1.9	0.5 (-31)	0.4 (-93)
		$C_{17:1\omega6}$	1.9 (-74)	nd	nd	0.1 (nd)
		cy$C_{17:0\omega5,6}$	7.1 (-82)	nd	nd	nd
		$C_{17:0}$	nd	nd	0.2 (nd)	0.1 (nd)
		$C_{18:1\omega9}$	1.0 (-27)	6.4 (-27)	0.2 (nd)	0.3 (-77)
		$C_{18:1\omega7}$	0.9 (-31)	13.7 (-31)	0.4 (-37)	1.5 (-84)
		$C_{18:0}$	0.2 (-25)	3.5 (-25)	1.8 (-28)	0.4 (-67)
	Archaeal lipids	Archaeol	1.0 (-90)	1.0 (-81)	1.0 (-97)	1.0 (-114)
		sn2-hydroxyarchaeol	1.7 (-92)	0.7 (-83)	tr	0.2 (-111)
		Crocetane / Phytane			0.5 (-47)	3.3 (-110)
		PMI:0			1.0 (-87)	1.0 (-111)
		ΣPMI:1			0.3 (nd)	4.6 (-113)
		ΣPMI:2			nd	8.3 (-113)
		ΣPMI:3			nd	0.3 (-101)
Concentration [µg g-dw^{-1}]	Bacterial fatty acids	i-$C_{15:0}$	0.08	0.01	0.1	8.7
		ai-$C_{15:0}$	0.1	0.09	0.15	16.77
		$C_{16:1\omega5}$	0.6	0.09	0.01	6.05
		$C_{17:1\omega6}$	0.14	nd	n d	0.5
		cy$C_{17:0\omega5,6}$	0.56	nd	n d	nd
	Archaeal lipids	Archaeol	0.14	0.4	2.39	41.58
		sn2-hydroxyarchaeol	0.23	0.3	0.02	8.31
		Crocetane / Phytane			0.23	4.59
		PMI:0			0.44	1.4
Putative origin			ANME2 Seep-SRB1	ANME1 Seep-SRB1 & ANME2 Seep-SRB1	ANME1 Seep-SRB1 (?)	ANME1 Seep-SRB1 & ANME2 Seep-SRB1

mixture in all of the hydrocarbon fractions. Similarly, specific archaeal diethers and bacterial FAs could not be resolved from this background below 40 cm sediment depth. The concentrations of diagnostic archaeal lipids were roughly one order of magnitude lower in comparison to specific bacterial FAs.

The FA fraction in sediments at the SMT was dominated by $C_{16:1\omega5}$ and $cyC_{17:0\omega5,6}$ and contained comparably high amounts of FA $C_{17:1\omega6}$ (Tab. 3). Both, $C_{16:1\omega5}$ and $cyC_{17:0\omega5,6}$ were the most ^{13}C-depleted FAs. However, all other FAs in the C_{14} to C_{17} range carried significantly ^{13}C-depleted isotope signatures as well with values ranging between -65‰ ($C_{16:1\omega9}$) to –75‰ ($C_{14:0}$). C_{18}-FAs were comparably enriched in ^{13}C as shown by $\delta^{13}C$ -values ranging between -25‰ ($C_{18:0}$) to -31‰ ($C_{18:1\omega7}$) most likely indicating a planktonic origin of these compounds. Concentrations of mono- and di-alkyl glycerol ethers (MAGEs and DAGEs, respectively) presumably of bacterial origin were low in all samples recovered during cruise SO-175. Thus, a detailed analysis of these compounds was not carried out. However, sediments at the SMT of Capt. Arutyunov Mud Volcano comprised comparably high contents of MAGEs relative to DAGES with $\delta^{13}C$ values ranging from –65‰ to -85‰ (data not shown). The MAGEs comprised a suite of alkyl moieties, which is comparable to those of the fatty acids found at Capt. Arutyunov MV. The suite of fatty acids extracted from the tube worms comprised dominant amounts of the FAs $C_{16:1\omega7}$ and $C_{18:1\omega7}$ and to a lesser degree $C_{16:0}$ and $C_{18:0}$ with uniform $\delta^{13}C$-values of about -40‰, indicating chemoautotrophic carbon fixation (data not shown). The alcohol and hydrocarbon fractions were not analysed.

3.2.4 Phylogenetic Diversity

Two clone libraries, one archaeal and one bacterial, were constructed to study the 16S rDNA-based microbial diversity in sediments at the SMT of Capt. Arutyunov MV (30-40 cm bsf). The 16S rDNA archaeal clone library consisted of 9 phylogenetic groups (Tab. 4). Closest relatives of these groups were found among seep-endemic, uncultured archaea and bacteria. The majority of sequences obtained were related to the ANME-2 group (59% ANME-2a, 3% ANME-2c of all archaeal sequences) which is known to mediate AOM (Boetius et al., 2000; Knittel et al., 2005; Orphan et al., 2002). The second most abundant group (18% of all archaeal sequences) was found to belong to the ANME-1 cluster which is also known to mediate AOM (Hinrichs et al., 1999; Michaelis et al., 2002; Orphan et al., 2002). The bacterial clone library consisted of 10 uncultivated bacterial lineages. Similar to the archaeal

Table 4. Archaeal and bacterial 16S rDNA clone libraries obtained from sediments of the SMT of Captain Arutyunov MV. The Archaeal clone library is dominated by sequences belonging to the ANME-2 cluster and the bacterial library by sequences belonging to the Seep-SRB1 cluster.

Phylogenetic group		Clones	Representative clone	Next relative	Sequence similarity
Archaea		39			
Euryarchaeota	ANME 2a	23	CAMV300A948 (DQ004662)	Uncultured cold seep archaeal clone BS-K-H6 (AJ578128)	99%
	ANME 2c	1	CAMV301A975 (DQ004668)	Uncultured hydrocarbon seep archaeal clone C1_R019 (AF419638)	99%
	ANME 1	7	CAMV300A952 (DQ004664)	Uncultured hydrocarbon seep archaeal clone HydCal61 (AJ578089)	99%
	Marine Benthic Group D	1	CAMV300A963 (DQ004667)	Uncultured hydrothermal vent archaeal clone pMC2A203 (AB019737)	98%
	Marine Benthic Group D	1	CAMV300A951 (DQ004663)	Uncultured contaminated aquifer archaeal clone WCHD3-02 (AF050616)	90%
	Uncalssified Archaea	3	CAMV301A993 (DQ004661)	Uncultured hydrothermal vent archaeal clone NT07-CAT-A24 (AB111475)	80%
	Unclassified Archaea	1	CAMV301A980 (DQ004669)	Uncultured hydrothermal vent archaeal clone VC2.1 Arc6 (AF068817)	87%
Crenarchaeota	Marine Benthic Group B	1	CAMV300A958 (DQ004665)	Uncultured archaeal clone BS-K-D4 (AJ578124)	99%
	Unclassivied Archaea	1	CAMV300A960 (DQ004666)	Uncultured cold seep archaeal clone BS-SR-H5 (AJ578148)	98%
Bacteria		47			
δ Proteobacteria	Seep SRB 1	38	CAMV300B922 (DQ004675)	Uncultured hydrocarbon seep bacterial clone Hyd89-04 (AJ535240)	99%
	Seep SRB 1	1	CAMV301B937 (DQ004679)	Uncultured Echinocardium cordatum hindgut bacterial clone Del 7 (AY845643)	96%
	Desulfobulbaceae	1	CAMV300B921 (DQ004674)	Uncultured hydrocarbon seep bacterial clone Hyd89-51 (AJ535252)	99%
γ Proteobacteria	Stenotrophomonas	1	CAMV301B944 (DQ004671)	Stenotrophomonas maltophilia (AB008509)	99%
Clostridia	Clostridiaceae	1	CAMV300B923 (DQ004676)	Uncultured hydrocarbon seep bacterial clone GCA025 (AF154106)	98%
	Thermoanaerobacteriaceae	1	CAMV300B902 (DQ004670)	Uncultured bacterial clone DR9IPCB16SCT8 (AY604055)	98%
Spirochaetes	Spirochaeta	1	CAMV301B941 (DQ004680)	Uncultured Spirochaeta sp. (AF424377)	96%
	Spirochaeta	1	CAMV300B915 (DQ004672)	Uncultured spirochete clone IE052 (AY605138)	96%
	Unclassified bacteria	1	CAMV300B916 (DQ004673)	Uncultured hydrocarbon seep bacterial clone Hyd24-12 (AJ535232)	97%
	Unclassified bacteria	1	CAMV301B934 (DQ004678)	Uncultured hydrocarbon seep bacterial clone 1B-41 (AY592596)	93%

sequences, the next relatives of all bacterial 16S rDNA sequences belonged to uncultivated organisms that are commonly found at methane seeps (Knittel et al., 2003, Tab. 4). The closest relatives of the most abundant cluster of sequences (81%) belonged to the Seep-SRB1 group which comprises the bacterial partners of ANME-1 and ANME-2 (Knittel et al., 2003). Other phylogenetic groups of bacteria were represented by single clone sequences (<2%).

3.3 Bonjardim MV

3.3.1 Methane, C_{2+}, Sulphate and Sulphide

A distinct SMT was observed in the top meter of the gravity core section. After alignment with the MUC-core section, the actual depth of the SMT was determined between 45 and 70 cm bsf (Fig. 5a). As the two core sections overlap, the concentration gradients can be determined from the gravity core section alone or from aligned profiles in the overlapping zone (Fig. 5a,d). Here, we used both approaches in order to investigate the potential range for the diffusive fluxes. The steepest methane and sulphate gradients in the gravity core section were determined with 0.09 and –0.76 µmol cm^{-4}, respectively (Fig. 5a, Tab. 2). Aligning the gravity core and MUC-core sections, the steepest sulphate gradient was –1.67 µmol cm^{-4}. Methane concentrations declined below the depth at which the two core sections overlap. Hence, no concentration gradient from core alignments was possible. Methane concentrations in surface sediments (0 – 52 cm sediment depth) were <0.001 mM indicating a complete consumption of methane in the SMT. C_{2+}-concentrations were comparably high with values of >0.25 mM at a sediment depth below 1 m (Fig. 5b). Similar to methane, concentrations of C_{2+}-compounds decreased across the SMT (Fig. 5b) indicating a consumption of these compounds. Gaseous hydrocarbons comprised methane (>81%), ethane (<14%), propane

(<4.5%) and Σbutane (<0.4%). Sulphide concentrations peaked in the SMT with 5.3 mM at 52.5 cm bsf (Fig. 5d). In the gravity core section, the steepest sulphide gradients were determined with 0.23 (upward) and –0.07 (downward) µmol cm^{-4}, respectively (Tab. 2). Aligning the two core sections, the steepest (upward) sulphide gradient was determined with 0.73 µmol cm^{-4}.

3.3.2 AOM, SR Rates and Diffusive Fluxes

AOM and SR rates were highest in the SMT at 58 cm bsf with maximum values of 2.6 and 15.4 nmol cm^{-3} d^{-1}, respectively. Comparably low values of AOM and SR rates were measured in over- and underlying sediment horizons. A 19.3-fold higher areal SR compared to AOM indicates a decoupling of these two processes (Tab. 2). Considering both concentration gradients (determined from unaligned and aligned profiles), the diffusive downward flux of sulphate was 5.1- to 11-fold higher compared to the upward methane flux. Similarly, the cumulative sulphide flux (upward and downward) accounted for 77% to 92% of the sulphate flux.

3.3.3 Lipid Biomarker

A moderate increase of diagnostic archaeal and bacterial lipid concentrations was observed at the SMT in sediments of Bonjardim MV (Fig. 5c,e). At this horizon (-57 cm), stable carbon isotope analysis revealed highest depletions in ^{13}C with minimum values of –83‰ (*sn2*-hydroxyarchaeol) in archaeal diether lipids and –49‰ ($C_{16:1\omega5}$) in bacterial FAs (Tab. 3, Fig. 5d,e). At the SMT, the ratio of *sn2*-hydroxyarchaeol relative to archaeol was 0.7:1 and

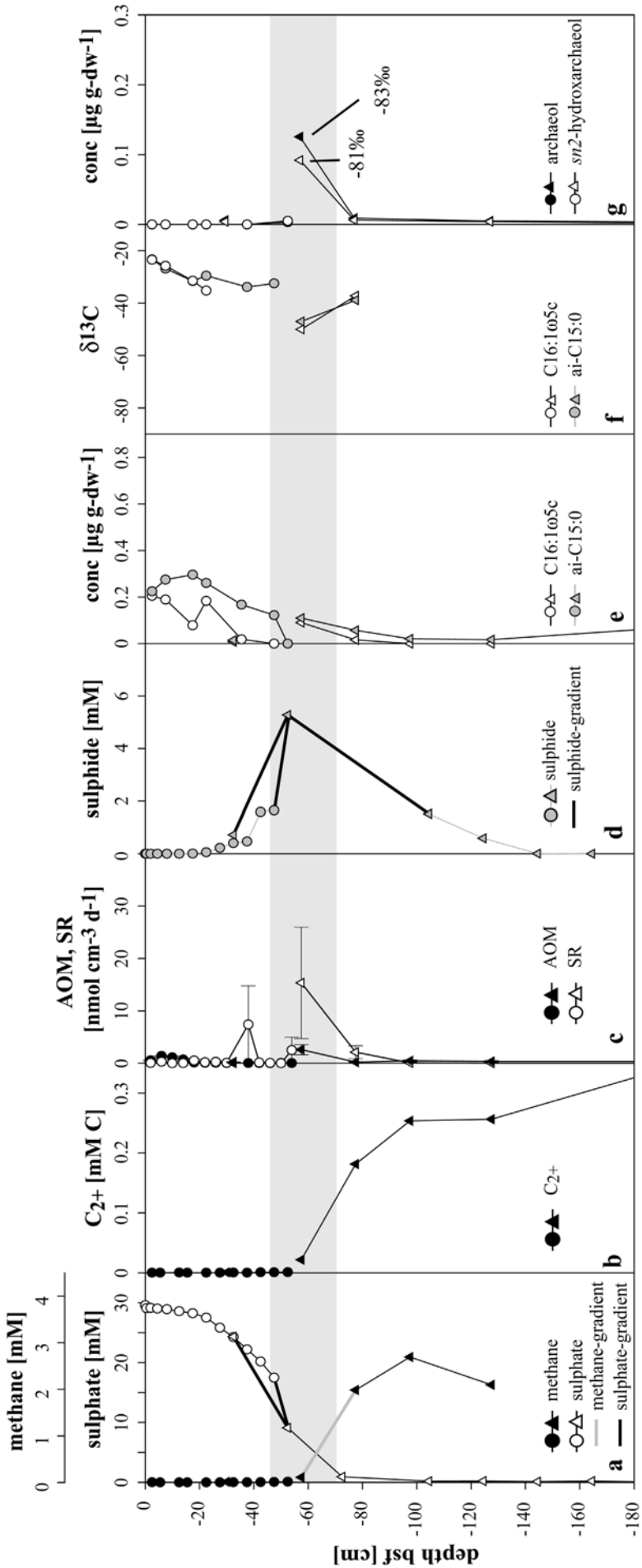

Figure 5. Bonjardim mud volcano. A distinct SMT, highlighted in grey, was found between 50 and 70 cm bsf (a). At this horizon, concentrations of higher hydrocarbons also decline (b). Note that concentrations of C_{2+}-compounds are ~35-fold higher compared to Captain Arutyunov MV. AOM and SR rates (c), sulphide concentrations (d), concentrations (e) and stable carbon isotope values of diagnostic, bacterial fatty acids (f) and concentrations of isoprenoidal diethers (g) peak at the SMT. Panel a and d illustrate steepest gradients determined for methane, sulphate and sulphide (bold lines). Concentration gradients for sulphate and sulphide were determined from gravity core samples and from aligned gravity core and multiple-corer samples. Circles represent multiple corer and triangles gravity corer samples. Errors are given as standard errors.

therefore lower in comparison to Capt. Arutyunov MV (Tab. 3). Similar to Capt. Arutyunov MV, other diagnostic archaeal isoprenoidal hydrocarbons could not be measured due to a high background from an unresolved complex mixture of hydrocarbons. Equally high amounts of the FAs $C_{16:1\omega5}$ and ai-$C_{15:0}$, both of which were the most ^{13}C-depleted FAs (Tab. 3), were detected in sediments at the SMT. The FA cy$C_{17:0\omega5,6,}$ which was abundant at Capt. Arutyunov MV could not be detected in sediments of Bonjardim MV. Furthermore, dominant FAs such as $C_{16:1\omega7}$, $C_{16:0}$, $C_{18:1\omega9}$ and $C_{18:1\omega7}$ carried $\delta^{13}C$-signatures ≥-34‰, indicating that these compounds are derived from processes other than AOM. In contrast to Capt. Arutyunov MV, the concentrations of diagnostic archaeal lipids were roughly 4-fold higher compared to specific bacterial FAs (Tab. 3). A further analysis of the diversity of microbial organism using 16S rDNA methods was not carried out at Bonjardim MV.

3.4 Ginsburg MV, Gemini MV and "No Name"

3.4.1 Methane, Sulphate and Sulphide

The SMT was located in the upper metre of the sediment cores retrieved from Ginsburg and Gemini MV and at 2-3 m bsf at the "No Name" structure, respectively (Fig. 6a, c, e). Methane concentrations in sediments overlying the SMT at these structures were <0.001 mM. Sediments retrieved from Ginsburg MV had a distinct smell of petroleum with depth below 40 cm. No depth corrections were made as only gravity cores were taken from these MVs.

The actual depth of the SMTs was therefore most likely 10 to 40 cm below the sediment depth indicated in figure 6. In contrast to the observed depletion of sulphate below the SMT at Gemini MV and the "No Name" structure, sulphate concentrations showed a minimum between 30 to 70 cm and an increase to values ≥17 mM with depth below 90 cm at Ginsburg MV. The total, diffusive sulphate flux was therefore calculated from both, the upward and the downward gradients at Ginsburg MV. At Ginsburg MV, Gemini MV and the "No Name" structure, methane and downward sulphate gradients ranged from 0.02 to 0.05 and –0.11 to -0.92 µmol cm^{-4}, respectively (Tab. 2). The upward sulphate gradient at Ginsburg MV was 0.35 µmol cm^{-4}. Sulphide concentrations peaked in the SMT with values between 4.7 to 7.6 mM and steepest gradients were determined with values between 0.04 to 0.32 (upward) and –0.06 to –0.15 (downward) µmol cm^{-4}, respectively (Tab. 2).

3.4.2 Diffusive Fluxes

The diffusive sulphate flux at Ginsburg MV, Gemini MV and the "No Name" structure exceeded the methane fluxes with 15.5-, 18.5- and 2.5-fold, respectively. This gives evidence for a decoupling of AOM and SR at these structures similar to the observations made at Bonjardim MV (Tab. 2). The cumulative (upward + downward) sulphide flux accounted for 66, 70 and 146% of the sulphate fluxes at Ginsburg MV, Gemini MV and the "No Name" structure, respectively. The composition of the microbial community was not investigated here.

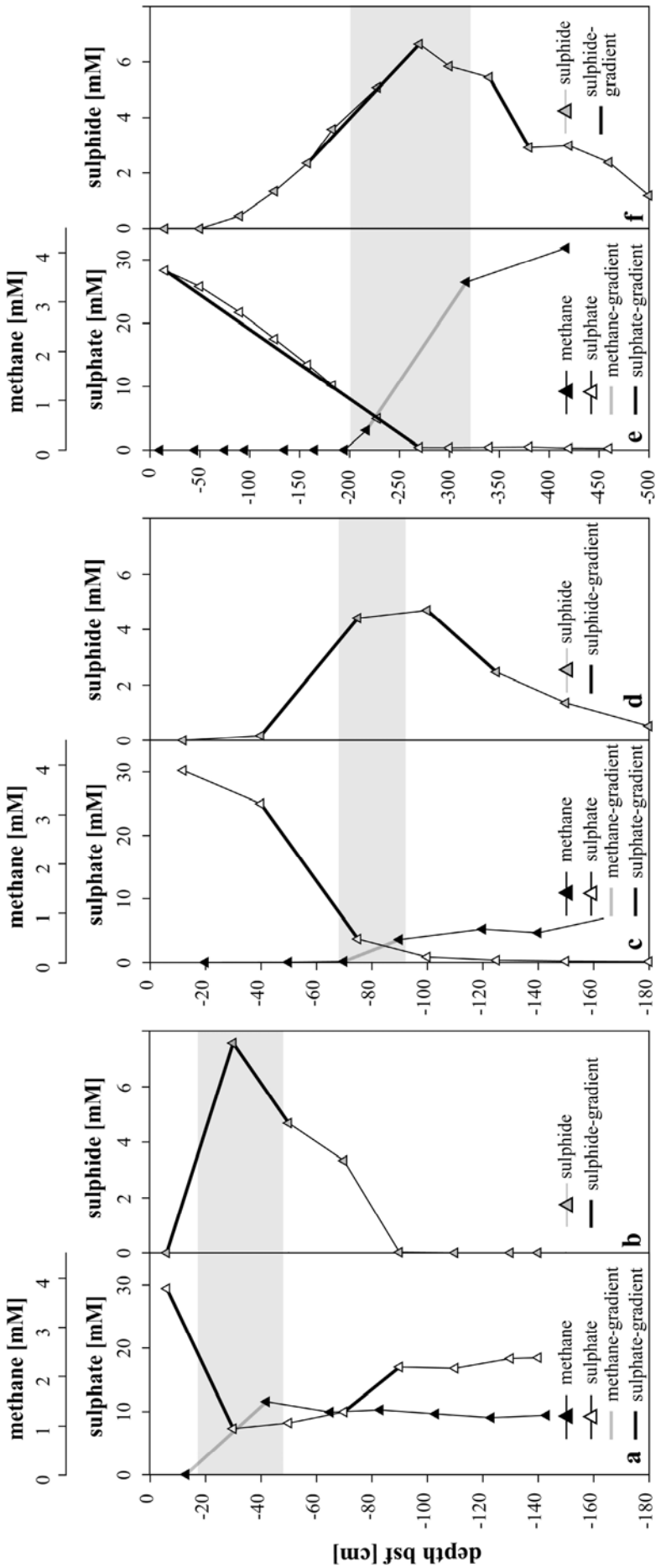

Figure 6. The SMT, highlighted in grey, was found in the top most m at Ginsburg (a) and Gemini (c) and between 2 and 3 m at No Name MV (e, note the different scale chosen for depth). In these horizons, also sulphide concentrations peak (b, d, f). Bold lines illustrate steepest gradients determined for methane, sulphate and sulphide.

3.5 Lipid Biomarkers of Carbonate Crusts

Exposed carbonate crusts were observed at the mud volcanoes Ginsburg, Hesperides and Faro. Additionally, high amounts of broken carbonate chimneys were found at Hesperides and Faro MV. Both crusts and chimneypieces were absent at Capt. Arutyunov MV, Bonjardim MV and the "No Name" structure according to our visual inspections. We could retrieve crust samples from the summits of Hesperides and Faro MV for further analyses of the lipid signatures of the crusts.

3.5.1 Hesperides MV

Carbonate crusts of Hesperides MV contained archaeal and bacterial lipids diagnostic for methanotrophic communities and processes. Archaeal lipids were strongly depleted in $\delta^{13}C$ with minimum values of –97‰ (archaeol) whereas bacterial FAs were only moderately depleted with minimum values of –43‰ (ai-$C_{15:0}$, Tab. 3). Only trace amounts of *sn2*-hydroxyarchaeol were detected among the archaeal diethers. Isoprenoidal hydrocarbons were dominated by 2,6,10,15,19-pentamethylicosane (PMI:0) and contained comparably low amounts of a crocetane / 2,6,10,14-tetramethylhexadecane (phytane) mixture and ΣPMI:1 (comprising 2 isomers). The FA fraction in the carbonate was dominated by $C_{16:0}$ followed by $C_{18:0}$ with $\delta^{13}C$-values >-28‰ (Tab. 3). FAs putatively specific for SRB involved in AOM such as $C_{16:1\omega5}$, i-$C_{15:0}$ and ai-$C_{15:0}$ (Blumenberg et al., 2004; Elvert et al., 2003), were approximately 3 to 4.8 times lower in concentration compared to $C_{16:0}$. However, in contrast to abundant FAs, stable carbon isotope compositions of i-$C_{15:0}$, ai-$C_{15:0}$ and $C_{16:1\omega5}$ showed a moderate depletion in ^{13}C (Tab. 3). Moreover, in comparison to specific archaeal lipids, diagnostic bacterial FAs were roughly an order of magnitude lower in concentration.

3.5.2 Faro MV

All archaeal and bacterial lipids found in carbonate crusts of Faro MV were strongly depleted in ^{13}C (Tab. 3). Stable carbon isotope analysis revealed minimum $\delta^{13}C$ values of –114‰ (archaeol) in diagnostic archaeal diether lipids and –99‰ (i-$C_{15:0}$) in specific bacterial FAs (Tab. 3). Archaeal diether lipids were dominated by archaeol and contained comparably low amounts of *sn2*-hydroxyarchaeol. Isoprenoidal hydrocarbons were dominated by PMI:2 (9 isomers) followed by PMI:1 (2 isomers) and relatively high amounts of crocetane/phytane. Specific FAs showed comparably small differences in abundance and $\delta^{13}C$-values (Tab. 3). However, ai-$C_{15:0}$ was the most dominant FA with a roughly 2-fold higher concentration compared to i-$C_{15:0}$ and $C_{16:1\omega5}$. The FA cy$C_{17:0\omega5,6}$ was not detected. Concentrations of specific FAs were comparable to specific archaeal lipids.

4. DISCUSSION

4.1 Methane-Driven Geochemical and Biological Activity at the Mud Volcanoes of the Gulf of Cadiz

Marine mud volcanoes have been identified as an important escape pathway of reduced hydrocarbon gases and may therefore contribute significantly to atmospheric green house gases (Dimitrov, 2002; Dimitrov, 2003; Judd et al., 2002; Kopf, 2002). Methane venting at such cold seeps provides an energy source for methanotrophic microbes which in turn may support enormous biomasses of seep-related macrofauna and thiotrophic, giant bacteria (Boetius and Suess, 2004; Cordes et al., 2005; Milkov et al., 2004; Olu et al., 1997; Sahling et al., 2002; Werne et al., 2002). Furthermore, methane venting is often associated with authigenic carbonates (Aloisi et al., 2000; Hensen et al., 2004; Kopf, 2002). The Gulf of Cadiz is characterised by numerous mud volcanoes which have been intensely surveyed since their discovery in 1999 (Kenyon et al., 2001; Kenyon et al., 2000; Pinheiro et al., 2003; Somoza et al., 2002). Among the findings indicative of past and present methane venting at several mud volcanoes are the occurrence of hydrate-bearing sediments, authigenic carbonates and seep related biota (Diaz-del-Rio et al., 2003; Gardner, 2001; Pinheiro et al., 2003; Somoza et al., 2003). Yet, the present activity of these structures in methane emission to the atmosphere remained unknown. Direct sea floor observations during cruise SO-175 revealed only few traces of methane seepage at the centres of the mud volcanoes Capt. Arutyunov, Bonjardim, Ginsburg and Hesperides, and the “No Name” structure. No visible fluid or gas escape was detected with video observations, indicating that the mud volcanoes may be relatively inactive and that methane is completely consumed within subsurface sediment horizons. In contrast, highly active seep systems such as Hydrate Ridge, the Gulf of Mexico

or Håkon Mosby Mud Volcano discharge methane into the hydrosphere through focused gas and fluid escape pathways, despite the high methane and sulphate turnover rates controlling substantial fractions of the methane flux (Boetius et al., 2000; Damm and Budeus, 2003; Joye et al., 2004; Treude et al., 2003).

The high anaerobic methane turnover at active seeps produces high sulphide fluxes, which are utilized by thiotrophic communities, e.g. mats of giant bacteria like *Beggiatoa sp.*, various chemosynthetic bivalves like *Calyptogena sp.*, *Acharax sp.*, *Bathymodiolus sp.* and by several tubeworm species (Sibuet and Olu, 1998). These organisms are adapted to different geochemical settings and can be used as indicators for high methane fluxes and turnover in subsurface or near surface sediments. Three types of indicator communities were so far observed at low abundances at the investigated mud volcanoes. Some small (ca. 20 cm diameter) blackish sediment patches covered with bacterial mats were found at Faro MV indicating locally elevated fluxes of methane and sulphide, which reach the surface of the seafloor (Fig. 6d). Few specimen of the deep dwelling thiotrophic bivalve *Acharax sp.* were recovered from Faro MV and previously from Ginsburg MV (Gardner, 2001). Members of the family *Solemyidae* are mostly deep burrowing and occur in seep habitats with low or moderate methane and sulphide fluxes where they can take up sulphide through their foot from subsurface accumulations (Sahling et al., 2002; Sibuet and Olu, 1998; Treude et al., 2003). At Hydrate Ridge for instance, *Acharax sp.* mines subsurface sediments for sulphide pockets below 15 cm sediment depth (Sahling et al., 2002). As a third indicator species, tube worms were recovered from Capt. Arutyunov and previously observed at Bonjardim MV (Pinheiro et al., 2003). Tube worms can extend their roots very deep into sediments to profit from subsurface methane and/or sulphide accumulations (Dando et al., 1994; Gebruk et al., 2003; Southward et al., 1981). At Capt. Arutyunov MV, the moderate depletion of worm-

derived membrane lipids indicates a thiotrophic feeding mode fuelled by AOM-derived sulphide rather than an aerobic methanotrophic mode.

4.2 Hotspots of Hydrocarbon Turnover at the Mud Volcanoes of the Gulf of Cadiz

The observed patterns of seep related biota is in good agreement with the observed geochemical gradients. All mud volcanoes investigated here showed a complete depletion of methane within the SMT. Elevated and corresponding AOM and SR rates within this zone give evidence that uprising methane is consumed anaerobically with sulphate by methanotrophic, microbial communities leading to a depletion of the two compounds in sediments of Capt. Arutyunov MV and Bonjardim MV at 25 to 40 cm and 45 to 70 cm bsf, respectively (Fig. 4a, 5a). Accordingly, concentration measurements of methane and sulphate and the resulting estimates of diffusive methane and sulphate fluxes at Ginsburg MV, Gemini MV and the "No Name" structure indicate that sulphate-dependent AOM is a wide spread microbial process in the centres of the mud volcanoes of the Gulf of Cadiz. With respect to methane fluxes and microbial turnover rates at the time of our investigation, Capt. Arutyunov MV is the most active of the investigated structures followed by Bonjardim, Ginsburg and Gemini MV, while "No Name" is the least active structure (Tab. 2). Furthermore, highest turnover rates and fluxes coincided with the shallowest SMT comparing all investigated MVs. Hence, compared to other marine gas seeps and methane-rich environments, the Gulf of Cadiz MVs investigated here showed a low or medium range in methane turnover rates, reflecting the relatively low methane fluxes. At the Namibian Shelf, the north western Black Sea Shelf and the western Argentinean Basin for instance, the SMT is located several meters bsf and methane fluxes are low with values usually <55 mmol m^{-2} yr^{-1} (Hensen et al., 2003; Jørgensen et al., 2001; Niewöhner et al., 1998). These values are comparable to Ginsburg and Gemini

MV as well as to the "No Name" sructure. The AOM activity and diffusive methane fluxes at Capt. Arutyunov and Bonjardim MV were substantially higher than those at Ginsburg MV, Gemini MV and the "No Name" structure. However, areal rates and diffusive fluxes at Capt. Arutyunov and Bonjardim MV are still two orders of magnitude lower in comparison to other cold seeps, which bear gas hydrates at their stability limit such as Hydrate Ridge and the Gulf of Mexico. In such environments with active fluid flow (>100 cm yr^{-1}) and gas emission via ebullition, methane fluxes were estimated with values >8.7 mol m^{-2} yr^{-1} (Luff and Wallmann, 2003; Torres et al., 2002) and AOM reached values >4 mol m^{-2} yr^{-1}, i.e. >0.5 µmol cm^{-3} d^{-1} (Joye et al., 2004; Treude et al., 2003).

At Bonjardim MV, integrated SR rates agreed best with the sulphate flux calculated from the aligned sulphate profile. Additionally, the deviation of integrated rates from diffusive fluxes calculated from the gravity core alone could be caused by the much lower resolution of subsamples taken from these cores. Integrated rate measurements were comparable to diffusive fluxes at Capt. Arutyunov and Bonjardim MV (Tab. 3). However, further modelling is required to assess a potential advective transport component in order to estimate total fluxes. Also, the roughly s-shaped sulphate concentration profile from Ginsburg MV can not be explained by a steady state, diffusive transport as this would require an additional sulphate source at about 80 cm bsf.

In vitro experiments with sediment slurries and ex situ tracer injection assays showed that AOM and SR are in a 1:1 molar stoichiometry if methane is the sole carbon source (Nauhaus et al., 2002; Treude et al., 2003). In spite of the disproportionate loss of methane and sulphate caused by degassing during sampling, the deviation from the 1:1 stoichiometry between AOM and SR as well as between the sulphate and methane fluxes (Tab. 2) indicates the presence of electron donors other than methane for SR at the investigated MVs. SRB can use a variety of

short and long chain alkanes and complex aliphatic and aromatic compounds (Rueter et al., 1994; Widdel and Rabus, 2001). The energy yield from the degradation of e.g. ethane coupled to sulphate reduction (reaction 4) is higher than syntrophic AOM (reaction 5) (refer to Hanselmann et al., (1991) for Gf^0-values of the reactants).

$$4C_2H_{6\,(aq)} + 7SO_4^{2-}{}_{(aq)} \rightarrow 8HCO_3^-{}_{(aq)} + 7HS^-{}_{(aq)} + 4H_2O_{\,(l)} + H^+{}_{(aq)},\ \Delta G^0 = -279\ kJ\ mol^{-1} \quad (4)$$

$$CH_{4\,(aq)} + SO_4^{2-}{}_{(aq)} \rightarrow HCO_3^-{}_{(aq)} + HS^-{}_{(aq)} + H_2O_{\,(l)},\ \Delta G^0 = -33\ kJ\ mol^{-1} \quad (5)$$

Hence, it is possible that a substantial fraction of SR is fuelled by the anaerobic oxidation of C_{2+}-compounds in sediments where methane and higher hydrocarbons co-occur. Besides the present observations on C_{2+} compounds at Capt. Arutyunov and Bonjardim MV, Mazurenko et al. (2003) observed a composition of hydrocarbon gases at Ginsburg MV, which is very similar to Bonjardim MV. The presence of substantial amounts of higher hydrocarbons in these MVs, as well as the likely presence of petroleum in sediments of Ginsburg MV indicate that methane is of a thermogenic origin in the Gulf of Cadiz, and that hydrocarbon-fuelled sulphate reduction could be an important microbial process in the sediments. Accordingly, AOM explained a smaller fraction of SR at Bonjardim MV, which had a higher C_{2+} concentration than Capt. Arutyunov MV (Fig. 4b-c, 5b-c, Tab. 2). This is comparable to previous findings from the Gulf of Mexico where SR rates exceeds AOM rates up to 10-fold, most likely due to the presence of a variety of hydrocarbons and petroleum in the sediments (Joye et al., 2004). The microbial hydrocarbon degraders at natural petroleum seeps have not been identified yet.

Another interesting, potentially microbial process is the oxidation of sulphide in anaerobic sediments just above and below the depth of the SMT (Fig. 4d-6d). At least at Capt. Arutyunov MV, a biological control of the upward sulphide flux seems likely. At many seep

systems, the upward sulphide flux is utilized by thiotrophic organisms such as endosymbiotic bacteria living in invertebrate organisms such as clams and tube worms (Felbeck, 1983; Fisher, 1990; Sahling et al., 2002; Sibuet and Olu, 1998; Southward et al., 1986) and by various giant sulphide-oxidizing bacteria like *Beggiatoa sp.* and *Thioploca sp.* which can use oxygen or nitrate as electron acceptors (Fossing et al., 1995; Huettel et al., 1996; Mussmann et al., 2003; Nelson et al., 1982). At Capt. Arutyunov MV, the tubes of the worms extend to 20 cm. The upper horizon where sulphide consumption takes place is at 20 to 40 cm bsf, hence it seems likely that the worms and/or gliding bacteria can be responsible for this process. In contrast, it appears very unlikely that organisms depending on oxygen or nitrate utilise sulphide below the horizon where sulphide is produced. Here, a reaction of downward diffusing sulphide with iron as proposed previously is a more likely explanation (Hensen et al., 2003; Jørgensen et al., 2004).

In conclusion, our biogeochemical measurements as well as biological and geological observations indicate that the MVs studied during cruise SO-175 are currently not emitting methane and other hydrocarbon gases to the hydrosphere. However, there is evidence for extensive fluid and/or gas escape in the past, as indicated by the widespread occurrence of massive carbonate chimneys and crusts along or in close proximity to the main channels of the Mediterranean outflow water in the northern part of the Gulf of Cadiz (Diaz-del-Rio et al., 2003; Somoza et al., 2003). Another geological evidence for temporally varying activities of mud volcanism in the Gulf of Cadiz are the typical “Christmas tree” structures observed on high-resolution seismic profiles (Somoza et al., 2003; Somoza et al., 2002). Such patterns are probably caused by eruptive events followed by phases of dormancy. This so-called multiphase activity is a common behaviour in many terrestrial mud volcanoes (e.g. Lokbatan MV; Aliyev et al., 2002; Dimitrov, 2003; Kholodov, 2002). It is therefore possible that mud volcanism in the Gulf of Cadiz is in a transient state of low activity at present.

4.4 Identity of Methane Oxidising Communities in Sediments and Carbonate Crusts

Fingerprinting of diagnostic lipids is a common tool for the chemotaxonomic identification of micro organisms (Boschker and Middelburg, 2002; Madigan et al., 2000). This approach has been used extensively to examine anaerobic methanotrophic organisms, because the carbon isotope fractionation associated with AOM leads to specific, very depleted $\delta^{13}C$-signatures of lipid biomarkers (Blumenberg et al., 2004; Elvert et al., 2001; Hinrichs et al., 1999). The dominance of bacterial and archaeal lipids with low $\delta^{13}C$-values in sediments and carbonates indicate that AOM is a dominant biomass-generating process at the explored MVs. Differences in the abundances of specific archaeal isoprenoidal diethers and hydrocarbons and varying contents of bacterial FAs, as well as varying $\Delta\delta^{13}C$ values of these lipids (compared to source methane) give evidence that several phylogenetic groups of methanotrophic communities mediate AOM in the Gulf of Cadiz. Elevated concentrations and associated low $\delta^{13}C$-signatures of specific archaeal and bacterial membrane lipids corresponded with elevated AOM and SR rates in sediments of the SMT at Capt. Arutyunov and Bonjardim MV (Fig. 4e-g, 5e-g, Tab. 3). The molecular analyses give evidence that AOM is mediated by a microbial community consisting of methanotrophic archaea and SRB phylogenetically related to those which were previously found at other methane seeps (Boetius et al., 2000; Michaelis et al., 2002; Orphan et al., 2002; Teske et al., 2002). Furthermore, the presence of a similar suite of ^{13}C-depleted lipids in abundant authigenic carbonates recovered from Hesperides and Faro MV (Tab.3) indicates higher activities and a more wide spread methane turnover in the past.

4.4.1 Methanotrophic Archaea

Previous publications revealed dominant amounts *sn2*-hydroxarchaeol relative to archaeol in ANME-2 dominated habitats, whereas the reverse was observed in ANME-1 dominated systems (Blumenberg et al., 2004; Boetius et al., 2000; Orphan et al., 2001a; Teske et al., 2002). Moreover, ANME-2 communities were found to comprise high contents of crocetane which is only present at low concentrations in ANME-1 (Blumenberg et al., 2004; Boetius et al., 2000; Elvert et al., 1999). Moreover, stable carbon isotope fractionations were found to be higher in ANME-2 compared to ANME-1 dominated habitats with $\Delta\delta^{13}$C-values (archaeol relative to source methane) ranging between 34 to 53‰ and 11 to 37‰, respectively (Blumenberg et al., 2004; Boetius et al., 2000; Elvert et al., 2001; Hinrichs et al., 1999; Orphan et al., 2002; Teske et al., 2002).

The high ratio of *sn2*-archaeol relative to archaeol and a $\Delta\delta^{13}$C-value of 42‰ of archaeol compared to source methane (-48‰, Nuzzo et al., 2005) at Capt. Arutyunov MV is in good agreement with the published lipid signatures of ANME-2 dominated habitats. Furthermore, the dominant abundance of ANME-2 compared to ANME-1 clone sequences, together with the lipid biomarker fingerprint suggest a dominance of ANME-2 in sediments of Capt. Arutyunov MV.

The comparably high ratio of archaeol relative to *sn2*-hydroxyarchaeol as well as a $\Delta\delta^{13}$C-value of -31.5‰ of archaeol compared to source methane at Bonjardim MV (-49.5 ‰, Nuzzo et al., 2005) lies between published values from systems dominated by ANME-1 and ANME-2. This suggests a mixed ANME community in these sediments.

The low ratio of *sn2*-hydroxyarchaeol relative to archaeol in carbonate crusts obtained from Hesperides MV is in very good agreement with the published values for ANME-1 communities. Our chromatography settings for hydrocarbon separation did not resolve crocetane from its isomer phytane, which is a known breakdown product of chlorophyll. However, the comparably heavy $\delta^{13}C$-value of this compound mixture provides evidence for a low crocetane content, which furthermore agrees with a dominant ANME-1 origin of archaeal lipid biomass in these carbonates. Similar to Bonjardim MV, the lipid imprint in carbonate crusts recovered from Faro MV shows characteristics of both, ANME-1 and ANME-2 systems. Comparably low amounts of *sn2*-hydroxyarchaeol relative to archaeol would be indicative for ANME-1. However, high amounts of crocetane also point to a substantial contribution of ANME-2 to the archaeal biomass preserved in the crusts.

4.4.2 Sulphate Reducing Bacteria

At many different cold seep settings, ANME-1 and ANME-2 archaea have been found in consortium with SRB of the Seep-SRB1 cluster belonging to the *Desulfosarcina/Desulfococcus* group (Seep-SRB1, Knittel et al., 2003). However, this cluster apparently comprises physiologically different ecotypes that are distinguished by very specific FA patterns according to their association to either ANME-1 or to ANME-2 (Blumenberg et al., 2004; Elvert et al., 2003; Knittel et al., 2003). FA signatures in environmental systems dominated by ANME-1 / Seep-SRB1 communities comprise high contents of ai-$C_{15:0}$ relative to i-$C_{15:0}$, whereas systems dominated by ANME-2 / Seep-SRB1 communities comprise the unusual FA cy$C_{17:1\omega5,6}$ and dominant contents of $C_{16:1\omega5}$ but almost balanced ratios of ai-$C_{15:0}$ relative to i-$C_{15:0}$ (Blumenberg et al., 2004; Elvert et al., 2003).

The dominance of the unusual FAs $C_{16:1\omega5}$ and $cyC_{17:1\omega5,6}$ and an almost equal ratio of the iso and anteiso branched $C_{15:0}$ FAs at Capt. Arutyunov MV are in very good agreement with the published lipid signatures of the Seep SRB 1 ecotype associated with ANME-2. This finding is in agreement with the predominance of Seep-SRB1 sequences in the bacterial clone library. As expected from the detection of potentially diverse ANME communities at Bonjardim MV, the FA signature shows characteristics of various SRB previously identified as bacterial partners in AOM. The high ratio of ai-$C_{15:0}$ compared to i-$C_{15:0}$ would be indicative for the Seep-SRB1 ecotype associated with ANME-1 while the high abundance of $C_{16:1\omega5}$ would indicate the ecotype associated with ANME-2. However, a further assignment of FAs to particular SRBs remains speculative as the FA $cyC_{17:0w5,6}$ specific for the Seep-SRB1 type associated with ANME-2 was not detected, which might be a result of the overall low concentrations of lipids in sediments at Bonjardim MV (Fig. 5e, f, Tab. 3). At Bonjardim MV, several FAs carry $\delta^{13}C$-signatures that are comparable to the source methane and do not show any fractionation. This indicates a contribution to carbon biomass from processes other than methane consumption, possibly related to the anaerobic oxidation of higher hydrocarbons. A similar mixture of carbon sources could also explain the unspecific signature of FAs in carbonates of Hesperides MV. Similar to Bonjardim MV, FA signatures of Seep-SRB1 cluster associated with ANME-1 and ANME-2 were found in carbonates recovered from Faro MV. The comparably high content of ai-$C_{15:0}$ relative to i-$C_{15:0}$ and the lack of $cyC_{17:0\omega5,6}$ is indicative for Seep-SRB1 associated to ANME-1 while relatively high amounts of $C_{16:1\omega5}$ are indicative for Seep-SRB1 associated to ANME-2. In contrast to Hesperides MV, the low $\delta^{13}C$-values of all lipid components analysed at Faro MV give evidence that AOM dominated biomass production.

Another striking difference is the comparably high lipid concentration in carbonates recovered from Faro compared to those recovered from Hesperides MV. A rather recent formation of the

sampled carbonates from Faro MV appears likely, as these were stained black from sulphide and recovered together with some living specimens of the chemosynthetic bivalve *Acharax sp.* A possible explanation for the difference in AOM-derived lipid content could be that the sampled carbonate crusts from Hesperides are older than those recovered from Faro MV and have been exposed to oxic sea water and lipid diagenesis for a longer time.

CONCLUSIONS

At the centres of the mud volcanoes Captain Arutyunov, Bonjardim, Ginsburg, Gemini and Faro as well as at the "No Name" structure, several indications for a slow fluid and gas transport were found. Our data suggest a complete consumption of methane and higher hydrocarbons in the sediments of the studied mud volcanoes at depths of 30-300 cm below seafloor. We found no indication of hydrocarbons reaching the hydrosphere, except from the visual observation of small patches of reduced sediments covered by giant sulphide-oxidizing bacteria. The overlap of methane and sulphate depletion with sulphide production shows that methane and higher hydrocarbon oxidation processes are mediated microbially under anaerobic conditions. Correspondingly, anaerobic oxidation of methane and sulphate reduction rates show a peak in a distinct, narrow methane-sulphate transition zone in the subsurface sediments of the mud volcano centres. Highest turnover rates and fluxes coincided with the shallowest SMT depths with Capt. Arutyunov MV as the most active system in the study area, followed by the mud volcanoes Bonjardim, Ginsburg, and Gemini and finally the "No Name" structure. In comparison to other gas seeps, methane fluxes and turnover rates are low to mid range in the Gulf of Cadiz. In addition to AOM, a substantial fraction of the SR is fuelled by the anaerobic oxidation of higher hydrocarbons, which rise from deep reservoirs

together with methane. Lipid biomarker and 16S rDNA clone library from the sediments and carbonates of the AOM hotspots provide evidence that both of the previously described ANME-1 / Seep-SRB1 and ANME-2 / Seep-SRB1 communities mediate AOM at mud volcanoes in the Gulf of Cadiz. The finding of their signatures in carbonate crusts at the centres of the investigated mud volcanoes indicates that at least some of the vast amounts of carbonates littering mud volcanoes and diapirs in the northern part of the Gulf of Cadiz are linked to methane seepage.

Acknowledgements

The authors thank the captain and crew as well as the shipboard scientific community of the R/V SONNE for their help at sea. We also thank Thomas Willkop, Imke Müller and Viola Beier for technical assistance with laboratory analyses. Scientific exchange and collaboration were supported by the CRUP-ICCTI/DAAD Portuguese/German Joint Action *Geophere/Biosphere Coupling Processes in the Gulf of Cadiz* (A-15/04; Boetius, Pinheiro). This work was also supported by the ESF Eurocores/Euromargins MVSEIS project (01-LEC_EMA24F; PDCTM72003/DIV/40018-MVSEIS), as well as by the IRCCM (International Research Consortium on Continental Margins at International University Bremen, Germany) and the Max Planck Society.

References

Aloisi G., Pierre C., Rouchy J.-M., Foucher J.-P., Woodside J., and Party t. M. S. (2000) Methane-related authigenic carbonates of eastern Mediterranean Sea mud volcanoes and their possible relation to gas hydrate destabilisation. *Earth and Planetary Science Letters* **184**(1), 321-338.

Blumenberg M., Seifert R., Reitner J., Pape T., and Michaelis W. (2004) Membrane lipid patterns typify distinct anaerobic methanotrophic consortia. *Proceedings of the National Academy of Sciences of the United States of America* **101**(30).

Boetius A., Ravenschlag K., Schubert C., Rickert D., Widdel F., Gieseke A., Amann R., Jørgensen B. B., Witte U., and Pfannkuche O. (2000) A marine microbial consortium apparently mediating anaerobic methane of oxidation. *Nature* **407**, 623-626.

Boetius A. and Suess E. (2004) Hydrate Ridge: a natural laboratory for the study of microbial life fueled by methane from near-surface gas hydrates. *Chemical Geology* **205**(3-4), 291-310.

Boschker H. T. S. and Middelburg J. J. (2002) Stable isotopes and biomarkers in microbial ecology. *Fems Microbiology Ecology* **40**(2), 85-95.

Boudreau B. P. (1997) *Diagenetic models and their implementation: modelling transport and reactions in aquatic sediments*. Springer.

Charlou J. L., Donval J. P., Zitter T., Roy N., Jean-Baptiste P., Foucher J. P., and Woodside J. (2003) Evidence of methane venting and geochemistry of brines on mud volcanoes of the eastern Mediterranean Sea. *Deep-Sea Research Part I-Oceanographic Research Papers* **50**(8), 941-958.

Cordes E. E., Arthur M. A., Shea K., Arvidson R. S., and Fisher C. R. (2005) Modeling the mutualistic interactions between tubeworms and microbial consortia. *Plos Biology* **3**(3), 497-506.

Damm E. and Budeus G. (2003) Fate of vent-derived methane in seawater above the Hakon Mosby mud volcano (Norwegian Sea). *Marine Chemistry* **82**(1-2), 1-11.

Dando P. R., Bussmann I., Niven S. J., O'Hara S. C. M., Schmaljohann R., and Taylor L. J. (1994) A methane seep area in the Skagerrak, the habitat of the pogonophore *Siboglinum poseidoni* and the bivalve mollusc *Thyasira sarsi*. *Marine Ecology Progress Series* **107**, 157-167.

Diaz-del-Rio V., Somoza L., Martinez-Frias J., Mata M. P., Delgado A., Hernandez-Molina F. J., Lunar R., Martin-Rubi J. A., Maestro A., Fernandez-Puga M. C., Leon R., Llave E., Medialdea T., and Vazquez J. T. (2003) Vast fields of hydrocarbon-derived carbonate chimneys related to the accretionary wedge/olistostrome of the Gulf of Cadiz. *Marine Geology* **195**(1-4), 177-200.

Dimitrov L. I. (2002) Mud volcanoes - the most important pathway for degassing deeply buried sediments. *Earth-Science Reviews* **59**(1-4), 49-76.

Dimitrov L. I. (2003) Mud volcanoes - a significant source of atmospheric methane. *Geo-Marine Letters* **23**(3-4), 155-161.

Elvert M., Boetius A., Knittel K., and Jorgensen B. B. (2003) Characterization of specific membrane fatty acids as chemotaxonomic markers for sulfate-reducing bacteria involved in anaerobic oxidation of methane. *Geomicrobiology Journal* **20**(4), 403-419.

Elvert M., Greinert J., Suess E., and Whiticar M. J. (2001) Carbon isotopes of biomarkers derived from methane-oxidizing microbes at Hydrate Ridge, Cascadia convergent margin. In *Natural gas hydrates: Occurrence, distribution, and dynamics*, Vol. 124 (ed. C. K. Paull and W. P. Dillon), pp. 115-129. American Geophysical Union.

Elvert M., Suess E., and Whiticar M. J. (1999) Anaerobic methane oxidation associated with marine gas hydrates: superlight C-isotopes from saturated and unsaturated C_{20} and C_{25} irregular isoprenoids. *Naturwissenschaften* **86**(6), 295-300.

Felbeck H. (1983) Sulfide Oxidation and Carbon Fixation by the Gutless Clam Solemya-Reidi - an Animal-Bacteria Symbiosis. *Journal of Comparative Physiology* **152**(1), 3-11.

Fisher C. R. (1990) Chemoautotrophic and Methanotrophic Symbioses in Marine-Invertebrates. *Reviews in Aquatic Sciences* **2**(3-4), 399-436.

Fossing H., Gallardo V. A., Jorgensen B. B., Huttel M., Nielsen L. P., Schulz H., Canfield D. E., Forster S., Glud R. N., Gundersen J. K., Kuver J., Ramsing N. B., Teske A., Thamdrup B., and Ulloa O. (1995) Concentration and Transport of Nitrate by the Mat-Forming Sulfur Bacterium Thioploca. *Nature* **374**(6524), 713-715.

Gardner J. M. (2001) Mud volcanoes revealed and sampled on the Western Moroccan continental margin. *Geophysical Research Letters* **28**(2), 339-342.

Gebruk A. V., Krylova E. M., Lein A. Y., Vinogradov G. M., Anderson E., Pimenov N. V., Cherkashev G. A., and Crane K. (2003) Methane seep community of the Hakon Mosby mud volcano (the Norwegian Sea): composition and trophic aspects. *Sarsia* **88**(6), 394-403.

Hanselmann K. W. (1991) Microbial Energetics Applied to Waste Repositories. *Experientia* **47**(7), 645-687.

Hensen C., Wallmann K., Schmidt M., Ranero C. R., and Suess E. (2004) Fluid expulsion related to mud extrusion off Costa Rica - A window to the subducting slab. *Geology* **32**(3), 201-204.

Hensen C., Zabel M., Pfeifer K., Schwenk T., Kasten S., Riedinger N., Schulz H. D., and Boettius A. (2003) Control of sulfate pore-water profiles by sedimentary events and the significance of anaerobic oxidation of methane for the burial of sulfur in marine sediments. *Geochimica Et Cosmochimica Acta* **67**(14), 2631-2647.

Hinrichs K.-U. and Boetius A. (2002) The anaerobic oxidation of methane: New insights in microbial ecology and biogeochemistry. In *Ocean Margin Systems* (ed. G. Wefer, D. Billett, and D. Hebbeln), pp. 457-477. Springer-Verlag, Berlin.

Hinrichs K.-U., Hayes J. M., Sylva S. P., Brewer P. G., and DeLong E. F. (1999) Methane-consuming archaebacteria in marine sediments. *Nature* **398**, 802-805.

Houghton J. T., Meira Filho L. G., Callander B. A., Harris N., Kattenberg A., and Maskell K. (1996) *Climate Change 1995: The Science of Climat Change*. Cambrige University Press for the Inter-governmental Panel on Climate Change, Cambridge.

Huettel M., Forster S., Kloser S., and Fossing H. (1996) Vertical migration in the sediment-dwelling sulfur bacteria Thioploca spp in overcoming diffusion limitations. *Applied and Environmental Microbiology* **62**(6), 1863-1872.

Iversen N. and Jørgensen B. B. (1985) Anaerobic methane oxidation rates at the sulfate-methane transition in marine sediments from Kattegat and Skagerrak (Denmark). *Limnology and Oceanography* **30**(5), 944-955.

Jørgensen B. B., Bottcher M. E., Luschen H., Neretin L. N., and Volkov, II. (2004) Anaerobic methane oxidation and a deep H2S sink generate isotopically heavy sulfides in Black Sea sediments. *Geochimica Et Cosmochimica Acta* **68**(9), 2095-2118.

Jørgensen B. B., Weber A., and Zopfi J. (2001) Sulfate reduction and anaerobic methane oxidation in Black Sea sediments. *Deep-Sea Research Part I-Oceanographic Research Papers* **48**(9), 2097-2120.

Joye S. B., Boetius A., Orcutt B. N., Montoya J. P., Schulz H. N., Erickson M. J., and Lugo S. K. (2004) The anaerobic oxidation of methane and sulfate reduction in sediments from Gulf of Mexico cold seeps. *Chemical Geology* **205**(3-4), 219-238.

Judd A. G., Hovland M., Dimitrov L. I., Gil S. G., and Jukes V. (2002) The geological methane budget at Continental Margins and its influence on climate change. *Geofluids* **2**(2), 109-126.

Kane M. D., Poulsen L. K., and Stahl D. A. (1993) Monitoring the Enrichment and Isolation of Sulfate-Reducing Bacteria by Using Oligonucleotide Hybridization Probes Designed from Environmentally Derived 16s Ribosomal-Rna Sequences. *Applied and Environmental Microbiology* **59**(3), 682-686.

Kenyon N. H., Ivanov M. K., Akhmetzhanov A. M., and Akhmanov G. (2001) Interdisciplinary Approaches to Geoscience on the North East Atlantic Margin and Mid-Atlantic Ridge. IOC Technical Series no. 60.

Kenyon N. H., Ivanov M. K., Akhmetzhanov A. M., and Akhmanov G. G. (2000) Multidisciplinary Study of Geological Processes on the North East Atlantic and Western Mediterranean Margins, pp. 102. IOC Technical Series no. 56.

Kholodov V. N. (2002) Mud Volcanoes: Distribution Regularities and Genesis (Communication 2. Geological–Geochemical Peculiarities and Formation Model). *Lithology and Mineral Resources* **37**(4), 293-310.

Kimura H., Sato M., Sasayama Y., and Naganuma T. (2003) Molecular characterization and in situ localization of endosymbiotic 16S ribosomal RNA and RuBisCO genes in the pogonophoran tissue. *Marine Biotechnology* **5**(3), 261-269.

Knittel K., Boetius A., Lemke A., Eilers H., Lochte K., Pfannkuche O., Linke P., and Amann R. (2003) Activity, distribution, and diversity of sulfate reducers and other bacteria in sediments above gas hydrate (Cascadia margin, Oregon). *Geomicrobiology Journal* **20**(4), 269-294.

Knittel K., Losekann T., Boetius A., Kort R., and Amann R. (2005) Diversity and distribution of methanotrophic archaea at cold seeps. *Applied and Environmental Microbiology* **71**(1), 467-479.

Kopf A., Bannert B., Brückmann W., Dorschel B., Foubert A. T. G., Grevemeyer I., Gutscher M. A., Hebbeln D., Heesemann B., Hensen C., Kaul N. E., Lutz M., Magalhaes V. H., Marquardt M. J., Marti A. V., Nass K. S., Neubert N., Niemann H., Nuzzo M., Poort J. P. D., Rosiak U. D., Sahling H., Schneider von Deimling J., Somoza L., Thiebot E., and Wilkop T. P. (2004) Report and preliminary results of Sonne Cruise SO175, Miami - Bremerhaven, 12.11 - 30.12.2003, pp. 218. Fachbereich Geowissenschaften der Universität Bremen.

Kopf A. J. (2002) Significance of mud volcanism. *Reviews of Geophysics* **40**(2).

Krueger D. M. and Cavanaugh C. M. (1997) Phylogenetic diversity of bacterial symbionts of Solemya hosts based on comparative sequence analysis of 16S rRNA genes. *Applied and Environmental Microbiology* **63**(1), 91-98.

Kvenvolden K. A. (2002) Methane hydrate in the global organic carbon cycle. *Terra Nova* **14**(5), 302-306.

Lane D. J., Pace B., Olsen G. J., Stahl D. A., Sogin M. L., and Pace N. R. (1985) Rapid-Determination of 16s Ribosomal-Rna Sequences for Phylogenetic Analyses. *Proceedings of the National Academy of Sciences of the United States of America* **82**(20), 6955-6959.

Luff R. and Wallmann K. (2003) Fluid flow, methane fluxes, carbonate precipitation and biogeochemical turnover in gas hydrate-bearing sediments at Hydrate Ridge, Cascadia Margin: Numerical modeling and mass balances. *Geochimica Et Cosmochimica Acta* **67**(18), 3403-3421.

Madigan M. T., Martinko J. M., and Parker J. (2000) *Brock Biology of Microorganisms*. Prentice-Hall, Inc.

Maldonado A. and Comas M. C. (1992) Geology and Geophysics of the Alboran Sea - an Introduction. *Geo-Marine Letters* **12**(2-3), 61-65.

Maldonado A., Somoza L., and Pallares L. (1999) The Betic orogen and the Iberian-African boundary in the Gulf of Cadiz: geological evolution (central North Atlantic). *Marine Geology* **155**(1-2), 9-43.

Manne A. S. and Richels R. G. (2001) An alternative approach to establishing trade-offs among greenhouse gases. *Nature* **410**(6829), 675-677.

Massana R., Murray A. E., Preston C. M., and DeLong E. F. (1997) Vertical distribution and phylogenetic characterization of marine planktonic Archaea in the Santa Barbara Channel. *Applied and Environmental Microbiology* **63**(1), 50-56.

Mazurenko L. L., Soloviev V. A., Belenkaya I., Ivanov M. K., and Pinheiro L. M. (2002) Mud volcano gas hydrates in the Gulf of Cadiz. *Terra Nova* **14**(5), 321-329.

Michaelis W., Seifert R., Nauhaus K., Treude T., Thiel V., Blumenberg M., Knittel K., Gieseke A., Peterknecht K., Pape T., Boetius A., Amann R., Jorgensen B. B., Widdel F., Peckmann J. R., Pimenov N. V., and Gulin M. B. (2002) Microbial reefs in the Black Sea fueled by anaerobic oxidation of methane. *Science* **297**(5583), 1013-1015.

Milkov A. V. (2000) Worldwide distribution of submarine mud volcanoes and associated gas hydrates. *Marine Geology* **167**(1-2), 29-42.

Milkov A. V., Sassen R., Apanasovich T. V., and Dadashev F. G. (2003) Global gas flux from mud volcanoes: A significant source of fossil methane in the atmosphere and the ocean. *Geophysical Research Letters* **30**(2).

Milkov A. V., Vogt P. R., Crane K., Lein A. Y., Sassen R., and Cherkashev G. A. (2004) Geological, geochemical, and microbial processes at the hydrate-bearing Hakon Mosby mud volcano: a review. *Chemical Geology* **205**(3-4), 347-366.

Moss C. W. and Lambert-Fair M. A. (1989) Location of Double Bonds in Monounsaturated Fatty Acids of Campylobacter cryaerophila with Dimethyl Disulfide Derivatives and Combined Gas Chromatography-Mass Spectrometry. *JOURNAL OF CLINICAL MICROBIOLOGY* **27**(7), 1467-1470.

Mussmann M., Schulz H. N., Strotmann B., Kjaer T., Nielsen L. P., Rossello-Mora R. A., Amann R. I., and Jorgensen B. B. (2003) Phylogeny and distribution of nitrate-storing Beggiatoa spp. in coastal marine sediments. *Environmental Microbiology* **5**(6), 523-533.

Muyzer G., Teske A., Wirsen C. O., and Jannasch H. W. (1995) Phylogenetic-Relationships of Thiomicrospira Species and Their Identification in Deep-Sea Hydrothermal Vent Samples by Denaturing Gradient Gel-Electrophoresis of 16s Rdna Fragments. *Archives of Microbiology* **164**(3), 165-172.

Nauhaus K., Boetius A., Kruger M., and Widdel F. (2002) In vitro demonstration of anaerobic oxidation of methane coupled to sulphate reduction in sediment from a marine gas hydrate area. *Environmental Microbiology* **4**(5), 296-305.

Nelson D. C., Waterbury J. B., and Jannasch H. W. (1982) Nitrogen-Fixation and Nitrate Utilization by Marine and Fresh-Water Beggiatoa. *Archives of Microbiology* **133**(3), 172-177.

Nichols P. D., Guckert J. B., and White D. C. (1986) Determination of monounsaturated fatty acid double-bond position and geometry for microbial monocultures and complex consortia by capillary GC-MS of their dimethyl disulphide adducts. *Journal of Microbiological Methods* **5**, 49-55.

Niewöhner C., Hensen C., Kasten S., Zabel M., and Schulz H. D. (1998) Deep sulfate reduction completely mediated by anaerobic methane oxidation in sediments of the upwelling area off Namibia. *Geochimica et Cosmochimica Acta* **62**(3), 455-464.

Nuzzo M., Hensen C., Hornibrook E., Brueckmann W., Magalhaes V. H., Parkes R. J., and Pinheiro L. M. (2005) Origin of Mud Volcano Fluids in the Gulf of Cadiz (E-Atlantic). *EGU General Assembly*.

Olu K., Lance S., Sibuet M., Henry P., Fiala-Médioni A., and Dinet A. (1997) Cold seep communities as indicators of fluid expulsion patterns through mud volcanoes seaward of the Barbados accretionary prism. *Deep-Sea Research I* **44**(5), 811-841.

Orphan V. J., Hinrichs K. U., Ussler W., Paull C. K., Taylor L. T., Sylva S. P., Hayes J. M., and Delong E. F. (2001a) Comparative analysis of methane-oxidizing archaea and sulfate- reducing bacteria in anoxic marine sediments. *Applied and Environmental Microbiology* **67**(4), 1922-1934.

Orphan V. J., House C. H., Hinrichs K. U., McKeegan K. D., and DeLong E. F. (2001b) Methane-consuming archaea revealed by directly coupled isotopic and phylogenetic analysis. *Science* **293**(5529), 484-487.

Orphan V. J., House C. H., Hinrichs K. U., McKeegan K. D., and DeLong E. F. (2002) Multiple archaeal groups mediate methane oxidation in anoxic cold seep sediments. *Proceedings of the National Academy of Sciences of the United States of America* **99**(11), 7663-7668.

Pancost R. D., Sinninghe Damsté J. S., de Lint S., van der Maarel M. J. E. C., Gottschal J. C., and party T. M. s. s. (2000) Biomarker evidence for widespread anaerobic methane oxidation in Mediterranean sediments by a consortium of methanogenic archaea and bacteria. *Applied and Environmental Microbiology* **66**(3), 1126-1132.

Peek A. S., Feldman R. A., Lutz R. A., and Vrijenhoek R. C. (1998) Cospeciation of chemoautotrophic bacteria and deep sea clams. *Proceedings of the National Academy of Sciences of the United States of America* **95**(17), 9962-9966.

Pinheiro L. M., Ivanov M. K., Sautkin A., Akhmanov G., Magalhaes V. H., Volkonskaya A., Monteiro J. H., Somoza L., Gardner J., Hamouni N., and Cunha M. R. (2003) Mud volcanism in the Gulf of Cadiz: results from the TTR-10 cruise. *Marine Geology* **195**(1-4), 131-151.

Reeburgh W. S. (1996) "Soft spots" in the global methane budget. In *Microbial Growth on C_1 Compounds* (ed. M. E. Lidstrom and F. R. Tabita), pp. 334-342. Kluwer Academic Publishers.

Rueter P., Rabus R., Wilkes H., Aeckersberg F., Rainey F. A., Jannasch H. W., and Widdel F. (1994) Anaerobic Oxidation of Hydrocarbons in Crude-Oil by New Types of Sulfate-Reducing Bacteria. *Nature* **372**(6505), 455-458.

Sahling H., Rickert D., Lee R. W., Linke P., and Suess E. (2002) Macrofaunal community structure and sulfide flux at gas hydrate deposits from the Cascadia convergent margin, NE Pacific. *Marine Ecology-Progress Series* **231**, 121-138.

Schmaljohann R. and Flugel H. J. (1987) Methane-Oxidizing Bacteria in Pogonophora. *Sarsia* **72**(1), 91-99.

Sibuet M. and Olu K. (1998) Biogeography, biodiversity and fluid dependence of deep-sea cold-seep communities at active and passive margins. *Deep-Sea Research Part Ii-Topical Studies in Oceanography* **45**(1-3), 517-+.

Somoza L., Diaz-del-Rio V., Leon R., Ivanov M., Fernandez-Puga M. C., Gardner J. M., Hernandez-Molina F. J., Pinheiro L. M., Rodero J., Lobato A., Maestro A., Vazquez J. T., Medialdea T., and Fernandez-Salas L. M. (2003) Seabed morphology and hydrocarbon seepage in the Gulf of Cadiz mud volcano area: Acoustic imagery, multibeam and ultra-high resolution seismic data. *Marine Geology* **195**(1-4), 153-176.

Somoza L., Diaz-del-Rio V., Vaszquez J. T., Pinheiro L. M., and Hernandez-Molina F. J. (2002) Numerous methane gas-related sea floor structures identified in Gulf of Cadiz. *EOS* **83**(47), 541-547.

Southward A. J., Southward E. C., Dando P. R., Barrett R. L., and Ling R. (1986) Chemoautotrophic Function of Bacterial Symbionts in Small Pogonophora. *Journal of the Marine Biological Association of the United Kingdom* **66**(2), 415-437.

Southward A. J., Southward E. C., Dando P. R., Rau G. H., Felbeck H., and Fluegel H. (1981) Bacterial symbionts and low $^{13}C/^{12}C$ ratios in tissues of Pogonophora indicate unusual nutrition and metabolism. *Nature* **293**, 616-620.

Summons R. E., Jahnke L. L., and Roksandic Z. (1994) Carbon isotopic fractionation in lipids from methanotrophic bacteria: Relevance for interpretation of the geochemical record of biomarkers. *Geochimica Et Cosmochimica Acta* **58**(13), 2853-2863.

Teske A., Hinrichs K. U., Edgcomb V., Gomez A. D., Kysela D., Sylva S. P., Sogin M. L., and Jannasch H. W. (2002) Microbial diversity of hydrothermal sediments in the Guaymas Basin: Evidence for anaerobic methanotrophic communities. *Applied and Environmental Microbiology* **68**(4), 1994-2007.

Thiel V., Peckmann J., Seifert R., Wehrung P., Reitner J., and Michaelis W. (1999) Highly isotopically depleted isoprenoids: molecular markers for ancient methane venting. *Geochimica et Cosmochimica Acta* **63**(23/24), 3959-3966.

Torres M. E., McManus J., Hammond D. E., de Angelis M. A., Heeschen K. U., Colbert S. L., Tryon M. D., Brown K. M., and Suess E. (2002) Fluid and chemical fluxes in and out of sediments hosting methane hydrate deposits on Hydrate Ridge, OR, I: Hydrological provinces. *Earth and Planetary Science Letters* **201**(3-4), 525-540.

Treude T., Boetius A., Knittel K., Wallmann K., and Jorgensen B. B. (2003) Anaerobic oxidation of methane above gas hydrates at Hydrate Ridge, NE Pacific Ocean. *Marine Ecology-Progress Series* **264**, 1-14.

Treude T., Niggemann J., Kallmeyer J., Wintersteller P., Schubert C. J., Boetius A., and Jorgensen B. B. (2005) Anaerobic oxidation of methane and sulfate reduction along the Chilean continental margin. *Geochimica et Cosmochimica Acta* **69**(11), 2767-2779.

Werne J. P., Baas M., and Damste J. S. S. (2002) Molecular isotopic tracing of carbon flow and trophic relationships in a methane-supported benthic microbial community. *Limnology and Oceanography* **47**(6), 1694-1701.

Whiticar M. J. (1999) Carbon and hydrogen isotope systematics of bacterial formation and oxidation of methane. *Chemical Geology* **161**(1-3), 291-314.

Whiticar M. J., Faber E., and Schoell M. (1986) Biogenic methane formation in marine and freshwater environments: CO_2 reduction *vs*. acetate fermentation - Isotope evidence. *Geochimica et Cosmochimica Acta* **50**, 693-709.

Widdel F. and Rabus R. (2001) Anaerobic biodegradation of saturated and aromatic hydrocarbons. *Current Opinion in Biotechnology* **12**(3), 259-276.

Wuebbles D. J. and Hayhoe K. (2002) Atmospheric methane and global change. *Earth-Science Reviews* **57**(3-4), 177-210.

Methane emission and consumption at a North Sea gas seep (Tommeliten area)

H. Niemann[1,2], M. Elvert[3], M. Hovland[4], B. Orcutt[5], A. Judd[6], I. Suck[2], J. Gutt[2], S. Joye[5], E. Damm[2], K. Finster[7], A. Boetius[1,8]

[1] Max Planck Institute for Marine Microbiology, 28359 Bremen, Germany,

[2]Alfred Wegener Institute for Polar and Marine Research, 27515 Bremerhaven, Germany

[3]Research Center Ocean Margins, University of Bremen, 28334 Bremen, Germany

[4]Statoil, 4001 Stavanger, Norway

[5]University of Georgia, Athens, Georgia 30602-3636, USA

[6]Wilderspool House, High Mickley, Stocksfield, Northumberland, NE43 7LU, UK

[7]University of Aarhus, 8000 Aarhus, Denmark

[8]International University Bremen, 28759 Bremen, Germany

Author to whom correspondence should be addressed:

Helge Niemann
Max Planck Institute for Marine Microbiology, Celsiusstr. 1, 28359 Bremen, Germany
email: hniemann@mpi-bremen.de, phone +49-421-2028653

ABSTRACT

The North Sea hosts large coal, oil and gas reservoirs of commercial value. Natural leakage pathways of subsurface gas to the hydrosphere have been recognized during geological surveys (Hovland and Judd, 1988). The Tommeliten seepage area is part of the Greater Ekofisk area, which is situated above the Tommeliten Delta salt diapir in the central North Sea. In this study, we report of an active seep site (56° 29.90' N, 2° 59.80' E) located in the Tommeliten area, Norwegian Block 1/9, at 75 m water depth. Here, cracks in a buried marl horizon allow methane to migrate into overlying clay-silt and sandy sediments. Hydroacoustic sediment echosounding showed several venting spots coinciding with the apex of marl domes where methane is released into the water column and potentially to the atmosphere during deep mixing situations. In the vicinity of the gas seeps, sea floor observations showed small mats of giant sulphide-oxidizing bacteria above patches of black sediments and carbonate crusts, which are exposed 10 to 50 cm above seafloor forming small reefs. These methane-derived authigenic carbonates (MDACs) contain ^{13}C-depleted, archaeal lipids indicating previous gas seepage and AOM activity. High amounts of *sn2*-hydroxyarchaeol relative to archaeol and low abundances of biphytanes in the crusts give evidence that anaerobic methane-oxidising archaea (ANME) of the phylogenetic cluster ANME-2 were the potential mediators of anaerobic oxidation of methane (AOM) at the time of carbonate formation. Small pieces of MDACs were also found subsurface at about 1.7 m sediment depth, associated with the sulphate-methane transition zone (SMTZ). The SMTZ of Tommeliten is characterized by elevated AOM and sulphate reduction (SR) rates, increased concentrations of ^{13}C-depleted tetraether derived biphytanes, and specific bacterial fatty acids (FA). Further biomarker and 16S rDNA based analyses give evidence that AOM at the Tommeliten SMTZ is mediated by archaea belonging to the ANME-1b group and sulphate reducing bacteria (SRB) most likely belonging to the Seep-SRB1 cluster. The zone of active methane

consumption was restricted to a distinct horizon of about 20 cm. Concentrations of ^{13}C-depleted lipid biomarkers (e.g. 500 ng g-dw^{-1} biphythanes, 140 ng g-dw^{-1} fatty acid ai-$C_{15:0}$), cell numbers (1.5 * 10^8 cells cm^{-3}), AOM and SR rates (3 nmol cm^{-3} d^{-1}) in the SMTZ are 2-3 orders of magnitude lower compared to AOM zones of highly active cold seeps such as Hydrate Ridge or the Gulf of Mexico.

1. INTRODUCTION

Hydrocarbon seepage in the ocean has been known for more than thirty years, but the contribution of this process to the global methane budget and the carbon cycle are not well constrained. Upwelling of hydrocarbon-rich geofluids from subsurface reservoirs to the hydro- and atmosphere could be a relevant process in the global carbon cycle, especially with regard to emissions of the greenhouse gas methane. Gas seepage from temperate shallow shelf seas is likely to contribute to methane emissions to the atmosphere, because of the seasonal deep mixing of the water column reaching the gas plumes above active seeps. The main challenge in constraining methane emission from the ocean is the need for quantitative estimates of the abundance and activity of cold seeps of ocean margins. As part of the OMARC cluster (Ocean Margin Deep-Water Research Consortium) of the 5th framework program of the European Commission, the project METROL (Methane flux control in ocean margin sediments) has been investigating methane fluxes from seep systems of the central and northern North Sea. Here we present results from biogeochemical and microbiological investigations of the Tommeliten seep area (56° 29.90' N, 2° 59.80' E) in the central North Sea. This and other active cold seeps have been detected during pipeline route and site surveys by oil companies (Hovland and Sommerville, 1985). Cold seeps have been reported from various geographic and geological settings (Judd, 2003). Once initiated, cold seeps may continuously emit gas, but they become inactive if subsurface gas and fluids are depleted, or undergo phases of dormancy where the shallow reservoir is recharged and none or little seepage occurs (Çifçi et al., 2003; Hovland and Judd, 1988). In the particular case of the central North Sea, thermogenic methane is produced in Jurassic sediments (Hovland and Judd, 1988). In the Tommeliten area, the enclosing sedimentary rocks have been pierced by a buried salt diapir, the so called Delta Structure, at about 1 km depth below sea floor (bsf). As a result, the methane reservoir lacks a proper seal and disturbances on seismic profiles

indicate that free gas migrates in sediments above the diapir to the sea floor (Hovland, 2002; Hovland and Judd, 1988). Previous expeditions to the Tommeliten seepage area with remotely operated vehicles (ROVs) documented streams of single methane bubbles of a thermogenic origin (–45.6‰ vs. Pee Dee Belemnite), small patches of filamentous, microbial mats and MDACs that outcrop on the sea floor (Hovland and Judd, 1988; Hovland and Sommerville, 1985; Thrasher et al., 1996). Such observations are typical for active seep systems, which have been found at passive and active continental margins.

High fluxes of methane usually lead to the development of methanotrophic microbial communities. Anaerobic methanotrophic archaea dominate submarine seep communities, because they profit from the abundance of sulphate utilised as an electron acceptor for AOM (Hinrichs and Boetius, 2002; Reeburgh, 1996). High AOM activities lead to high fluxes of sulphide and the development of microbial mats of giant sulphide-oxidizing bacteria (e.g. *Beggiatoa sp.*) and other thiotrophic organisms (Boetius and Suess, 2004; and literature therein). Furthermore, methane venting at various cold seeps is associated with the precipitation of MDACs which often contain lipid biomarkers of AOM communities (Bohrmann et al., 1998; Diaz-del-Rio et al., 2003; Hovland et al., 1985; Hovland et al., 1987; Michaelis et al., 2002; Peckmann et al., 1999; Roberts and Aharon, 1994; Thiel et al., 2001). The phylogenetic origin of methanotrophic communities has been determined using combinations of lipid analysis and 16S rDNA methods in several methane seep environments (Boetius et al., 2000; Elvert et al., 1999; Hinrichs et al., 1999; Hoehler and Alperin, 1996; Knittel et al., 2003; Knittel et al., 2005; Michaelis et al., 2002; Orphan et al., 2001b). Previous works identified two groups of anaerobic methane oxidising (ANME) archaea, which are phylogenetically related to methanogens (*Methanosarcina sp*.). Both ANME-1 and ANME-2 occur in consortia with relatives of a SRB cluster (Seep-SRB1) within the *Desulfosarcina/Desulfococcus* branch (Knittel et al. 2003). Although the geology and biology

of a variety of shallow water cold seeps have been well investigated, there is still very little known on the biogeochemistry and relevance of microbial methane consumption (Barry et al., 1996; Barry et al., 1997; Bian et al., 2001; Bussmann et al., 1999; Dando and Hovland, 1992; Garcia-Garcia et al., 2003; Thomsen et al., 2001). The aim of this investigation was to study microbial processes related to methane seepage in shelf sediments. The main tasks were to reveal the distribution and identity of methanotrophic microorganisms, the zonation and magnitude of methane oxidation and to analyse the impact of methane venting on a sandy benthic habitat of the North Sea.

2. MATERIALS AND METHODS

2.1 Field Observations

Visual observations of the Tommeliten sea floor were carried out with a remotely operated vehicle (ROV "Sprint 103" of the Alfred Wegener Institute of Polar and Marine Research) during a cruise with R/V Heincke in June 2002 (HE-169) and with a towed video camera in October 2002 (HE-180). Gas flares in the water column were detected with a SES-2000 echosounder operated at different frequencies in the range of 10 to 100 kHz. The same parametric echosounder was used for high-resolution sub-bottom profiling at frequencies between 8 and 15 kHz. Video and echosounder images were used to select positions for sediment sampling.

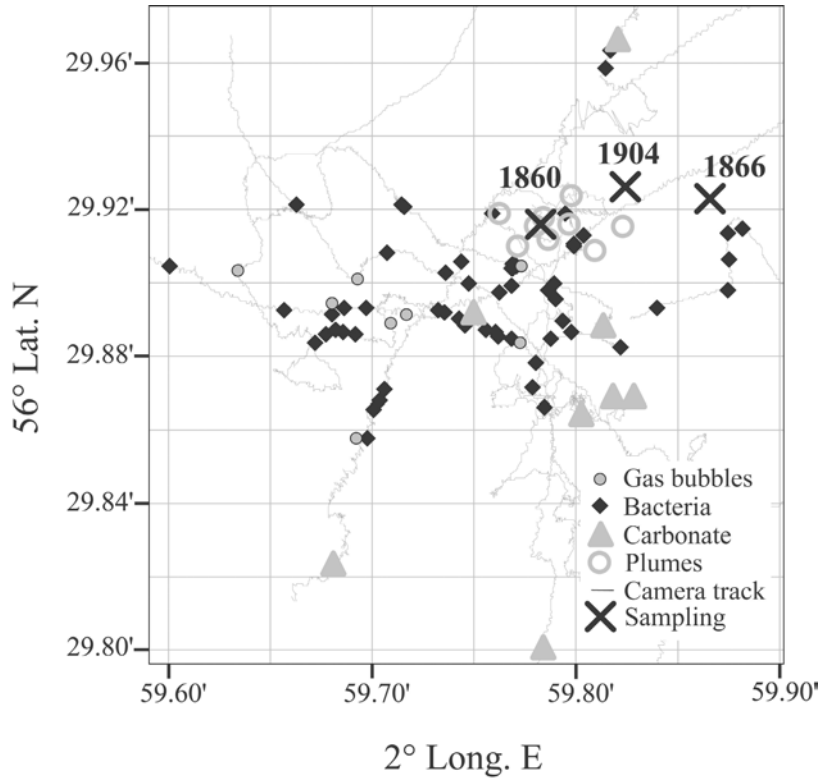

Figure 1. A chart of the survey area at Tommeliten showing sampling positions of vibrocoring, sea floor and hydroacoustic observations.

2.2 Sample Collection and Storage

Sediment samples were collected by vibrocoring (Institute of Baltic Sea Research) during the cruise HE180 in October 2002. Three cores were recovered from seep areas (core 1860, 1866, 1904, Fig. 1) and one from a reference station (core 1867). Upon recovery, cores were sectioned in 1 m pieces and kept in their plastic bags during subsampling of porewater constituents (methane, sulphate, sulphide) and turnover rate measurements of methane and sulphate. Replicate subsamples were obtained from a 10 cm section every 10 (cores 1866 and 1904) or 20 cm (core 1860). Samples for lipid biomarkers, cell counts and DNA were collected from the same 10 cm sections of core 1904. Sediment samples for lipid analysis were transferred into pre-cleaned glass vials and stored at –25 °C until extraction. Sediments for microbiological analysis were fixed for fluorescent *in situ* hybridisation (FISH) or frozen for DNA extraction. Pieces of MDACs were collected from the SMTZ at station 1904 and stored at –25°C until extraction. MDACs from the surface of the sea floor were collected earlier during a ROV expedition in 1998 (Hovland, 2002). Detailed protocols for the following methods can be obtained from www.metrol.org.

2.3 Methane Concentrations

Methane concentrations from selected sediment horizons were determined according to the "head space" method from 5 ml sediment fixed with 25 ml NaOH (2.5%, w/v) in gas-tight glass vials as described previously (Treude et al., 2003). Immediately after sub-sampling, methane concentrations were determined on board using a gas chromatograph as described elsewhere (Treude et al., 2003).

2.4 Sulphate Concentrations

5ml of wet sediment were fixed in 50 ml corning vials with 25 ml zinc acetate solution (20%, w/v). After vigorous shaking, sediment particles were separated by centrifugation and filtration. Sulphate concentrations were determined from an aliquot of the supernatant using a Waters HPLC system (Waters 512 HPLC pump, I.C.-Pak anion-column (Waters; WAT007355) 4.6 x 50 mm, Waters 730 conductivity detector). Isophtalic acid (1mM) was used as a solvent at a constant flow rate of 1ml min^{-1}. Sulphate concentrations were corrected for porosity, which was determined according to Treude et al. (2003).

2.5 Sulphide Concentrations

Total sulphide concentrations were determined using a combination of a WTW Multiline P4 multi meter equipped with a WTW pH/ION 340i ion meter with two coupled electrodes (WTW Ag 500 / WTW Ag/S 5001) for S^{2-} concentration measurements and a WTW SenTix 41-3 electrode for pH measurements. The S^{2-} measuring section was calibrated against standards of $H_2S/HS^-/S^{2-}$ at pHs of 6, 7, 8 and 9.

2.6 *Ex situ* AOM and SR Measurements

Subsamples for turnover rate measurements were collected from core 1904 by plugging glass tubes (1 x 6 cm) into a defined sediment horizon of ca 10 cm (n = 5 for AOM and SR, respectively) as described previously (Treude et al. 2005 and references therein). To prevent gas exchange, the tubes were sealed with butyl rubber stoppers and only briefly opened for radiotracer injection, i.e., 50 µl ^{14}C-labelled methane and 5 µl ^{35}S-labelled sulphate (tracer

dissolved in water, 10 kBq and 50 kBq, respectively). Sediment samples were incubated on board at *in situ* temperature (4 °C) for 24 h in the dark. After incubation, AOM and SR samples were fixed like the methane and sulphate samples (see above). Further processing of AOM and SR samples was performed according to Treude et al. (2003) and references therein. Turnover rates were calculated according to the following formulas:

$$\mathrm{AOM} = \frac{^{14}\mathrm{CO_2}}{^{14}\mathrm{CH_4} + ^{14}\mathrm{CO_2}} \times \frac{\mathrm{conc.CH_4}}{\mathrm{incubat.Time}} \quad (1)$$

$$\mathrm{SRR} = \frac{\mathrm{TRI}^{35}\mathrm{S}}{^{35}\mathrm{SO_4}^{2-} + \mathrm{TRI}^{35}\mathrm{S}} \times \frac{\mathrm{conc.SO_4}^{2-}}{\mathrm{incubat.Time}} \quad (2)$$

Here, $^{14}CO_2$, $^{35}SO_4^{2-}$ and $TRI^{35}S$ are the activities (Bq) of carbon dioxide, sulphate and total reduced sulphur species, respectively, whereas conc. CH_4 and conc. SO_4^{2-} are the concentrations of methane and sulphate at the beginning of the incubation.

2.7 *In Vitro* Potential Rates

The applied subsampling techniques of this work have been proven useful for muddy sediments (Treude et al., 2003). To test the suitability for sandy sediments, we compared short-term AOM and SR measurements with long-term *in vitro* measurements (1 wk) of sediments collected from three horizons (surface, at the sulphide peak, and deep horizons) according to a modified method of Nauhaus et al. (2002). For this study, 20 ml sediment slurries were incubated with radio-labelled methane and sulphate (n = 5 for AOM and SR, respectively). The slurries consisted of 1 cm^3 fresh sediment and methane saturated (1.4 mM),

artificial sea water media with 28 mM sulphate (Widdel and Bak, 1992). As a control, slurries from one horizon (100-150 cm, core 1904) were incubated without methane. After incubation, sediment slurries were processed like those from short-term incubations.

2.8 Extraction of Sediment and MDAC Samples and Preparation of Derivatives

The extraction procedure and preparation of fatty acid methyl esters was carried out according to Elvert and co-workers (2003). Briefly, total lipid extracts (TLE) were obtained from ca. 25g of wet sediment collected from core 1904 and from two MDAC pieces (one collected from the surface of the sea floor and one from the SMTZ in core 1904). Prior to extraction, the MDAC pieces were disintegrated with HCL (2M). The TLE was extracted by subsequent ultrasonification using organic solvents of decreasing polarity. Internal standards of known concentration and carbon isotopic compositions were added prior to extraction. Esterified fatty acids (FAs) present in glyco- and phospholipids were cleaved by saponification with methanolic KOH-solution. After extraction of the neutral lipid fraction from this mixture, FAs were methylated for analysis with BF_3 in methanol yielding fatty acid methyl esters (FAMES).

Neutral lipids were further separated into hydrocarbons, ketones and alcohols on a SPE silica glass cartridge (0.5 g packing). Prior to separation, the column was rinsed with 15 ml *n*-hexane/dichloromethane (95:5, v/v). After application of the neutral fraction, solvent mixtures of increasing polarity were subsequently added: (I) 5 ml *n*-hexane/dichloromethane (95:5, v/v), (II) 5 ml *n*-hexane/dichloromethane (2:1, v/v) and (III) 5 ml dichloromethane/acetone (9:1, v/v). Neutral lipid fractions (hydrocarbons (I), ketones (II) and alcohols (III), respectively) were collected and concentrated to 100 µl using rotary evaporation. Finally,

neutral lipid fractions were stored at –20 °C until further processing and/or analysis. Alcohols were analysed as trimethylsilyl (TMS) ethers. Shortly before analysis (<1 wk), aliquots from selected alcohol fractions were dried under a stream of nitrogen. 100 µl pyridine and 50 µl bis(trimethylsilyl)triflouracetamid were added and the reaction was carried out for 1 h at 70 °C. After cooling, excess solvent was evaporated and the remaining TMS adducts were re-suspended in 50 µl of *n*-hexane. TMS adducts were stored at –20 °C until GC and GC-MS analysis.

Sediments and the two MDAC pieces were additionally analysed for the content of tetraether lipids. Tetraether lipids, which are contained in the alcohol fractions, were subjected to ether cleavage through HI treatment as reported previously yielding phytanes and biphytanes which can be analysed by GC (-MS and IRMS) analysis (Blumenberg et al., 2004; Kohnen et al., 1992). Briefly, 500 µl HI (57%) and 500 µl acetic acid (100%) were added to a dried alcohol fraction and iodisation of ether bonds was promoted at 110 °C for 4 h. After cooling, alkyl iodides were extracted with *n*-hexane. Excess iodine was removed by adding sodium thiosulphate solution (5%, w/v in water). Subsequently, the hexane phase was removed and dried. Alkyl iodides were reduced to alkanes in 0.5 ml of tetrahydrofurane (THF) by adding lithium-aluminium hydride (2 spatula tips). Reduction of iodides was carried out at 110 °C for 3 h. After cooling, excess lithium-aluminium hydride was deactivated by the addition of deionised water. The supernatant solvent phase was removed, dried and stored at -20 °C.

2.9 Preparation of Dimethyl Disulphide (DMDS) Adducts

Double bond positions of monoenoic FAs were determined by analysis as DMDS adducts according to previously reported methods (Moss and Lambert-Fair, 1989; Nichols et al.,

1986). Briefly, an aliquot of a selected sample (dissolved in 50µl *n*-hexane) was treated with DMDS (100 µl) and iodine-diethyl ether solution (20 µl, 6% w/v). Formation of DMDS adducts was carried out at 50 °C for 48 h. After cooling, excess iodine was reduced with sodium thiosulphate (5% w/v in water). The organic phase was removed, dried and stored at –20 °C.

2.10 Gas Chromatography (GC), Gas Chromatography-Mass Spectrometry (GC-MS), Gas Chromatography-Isotope Ratio Mass Spectrometry (GC-IRMS)

Concentrations, identities and stable carbon isotope ratios of individual compounds were determined by GC, GC-MS and GC-IRMS analyses, respectively. Instrument specifications and operation modes of the GC, GC-MS and GC-IRMS were set according to Elvert and co-workers (2003). Concentrations were calculated against internal standards. Identities of acquired mass spectra were compared to known standards and published data. The chemical structure of biphytanes are reviewed in Schouten et al. (1998): monocyclic biphytane reported here equals compound IV and bicyclic biphytane compound V. Stable isotope ratios are given in the δ-notation against PDB. δ^{13}C-values of FAs and alcohols were corrected for the introduction of additional carbon atoms during derivatisation. Internal standards were used to monitor precision and reproducibility during measurements. Reported δ^{13}C-values have an analytical error of 1-2 ‰.

2.11 Cell Counts and Fluorescence *In Situ* Hybridisation

Selected sediment samples from core 1904 were fixed with 2 % formaldehyde and stored at 4°C until further analysis. Total cell numbers were quantified with the aid of epifluorescence microscopy after staining the cells with Acridine Orange according to Knittel et al. (2003). Sediments from above, below and within the SMTZ were analysed for the presence of archaea and bacteria by fluorescence in situ hybridization with horseradish peroxidase (HRP)-labelled oligonucleotide probes and tyramide signal amplification (CARD-FISH) according to the method of Pernthaler et al. (2002). The CARD-FISH probes used in this study were EUB338, ARCH915 and ANME1-350, purchased from biomers.net GmbH, Ulm, Germany. Oligonucleotide probes and instrument specification are presented in Knittel et al. (2005). Briefly, after 2 hours fixation at 4°C, formaldehyde fixed sediments were washed with 1xPBS (10 mM sodium phosphate, 130 mM NaCl) and stored in 1xPBS/EtOH (1:1) at -20°C. These samples were diluted 1:10, treated by sonification and filtered on 0.2 µm GTTP polycarbonate filters. Prior to filtration, filters were coated with agarose to prevent cell loss. In addition to ultrasonification, cells were permeabilised with lysozyme solution for 1 h at 37° C and subsequently hybridised with HRP labelled probe for 2 h at 35 °C. Finally, filters were incubated for 15 min in tyramide solution labelled with the fluorochrome Cy-3.

2.12 DNA Extraction and Clone Library Construction

Total community DNA was directly extracted from ca. 5 g of wet sediment from the SMTZ of core 1904 according to Zhou et al. (1996). Crude DNA was purified with the Wizard DNA Clean-Up Kit (Promega, Madison, WI). Almost full-length archaeal and bacterial 16S rRNA genes from the extracted chromosomal DNAs were amplified using primers 20f (Massana et

al., 1997) and Uni1392R (Lane et al., 1985) for archaea and GM3F (Muyzer et al., 1995) and GM4R (Kane et al., 1993) for bacteria. Polymerase chain reactions (PCRs) were performed with a Mastercycler Gradient (Eppendorf, Hamburg, Germany) as described previously (Ravenschlag et al., 1999), except that the annealing temperature was 58°C and 42°C for archaea and bacteria, respectively. PCR products of several reactions were combined and purified with the QiaQuick PCR Purification Kit (Qiagen, Hilden, Germany). DNA was ligated in the pGEM T-Easy vector (Promega, Madison, WI) and transformed into *E. coli* TOP10 cells (Invitrogen, Carlsbad, CA) according to the manufacturer's recommendations. Sequencing was performed by *Taq* cycle sequencing with a model ABI1377 sequencer (Applied Biosystems) with insert-specific and vector primers. The absence of chimeric sequences in the clone libraries was verified with the CHIMERA_CHECK program of the Ribosomal Database Project II (http://rdp.cme.msu.edu/html/analyses.html). A total of 57 archaeal and 54 bacterial clones were partially sequenced (~ 0.5 kb). Using the ARB software package, these sequences were calculated into existing phylogenetic trees by parsimony without allowing changes in the tree topology. Representative sequences of each cluster were then fully sequenced (~1.3 kb) and matched against the NCBI data base (http://www.ncbi.nlm.nih.gov/BLAST). The sequence data reported here will appear in the EMBL, GenBank, and DDBJ nucleotide sequence databases under the accession numbers DQ007532 to DQ007540.

3. RESULTS

3.1 Field Observations

Echosounder transects revealed several gas flares reaching from the sea floor to the sea surface (transducer depth) at 6° 29.92' N, 2° 59.80'E in an area of ca. 3500 m^2 (Fig. 1, 2). A small area with 4 single plumes was also found at 6° 29.56' N, 2° 59.25'E. No plumes were detected outside of the seep areas within a larger area of 12 km^2. Echosounder guided sampling of the gas flares and subsequent gas extraction showed high concentrations of methane within the plumes (500 nM), which were up to 2 orders of magnitude above the background concentration (5 nM, data not shown). Similar to earlier findings (Hovland, 2002; Hovland and Judd, 1988), sea bottom observations with the ROV and the towed camera showed the presence of bubble streams emanating from small point sources of a few cm in diameter (Fig. 3a). White bacterial mats, most likely formed by giant sulphide oxidizing bacteria with a patch size of some decimetres were found in the same area (Fig. 1, 3b). No bubble emission was observed directly from bacterial mats.

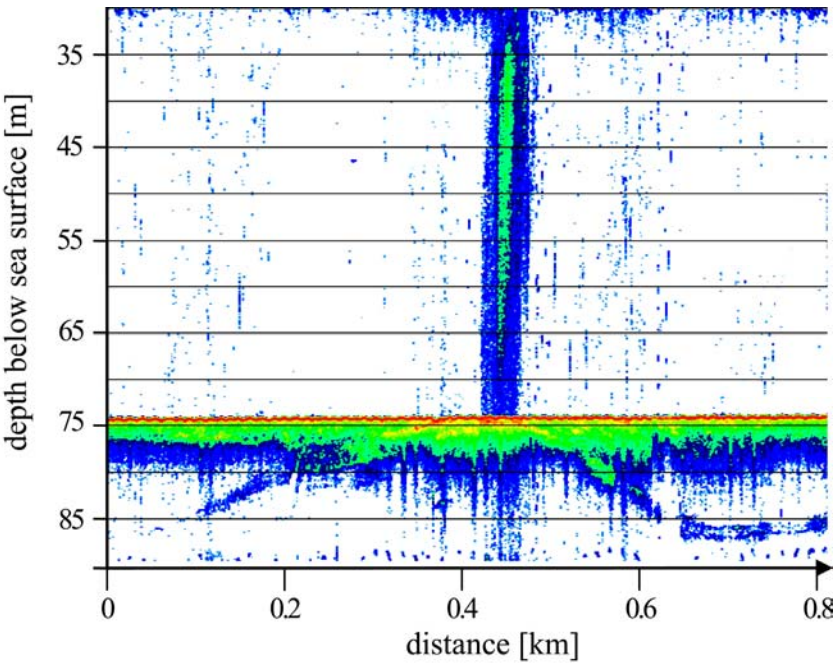

Figure 2. Hydro acoustic image of a methane plume reaching from the sea floor to the sea surface. Ascending sub-surface horizons forming dome-like structures are visible. The image was recorded with a SES-2000 echosounder operated at 8 to 100 kHz.

At various locations mostly situated north of the plume cluster, carbonate crusts with diameters ranging from decimetres to metres were exposed 10 – 50 cm above the sea floor (Fig. 1, 3c). These crusts were densely covered by several species of anthozoa and other sessile macrofauna typical of hard grounds (Fig. 3c). These animals were not found in the surrounding area characterized by sandy sediments. Furthermore, a comparably high density of demersal fish was observed in the vicinity of the crusts.

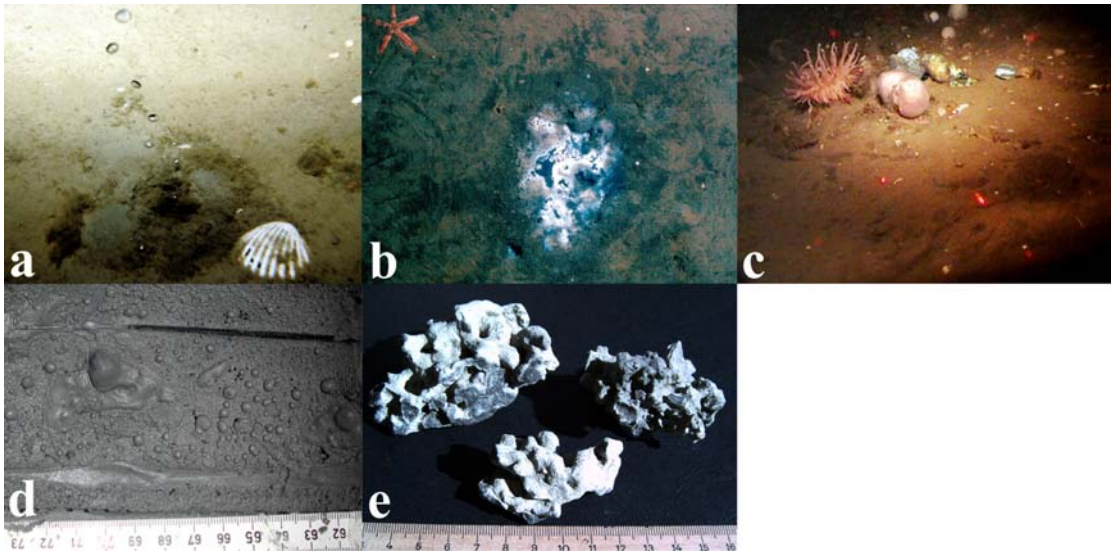

Figure 3. Images of the seafloor observations showing (a) a stream of methane bubbles, (b) bacterial mats and (c) sessile macro fauna on exposed carbonates. (d) A lower section of core 1904 comprising methane-rich, clay-silt sediments and (e) MDACs recovered at the interface between methane-rich, clay-silt and overlying sandy sediments.

3.2 Sediment Layers and Geochemical Profiles

The echosounder profiles showed several dome like structures in the seep area with a distinct sequence of layers narrowing towards the apex of each dome where the gas plumes were situated (Fig. 2). Station 1904 was furthest away from the plume, and station 1860 was closest. All cores obtained from the Tommeliten seep area (1904, 1866 and 1860, Fig. 1)

contained four different horizons of sediments (Fig. 4a-6a): (1) the lowest (350 – 240 cm bsf in core 1904; 300 – 200 cm bsf in core 1860) consisted of stiff marl followed by (2) a gassy layer of clay-silt (Fig. 3d) (240 – 175 cm bsf in core 1904; 230 – 160 cm bsf in core 1866; 200 – 125 cm bsf in core 1860). (3) 10 to 40 cm of sand comprising MDACs (Fig. 3e) were overlying the clay-silt in cores 1904 and 1860. The presence of gas bubbles of ca 0.1-1 cm in diameter in the clay-silt (2), MDAC bearing sediments (3) and the first 10 to 20 cm just above the carbonate bearing sections gave the sediments a spongy appearance (Fig. 3d). (4) The upper most sediment layer consisted of carbonate-free sand (165 – 0 cm bsf in core 1904; 85 – 0 cm bsf in core 1860). Hence, the narrowing of layers towards the apex of the dome visualized by echosounder images (Fig. 2) was reflected in the sedimentology (Fig. 4a, 6a). The sediment layering at station 1866 was different from station 1904 and 1860 as the (3) horizon containing MDACs was found at ca 75 to 85 cm bsf within the (4) sandy sediments (Fig. 5a). No (1) marl section was recovered from core 1866, which was 230 cm long. Sediments at the reference station (recovered ca. 5 km away from the seep area) consisted of (4) a sandy surface horizon (0 to 100 cm bsf) and an underlying (3) clay-silt horizon (100 - 400 cm bsf). No gas bubbles or carbonates were observed at this station (data not shown).

The methane, sulphate and sulphide gradients in the cores from the Tommeliten seep area were influenced by their proximity to the gas plume and by the sediment layering. Because of the artefacts introduced by vibrocoring and subsequent sampling of the gassy and sandy sediments, fluxes of methane and sulphate cannot be calculated from the profiles. Nevertheless, the data indicate a distinct zonation of the processes of anaerobic methane consumption and associated sulphide production. At the reference station away from the seep, sediments contained methane concentrations <0.1 µM (quantification limit) throughout the core. In contrast, within the seep area, methane concentrations reached supersaturation in the (2) clay horizon and the (3) MDAC-bearing sediments (core 1860 = 2.5, 1866 = 1.4, 1904 =

1.6 mM). Within the stiff marl sediments (1), the methane concentration was comparably low (<0.2 mM) (Fig. 4a-6a). The sulphate-methane transition zone (SMTZ) is defined here as the horizon with a distinct dip in methane and sulphate concentrations as well as a peak in sulphide concentrations. This was located between the (3) MDAC-bearing sediments and (4) the overlying sandy sediments in cores 1904 and 1860, and in the lower sand section in core 1866. In contrast to a typical SMTZ, sulphate was not depleted in the methane-rich zone. However, this is most likely a result of sampling artefacts. Above the SMTZ, methane concentrations declined to values <0.04 mM. In core 1860, methane concentrations remained comparably high above the carbonate-bearing horizon (>0.25 mM) but declined to <0.04 mM in the top sediment horizon. At station 1904 and 1866, methane concentrations were below 0.01 mM in the top 40 cm of the seabed (Fig. 4a, 5a). Sulphate concentrations declined slightly at the methane transition zone (SMTZ) from seawater values (28 mM) to values between 23 (core 1904, 1866; Fig. 4a, 5a) and 15 mM (core 1860; Fig. 6a). In each core, a distinct sulphide peak was measured just above the horizon in which methane declined with concentrations of 3.1 mM (core 1904, 135 cm bsf), 1.9 mM (core 1866, 115 cm bsf) and 2.1 mM (core 1860, 55 cm bsf), respectively (Fig. 4b-6b). Sulphide concentrations declined to values below detection limit in surface and bottom horizons. Sediments of the reference station did not show any detectable sulphide concentrations (data not shown).

3.3 *Ex situ* AOM and SR

In short-term *ex situ* incubations, AOM reached a maximum rate of 2.4 nmol cm^{-3} d^{-1} at 170 cm bsf in core 1904 within the SMTZ. Sulphate reduction rates were also elevated at the SMTZ reaching 2 nmol cm^{-3} d^{-1}. Unfortunately, no SR could be measured below this horizon due to sample loss. Rates in overlying horizons decreased to values ranging between 0.8 and

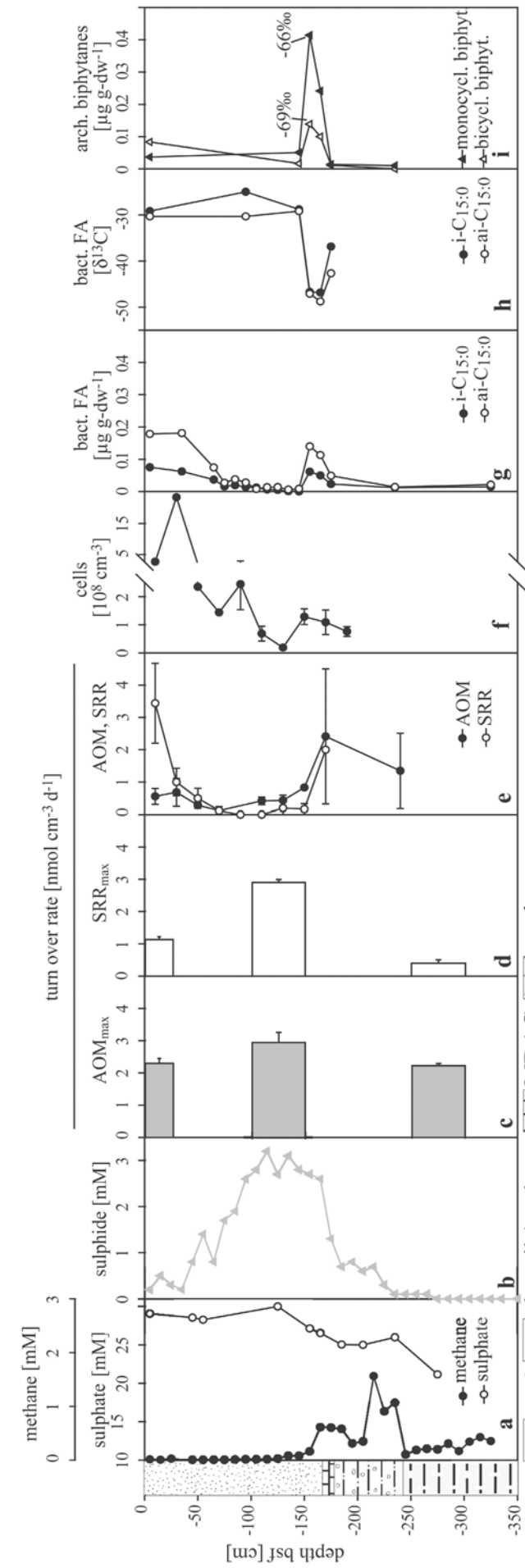

Figure 4. Station 1904. (a) Methane and sulphate concentrations decline at depth of MDAC bearing sediments (150 cm bsf.). (b) Note that sulphide concentrations, (c) potential methane oxidation and (d) sulphate reduction rates, (e) ex situ measured methane oxidation and sulphate reduction rates, (f) cell counts, (g) concentrations and (h) stable carbon isotope values of selected, bacterial fatty acids and (i) concentrations of cleaved, archaeal tetraether lipids peak at the methane-sulphate transition zone. Errors are given as standard errors.

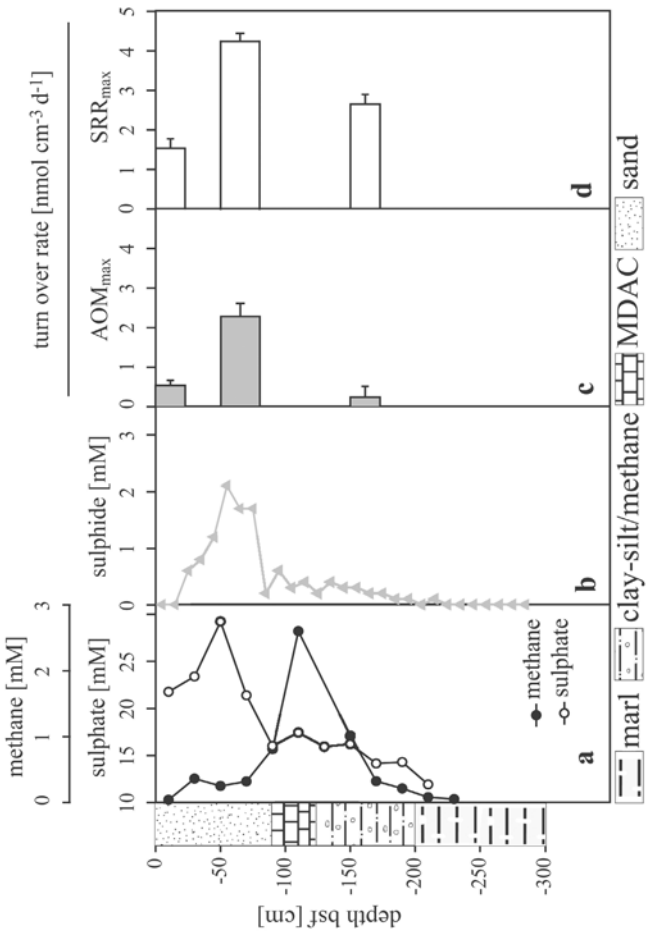

Figure 5. Station 1866. (a) Methane and sulphate concentrations decline below carbonate bearing sediments (100 cm bsf). Homologous to core 1904, (b) sulphide concentrations and potential rates of (c) methane oxidation and (d) sulphate reduction are highest at the sulphate-methane transition zone. Errors are given as standard errors.

Figure 6. Station 1860. (a) Methane and sulphate concentrations decline at depth of carbonate bearing sediments (70 cm bsf). Homologous to core 1904, (b) sulphide concentrations and potential rates of (c) methane oxidation and (d) sulphate reduction are highest at the sulphate-methane transition zone. Errors are given as standard errors.

0.1 nmol cm^{-3} (Fig. 4e). Highest SR were detected in the surface horizon (3.5 nmol cm^{-3} d^{-1}). AOM and SR were highly variable between replicate subsamples within one horizon leading to standard errors of up to 83 % of the mean (Fig. 4e).

3.4 *In Vitro* Rates at Methane Saturation

Potential AOM and SR rates (AOM_{max}, SR_{max}) measured in long-term incubations were highest in sediments collected from the SMTZ with 1.4 to 3 and 2.9 to 4.6 nmol cm-3 d^{-1}, respectively (Fig. 4c, d - 6c, d). In these incubations, the ratio of AOM to SR was 1:1 in core 1904, 0.3:1 in core 1866 and 0.5:1 core 1860. In sediment slurries from the SMTZ at station 1904, SR without methane was 70% lower compared to incubations with methane. This indicates a close coupling between AOM and SR. AOM_{max} and SR_{max} were substantially lower in slurries obtained from horizons above and below the SMTZ (Fig. 4c,d-6c,d).

3.5 Biomarker Signatures

3.5.1 Sediments

Concentration measurements of single lipid compounds showed maxima of specific bacterial FAs and archaeal isoprenoidal lipids in sediments from the SMTZ of core 1904 (150 – 180 cm bsf; Fig. 4g, i, Tab. 1). At this horizon, stable carbon isotope analysis revealed the highest depletion in ^{13}C with minimum values of –79‰ (*sn2*-hydroxyarchaeol) in archaeal diether lipids (Fig. 7) and –50‰ (ai-$C_{15:0}$) in bacterial FAs (Fig. 4h, Fig. 9). The concentration of both archaeal and bacterial lipids decreased just above and below the SMTZ where these

Table 1. Lipid biomarker concentrations extracted from sediments at the sulphate-methane transition zone (155 cm bsf) of core 1904.

Bacterial fatty acids

Component	Concentration [ng g-dw^{-1}]
C14:0	145
i-C15:0	61
ai-C15:0	140
C15:0	72
i-C16:0	25
C16:1ω9c	88
C16:1ω7c	21
C16:1ω5c	11
C16:0	604
i-C17:0	15
ai-C17:0	43
C17:0	39
C18:2ω6,9c	215
C18:1ω9c	270
C18:1ω7c	58
C18:0	345

Archaeal ether lipids

Component	Concentration [ng g-dw^{-1}]
crocetane	21
PMI:0	56
PMI:1	36
ΣPMI:2	158
ΣPMI:3	-
ΣPMI:4	15
archaeol	473
sn2-hydroxyarchaeol	84
sn3-hydroxyarchaeol	105
phytane	918
biphytane	504
monocycl. biphytane	414
bicycl. biphytane	139
crenarchaeol	4

biomarkers were also less depleted. Archaeal lipids found at the SMTZ were dominated by the glycerol diether archaeol and the decomposition products of both diether and tetraether lipids, i.e. phytane and biphytanes with δ^{13}C-values ranging from –60‰ to -70‰ (Tab. 1, Fig 7). *sn2*- and *sn3*-hydroxy-archaeol (Σhydroxyarcha-eol) were less abundant relative to archaeol with a ratio of 0.4:1. Concentrations of the biphytanes decreased with increasing degree of cyclisation (Fig. 7). Compared to the di- and tetraethers, archaeal isoprenoidal hydrocarbons were approximately one order of magnitude lower in concentration (Tab. 1). As a result, the stable isotope composition of these compounds could not be measured (required minimum concentration: ~100 ng g-dw^{-1}). Isoprenoidal hydrocarbons were dominated by 2,6,10,15,19-pentamethylicosenes with two double bonds (ΣPMI:2; 3 isomers) followed by PMI:0 and PMI:1 (Fig. 8). The FA fraction in sediments of the SMTZ was dominated by $C_{16:0}$, followed by $C_{18:1\omega9}$, $C_{18:0}$ and $C_{18:2}$. FAs that are putatively specific for SRB involved in AOM such as $C_{16:1\omega5}$, i-$C_{15:0}$ and ai-$C_{15:0}$ (Blumenberg et al., 2004; Elvert et al., 2003), were approximately 5 to 50 times lower in concentration compared to $C_{16:0}$ in Tommeliten sediments (Tab. 1). However, in contrast to abundant FAs, stable carbon isotope compositions of i-$C_{15:0}$ and ai-$C_{15:0}$ showed a depletion in ^{13}C (Fig 4h, 9).

3.5.2 Methane Derived Authigenic Carbonates

Lipid analysis revealed that MDACs from the Tommeliten seep contained specific archaeal and bacterial lipids. $\delta^{13}C$-values of these compounds were 20-30‰-lower in comparison to those extracted from sediment at the SMTZ of station 1904 (Fig. 7-9). In contrast to the SMTZ sediments, the di- and tetraether fraction in the subsurface MDACs was dominated by *sn2*-hydroxyarchaeol, which was slightly more abundant than archaeol (archaeol: Σhydroxyarchaeol = 1:1.6). The surface MDACs even reached a ratio of archaeol to Σhydroxyarchaeol of 1:1.9 (Fig. 7). The suite of biphytanes found in sediments of the SMTZ was also present in the subsurface and surface MDACs. Furthermore, the biphytanes in the MDACs and in sediments of the SMTZ showed a similar abundance pattern. I.e.,

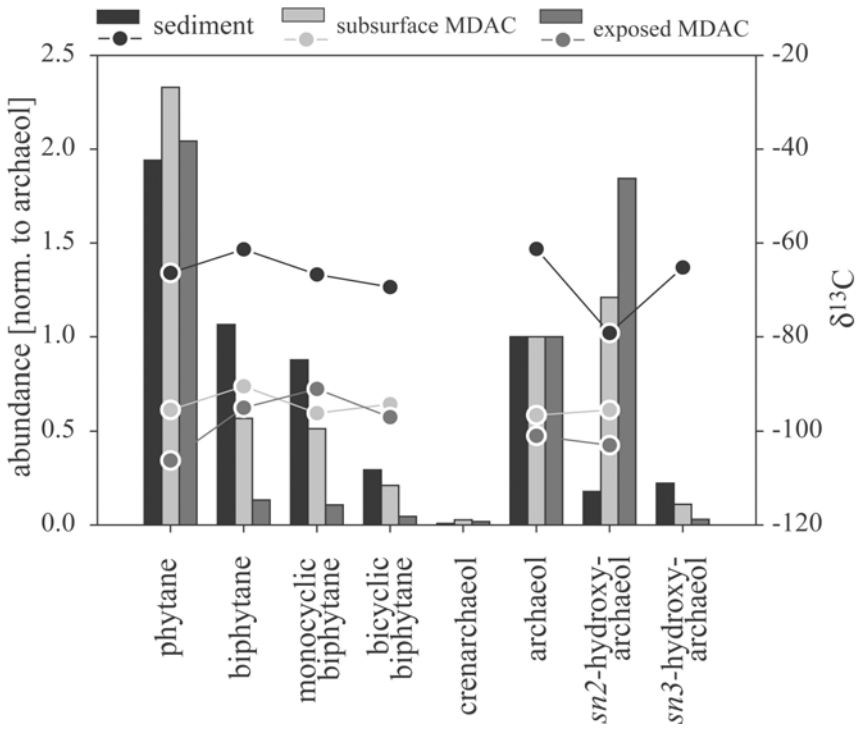

Figure 7. Abundance (bars) and stable carbon isotope composition (circles) of cleaved, archaeal tetraether and whole diether lipids extracted from sediments and MDACs at the sulphate-methane transition zone (155 cm bsf) of core 1904 and from surface MDACs recovered by a ROV. Abundances were normalised to archaeol. Note the constant offset in $\delta^{13}C$-values between sediments and MDACs.

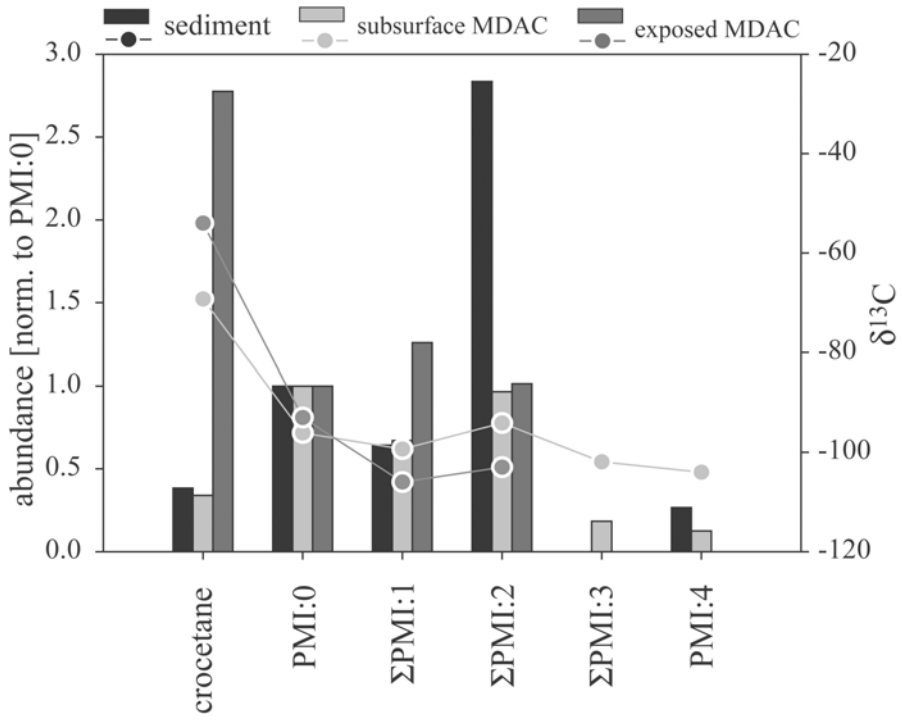

Figure 8. Abundance (bars) and stable carbon isotope composition (circles) of archaeal, isoprenoid hydrocarbon lipids extracted from sediments and MDACs at the sulphate-methane transition zone (155 cm bsf) of core 1904 and from surface MDACs recovered by a ROV. Abundances were normalised to PMI:0. Note that concentrations of crocetane are ca. 7.5-fold increased in surface MDACs. Low concentrations prohibited $\delta^{13}C$-measurements of hydrocarbons in the sediment.

concentrations of the biphytanes decreased with higher degrees of cyclisation. However, in contrast to sediments of the SMTZ, the abundance of biphy-tanes relative to archaeol and phytane was lower in the subsurface MDACs and lowest in surface MDACs (Fig. 7). Furthermore, PMIs in the MDACs showed higher degrees of saturation (Fig. 8) and a higher number of isomers compared to sediments of the SMTZ. ΣPMI:1 comprised 4, ΣPMI:2 5 and ΣPMI:3 2 isomers. Notably, surface MDACs contained very high amounts of crocetane. Stable carbon isotope compositions of diethers, tetraethers and isoprenoid hydrocarbons were uniformly <-90 ‰, both in the subsurface and the surface MDACs. An exception was crocetane showing $\delta^{13}C$ values of –70 and –55 ‰ in the subsurface and the surface MDACs, respectively (Fig. 8). Variations in $\delta^{13}C$-values among the PMI isomers were small with a

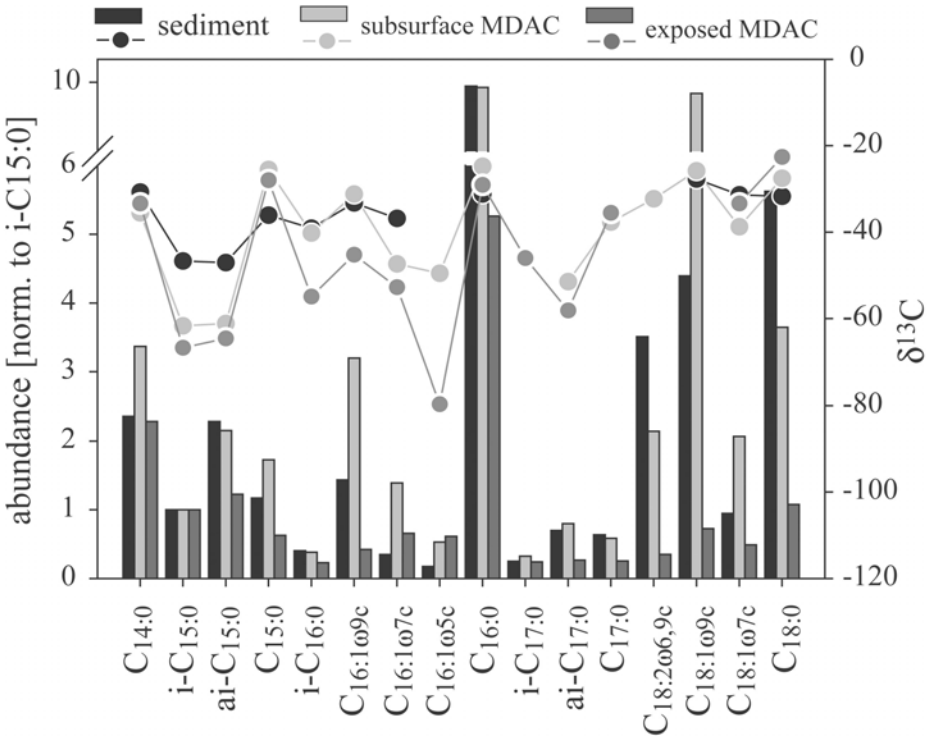

Figure 9. Abundance (bars) and stable carbon isotope composition (circles) of fatty acids extracted from sediments and MDACs at the sulphate-methane transition zone (155 cm bsf) of core 1904 and from surface MDACs recovered by a ROV. Abundances were normalised to i-$C_{15:0}$. i-$C_{15:0}$, ai-$C_{15:0}$ and $C_{16:1\omega5}$, are among the most depleted fatty acids. Note the offset in $\delta^{13}C$-values between sediments and MDACs.

maximum of ±2 ‰. As with the biphytanes, the FA abundance pattern of the subsurface MDACs showed comparably high similarities to the pattern found in sediments of the SMTZ, whereas the abundance pattern of the surface MDACs showed lower similarities (Fig. 9). Subsurface MDACs contained roughly twice as much i-$C_{15:0}$ than ai-$C_{15:0}$ while this ratio was almost 1:1 in surface carbonates. In the subsurface MDACs, i-$C_{15:0}$ and ai-$C_{15:0}$ were the most ^{13}C-depleted FAs with values down to -62‰. In contrast, the most ^{13}C-depleted FA found in the surface MDACs was $C_{16:1\omega5}$ with a $\delta\ ^{13}C$-value of –80‰ while i-$C_{15:0}$ and ai-$C_{15:0}$ showed values of -67‰ and -65‰, respectively (Fig. 9).

3.6 Archaeal and Bacterial Clone Libraries

One archaeal and one bacterial clone library were constructed from a sediment sample from the SMTZ of station 1904 to study the microbial diversity in the AOM zone. A total of 57 archaeal and 54 bacterial clones were partially sequenced (~ 0.5 kb). From each phylogenetic group, one representative sequence was almost fully (~1.5 kb) sequenced. The obtained 16S rDNA archaeal clone library showed a low diversity in comparison to previous publications of methane seep systems (Mills et al., 2003; Orphan et al., 2002; Teske et al., 2002). Two different phylogentic groups of archaea were detected (Tab. 2). The ANME-1b cluster (*Methanosarcinales*) accounted for 98 % of obtained sequences. The second group comprised a single clone sequence, which belongs to the Marine Benthic Group D (Thermoplamatales). Other ANME groups or methanogens were not detected.

The bacterial clone library consisted of seven uncultivated, methane seep-related lineages. The next relatives to all sequences obtained are commonly found in marine cold seeps (Tab. 2). Most abundant were clones of the δ-Proteobacteria comprising sequences of the putative bacterial partner for AOM (26% of bacterial clone sequences), i.e. the Seep-SRB1 cluster (Knittel et al., 2003). One other abundant group among the δ-Proteobacteria were the Desulfoarculaceae (26%). 38% of bacterial sequences were distantly related to the Haloanaerobiales, which belong to the Firmicutes.

3.7 Total Cell Counts and ANME-1 Abundance

Direct cell counts showed highest numbers in surface sediment horizons (23.2 $*10^8$ cells cm^{-3} at 30 cm bsf). Cell counts decreased below this horizon to values $<0.2*10^8$ cells cm^{-3} at 130 cm bsf but showed an increase in sediments of the SMTZ (1.1 – 1.3 $*10^8$ cells cm^{-3} at 150 –

Table 2. Archaeal and bacterial 16S rDNA clone libraries obtained from sediments at the methane transition zone (155 cm bsf) of core 1904.

Phylogenetic group		Clones	Representative clone	Next relative	Sequence similarity
Archaea		57			
Euryarchaeota	ANME-1b	56	Tommeliten_ARCH1FL (DQ007532)	Hydrate Ridge Sediment Clone HydCal61 (AJ578089)	≥98 %
	Marine Benthic Group D	1	Tommeliten_ARCH69FL(DQ007533)	Uncultured archaeon clone Napoli-3A-13 (AY592524)	99 %
Bacteria		54			
δ Proteobacteria	Seep-SRB1	14	Tommeliten_BAC57FL (DQ007534)	Hydrate Ridge clone Hyd89-22 (AJ535247)	≥93 %
	Seep-SRB2	2	Tommeliten_BAC13FL (DQ007535)	Hydrate Ridge clone Hyd89-19 (AJ535233)	98 %
	Desulfoarculaceae	14	Tommeliten_BAC62FL (DQ007536)	Eel River Basin clone Eel-BE1B4 (AF354145)	≥95 %
	distantly to Myxococcales	1	Tommeliten_BAC81FL (DQ007537)	Eel River Basin clone Eel-TE1A7 (AF354155)	93 %
Clostridia	distantly to Haloanaerobiaceae	20	Tommeliten_BAC55FL (DQ007538)	hydrocarbon seep clone GCA025 (AF154106)	≥95 %
Acidobacteria	distantly to Acidobacteriaceae	2	Tommeliten_BAC4FL (DQ007539)	Gyamas sediment clone C1_B017 (AF419691)	96 %
Thermotogae	distantly to Thermotoga	1	Tommeliten_BAC43FL (DQ007540)	Nankai Trough clone MB-C2-106 (AY093477)	94 %

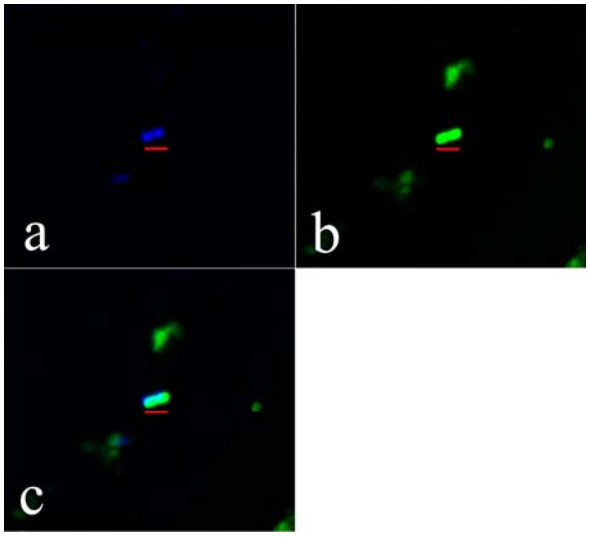

Figure 10. Individual cells of ANME-1 archaea from sediments at the sulphate-methane transition zone (155 cm) of core 1904 (a) visualised with 4′,6′-diamidino-2-phenylindole (DAPI), (b) cy-3 horseradish peroxidase-labeled oligonucleotide probe ANME1-350 and tyramide signal amplification (CARD-FISH) and (c) an overlay of both images. The red scale bar represents 2µm.

170 cm bsf). In this horizon, probing with CARD-FISH targeting ANME-1 cells resulted in positive signals (Fig. 10). Only single cells or chains of up to three cells were observed. Bacterial partners physically attached to ANME-1 were not observed. Specific CARD-FISH counts resulted in $1.45 * 10^7$ ANME-1 cells cm^{-3} sediment. The overlying horizon (110 cm bsf) contained very low numbers of ANME-1 cells ($<3* 10^5$ cells cm^{-3}), whereas ANME-1 could not be detected in an underlying horizon (190 cm bsf.).

4. DISCUSSION

4.1 Methane Emission from the Tommeliten Seep Area

Two decades after the discovery of gas seeps in the Tommeliten area by Hovland and Judd (1988), we revisited this area for video and biogeochemical surveys. The Tommeliten area is located in the central North Sea (56° 29.90' N, 2° 59.80' E) above three salt diapiers. Here, the so-called Delta structure has pierced the enclosing sedimentary rocks allowing methane to migrate to surface sediments. During ROV surveys, Hovland and Judd (1988) identified several small gas vents emitting single streams of methane bubbles from the sandy seabed into the hydrosphere. High reflective, small patches (<5 m across, ~0.5 m deep) noted on short-range side-scan sonar records, which the authors termed "eyed pockmarks", were found to comprise MDAC crusts serving as a hard substrate for a variety of anthozoa such as sea-anemones and sea pens. Furthermore, it was estimated that the flux of gas from the wider seep area of 6500 m^2 was 47 g CH_4 m^{-2} yr^{-1} (Hovland and Judd, 1992; Hovland et al. 1993). Two decades later, our observations provide evidence that the Tommeliten seep area is still active. Here, several gas flares reaching almost to the sea surface were recorded by hydroacoustic profiling (Fig. 2) and video surveys provided evidence for bubble streams being emitted from the sandy sea floor (Fig. 3a). From these observations it can be concluded that the seeps of the Tommeliten area contribute to atmospheric methane, especially during deep mixing situations in the North Sea. Video observations also showed microbial mats of filamentous, presumably thiotrophic bacteria (Fig. 3b) and reef like structures of MDACs as already described by Hovland and Judd (1988).

Such features as observed at Tommeliten are typical for active cold seeps on continental margins and generally indicate high methane fluxes and turnover rates (Boetius and Suess, 2004; Joye et al., 2004; Michaelis et al., 2002; Orphan et al., 2004; Treude et al., 2003). However, we found only few highly focused point sources in the sandy seabed and very patchy, small microbial mats pointing to very restricted AOM zones close to the sea floor.

4.2 Control of Methane Efflux from Seep Sediments

Our study provides evidence that methane flux at the Tommeliten seeps is controlled by a combination of geological and microbial processes as illustrated in figure 11. The shallow seismic profiles show strong, ascending reflectors in the sediment (Fig. 2). Moreover, ascending and discontinuous reflectors on seismic plots of deep sediment layers (Hovland, 2002; Hovland and Judd, 1988) indicate that the process of local gas venting may have occurred several times in the history of Tommeliten. At present, the position of the methane plumes together with direct observations of methane bubbles (Fig 1, 3a) give evidence for seepage pathways at the crest of the marl domes that allow for emission of free gas, circumventing microbial consumption (Fig. 11-II). Our observations from vibrocorer sampling indicate that the marl sediments represent a barrier to gas flow. A shallower depth and narrowing of the marl boundary in the vicinity of plumes as observed previously (Hovland and Judd, 1988) and in this study (Fig. 4a, 6a) suggests that subsurface gas pressure lifts sediments (Fig. 11-I). As a consequence, the marl may locally crack, allowing an advection of methane into and within the overlying clay-silt sediments. At the station 1860 closest to the gas plume, the marl horizon was missing. It is possible that the position of the gas vents is connected to the distribution of sands, which facilitate the passage of free gas bubbles compared to clays.

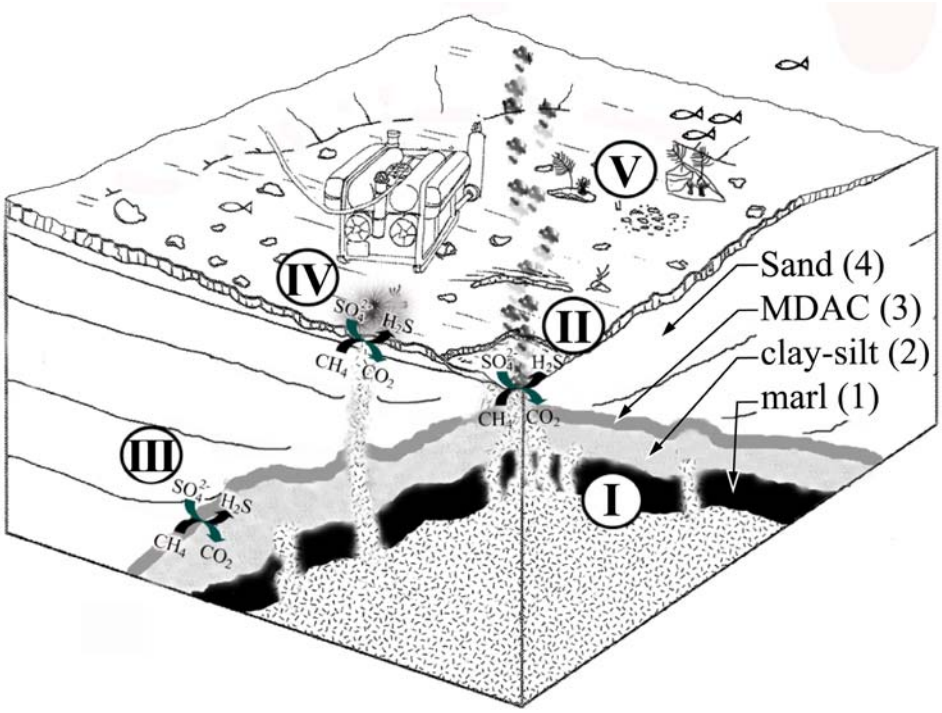

Figure 11. Schematic overview of seepage and related processes at Tommeliten modified from Hovland & Judd (1988). The different sediment horizons are indicated. (I) methane migrates through cracks in the uplifted marl into overlying, clay-silt sediments sediments. (II) sedimentary pathways at the crest of the marl dome permit the escape of free gas, circumventing microbial consumption. (III) subsurface, AOM depletes uprising methane at the interface between clay silt and sandy sediments where MDACs precipitate. With time and/or reduced methane fluxes, seepage at Tommeliten is sealed of as indicated by (IV) patches of thiotrophic, bacterial mats on the seafloor. These are commonly associated to high AOM rates in shallow surface sediments consuming uprising methane. (V) MDACs are precipitated in near-surface sediments. These provide a hard substrate for sessile macro fauna after exposure.

Within the sediments, methane is most likely advecting horizontally in the clay-silt layer above the marl. Here, it is partially consumed in a very distinct subsurface horizon of no more than 20 cm located at the SMTZ between the MDACs (horizon 3) and the sandy sediments (horizon 4) (Fig. 11-III). The decline of methane concentrations in this sediment layer coincided with increased concentrations of ^{13}C-depleted lipid biomarkers, cell abundances as well as with relatively elevated rates of AOM and SR measured by *in vitro* and *ex situ* incubations.

The *ex situ and in vitro* AOM and SR rates at the Tommeliten seep SMTZ are 2 to 3 orders of magnitude lower in comparison to highly active cold seeps such as Hydrate Ridge and the Gulf of Mexico (Boetius et al., 2000; Joye et al., 2004; Treude et al., 2003), Nevertheless, AOM apparently consumes all the methane diffusing into the sands. With respect to the abundance of ANME-1 cells ($1.5 * 10^7$ cells cm^{-3}) and the average AOM rate in sediments at the SMTZ (2.4 nmol cm^{-3} d^{-1}), the cell-specific AOM rate at Tommeliten was ~0.17 fmol d^{-1}. This value is comparable to highly active seeps. At Hydrate Ridge, *ex situ* measurements of AOM showed near surface peaks with average values of 1.1 and 1.3 µmol cm^{-3} d^{-1}, respectively (Treude et al., 2003; study site *Beggiatoa* field 2 at 2.5 and 6.5cm bsf). In these horizons, ca. $0.9*10^8$ and $0.6*10^8$ ANME-2 / Seep-SRB1 aggregates per cm^3 were detected, respectively (Treude et al., 2003). An average aggregate at Hydrate Ridge was found to consist of ca. 100 archaeal and 200 SRB cells (Boetius et al., 2000). Hence, cell-specific AOM rates are ranging between 0.13 and 0.21 fmol d^{-1}. These values are in good agreement with *in vitro* measurements from Hydrate Ridge. Nauhaus et al. (2005) measured *in vitro* AOM rates of 2.5 µmol g-dw^{-1} d^{-1} in sediments from a *Beggiatoa* site, which contained $0.9*10^8$ aggregates g-dw^{-1}. This corresponds to a cell specific rate of 0.28 fmol d^{-1}. Other AOM systems such as the ANME-1 dominated microbial mats from the Black Sea were found to contain ca. $4*10^{10}$ ANME-1 cells cm^{-3} (Knittel et al., 2005). Corrected for porosity (~87%, Treude pers. com.), *in vitro* AOM at the Black Sea microbial mats was ca. 5.3 µmol cm^{-3} d^{-1} (Nauhaus et al., 2005) which corresponds to a cell-specific rate of 0.13 fmol d^{-1}. In conclusion, the capacity for AOM at methane seep systems appears to be mainly related to the biomass and distribution of the AOM community, which is in turn regulated by the availability of methane and sulphate.

The sea floor observations of patches of presumably thiotrophic mats, above blackish, reduced sediments (Fig.6b, Fig. 11-IV), give evidence for another type of patchy hot spot of

microbial activity just beneath the sea floor, possibly AOM as indicated by previous observations of free methane trapped below microbial mats (Hovland, 2002). However, we were not able to sample these sediments with our tools during the R/V Heincke expeditions. The imprint of ^{13}C-depleted archaeal and bacterial lipids in MDACs exposed at the sea floor also provide evidence of AOM activity and resulting carbonate precipitation in near surface sediments at Tommeliten. However, at present, no seepage was observed at the crusts (Hovland, 2002; Hovland and Judd 1988; this work). It is possible that the precipitation of carbonates in the AOM zone leads to a self-sealing of gas leakage pathways (Hovland, 2002). The surface MDAC crusts found at the Tommmeliten site may have formed in near-surface horizons just like the MDAC pieces found in the SMTZ, and may have been exposed due to sediment erosion. Today they are providing a niche for sessile hard substrate fauna, which is unusual for the sandy seabed of the central North Sea (Fig.3c, Fig. 11-V). Furthermore, the crusts also attract demersal fish. Hence, these observations indicate that seepage related carbonates, which outcrop the sea floor have a stimulating effect on the abundance of mega fauna.

4.3 Distribution and Identity of Methanotrophic Communities

Specific lipid biomarkers with typically low δ^{13}C-values in sediments and MDACs of the Tommeliten seep area provide evidence for anaerobic methanotrophic communities associated with gas seepage. The differences in the biomarker patterns in sediments at the SMTZ and in the surface and subsurface MDACs indicate the presence of different groups of methanotrophs. Sediments of the SMTZ host a methanotrophic community dominated by ANME-1. MDAC pieces at the SMTZ show a lipid pattern indicative of a mixed ANME-1 /

ANME-2 community whereas the exposed MDAC crusts contain a biomarker signature typical of ANME-2 communities, as discussed in the following:

4.3.1 ANME-1 Community in Sediments of the SMTZ

^{13}C-depleted acyclic and cyclic biphytanes were found in relatively high abundances in sediments at the SMTZ (Fig. 7). Biphytanes are present in various methanogenic archaea and planktonic crenarchaeota (De Rosa and Gambacorta, 1988; Koga et al., 1993; Schouten et al., 2002). However, a substantial δ^{13}C-depletion as observed here and in other seep environments points to methanotrophic organisms. A similar lipid pattern as in the Tommeliten SMTZ was found in microbial mats from the Black Sea. These mats were dominated by ANME-1, as shown by microscopic observation based on FISH (Blumenberg et al., 2004; Knittel et al., 2005; Michaelis et al., 2002). Blumenberg et al. (2004) also showed that biphytanes are absent or rare in ANME-2 dominated microbial mats and proposed to use biphytanes as specific indicators for ANME-1 communities. Furthermore, in sediments of the SMTZ, the low ratio of *sn2*-hydroxyarchaeol relative to archaeol (0.2:1, Fig. 7), both of which are ^{13}C-depleted, matches typical ANME-1 signatures known from other cold seep sediments and MDACs (Aloisi et al., 2002; Blumenberg et al., 2004; Hinrichs et al., 1999; Hinrichs et al., 2000; Teske et al., 2002). In contrast, a ratio of 2:1 or higher was found in ANME-2 dominated systems (Blumenberg et al., 2004; Elvert et al., submitted; Hinrichs et al., 2000; Orphan et al., 2001a). The predominance of ANME-1 in the SMTZ of Tommeliten seeps is confirmed by 16S rDNA and FISH analysis. We found a very low diversity of archaeal 16S rDNA clone sequences, which belonged almost entirely to the ANME-1b sub-cluster (98 % of the retrieved archaeal sequences, Tab. 2). Epifluorescence microscopy of CARD-FISH targeted cells detected ANME-1 in the SMTZ zone (Fig. 10). In contrast, probes targeting

ANME-2a, ANME-2c or ANME-3 gave no positive results in sediments from the SMTZ or around it.

Usually, ANME cells are found physically associated with SRB in samples from AOM zones of most seep systems. It is generally assumed that these SRB are syntrophic partners of ANME, however, so far, the mechanistic nature of their interaction remains unknown (Boetius et al., 2000; Hoehler et al., 1994; Nauhaus et al., 2002; Orphan et al., 2001b). Fingerprints of ^{13}C-depleted bacterial FAs and microscopic observations using FISH showed, that the most common partners of ANME-1 and ANME-2 communities are SRB of the Seep-SRB1 cluster (Blumenberg et al., 2004; Elvert et al., 2003; Knittel et al., 2003). Accordingly, the 16S rDNA clone library from sediments of the SMTZ contained high abundances of Seep-SRB1 sequences. Although sequences of the Seep-SRB1 in ANME-1 and ANME-2 dominated habitats form one cluster, FA lipid patterns suggest the existence of two distinct ecotypes of Seep-SRB1 with different FA fingerprints when associated to ANME-1 or ANME-2 (Blumenberg et al., 2004; Elvert et al., 2003). In the Tommeliten SMTZ sediments, the high content of ai-$C_{15:0}$ relative to i-$C_{15:0}$ and the lack of abundant amounts of $C_{16:1\omega5}$ suggest the presence of the Seep-SRB1 type associated to ANME-1 (Blumenberg et al. 2004).

4.3.2 ANME-1 / ANME-2 Communities in MDACs

Previous investigations showed that biomarker patterns in MDACs may be derived from living biomass or represent fossilized materials, or a mixture of both (Aloisi et al., 2002; Peckmann et al., 2002; Thiel et al., 2001). The presence of ^{13}C-depleted archaeal lipids in subsurface and exposed MDACs indicate that carbonate precipitation at Tommeliten is associated with processes of seepage and AOM. The shapes of subsurface MDACs suggest

that these were precipitated in pore spaces and channels formed by gas bubble streams. It is interesting to note that the subsurface and exposed MDACs contained different biomarker patterns. The subsurface MDACs were found to contain archaeal lipids which indicate a mixed ANME-1 / ANME-2 community. Compared to sediments at the SMTZ, the relative abundance of ANME-1 specific biphytanes was low (Fig. 7). The ratio of *sn2*-hydroxyarchaeol relative to archaeol was comparable to available values from settings comprising a mixed community consisting of ANME-1 / ANME-2 or dominated by ANME-2 (Blumenberg et al., 2004; Elvert et al., submitted; Hinrichs et al., 1999; Hinrichs et al., 2000; Orphan et al., 2001a). In contrast to the subsurface MDACs, the MDACs exposed at the seafloor contained a biomarker signature typical for ANME-2 communities. Low amounts of biphytanes and high amounts of *sn2*-hydroxyarchaeol relative to archaeol (1:1.9, Fig. 7) as well as substantial amounts of ^{13}C-depleted crocetane (Fig. 8) are in good agreement with published data for ANME-2 dominated systems (Blumenberg et al., 2004; Elvert et al., 2001; Elvert et al., submitted; Elvert et al., 1999; Orphan et al., 2001a). The subsurface as well as the surface MDACs also contained lipid signatures typical of the Seep-SRB1 cluster commonly associated with ANME-1 or ANME-2. High amounts of ai-$C_{15:0}$ relative to i-$C_{15:0}$ (2.1:1, Fig. 9) in surface MDACs are indicative of Seep-SRB1 associated with ANME-1, whereas in exposed MDACs, a ratio of nearly 1:1 and substantial amounts of $C_{16:1\omega5}$ point to the Seep-SRB1 ecotype associated to ANME-2 (Blumenberg et al., 2004; Elvert et al., 2003). It is possible that the MDACs found at Tommeliten preserve signatures of previous ANME-2 communities once populating the surface sediments of this seep. At present, such a niche could exist in the reduced patches covered by bacterial mats, which we unfortunately were not able to sample because of their small size and patchy distribution. Previous studies at the cold seep systems of Hydrate Ridge showed a similar trend in the distribution of ANME-1 and ANME-2 communities. Here, surface sediments are dominated by ANME-2 whereas the abundance of ANME-1 was found to increase subsurface (Knittel et al. 2003, 2005).

However, the environmental factors selecting for these different phylogenetic groups and their bacterial partner remain unknown.

CONCLUSIONS

So far, only very little is known on the identity, activity and distribution of AOM communities of shallow water cold seeps. In this investigation we revisited the Tommeliten area, a seepage site of the central North Sea. Here, an impermeable horizon of stiff marl sediments represents a natural barrier for methane rising from a deep gas reservoir. Methane pressure lifts this horizon forming dome-like subsurface structures. As a consequence, the marl may crack, allowing methane to advect into overlying, sediments of clay-silt. At the interface between silty and sandy sediments, methane is oxidised anaerobically by a community of ANME-1 archaea and SRB of the Seep-SRB1 group in a defined subsurface horizon of ca. 20 cm. This horizon also bears methane-derived authigenic carbonates and shows the highest AOM activity. AOM and SR rates are several orders of magnitude lower in comparison to AOM zones of highly active cold seeps. Nevertheless, the specific activity of methanotrophic cells detected in the sediments is comparable. All uprising methane is consumed within the sediments, except for a few locations with active gas venting to the hydrosphere. Here, at the crest of the marl domes, the ebullition of free gas circumvents microbial consumption most likely due to the presence of gas channels through sandy sediments. Thiotrophic bacterial mats as well as methane-derived authigenic carbonates exposed at the sea floor also indicate the presence of local gas escape routes.

Acknowledgements

This study was conducted as part of the METROL project (www.metrol.org) of the 5th framework program of the European Commission (EVK-3-CT-2002-00080). We thank captain, crew and shipboard scientists of R/V Heincke cruise HE-169 and HE-180 for their excellent support with work at sea. We thank Gert Wendt and Jens Wunderlich from Rostock University and Innomar Technologie GmbH for providing and operating the echosounder SES-2000 and Werner Dimmler from the Alfred Wegener Institute for Polar and Marine Research for ROV maintenance and operation. We thank Regina Usbeck from FIELAX for support with mapping and geo-referencing, Imke Busse, Viola Beyer and Thomas Wilkop for laboratory analyses and Gerd Bening for handling the vibrocorer of the Institute for Baltic Sea Research (IOW). This study would not have been possible without the technical support by the Geology Department of the IOW. Rebecca Rendle-Bühring, Johanna Schwarz and Stephan Steinke of the University Bremen are acknowledged for their help with sedimentological descriptions. We also thank Thomas Pape of the University Hamburg for the provision of analytical protocols.

References

Aloisi G., Bouloubassi I., Heijs S. K., Pancost R. D., Pierre C., Damste J. S. S., Gottschal J. C., Forney L. J., and Rouchy J. M. (2002) CH4-consuming microorganisms and the formation of carbonate crusts at cold seeps. *Earth and Planetary Science Letters* **203**(1), 195-203.

Barry J. P., Greene H. G., Orange D. L., Baxter C. H., Robison B. H., Kochevar R. E., Nybakken J. W., Reed D. L., and McHugh C. M. (1996) Biologic and geologic characteristics of cold seeps in Monterey bay, California. *Deep-Sea Research Part I-Oceanographic Research Papers* **43**(11-12), 1739-&.

Barry J. P., Kochevar R. E., and Baxter C. H. (1997) The influence of pore-water chemistry and physiology on the distribution of vesicomyid clams at cold seeps in Monterey Bay: Implications for patterns of chemosynthetic community organization. *Limnology and Oceanography* **42**(2), 318-328.

Bian L. Q., Hinrichs K. U., Xie T. M., Brassell S. C., Iversen H., Fossing H., Jorgensen B. B., and Hayes J. M. (2001) Algal and archaeal polyisoprenoids in a recent marine sediment: Molecular isotopic evidence for anaerobic oxidation of methane. *Geochemistry Geophysics Geosystems* **2**, U1-U22.

Blumenberg M., Seifert R., Reitner J., Pape T., and Michaelis W. (2004) Membrane lipid patterns typify distinct anaerobic methanotrophic consortia. *Proceedings of the National Academy of Sciences of the United States of America* **101**(30).

Boetius A., Ravenschlag K., Schubert C., Rickert D., Widdel F., Gieseke A., Amann R., Jørgensen B. B., Witte U., and Pfannkuche O. (2000) A marine microbial consortium apparently mediating anaerobic methane of oxidation. *Nature* **407**, 623-626.

Boetius A. and Suess E. (2004) Hydrate Ridge: a natural laboratory for the study of microbial life fueled by methane from near-surface gas hydrates. *Chemical Geology* **205**(3-4), 291-310.

Bohrmann G., Greinert J., Suess E., and Torres M. (1998) Authigenic carbonates from the Cascadia subduction zone and their relation to gas hydrate stability. *Geology* **26**(7), 647-650.

Bussmann I., Dando P. R., Niven S. J., and Suess E. (1999) Groundwater seepage in the marine environment: role for mass flux and bacterial activity. *Marine Ecology-Progress Series* **178**, 169-177.

Çifçi G., Dondurur D., and Ergün M. (2003) Deep and shallow structures of large pockmarks in the Turkish shelf, Eastern Black Sea. *Geo-Marine Letters* **23**(3-4), 311-322.

Dando P. R. and Hovland M. (1992) Environmental-Effects of Submarine Seeping Natural-Gas. *Continental Shelf Research* **12**(10), 1197-&.

De Rosa M. and Gambacorta A. (1988) The lipids of archaebacteria. *Progress in Lipid Research* **27**, 153-175.

Diaz-del-Rio V., Somoza L., Martinez-Frias J., Mata M. P., Delgado A., Hernandez-Molina F. J., Lunar R., Martin-Rubi J. A., Maestro A., Fernandez-Puga M. C., Leon R., Llave E., Medialdea T., and Vazquez J. T. (2003) Vast fields of hydrocarbon-derived carbonate chimneys related to the accretionary wedge/olistostrome of the Gulf of Cadiz. *Marine Geology* **195**(1-4), 177-200.

Elvert M., Boetius A., Knittel K., and Jorgensen B. B. (2003) Characterization of specific membrane fatty acids as chemotaxonomic markers for sulfate-reducing bacteria involved in anaerobic oxidation of methane. *Geomicrobiology Journal* **20**(4), 403-419.

Elvert M., Greinert J., Suess E., and Whiticar M. J. (2001) Carbon isotopes of biomarkers derived from methane-oxidizing microbes at Hydrate Ridge, Cascadia convergent

margin. In *Natural gas hydrates: Occurrence, distribution, and dynamics*, Vol. 124 (ed. C. K. Paull and W. P. Dillon), pp. 115-129. American Geophysical Union.

Elvert M., Hopmans E. C., Boetius A., and Hinrichs K.-U. (submitted) Spatial variatons of archaeal-bacterial assambladges in gas hydrate bearing sediments at a cold seep: Implications from a high resolution molecular and isotopic approach.

Elvert M., Suess E., and Whiticar M. J. (1999) Anaerobic methane oxidation associated with marine gas hydrates: superlight C-isotopes from saturated and unsaturated C_{20} and C_{25} irregular isoprenoids. *Naturwissenschaften* **86**(6), 295-300.

Garcia-Garcia A., Garcia-Gil S., and Vilas F. (2003) Monitoring the Spanish gas fields in the Ria de Vigo (1991-2001). *Geo-Marine Letters* **23**(3-4), 200-206.

Hinrichs K.-U. and Boetius A. (2002) The anaerobic oxidation of methane: New insights in microbial ecology and biogeochemistry. In *Ocean Margin Systems* (ed. G. Wefer, D. Billett, and D. Hebbeln), pp. 457-477. Springer-Verlag, Berlin.

Hinrichs K.-U., Hayes J. M., Sylva S. P., Brewer P. G., and DeLong E. F. (1999) Methane-consuming archaebacteria in marine sediments. *Nature* **398**, 802-805.

Hinrichs K. U., Summons R. E., Orphan V., Sylva S. P., and Hayes J. M. (2000) Molecular and isotopic analysis of anaerobic methane-oxidizing communities in marine sediments. *Organic Geochemistry* **31**(12), 1685-1701.

Hoehler T. M. and Alperin M. J. (1996) Anaerobic methane oxidation by a methanogen-sulfate reducer consortium: geochemical evidence and biogeochemical considerations. In *Microbial Growth on C_1 Compounds* (ed. M. E. Lidstrom and F. R. Tabita), pp. 326-333. Kluwer Academic Publishers.

Hoehler T. M., Alperin M. J., Albert D. B., and Martens C. S. (1994) Field and laboratory studies of methane oxidation in an anoxic marine sediment: Evidence for a methanogenic-sulfate reducer consortium. *Global Biogeochemical Cycles* **8**(4), 451-463.

Hovland M. (2002) On the self-sealing nature of marine seeps. *Continental Shelf Research* **22**(16), 2387-2394.

Hovland M. and Judd A. G. (1988) *Seabed Pockmarks and Seepages: Impact on Geology, Biology and the Marine Environment*. Graham & Trotman.

Hovland M. and Sommerville J. H. (1985) Characteristics of two natural gas seepages in the North Sea. *Marine and Petroleum Geology* **2**(4), 319-326.

Hovland M., Talbot M., Olaussen S., and Aasberg L. (1985) Recently formed methane-derived carbonates from the North Sea floor. In *Petroleum Geochemistry in Exploration of the Norwegian Shelf* (ed. B. M. Thomas), pp. 263-266. Norwegian Petroleum Soc., Graham & Trotman.

Hovland M., Talbot M. R., Qvale H., Olaussen S., and Aasberg L. (1987) Methane-Related Carbonate Cements in Pockmarks of the North-Sea. *Journal of Sedimentary Petrology* **57**(5), 881-892.

Joye S. B., Boetius A., Orcutt B. N., Montoya J. P., Schulz H. N., Erickson M. J., and Lugo S. K. (2004) The anaerobic oxidation of methane and sulfate reduction in sediments from Gulf of Mexico cold seeps. *Chemical Geology* **205**(3-4), 219-238.

Judd A. G. (2003) The global importance and context of methane escape from the seabed. *Geo-Marine Letters* **23**(3-4), 147-154.

Kane M. D., Poulsen L. K., and Stahl D. A. (1993) Monitoring the Enrichment and Isolation of Sulfate-Reducing Bacteria by Using Oligonucleotide Hybridization Probes Designed from Environmentally Derived 16s Ribosomal-Rna Sequences. *Applied and Environmental Microbiology* **59**(3), 682-686.

Knittel K., Boetius A., Lemke A., Eilers H., Lochte K., Pfannkuche O., Linke P., and Amann R. (2003) Activity, distribution, and diversity of sulfate reducers and other bacteria in

sediments above gas hydrate (Cascadia margin, Oregon). *Geomicrobiology Journal* **20**(4), 269-294.

Knittel K., Losekann T., Boetius A., Kort R., and Amann R. (2005) Diversity and distribution of methanotrophic archaea at cold seeps. *Applied and Environmental Microbiology* **71**(1), 467-479.

Koga Y., Nishihara M., Morii H., and Akagawa-Matsushita M. (1993) Ether polar lipids of methanogenic bacteria: Structures, comparative aspects, and biosyntheses. *Microbiological Reviews* **57**(1), 164-182.

Kohnen M. E. L., Schouten S., Sinninghé Damste J. S., de Leeuw J. W., Merritt D. A., and Hayes J. M. (1992) Recognition of paleobiochemicals by a combined molecular sulfur and isotope geochemical approach. *Science* **256**, 358-362.

Lane D. J., Pace B., Olsen G. J., Stahl D. A., Sogin M. L., and Pace N. R. (1985) Rapid-Determination of 16s Ribosomal-Rna Sequences for Phylogenetic Analyses. *Proceedings of the National Academy of Sciences of the United States of America* **82**(20), 6955-6959.

Massana R., Murray A. E., Preston C. M., and DeLong E. F. (1997) Vertical distribution and phylogenetic characterization of marine planktonic Archaea in the Santa Barbara Channel. *Applied and Environmental Microbiology* **63**(1), 50-56.

Michaelis W., Seifert R., Nauhaus K., Treude T., Thiel V., Blumenberg M., Knittel K., Gieseke A., Peterknecht K., Pape T., Boetius A., Amann R., Jorgensen B. B., Widdel F., Peckmann J. R., Pimenov N. V., and Gulin M. B. (2002) Microbial reefs in the Black Sea fueled by anaerobic oxidation of methane. *Science* **297**(5583), 1013-1015.

Mills H. J., Hodges C., Wilson K., MacDonald I. R., and Sobecky P. A. (2003) Microbial diversity in sediments associated with surface-breaching gas hydrate mounds in the Gulf of Mexico. *Fems Microbiology Ecology* **46**(1), 39-52.

Moss C. W. and Lambert-Fair M. A. (1989) Location of Double Bonds in Monounsaturated Fatty Acids of Campylobacter cryaerophila with Dimethyl Disulfide Derivatives and Combined Gas Chromatography-Mass Spectrometry. *JOURNAL OF CLINICAL MICROBIOLOGY* **27**(7), 1467-1470.

Muyzer G., Teske A., Wirsen C. O., and Jannasch H. W. (1995) Phylogenetic-Relationships of Thiomicrospira Species and Their Identification in Deep-Sea Hydrothermal Vent Samples by Denaturing Gradient Gel-Electrophoresis of 16s Rdna Fragments. *Archives of Microbiology* **164**(3), 165-172.

Nauhaus K., Boetius A., Kruger M., and Widdel F. (2002) In vitro demonstration of anaerobic oxidation of methane coupled to sulphate reduction in sediment from a marine gas hydrate area. *Environmental Microbiology* **4**(5), 296-305.

Nauhaus K., Treude T., Boetius A., and Kruger M. (2005) Environmental regulation of the anaerobic oxidation of methane: a comparison of ANME-I and ANME-II communities. *Environmental Microbiology* **7**(1), 98-106.

Nichols P. D., Guckert J. B., and White D. C. (1986) Determination of monounsaturated fatty acid double-bond position and geometry for microbial monocultures and complex consortia by capillary GC-MS of their dimethyl disulphide adducts. *Journal of Microbiological Methods* **5**, 49-55.

Orphan V. J., Hinrichs K. U., Ussler W., Paull C. K., Taylor L. T., Sylva S. P., Hayes J. M., and Delong E. F. (2001a) Comparative analysis of methane-oxidizing archaea and sulfate- reducing bacteria in anoxic marine sediments. *Applied and Environmental Microbiology* **67**(4), 1922-1934.

Orphan V. J., House C. H., Hinrichs K. U., McKeegan K. D., and DeLong E. F. (2001b) Methane-consuming archaea revealed by directly coupled isotopic and phylogenetic analysis. *Science* **293**(5529), 484-487.

Orphan V. J., House C. H., Hinrichs K. U., McKeegan K. D., and DeLong E. F. (2002) Multiple archaeal groups mediate methane oxidation in anoxic cold seep sediments. *Proceedings of the National Academy of Sciences of the United States of America* **99**(11), 7663-7668.

Orphan V. J., Ussler W., Naehr T. H., House C. H., Hinrichs K. U., and Paull C. K. (2004) Geological, geochemical, and microbiological heterogeneity of the seafloor around methane vents in the Eel River Basin, offshore California. *Chemical Geology* **205**(3-4), 265-289.

Peckmann J., Goedert J. L., Thiel V., Michaelis W., and Reitner J. (2002) A comprehensive approach to the study of methane-seep deposits from the Lincoln Creek Formation, western Washington State, USA. *Sedimentology* **49**(4), 855-873.

Peckmann J., Paul J., and Thiel V. (1999) Bacterially mediated formation of diagenetic aragonite and native sulfur in Zechstein carbonates (Upper Permian, Central Germany). *Sedimentary Geology* **126**(1-4), 205-222.

Pernthaler A., Preston C. M., Pernthaler J., DeLong E. F., and Amann R. (2002) Comparison of fluorescently labeled oligonucleotide and polynucleotide probes for the detection of pelagic marine bacteria and archaea. *Applied and Environmental Microbiology* **68**(2), 661-667.

Ravenschlag K., Sahm K., Pernthaler J., and Amann R. (1999) High bacterial diversity in permanently cold marine sediments. *Applied and Environmental Microbiology* **65**(9), 3982-3989.

Reeburgh W. S. (1996) "Soft spots" in the global methane budget. In *Microbial Growth on C_1 Compounds* (ed. M. E. Lidstrom and F. R. Tabita), pp. 334-342. Kluwer Academic Publishers.

Roberts H. H. and Aharon P. (1994) Hydrocarbon-Derived Carbonate Buildups of the Northern Gulf-of-Mexico Continental-Slope - a Review of Submersible Investigations. *Geo-Marine Letters* **14**(2-3), 135-148.

Schouten S., Hoefs M. J. L., Koopmans M. P., Bosch H.-J., and Sinninghe Damsté J. S. (1998) Structural characterization, occurrence and fate of archael ether-bound acyclic and cyclic biphytanes and corresponding diols in sediments. *Organic Geochemistry* **29**(5-7), 1305-1319.

Schouten S., Hopmans E. C., Schefuss E., and Damste J. S. S. (2002) Distributional variations in marine crenarchaeotal membrane lipids: a new tool for reconstructing ancient sea water temperatures? *Earth and Planetary Science Letters* **204**(1-2), 265-274.

Teske A., Hinrichs K. U., Edgcomb V., Gomez A. D., Kysela D., Sylva S. P., Sogin M. L., and Jannasch H. W. (2002) Microbial diversity of hydrothermal sediments in the Guaymas Basin: Evidence for anaerobic methanotrophic communities. *Applied and Environmental Microbiology* **68**(4), 1994-2007.

Thiel V., Peckmann J., Richnow H. H., Luth U., Reitner J., and Michaelis W. (2001) Molecular signals for anaerobic methane oxidation in Black Sea seep carbonates and a microbial mat. *Marine Chemistry* **73**(2), 97-112.

Thomsen T. R., Finster K., and Ramsing N. B. (2001) Biogeochemical and molecular signatures of anaerobic methane oxidation in a marine sediment. *Applied and Environmental Microbiology* **67**(4), 1646-1656.

Thrasher J., Fleet S. J., Hovland M., and Düppenbecker S. (1996) Understanding geology as the key to using seepage in exploration: spectrum of seepage styles. In *Hydrocarbon migration and its near-surface expression* (ed. D. Schumacher and M. A. Abrams), pp. 223-241. AAPG Memoir.

Treude T., Boetius A., Knittel K., Wallmann K., and Jorgensen B. B. (2003) Anaerobic oxidation of methane above gas hydrates at Hydrate Ridge, NE Pacific Ocean. *Marine Ecology-Progress Series* **264**, 1-14.

Treude T., Niggemann J., Kallmeyer J., Wintersteller P., Schubert C. J., Boetius A., and Jorgensen B. B. (2005) Anaerobic oxidation of methane and sulfate reduction along the Chilean continental margin. *Geochimica et Cosmochimica Acta* **69**(11), 2767-2779.

Widdel F. and Bak F. (1992) The gram negative mesophilic sulfate reducing bacteria. In *The prokaryotes* (ed. M. Dworkin). Springer.

Final discussion and conclusion

PREFACE

In this thesis, a variety of different cold seep systems were investigated in three oceanic regions (Fig 1). The focus was on methane turnover at mud volcanoes (MVs) and coastal gas seeps, which have not been investigated before with regard to their geomicrobiology. The studies presented here combined biogeochemical, microbiological and geological tools for a system-oriented investigation of those methane seeps. Major aims were to detect and to quantify hot spots of methane oxidation as well as to assess environmental factors determining the activity and the distribution of methanotrophic communities. Furthermore, key microbial players mediating methanotrophy were identified and the impact of the anaerobic oxidation of methane (AOM) and the aerobic oxidation of methane (MOx) on the surrounding, marine environment was analysed. The studies were carried out at:

- The highly active Håkon Mosby Mud Volcano (HMMV)
- Quiescent mud volcanoes of the Gulf of the Cadiz
- The Tommeliten gas seeps

In the first part of the final discussion, the magnitude of turnover rates and environmental factors determining the distribution of AOM and MOx are summarized. Furthermore, the dependency of methanotrophic activity and concentrations of diagnostic lipid biomarkers are discussed. The second part focuses on the identity of methanotrophic communities and diagnostic lipid signatures expressed by the key microbial players. The third part investigates how methanotrophic activity changes a marine habitat. The last section of gives an outlook on further research questions.

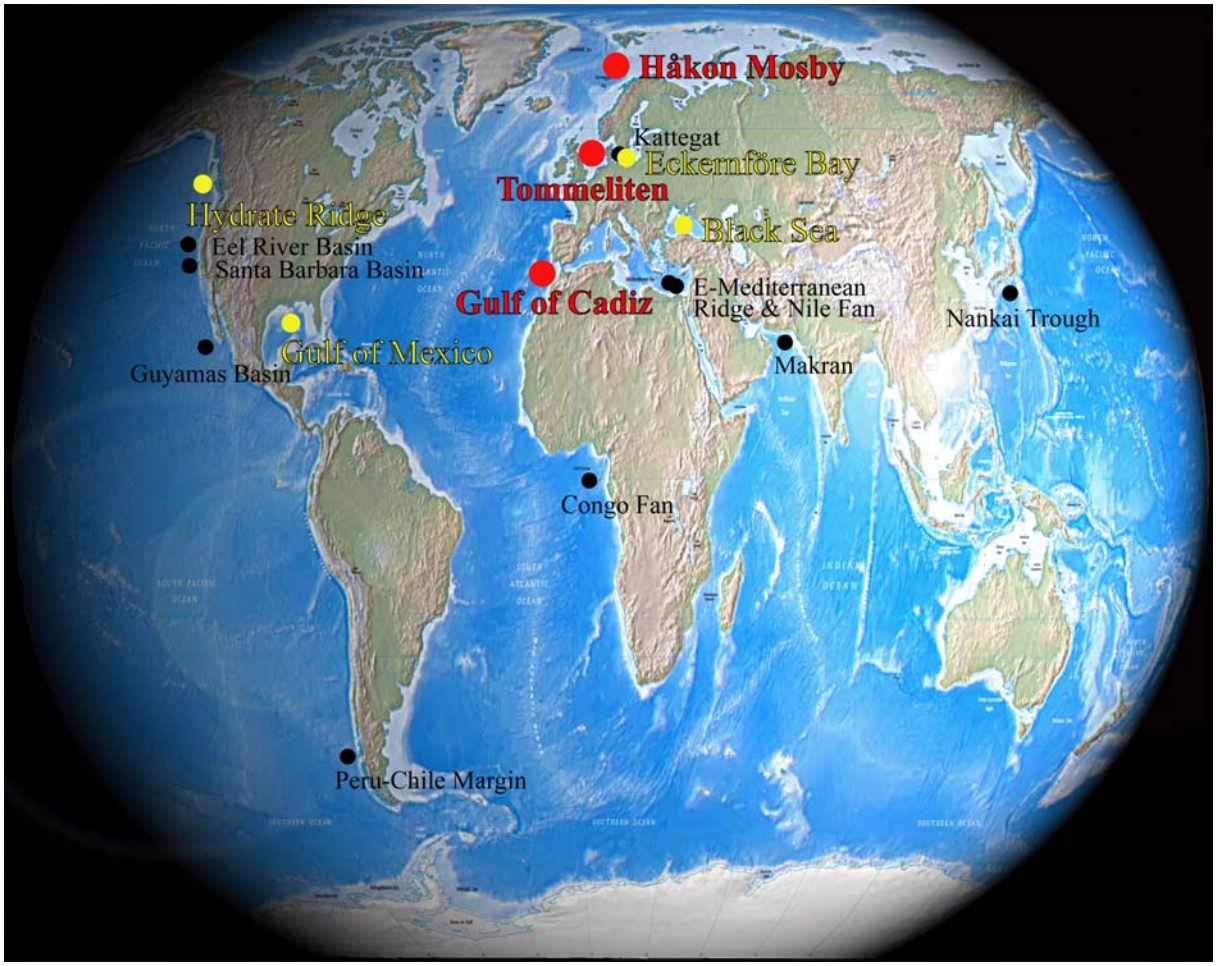

Figure 1. Selected cold seeps in the world oceans. Locations investigated in this thesis are indicated in red. Other seep locations with known identities and activities of the key methanotrophs are highlighted in yellow. Black dots denote seeps where either key methanotrophs and/or activities have not been fully determined yet.

1. METHANE OXIDATION RATES IN DIFFERENT MARINE HABITATS

The average turnover rates of methane in different habitats are illustrated in Figure 2. The magnitude of AOM and MOx as well as the main characteristics of the investigated habitats are shown in Table 1. On average, methane turnover rates varied by 2 orders of magnitude within the AOM and MOx zones in the investigated areas. The end member with the highest fluid flow rates was the HMMV. Here, AOM and MOx consume 22 – 55 % ($7 * 10^{-5}$ Tg yr^{-1}) of the estimated methane efflux (Chapter 2, 4). The magnitude of AOM at HMMV is

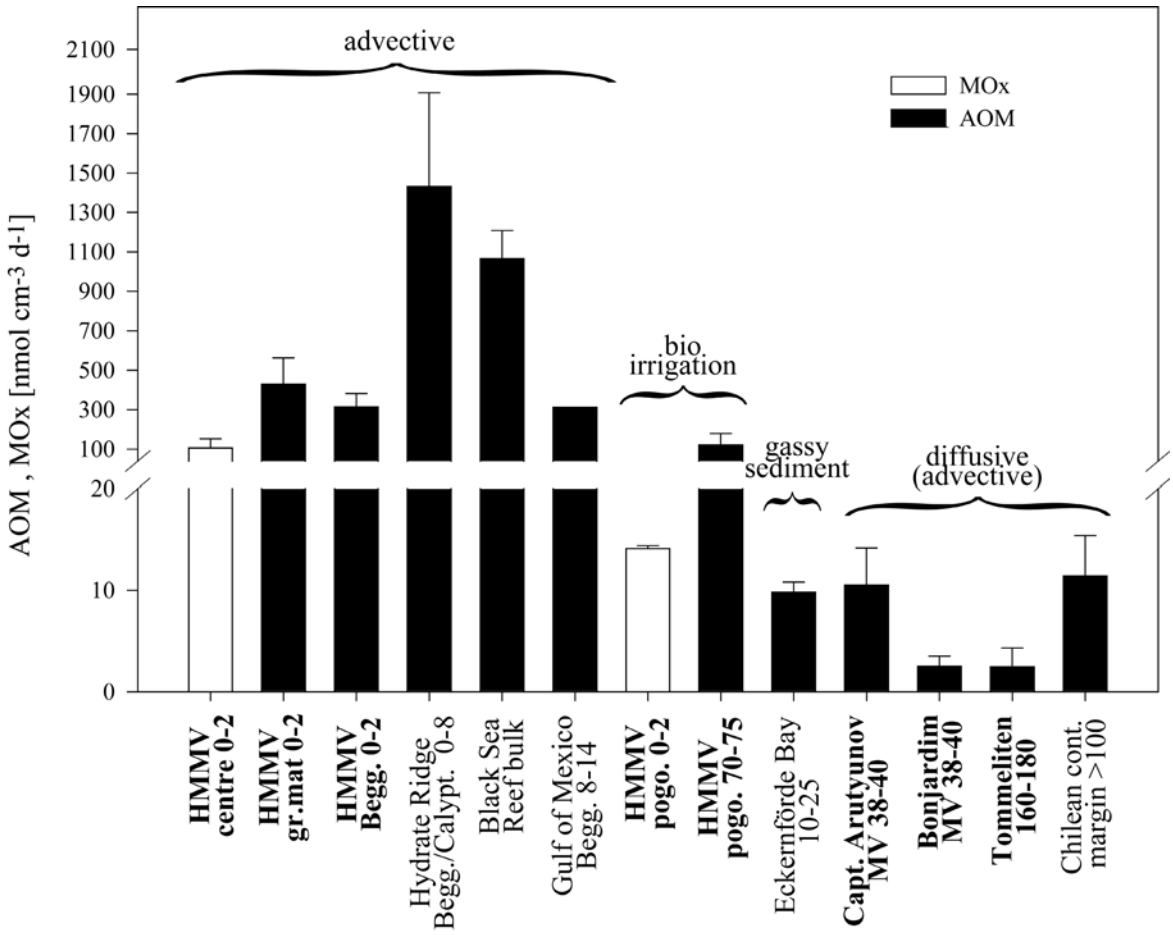

Figure 2. Mean methane turnover rates at the hot spots of AOM and MOx at methane-rich habitats. The dominant modes of substrate transport and the depth interval of maximum rates are indicated. Habitats investigated in this thesis are highlighters in bold face type. Data from Hydrate Ridge, the Black Sea, Eckernförde Bay and the Chilean continental margin are modified from Treude (2003). Data from the Gulf of Mexico are modified after Joye et al. (2004).

comparable to other highly active seep systems such as Hydrate Ridge, the Gulf of Mexico and the Black Sea where areal AOM of up to 35 mol m^{-2} yr^{-1} and maximum rates of 1.4 µmol cm^{-3} d^{-1} were detected. On average, AOM was estimated to consume 60 % of the methane at sites of Hydrate Ridge with the highest flux rates (Treude et al., 2003). The Gulf of Cadiz mud volcanoes investigated in this thesis (Chapter 5) showed a low or medium range activity. Areal AOM rates at Capt. Arutyunov and Bonjardim MV were substantially lower compared

Table 1. Charcteristics of methane-rich habitats

Location	Methane origin	Habitat	Methane transport	Methane ox. mode	‡Methane disappearance [cm]	‡Sulphate penetration [cm]	AOM, MOx hot spot [cm]	Areal AOM,MOx [mol m^{-2} yr^{-1}]	Methane fluxes [mol m^{-2} yr^{-1}]
HMMV	mixed	centre	advective	MOx	na*	8-20	0-2	1.7	na
	microbial	gr. mat	advective	AOM	na*	>20	0-20	12.4	na
	thermogenic	Beggiatoa	advective	AOM	na*	3-15	0-5	4.5	na
		Pogo. surface	bioventilation	MOx	low conc.+			0.22	na
		Pogo. subsurface	bioventilation	AOM	30-50	ca. 80	70-75	7.1	na
Hydrate Ridge	thermogenic	Beggiatoa	advective	AOM	na*	ca. 4	0-10	2-36	5-7
		Calyptogena	advective	AOM	na*	8	2-5	20	na
		Acharax	diffusive (advective)	MOx	low conc.+	>10	0-5	0.8	na
Gulf of Mexico	thermogenic	Beggiatoa	advective	AOM	0-13	2-10	8-14	2-5	na
Eckernförde Bay	microbial	gassy sediment	diffusive (advective)	AOM	0-5	30	20-25	0.1-0.5	0.2-05
Capt. Arutyunov MV	thermogenic	centre	diffusive (advective†)	AOM	25	75	25-40	0.4	0.4
Bonjardim MV	thermogenic	centre	diffusive (advective†)	AOM	50	75	45-70	0.04	0.07
Ginsburg MV	na	centre	diffusive (advective†)	AOM	20	>140	15-50	na	0.06
Gemeni MV	na	centre	diffusive (advective†)	AOM	70	100	70-90	na	0.02
No Name MV	na	centre	diffusive†	AOM	200	275	200-350	na	0.03
Tommeliten	thermogenic	gas seep	diffusive	AOM	150	>250	155-175	na	na
Chilean cont margin	microbial		diffusive	AOM	>110	>150	>115	0.1-2	<0.1

†advective flux components are presently unquantified (Hensen pers. com.), ‡methane disappearance and sulphate penetration depth were estimated from ex istu data. *the depth of methane disappearance could not be determined due to gas ebullition during core retrieval. +Methane concentrations were <0.05 mM.
Data from hydrate Ridge the Guf of Mexico, Eckernförde Bay and the Chilean continental margin were modified from Treude (2003). Data from the Gulf of Mexico were modifeid from Joye et al. (2004).

to HMMV but higher than those in diffusion dominated ocean sediments with AOM rates <0.06 mol m^{-2} yr^{-1} (Hensen et al., 2003; Jørgensen et al., 2001; Niewöhner et al., 1998). These values are comparable to Ginsburg MV Gemini MV and the "No Name" structure.

AOM at the Tommeliten seep area (Chapter 6) is very low and comparable to the gassy sediments of Eckernförde Bay and some diffusive systems at the Chilean continental margin where maximum rates of <0.01 µmol cm^{-3} d^{-1} were measured (Treude, 2003).

Today, less is known on MOx rates than on AOM in gassy sediments. The MOx rates in surface sediments of the centre at HMMV (Chapter 2, 4) are to our knowledge among the highest ever measured in marine sediments. However, since the penetration depth of oxygen into the sediment was limited to a few millimetres (de Beer et al., submitted), the MOx zone was very small, as was the proportion of total methane consumed by MOx.

MOx at HMMV's centre was >1.5-fold higher in comparison to oxygenated surface sediments of a methane seep in the Baltic Sea (Jensen et al., 1992) and in low-flux seep sediments at Hydrate Ridge which are populated by the ventilating bivalve *Acharax* (Treude et al., 2003).

1.1 Environmental Factors Determining Methane Turnover

Generally, the AOM rates correlate with the methane flux (Tab.1). At HMMV (Chapter 2, 4), the high methane oxidation rates associated with the mats of sulphide oxidizing bacteria (*Beggiatoa* site) are supported by high rates of methane flow from deeper sediment layers. The deeper penetration depth of sulphate at the grey mat areas supported a 2-fold higher

AOM activity compared to the *Beggiatoa* site, indicating the relevance of the availability of electron acceptors. At the *Pogonophora* site, high AOM rates were found just beneath the roots of the worms (Fig. 2, Tab. 1, Chapter 4). Here, fluid flow is relatively small and methane is sequestered as clathrate in the sediment below 100 cm bsf. The bioirrigation activities of the worms pump sulphate to the methane-bearing sediment layers thereby fostering a high AOM activity. In contrast, AOM was substantially lower at the mud volcanoes in the Gulf of Cadiz and at the Tommeliten seep area (Fig. 2, Tab.1, Chapter 5, 6). Although no advective fluxes were estimated for Capt. Arutyunov and Bonjardim MV, the good agreement of AOM and diffusive methane fluxes indicate that the advective flux is within the same order of magnitude as the diffusive transport component.

Increasing methane concentrations during *in vitro* incubations had a positive effect on MOx and AOM activity (Nauhaus et al., 2002; Nauhaus et al., 2005; Chapter 4). AOM is the reaction of the electron donor methane with the electron acceptor sulphate (Barnes and Goldberg, 1976; Iversen and Jørgensen, 1985; Nauhaus et al., 2002; Nauhaus et al., 2005; Treude et al., 2003). This thesis and previous work (Treude, 2003; Treude et al., 2003) provide evidence that AOM hotspots are found where both substrates are available at milimolar concentrations. If either methane or sulphate is depleted, other processes take over. For example, the central area of HMMV is dominated by MOx because upward fluid flow rates of 4 μm s^{-1} limit the penetration depth of sulphate to the top few millimetres where it co-occurs with oxygen (de Beer et al., submitted). These are unfavourable conditions for AOM but allow for comparably high MOx rates. Similarly, bioirrigation of pogonophoran worms lead to an oxygen penetration depth of up to 10 cm sediment depth, which supports MOx but excludes AOM in this horizon (de Beer et al., submitted; Chapter 2, 4).

An additional factor that controls the magnitude of methane turnover rates is the biomasses of AOM and MOx communities. At Tommeliten, the magnitude of AOM (2.4 nmol cm^{-3} d^{-1}) and the abundance of ANME-1 cells (1.45 * 10^7 cells cm^{-3}) correspond to a cell specific rate of 0.17 fmol d^{-1} (Chapter 6). This value is in good agreement with highly active seeps such as Hydrate Ridge and the Black Sea which have much higher population densities of methanotrophs (Nauhaus et al., 2002; Nauhaus et al., 2005; Treude et al., 2003). A correlation between AOM rates and cell counts of methanotrophs is also present on a smaller scale, i.e. within the core. The vertical profiles of ANME-1 cell counts at Tommeliten and counts of microbial aggregates consisting of ANME-3 and sulphate reducing bacteria (SRB) of the *Desulfobulbus* (DBB) group matched the vertical distribution of AOM activity at Tommeliten and HMMV, respectively. Similarly, highest counts of the type I methanotroph *Methylobacter sp.* coincided with peaks in MOx activity at the centre of HMMV.

1.2 Hot Spots of AOM and MOx

Within the seabed, the hot spot of AOM and MOx were restricted to a few cm in the investigated sites (Tab. 1). The dimension of these zones of maximum methane turnover was controlled by (1) fluid flow, (2) bioirrigation activities, (3) diffusion and by (4) sedimentology. At the vertical boundaries of the hot spots, AOM and MOx most probably become unfavourable due to thermodynamic limitations.

(1) Fluid and/or gas flow is a defining characteristic of cold seep geosystems (Boetius and Suess, 2004; Judd et al, 2002). At sites of high fluid and/or gas flow, sediments are often covered by thiotrophic bacteria (Barry et al., 1996; Torres et al., 2002; Tryon et al., 2002) indicating elevated rates of chemoautotrophic metabolism fuelled by the upward flux of

electron donors (Boetius et al., 2000; Joye et al., 2004; Treude et al., 2003). However, with respect to the chemical composition of fluids and/or gases, high flow rates may also hinder the influx of electron acceptors such as sulphate, oxygen and nitrate, thus limiting microbial activity to near surface sediments. At HMMV, fluid flow and bioirrigation activities are dominant factors controlling the vertical distribution of AOM and MOx. Hot spots of MOx activity were generally restricted to the top mm surface sediments due to oxygen limitations. The thickness of the MOx hot spot at the centre of HMMV is controlled by fluid flow. Here, a pore water flow velocity of 4 μm s^{-1} restricts the *in situ* penetration depth of oxygen to about 2 - 3 mm (de Beer et al., submitted) allowing for comparably high MOx rates. These high upward fluid flow rates also restrict the penetration depth of sulphate to a few centimetres into the sediment at the *Beggiatoa* site, thus limiting AOM to the top of the seafloor due to thermodynamic limitations. Unfortunately, *in situ* concentrations of AOM-reactants are unknown, thus prohibiting further analysis of thermodynamics. At the grey mat sites, the overlap of sulphate and methane over a larger depth interval allows for a comparably broad AOM zone. The reason for the deeper penetration depth of sulphate in these patches of 1-2 m in diameter remains unknown.

(2) Benthic animals can play an important role in the biogeochemical zonation by activities like dwelling, burrowing and bioventilation. At cold seeps, a variety of symbiotic chemosynthetic animals may occur which are adapted to transport sulphide and/or methane as well as oxygen to their symbionts. The most important groups are vestimetiferan and pogonophoran tubeworms, and the bivalves *Calyptogena*, *Acharax* and *Bathymodiolus* (Cordes et al., 2005; Sahling et al., 2002; Treude et al., 2003). At the HMMV, the most abundant chemosynthetic animals are two types of pogonophoran tubeworms (*Oligobrachia haakonmosbiensis*, *Sclerolinum contortum*; Smirnov, 2000). The larger species (*O. haakonmosbiensis*) form up to 60 cm long but thin (~1 mm) tubes and transports oxygen

and sulphate into methane rich sediments. The thickness of the MOx horizon at the *Pogonophora* site is controlled by the irrigation activities of the worms, which oxygenate the upper 10 cm of the sediment. The AOM horizon is also controlled by the bioirrigation activities of the worms, indicated by its position directly below the lower end of the tubes (> 60 cm sediment depth). Bioirrigation activities of macrofauna organisms irrigating methane-rich sediments with sulphate, thereby fueling AOM, were also reported from Hydrate Ridge and the Gulf of Mexico (Cordes et al., 2005; Sahling et al., 2002; Treude et al., 2003).

(3) Diffusion controlled methane-rich sediments generally show the lowest methane turnover and methanotrophic biomasses (Treude, 2003; Treude et al., 2005). Diffusion rather than advection was the dominant factor controlling the fluxes of methane and sulphate at the MVs of the Gulf of Cadiz. The depth of the sulphate methane transition zones (SMTs) at the studied mud volcanoes in the Gulf of Cadiz was matching the magnitude of methane fluxes (Tab. 1). At Capt. Arutyunov MV where the highest methane flux was encountered, the SMT was at about 30 cm bsf, whereas at the "No Name" structure, the methane flux was 10-fold lower and the SMT was at about 275 cm bsf. As an example of energy availability in diffusion controlled systems, a simplified, high-resolution ΔG profile from methane, sulphate and sulphide concentrations is calculated according to the following reactions:

$$CH_{4\,(aq)} + 3H_2O_{\,(l)} \rightarrow HCO_3^-{}_{(l)} + 4H_{2\,(aq)} + H^+_{(aq)} \quad (1)$$

$$SO_4^{2-}{}_{(aq)} + 4H_{2\,(aq)} + H^+_{(aq)} \rightarrow HS^-{}_{(aq)} + 4H_2O_{\,(l)} \quad (2)$$

Single ΔG values were calculated with the program Thermodyn© and concentrations of protons (10 nM), DIC (10 mM) and H_2 (0.1 pM) were assumed without any changes over depth. The ΔG profile roughly follows the vertical distribution of AOM (Fig. 3). Background values of methane at the sediment surface (0-10 cm) make AOM unfavourable with

ΔG-values of ca -10 kJ mol^{-1}. At the hot spot of AOM, ΔG decreases to a minimum of about -26 kJ mol^{-1} and then increases with depth due to sulphate limitations and increasing sulphide concentrations.

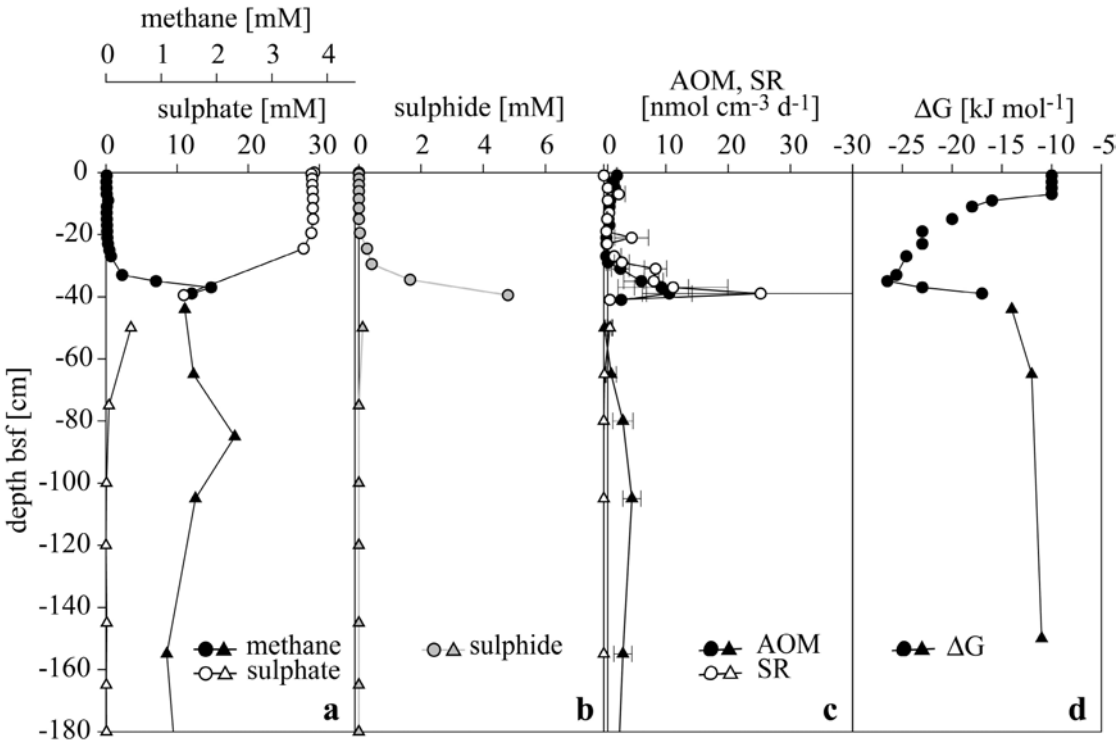

Figure 3. Geochemical gradients in sediments of Capt. Arutyunov MV. (a) Methane and sulphate, (b) sulphide, (c) AOM and SR rates, (d) free energy yield of AOM. Circles and triangles denote multi-core and gravity core samples, respectively.

(4) The sedimentology of a site can influence pathways of methane flow, both for free as well as dissolved gas. Some sediments like marl act as barriers to methane flux. An example is Tommeliten where the depth of the methane transition zone is controlled by the sedimentary regime. At Tommeliten, subsurface methane pressure was observed to lift a marl horizon developing dome-like structures visible in acoustic sediment imaging. Methane advects most probably through cracks of this marl horizon into overlying clay-silt sediments. At the interface of the clay-silt to overlying sandy sediments, methane is consumed in a defined SMT. This AOM hot spot was found to follow the depth of the marl horizon.

1.3 Correlating Distribution of Microbial and Geochemical Signatures in Marine Sediments.

The investigated habitats can be divided into two categories according to the location of the hot spot of methane turnover in (1) surface or (2) subsurface sediment horizons (Fig. 4). The first category encompasses the centre, *Beggiatoa* and grey mat site of HMMV. The *Pogonophora* site with its deep AOM hotspot as well as the studied mud volcanoes in the Gulf of Cadiz and the Tommeliten pockmarks represent the second category.

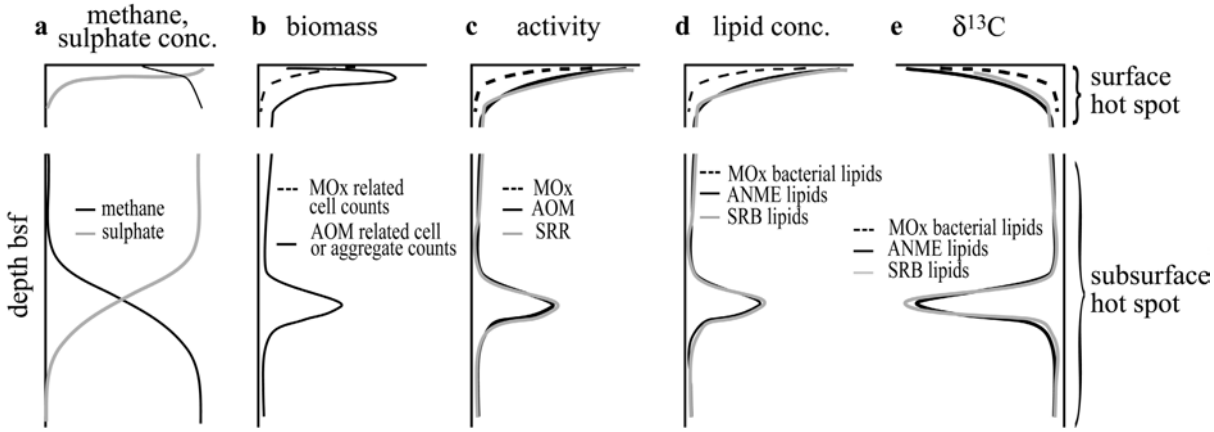

Figure 4. Scheme of the vertical distribution of (a) methane and sulphate concentrations, (b) methanotrophic biomass, (c) AOM, SRR and MOx activity, (d) diagnostic archaeal and bacterial lipid concentrations and (e) their associated $\delta^{13}C$-values in methane bearing habitats. The upper and lower sections illustrate a methanotrophic hot spot in surface and subsurface sediments, respectively.

A surface AOM hot spot characterized by high methane and sulphate concentrations, coinciding peaks in methane and sulphate turnover, biomarker and cell counts was first described at Hydrate Ridge (Boetius et al., 2000; Elvert et al., submitted; Treude, 2003; Treude et al., 2003). The biomass of key microbial players (Fig. 4b), methane turn over rates (Fig. 4c), concentrations of membrane lipids specific for the key microbial players (Fig. 4d) and their associated $\delta^{13}C$-values (Fig. 4e) showed a matching vertical distribution. Hence, an

increase in AOM and MOx biomass appears to be associated to elevated methane turn over rates (see section 1.1) as well as to elevated lipid biomarker concentrations and depleted isotope signatures. With respect to the data presented in this work and those available in the literature, the correlation of these parameters needs further investigation for quantitative estimates. Cell specific lipid concentrations are available from only three habitats, i.e., Tommeliten (ANME-1 dominated; chapter 6), Hydrate Ridge (ANME-2 dominated; Elvert et al., submitted) and from HMMV (ANME-3 dominated; chapter 3). Here, the cell specific values of for instance archaeol were: 20 fg (Tommeliten), 0.25 fg (Hydrate Ridge) and 3.7 fg (HMMV). In previous works, biomarker analyses and cell counts were usually not carried out on the same sample but on replicate samples from one core or even replicate cores. As both methods are very time consuming, the data are usually based on single measurements and not averages of replicates. Hence, there is an additional error associated with both sets of data since the methods do not account for small-scale heterogeneity.

One other interesting observation is the distinct minimum in $\delta^{13}C$ of lipid biomass associated with the maximum activity (Fig. 4c, e). Subsurface AOM hot spots usually coincide with the methane-sulphate transition zone (Iversen and Jørgensen, 1985). Here, methane with a given carbon isotope signature rises upward and is completely consumed within the hot spot. The AOM metabolism was found to discriminate against the heavy isotope ^{13}C leading to a depletion in the lipid biomass (Elvert et al., 1999; Hinrichs et al., 1999; Orphan et al., 2001b). Hence, the uprising methane becomes progressively heavier according to Raleigh distillation processes (Whiticar, 1999). This explains the enrichment of ^{13}C in the lipid biomass at the upper boundary of the AOM biomass peak at subsurface hot spots (Fig. 3e). However, the same trend was also found at the lower boundary, which cannot be explained by Raleigh distillation processes. Here, the uprising methane carries its source $\delta^{13}C$-signal. Hence, methanotrophic activity should lead to very low $\delta^{13}C$-values of the lipid biomass. However, at

the lower boundary, sulphate is limiting making AOM unfavourable. This raises the question whether the AOM community could switch from a methanotrophic to a methanogenic mode once AOM becomes unfavourable.

2. IDENTITY OF METHANOTROPHIC MICROBES

At most of the study sides investigated here, i.e., HMMV, Capt. Arutyunov MV and at Tommeliten, the microbial communities mediating AOM and MOx were identified by 16S rDNA methods combined with biomarker analysis. All known archaea mediating AOM are distantly related to methanogens of the orders *Methanosarcinales* and *Methanomicrobiales* (Knittel et al., 2005). At HMMV, a novel AOM community was discovered (Chapter 2, 4). It consists of archaea forming a distinct cluster closely related to ANME-2 and more distantly to ANME-1. Previously, a few sequences clustering with this group were detected in the Santa Barbara basin (Knittel et al., 2005; Orphan et al., 2001a). The new group was termed ANME-3. Like the ANME-2, this group often forms shell-like, dense aggregates with SRB enclosing the archaea. However, in contrast to ANME-2 which is associated with the Seep-SRB1 group (Boetius et al., 2000; Knittel et al., 2003; Knittel et al., 2005; Orphan et al., 2002), ANME-3 has been found in association with SRB of the *Desulfobulbus* group (Chapter 2, 3).

At Capt. Arutyunov MV (Gulf of Cadiz), 16S rDNA clone libraries indicate, that AOM is mediated by ANME-2 and Seep-SRB1 (Tab. 2; Chapter 5). ANME-2 / Seep-SRB1 dominated habitats were previously found in surface sediments at the cold seeps of Hydrate Ridge (Boetius et al., 2000; Boetius and Suess, 2004; Knittel et al., 2003; Knittel et al., 2005), the

Eel River and Santa Barbara Basin (Orphan et al., 2001a; Orphan et al., 2002), cold seeps at the Eckernförde Bay (Treude, 2003) and in the Black Sea (Knittel et al., 2003; Knittel et al., 2005; Michaelis et al., 2002) but also in surface sediments of the hydrothermal vents of the Guaymas Basin (Teske et al., 2002). At Tommeliten, a predominance of ANME-1 and Seep-SRB1 was found in subsurface sediments (Chapter 6). Here, ANME-1 occurred as single cells or small chains of up to three cells. ANME-1 associated with Seep-SRB1 was previously found in surface sediments at the cold seeps of the Eel River- (Hinrichs et al., 1999; Orphan et al., 2001a; Orphan et al., 2002) as well as at the hydrothermal vents at the Guaymas Basin (Teske et al., 2002), microbial mats at cold seeps of the Black Sea (Knittel et al., 2005; Middelburg et al., 2002), and carbonate crusts at the Napoli Mud Volcano (Aloisi et al., 2002). Obviously, different phylogenetic groups of archaea and SRB with some morphological variation in the form of their consortia can mediate AOM in a great variety of oceanic settings. Unfortunately, the specific environmental conditions selecting for a particular AOM community are still unknown.

In addition to AOM communities, also MOx bacteria were found at HMMV (Chapter 2, 4). These were type I methanotrophs of the *Methylobacter sp.,* belonging to the class *α-Proteobacteria*. In the HMMVs centre and in shallow sediments of the *Pogonophora* site these methanotrophs consume a significant amount of methane. The ice-cold (-1°C) ambient sea water temperature might be one parameter selecting for type I methanotrophs (Hanson and Hanson, 1996). However, in most marine sediments, oxygen and methane do not overlap, which makes MOx a minor sink of methane in marine sediments.

Table 2. Diagnostic archaeal and bacterial lipids in methane-dominated environments hosting particular groups of AOM communities

					Diagnostic archaeal lipids‡					Diagnostic bacterial lipids‡						
#	Structure, environment	Sample (depth in cm)	ANME	SRB	archaeol	*sn2*-hydroxy archaeol	croc.	PMIΔ	GDGT	i-$C_{15:0}$	ai-$C_{15:0}$	$C_{16:1\omega5}$	cy$C_{17:0\omega5,6}$	MAGE	DAGE	δ^{13}C-CH_4
1	Tommeliten [1]	sed. (155)	1a	DSS	++(-61)	+(-79)	tr	+;0-4	++(<-62)	+(-47)	++(-47)	tr	–	na	na	-46[2]
2	BS, microbial reef [3-5]	microbial mat	1b	DSS	++(-78)	+(-89)	tr(-85)	+;0-5(<-90)	++(<-91)	+(-84)	++(-79)	+(-72)	–	tr(na)	++(-80)	-65[6]
3	ER, PC26, Clam, bact. mat [7,8]	sed. (13-15)	1x	DSS	++(-100)	+(-106)	-	-	na	+(na)	++(na)	+(-76)	–	tr(-90)	+(-75)	-64[9]
4	GB, core A, Beggiatoa [10]	hyd.th.sed. (1-2)	1a,b	DSS	++(-60)	tr(na)	na	na	+?(-68)	na	na	na	na	+(-37)	++(-47)	-47[11]
5	GB, core T, Beggiatoa [10]	surf. sed. (0-2.5)	1a,b	DSS	++(-72)	++(-89)	na	na	++?(-68)	na	na	na	na	na	+(-45)	-47[11]
6	Napoli MV, MN16BT2 [12,4,5]	carbonate crust	1a,b	DSS	++(-88)	+(-91)	tr	+;0,X (-85)	++(-91)	na	na	na	na	-	++(-55)	-37[13]
7	CAMV [14]	sed. (31)	2a	DSS	+(-90)	++(-92)	na	na	na	+(-71)	+(-73)	++(-80)	++(-82)	+(ca.-75)	tr(na)	-48[15]
8	HR, Beggiatoa [16,4,5]	sed. (0-1)	2a,c	DSS	+(-114)	++(-133)	na	na	na	+(-63)	+(-75)	na	na	na	na	-67[17]
9	HR, Beggiatoa [18-21,4,5]	sed. (2-4)	2a,c	DSS	+(-120)	++(-124)	+(-119)	+;0-4(ca.-125)	+(na)	+(-69)	+(-74)	++(-80)	+(-101)	+(ca.-94)	+(ca.-95)	-67[17]
10	HR, Calyptogena [21,4,5]	sed. (4-6)	2c,a	DSS	+(-103)	++(-120)	+(-112)	+;3,4(ca.-117)	++(na)	+(-69)	+(-84)	+(-85)	+(-100)	+(ca.-87)	++(ca.-75)	-67[17]
11	BS, microbial reef [3-5]	microbial mat	2a	DSS	+(-99)	++(-102)	+(-105)	+;0-4(<-100)	tr	+(-94)	+(-88)	++(-84)	+(-85)	+(na)	+(na)	-65[6]
12	ER, PC36, Clam [22]	sed. (3-6)	2b,c	DSS	+(-101)	++(-106)	+(-92)	+;0,X(na)	na	na	na	na	na	+(-78)	+(na)	-64[9]
13	GB, core C, petroleum ooze [10]	hyd.th.sed. (0-1)	2c	DSS	+(-81)	+(-81)	na	na	-?	na	na	na	na	-	-	-47[11]
14	SBB, PC24, Calyptogena [8,22]	sed. (13-18)	2a,b	DSS	+(-119)	++(-128)	+(-119)	+;0,X	na	+(-56)	++(-58)	++(-103)	+(-114)	+(-105)	+(-110)	na
15	Kazan MV, MNLBC19 [23-25]	sed. (10-12)	2x*	DSS*	+(-95)	++(-107)	tr(na)	+;3(-87)	-	na	na	na	na	na	+(-85)	-33†[26]
16	HMMV, Beggiatoa [27,28]	sed. (0-2)	3	DSB	+(-98)	++(-107)	-	+;4,5(-105)	-	+(-65)	+(-62)	++(-71)	-	+(-80)	tr(na)	-60[29]
17	HMMV, Beggiatoa [27,30]	sed. (0-5)	3	DSB	+(-54)	++(-78)	-	+;4,5(-82)	-	+(-64)	+(-63)	++(-64)	-	-	tr(-57)	-60[29]

‡ Number of + signs designates the relative abundance of diagnostic archaeal and bacterial lipids. -signs denote the absence of a compound. Numbers in () brackets designate δ^{13}C-values vs. PDB; PMI double bond numbers are denoted by numbers; * denotes estimated identity, x indicates unknown ANME sub-cluster, † designates estimated δ^{13}C-methane value. δ^{13}C-values of MAGEs and DAGEs were averaged.

Abrevations: surf., surface; bact., bacterial; sed., sediment; hydroth., hydrothermal; MV, mud volcano;. tr, trace amounts; na, data not available

AOM environments: BS, Black Sea; ER, Eel River Basin; GB, Guaymas Basin; CAMV, Captain Arutyunov Mud Volcano; HR, Hydrate Ridge; SBB, Santa Barbara Basin; HMMV, Håkon Mosby Mud Volcano.

Cited references: [1] Chapter 5, this thisis [2] Hovland, 2002; [3] Blumenberg et al., 2004; [4] Knittel et al., 2005; [5] Knittel et al., 2003; [6] Michaelis et al., 2002; [7] Hinrichs et al., 1999; [8] Hinrichs et al., 2000; [9] Brooks et al., 1991; [10] Teske et al., 2002; [11] Welhan, 1988; [12] Aloisi et al., 2002; [13] Egorov and Ivanov, 1998; [14] Chapter 4, this thesis [15] Nuzzo et al. 2005; [16] Boetius et al., 2000; [17] Suess et al., 1999;[18] Elvert et al., 1999; [19] Elvert et al., 2001; [20] Elvert et al., 2003; [21] Elvert et al., submitted.; [22] Orphan et al., 2001; [23] Werne et al., 2002; [24] Werne et al., 2004; [25]Werne and Sinninghe Damste, 2005; [26] Haese et al., 2003; [27] Chapter 1, this thesis; [28] Chapter 2, this thesis [29] Lein et al., 1999; [30] Felden and Niemann, unpubl.

2.1 Lipid Fingerprints of Active Communities of Anaerobic Methanotrophs

Methanotrophic communities were identified by independent, molecular techniques, i.e. lipid biomarker patterns, 16S rDNA clone libraries and/or FISH. 16S rDNA clone libraries and FISH directly provide information on the phylogentic relations of microbes. Furthermore, FISH allows to quantify key microbial players. Lipid biomarker analysis provides information on dominant metabolic pathways (Boschker et al., 1998; Elvert et al., 2003; Hinrichs et al., 1999). Furthermore, phylogentic information can be gained by analysing the pattern of diagnostic lipids (Blumenberg et al., 2004; Elvert et al., 2003). This thesis and previous work provide a database to assign lipid patterns to the known groups of methane oxidizing archaea and to test the statistical relevance of these patterns. For identifying diagnostic lipid signatures of particular ANME groups and their associated, sulphate reducing bacteria, I compared literature data from methane–rich environments of which information on both, lipid signatures and the identity of dominant key microbial players are available. Information on the particular habitats, the dominant ANME and SRB groups, abundances and isotope signatures of diagnostic lipids as well as $\delta^{13}C$-values of the source methane is provided in Table 2.

2.1.1 Archaeal Biomarkers

A variety of lipid signatures putatively indicative for particular ANME-archaea have been discussed in the literature during the last decade. These include the glycerol dialkyl diethers archaeol and *sn2*-hydroxyarchaeol, the C_{20} and $C_{25,}$ irregular tail-to-tail linked, isoprenoidal hydrocarbons 2,6,11,15-tetramethylhexadecane (crocetane) and 2,6,10,15,19-pentamethyleicosane (PMI) and their unsaturated analogues (crocetenes and PMIΔ) as well as a variety of isoprenoidal glycerol dialkyl tetraethers (GDGT). With the exception of

crocetane, all of these molecules were also found in methanogenic archaea utilising bicarbonate, acetate or methylated substrates.

Archaeol was found in a variety of archaea and therefore appears to be ubiquitous, whereas significant amounts of hydroxyarchaeols where only detected in certain strains of the *Methanosarcinales* (Koga et al., 1998; Koga et al., 1993; Kushwaha and Kates, 1978). PMIs were also previously detected in methanogenic archaea (Brassell et al., 1981; Schouten et al., 1997). GDGTs were found in variety of thermophilic and planktonic archaea (De Rosa and Gambacorta, 1988; Schouten et al., 1998; Schouten et al., 2000). However, the incorporation of methane-derived carbon into these compounds is indicated by very low $\delta^{13}C$-values of the lipids. This is caused by the uptake of already ^{13}C-depleted methane in combination with a subsequent carbon isotope fractionation (Elvert et al., 1999; Hinrichs et al., 1999; Michaelis et al., 2002; Orphan et al., 2001b; Thiel et al., 1999).

Significant amounts of $\delta^{13}C$-depleted archaeol and *sn2*-hydroxyarchaeol were reported from every ANME dominated habitat (Tab. 2). However, ANME-2 dominated microbial mat sections at cold seeps of the Black Sea were found to contain considerably higher amounts of *sn2*-hydroxyarchaeol relative to archaeol in comparison to ANME-1 dominated sections (Blumenberg et al., 2004). The ratio of these compounds was therefore proposed as a specific fingerprint pattern for either ANME-1 or ANME-2 (Blumenberg et al., 2004). With respect to the currently available literature data, the ratio of *sn2*-hydroxyarchaeol to archaeol ranges between 0.05 and 0.78 (mean = 0.34, ± 0.1 S_E) in systems clearly dominated by ANME-1, and between 1 and 5.50 (mean = 2.38, ± 0.46 S_E) in systems predominated by ANME-2 (Fig. 5a). This difference is statistically significant when comparing all available data (t-test, $p = 0.02$, $n = 14$). Ratios of ANME-3 are within the range of ANME-2 and show values of 2.44 and 1.78 in two environmental samples analysed (Felden and Niemann, unpubl.; Chapter 2, 3).

Therefore, a *sn2*-hydroxyarchaeol to archaeol ratio >1 is a robust indicator for the distinction of ANME-1 from ANME-2 and ANME-3 (Fig. 4a).

The first discovery of a biomarker originating from archaea using methane as a carbon source was made in subsurface sediments at the SMT in the Kattegat, North Sea (Bian, 1994; Bian et al., 2001). Here, Bian and co-workers (1994, 2001) found elevated concentrations of crocetane, carrying a significant depleted ^{13}C-signal. High concentrations of strongly ^{13}C-depleted crocetane and crocetenes were also found in ANME-2 dominated habitats (Tab. 2). In contrast, only minor amounts of crocetane were found in ANME-1 systems. Consequently, the presence of substantial amounts of δ^{13}C-depleted crocetane appear to be a second indicator for the presence of ANME-2 (Blumenberg et al., 2004).

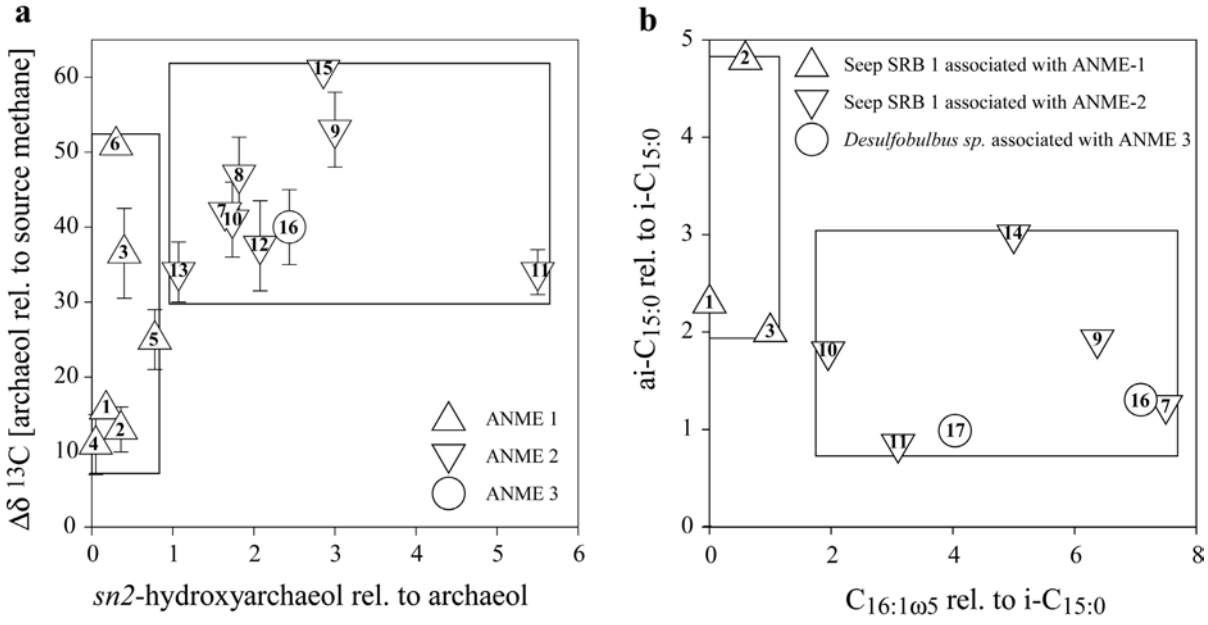

Figure 5. Diagnostic lipid patterns of methanotrophic archaeal (a) and sulphate reducing bacterial key players (b) in AOM environments. Error bars in panel a indicate maxima and minima of δ^{13}C-values of the source methane. The ratios of *sn2*-hydroxyarchaeol relative to archaeol and the $\Delta\delta^{13}$C-values of archaeol are significantly different in ANME-1 and ANME-2 dominated systems (t-test, p = 0.02, n = 14). Ratios of C16:1ω5 relative to i-C15:0 are significantly different in AOM environments dominated by eco-types of Seep-SRB1 associated with ANME-1 and ANME-2, respectively (t-test, p = 0.02, n = 8). Numbers denote locations of finding (see Table 1).

^{13}C-depleted PMI:0 and unsaturated PMIs were detected in virtually all studied AOM environments (Tab. 2). Nevertheless, ANME-1 and ANME-2 systems were found to contain a suite of PMIs ranging from PMI:0 to PMI:5 whereas ANME-3 was found to contain exclusively PMI:4 accompanied by more abundant PMI:5. The presence of only PMI:4 and PMI:5 and the absence of higher saturated PMI analogues may thus provide a tool to distinguish ANME-3 from ANME-2 (Chapter 2, 3).

Concentration measurements of GDGTs require a high performance liquid chromatography (HPLC) instrumentation. In the absence of this technique, GDGT contents have been inferred from their decomposition products, the acyclic and cyclic biphytanes (Blumenberg et al., 2004; Schouten et al. 1998; Chapter 6), but also free biphytanediols and biphytanic acids have been detected (Teske et al., 2002). Significant amounts of GDGTs were commonly detected in ANME-1 systems (Blumenberg et al., 2004; Hinrichs et al., 2000). Released biphytanes were generally dominated by acyclic biphytane followed by monocyclic biphytane (one cyclopentane ring) and bicyclic biphytane (two cylcopentane rings). The presence of δ^{13}C-depleted biphytanes released from GDGTs was consequently used as an indicator for ANME-1 (Blumenberg *et al.,* 2004; Chapter 6). However, recently, Elvert and co-workers (submitted) found GDGTs in ANME-2 dominated sediments (Tab. 2). At Hydrate Ridge, these authors detected comparably high contents of intact GDGTs at a *Calyptogena* site where 80 % of the ANME-2 cells belonged to the ANME-2c and 20 % to the ANME-2a sub-cluster (Knittel et al., 2005). Significantly lower GDGT contents were found at a *Beggiatoa* site were the ANME-2c / ANME-2a ratio was reverse to the *Calyptogena* site, indicating that the GDGTs were probably derived from archaea of the ANME-2c subgroup (Elvert et al., submitted). An ANME-1 origin is unlikely here, as the total content of ANME-1 cells was <10 % of detected single cells (Elvert et al., submitted; Knittel et al., 2005). No biphytanediols were detected at the Guaymas Basin at an ANME-2c dominated site (Teske et al., 2002). However, this is no

prove for the absence of intact GDGTs which were detected at high concentrations in other cores obtained from this region (Schouten et al., 2003). Substantial amounts of ^{13}C-depleted GDGTs are therefore indicative for ANME-1 and most probably ANME-2c.

2.1.2 Bacterial Biomarkers

Biomarker surveys in AOM environments found ^{13}C-depleted lipid compounds of presumably bacterial origin that co-occur with ^{13}C-depleted archaeal lipids. As for the archaeal partners, the strong depletion in ^{13}C is indicative for an incorporation of methane-derived carbon (Blumenberg et al., 2004; Elvert et al., 2003; Hinrichs et al., 2000; Michaelis et al., 2002; Zhang et al., 2002). At many different cold seep settings, ANME-1 and ANME-2 archaea have been found in consortia with SRB of the Seep-SRB1 cluster belonging to the *Desulfosarcina/Desulfococcus* group (Knittel et al., 2003). However, the suite of ^{13}C-depleted, bacterial lipids is surprisingly diverse (Blumenberg et al., 2004; Elvert et al., 2003; Hinrichs et al., 2000). This may indicate that the Seep-SRB1 cluster comprises physiologically different ecotypes of the same species. Intriguingly, the physical association of the same partner bacteria in the consortia also expresses morphological differences, e.g. in the ANME-1 / Seep-SRB1 and ANME-2 / Seep-SRB1 communities (shell type, mixed type, mat type, see also Knittel et al. 2005). ANME-3 has been found in close association with SRB of the *Desulfobulbus sp.* that express lipid signatures substantially different from those detected in Seep-SRB1 (Chapter 2, 3). Of particular value for typifying the sulphate reducing AOM-partners are fatty acid glycerol esters of which the fatty acid (FA) moieties are commonly cleaved off and separately analysed as fatty acid methyl esters (FAMEs). The second class of compounds putatively derived from SRB involved in AOM encompasses the non-isoprenoidal mono and dialkyl glycerol ethers (MAGE, DAGE) (Hinrichs et al., 2000;

Pancost et al., 2001; Rütters et al., 2001). Similar to the archaeal biomarker used for identifying particular ANME groups, none of the bacterial lipid compound classes discussed in the following is exclusively restricted to a particular group of SRB (Hinrichs and Boetius, 2002).

The iso and anteiso branched $C_{15:0}$ fatty acid have been found in virtually all AOM environments (Tab. 2). Similar to the use of the *sn2*-hydroxyarchaeol / archaeol ratio as an archaeal fingerprint, the ratio of ai-$C_{15:0}$ relative to i-$C_{15:0}$ shows higher values in ANME-1 / Seep-SRB1 compared to ANME-2 / Seep-SRB1 dominated systems and has consequently been proposed to distinguish the two Seep-SRB1 eco-types (Blumenberg et al., 2004). A value >>2 appears to be indicative for ANME-1-associated SRB (Fig. 5b). However, a statistical analysis of a larger set of data shows that there is a comparably large overlap between the two Seep-SRB1 eco-types and from a statistical point of view, the ai-$C_{15:0}$ / i-$C_{15:0}$ ratios are not significantly different (t-test, $p>0.5$, $n = 8$). This is probably a result of the still relatively small data pool available in the literature.

High concentrations of the fatty acid $C_{16:1\omega5}$ were observed in ANME-2 / Seep-SRB1 dominated systems and thus suggested as an indicator for this Seep-SRB1 eco-type (Blumenberg et al., 2004; Elvert et al., 2003). Relative to i-$C_{15:0}$, the $C_{16:1\omega5}$ content is significantly higher (t-test, $p = 0.02$, $n = 8$) in ANME-2 / Seep-SRB1 systems (mean = 4.8 ±1 S_E) compared to ANME-1 / Seep-SRB1 systems (mean = 0.5 ±0.3 S_E). A value <1.8 is hence a robust indicator for the Seep-SRB1 ecotype associated with ANME-1 (Fig. 4b). However, both ratios appear to be comparable in the Seep-SRB1 ecotype associated to ANME-2 and in *Desulfobulbus sp.* (Fig. 4b). Elvert et al. (2003) suggested that the presence of the unusual fatty acid cy$C_{17:0\omega5,6}$ is restricted to the Seep-SRB1 ecotype associated to ANME-2 which is consistent with the available literature data. *Dseulfobulbus* at HMMV was

found to express comparably high amounts of the unusual fatty acid $C_{17:1\omega6}$ additionally discerning these SRB (Felden and Niemann unpubl.; Chapter 2, 3)

^{13}C-depleted MAGEs and DAGEs were detected in most AOM environments (Tab. 2) The former seem to be a robust markers of the SRB involved in AOM because of their very similar chain-length distribution and pattern of unsaturated bonds (Hinrichs et al., 2000). Both, MAGEs and FAs have been detected in cultures of *Desulfosarcina variabilis* and *Desulforhabdus amnigenus* (Rütters et al., 2001). The DAGEs have so far only been found in deeply-branching thermophilic and halophilic bacteria (Huber et al., 1992; Langworthy et al., 1983; Ollivier et al., 1991). DAGEs detected in AOM environments have been found to comprise alkyl moieties with cyclohexane rings (Elvert et al., submitted; Pancost et al., 2001), which is in stark contrast to the pattern of alkyl moieties in the FA fraction. Thus, the question arises if DAGEs are directly produced by the syntrophic SRB or by an up to now unknown source organism heterotrophically feeding on AOM biomass. Substantial amounts of MAGEs appear to be restricted to the ANME-2 associated Seep-SRB1 ecotype and to *Dseulfobulbus* (Tab. 2). Thus, in addition to the ratios of diagnostic fatty acids discussed above, substantial amounts of MAGEs additionally point to these SRBs.

With respect to the currently available data on fatty acids as well as MAGEs and DAGEs, the ratio of $C_{16:1\omega5}$ relative to i-$C_{15:0}$ and the presence or absence of cy$C_{17:0\omega5,6}$ and $C_{17:1\omega6}$ appear to be the most robust fingerprints for discerning the different SRB types associated to the ANMEs. However, further investigations have to be carried out to assess the role and a potential involvement of other seep related bacteria such as Seep-SRB2 (Knittel et al., 2003) in AOM.

2.1.3 Carbon Isotope Systematics of AOM

In comparison to ANME-1, ANME-2 shows a higher stable carbon isotope fractionation as indicated by the respective $\Delta\delta^{13}C$-values of archaeol and *sn2*-hydroxyarchaeol. Compared to the source methane, $\Delta\delta^{13}C$-values of archaeol range between -11‰ and -51‰ (mean = -25‰ ±6 S_E) in ANME-1 dominated systems and between -34‰ and -61‰ (mean = -44‰ ±3 S_E) in ANME-2 dominated systems (Fig. 4a, b). For *sn2*-hydroxyarchaeol, $\Delta\delta^{13}C$-values are shifted by ca. -10‰ compared to archaeol ranging between -24‰ and -54‰ (mean = -39‰ ±5 S_E) and between -34‰ and -74‰ (mean = -49 ±5 S_E) in ANME-1 and ANME-2 dominated systems, respectively. Both compounds are thus more strongly ^{13}C-depleted in ANME-2 (t-test, $p = 0.05$, $n = 14$). A comparable isotope shift between ANME-1 and ANME-2 was previously observed by Orphan et al. (2002). Similar to the ratio of *sn2*-hydroxyarchaeol relative to archaeol, $\Delta\delta^{13}C$-values of ANME-3 are within the range of ANME-2 (Fig. 4a). However, at one site at HMMV, ANME-3 derived archaeol was found with a higher $\delta^{13}C$-value compared to the source methane (Tab. 2). The reason for this phenomenon is unknown. The comparison of $\Delta\delta^{13}C$-values of archaeol and *sn2*-hydroxyarchaeol show a considerable overlap between the three ANME groups. Hence, $\Delta\delta^{13}C$-values have to be regarded with caution.

Compared to the archaeal lipids, $\Delta\delta^{13}C$-values of specific bacterial fatty acids show an even weaker difference among the two Seep-SRB1 ecotypes and *Dseulfobulbus*. The available $\delta^{13}C$-values of i-$C_{15:0}$ for instance show a depletion of -20‰ compared to the source methane in ANME-1 / Seep-SRB1 systems in the Black Sea whereas source methane and ai-$C_{15:0}$ have comparable $\delta^{13}C$-values at Tommeliten (Tab. 2). In ANME-2 / Seep-SRB1 systems the carbon isotope fractionation appears to be slightly stronger ranging between –7‰ and -25‰

(mean = -14 ±4 S_E). At HMMV, ai-$C_{15:0}$ was only slightly depleted in comparison to the source methane (Tab. 2). However, unlike ANMEs often accounting for the bulk of archaeal cells, e.g. >90 % in Hydrate Ridge sediments (Knittel et al., 2005), up to 70 % in Black Sea microbial mats (Michaelis et al., 2002), a comparably high diversity of bacteria was detected in most AOM environments (Knittel et al., 2003; Lösekann et al., unpubl.; Orphan et al., 2001a; Teske et al., 2002; Chapter 5, 6). A mixture of the methane-derived $\delta^{13}C$-signal of Seep-SRB1 or DBB with non-AOM sources is thus likely (Elvert et al., 2003). Furthermore, an utilisation of multiple carbon sources by the syntrophic SRB can not be excluded.

2.1.4 Archaeal and Bacterial Biomass Ratios of AOM Communities

ANME-1 was found to comprise up to 70 % of cell counts (average 40 %, Knittel et al. unpublished) in microbial mats of the Black Sea (Michaelis et al., 2002), whereas aggregates at Hydrate Ridge are characterised by an ANME-2 relative to Seep-SRB1 ratio of 1:2 (Boetius et al., 2000). In several subsurface sediments, ANME-1 was observed without an associated bacterial partner (Orphan et al., 2002; Chapter 6). Hence, the content of archaeal lipid biomass relative to the bacterial one is most likely higher in ANME-1 systems compared to ANME-2 systems. For ANME-3 systems, this has not been determined yet. However, it remains entirely speculative if the ratio of archaeal relative to SRB cells as well as the archaeal relative to the bacterial lipid content is constant to the ratio of total archaeal vs. bacterial biomass in ANME-1, -2 and -3 dominated systems. Hence, the biomarker ratio presented in the following should be regarded as a tool for discerning the syntrophic SRB and not as an expression of biomass ratios. In order to estimate differences in the relative lipid contents, one has to use ratios of diagnostic archaeal and bacterial lipids, which have

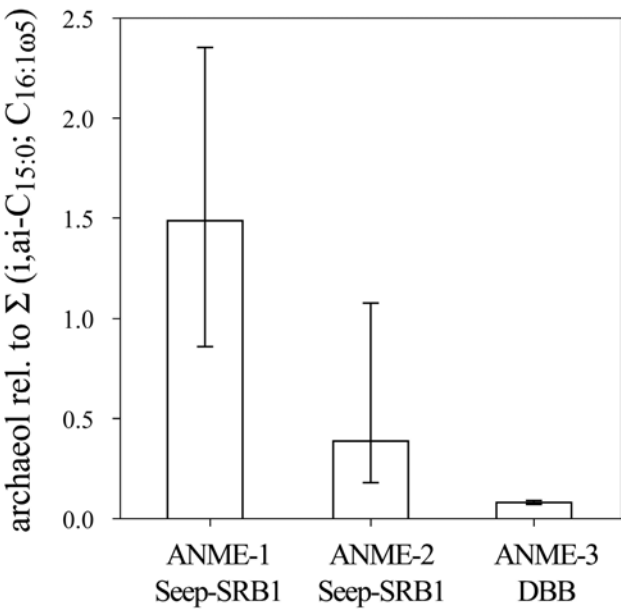

Figure 6. ratios of archaeol relative to selected bacterial FA. ANME-1 / Seep-SRB1 comprise significantly lower FA contents than ANME-2 / Seep-SRB1 and ANME-3 / *Dseulfobulbus* (T-test, $p < 0.05$). Error bars = maxima and minima.

been detected and quantified in all of the three known ANME / SRB communities. The ratio of the archaeal biomarker archaeol relative to the sum of the bacterial fatty acids i-$C_{15:0}$, ai-$C_{15:0}$ and $C_{16:\omega5}$ can be used as an approximation to discern the different AOM communities (Fig. 6). With respect to the currently available literature data, the ratio of archaeol relative to the sum of i-$C_{15:0}$, ai-$C_{15:0}$ and $C_{16:\omega5}$ ranges between 0.9 and 2.4 (mean = 1.5 ±0.4 S_E) in ANME-1 / Seep-SRB1 dominated systems and between 0.2 and 1.1 (mean = 0.4 ±0.1 S_E) in ANME-2 / Seep-SRB1 dominated systems (Fig. 6). This ratio is thus significantly higher in ANME-1 systems (t-test, $p = 0.02$). For ANME-3 / DBB, this ratio is within the range of ANME-2 / Seep-SRB1. Hence, a value >1.5 is an additional, robust indicator for ANME-1 / Seep-SRB1 systems and a value <0.4 for ANME-2 / Seep-SRB1 or ANME-3 / *Dseulfobulbus* systems.

In conclusion, the combination of $\Delta\delta^{13}C$ values and ratios of diagnostic archaeal and bacterial lipids presented in this section provide a robust tool to distinguish all of the three known AOM communities. This is of particular value to gain information on the identity of AOM communities and to interpret fossil lipid biomarker patterns in e.g. carbonates (Chapter 5, 6).

3. BIO-GEOSPHERE INTERACTION IN METHANE-BEARING, MARINE SEDIMENTS

This thesis and previous works provide evidence that the chemoautotrophic activity of methanotrophic organisms influence the benthic habitat (e.g. by mixing, by providing hard-substrate in the form of shells or tubes) and channel methane-derived carbon into higher trophic levels. At active cold seeps, fluids enriched in hydrocarbons are advected into surface sediments where the activity of methanotrophic and sulphate reducing communities form ecosystems that are almost independent from photosynthetic, primary production. The biogeochemical activities at these cold seeps exceed the biomass production in the adjacent none-seep sediments by orders of magnitude (Chapter 3). In near surface sediments, AOM supports enormous biomasses of filamentous, sulphide oxidising bacteria, chemosynthetic clams and vestimentiferan or pogonophoran worms (Boetius and Suess, 2004; Joye et al., 2004; Levin et al., 2003; Olu et al., 1997; Orphan et al., 2004; Sahling et al., 2002; Chapter 2, 3). For instance, AOM-related SR accounts for approximately all of the sulphide production at the *Beggiatoa* site at HMMV (Chapter 2, 4). Apart from the indirect support of thiotrophic biomass by AOM-derived sulphide, AOM communities may also represent a food source for organisms of higher trophic levels (Levin and Michener, 2002; Werne et al., 2002).

Where oxygen or nitrate is available, all of the produced sulphide - representing an enormous reducing power - is oxidised. However, the mechanisms removing free sulphide in deeper sediment layers (>1m bsf), are poorly understood. Here, it appears unlikely that gliding bacteria, burrowing clams or tubeworms are the mediators for sulphide oxidation (Chapter 5). Hence a geochemical reaction of sulphide with iron as proposed previously is a more likely explanation (Hensen et al., 2003; Jørgensen et al., 2004).

Free living cells of MOx bacteria may play an important role in the hydrosphere, reducing methane which has circumvented the benthic microbial filter system (Larock et al., 1994). However, very little is known about the identity and distribution of these microbes and the magnitude of MOx in the marine water column. It appears that free-living MOx bacteria play an important role if fluid flow limits the penetration depth of sulphate or if the comparably fast growth rates of these bacteria allow to colonise the sea bed around newly created methane sources (Chapter 2, 3). However, once oxygen is limiting and sulphate and methane overlap, it is expected that AOM out-competes MOx. In contrast, endosymbiontic MOx bacteria and some megafauna organisms have apparently formed a very successful symbiosis (Fisher, 1990; Hanson et al., 1993). At HMMV two species of *Pogonophora*, *Oligobrachia haakonmosbiensis* and *Sclerolinum contortum* build up biomass volumes of about 2 kg m^{-2} (Chapter 2). Of these two species, at least *O. haakonmosbiensis* harbours methanotrophic endosymbionts (Gebruk et al., 2003; Smirnov et al., 2000; Chapter 2). Little is known about mechanisms selecting for either free-living AOM communities or symbiotic MOx-containing animals. However, pogonophoran worms at HMMV were found to be confined to habitats characterised by comparably low fluid flow rates (Chapter 2, 4).

The most striking geochemical process related to AOM is the build up of large structures due to the precipitation of methane-related, authigenic carbonates. It is currently not known if this process is directly induced by methane turnover or by other geochemical processes. However, lipid biomarker analyses have provided evidence that AOM and carbonate precipitation are spatially connected (Michaelis et al., 2002; Peckmann and Tiel, 2004; Thiel et al., 1999; Chapter 5, 6). Such authigenic carbonates were found to form subsurface layers in marine sediments or reef-like structures and chimneys. In permanently anoxic waters of the Black Sea, calcified microbial reefs were also found to grow into the water column (Michaelis et al., 2002). In oxic waters, the carbonate crusts may then serve as a hard substrate for sessile

organisms (Chapter 6; Bohrmann et al., 1998; Hovland and Judd, 1988; Hovland et al., 1987). Similar to artificial reefs, carbonate reefs were also found to attract several fish species and other non-endemic species to the seeps (Hovland and Judd 1988; Chapter 6).

4. FUTURE RESEARCH QUESTIONS

This thesis combined independent analytical tools to investigate dominant modes and magnitudes of methane oxidation, the mechanisms controlling the vertical and horizontal distribution of methane turnover, the identity of key methanotrophs and the impact of methanotrophy on the habitat at active methane seeps. Yet, a quantitative and systematic understanding of methane seeps as ecosystems and sources of methane to the ocean still seems far away. In principle, a similar set of questions as addressed in the beginning of this thesis should be asked again when it is possible to measure methane and sulfide gradients as well as their turnover *in situ* at the seafloor:

What is the magnitude of methane oxidation?

What is the heterogeneity in the system?

How much methane escapes into the water column and potentially to the atmosphere?

What are the environmental conditions selecting for particular groups of methanotrophs?

How do methane seeps change over time?

It is still speculative how much methane is turned over *in situ* as sample recovery and changing environmental conditions during *ex situ* measurements introduce artefacts. Hence, an important research task would be to develop analytical tools allowing to measure substrate

concentrations and methane turnover *in situ*. With respect to a higher availability of submarine technology such as submersibles, ROVs and AUVs, a combination of sea floor mapping and high resolution *in situ* measurements of substrate turnover as well as flux calculations from *in situ* pore water solute concentrations provide possibilities for accurate estimates of microbial activity, environmental heterogeneity and to asses the controlling mechanisms.

Estimates on methane emission to the hydrosphere and potentially to the atmosphere are preliminary at most. One interesting task would therefore be to measure methane oxidation rates in the water column as well as to develop methods allowing to estimate the amount of methane that is leaving the benthos. For this purpose, instruments are needed which can measure fluid flow as well as gas ebullition. Some prototypes for these tasks are already available, but need further development.

Three types of AOM communities were discovered in the last five years and it is possible that some have remained undiscovered. For example, it is not known which types of methanotrophs could consume methane anaerobically at high temperatures. Also it is not clear if terrestrial habitats and the deep biosphere host new groups of anaerobic methanotrophs. The environmental factors determining for particular AOM communities are entirely speculative. The morphology and varying contents of membrane lipids of the known, closely related AOM communities may indicate a different physiological functioning or adaptation to yet unknown environmental conditions. Very little is known on the phylogeny and membrane lipids of symbiotic and free living MOx bacteria, and almost nothing is known on environmental parameters selecting for particular groups of these bacteria. Hence, a first approach would be

to obtain AOM and MOx communities in pure culture for manipulation experiments. Moreover, further analyses on phylogeny and intact membrane lipids in combination with field studies on environmental conditions should be carried out in the future.

One additional gap in our knowledge on methane seeps and methane-bearing habitats is their temporal behaviour. Future research should thus attempt to elucidate the variations in methane fluxes and seep activities over time and the response of the ecosystem to such variations.

References

Aloisi G., Bouloubassi I., Heijs S. K., Pancost R. D., Pierre C., Damste J. S. S., Gottschal J. C., Forney L. J., and Rouchy J. M. (2002) CH4-consuming microorganisms and the formation of carbonate crusts at cold seeps. *Earth and Planetary Science Letters* **203**(1), 195-203.

Barnes R. O. and Goldberg E. D. (1976) Methane Production and Consumption in Anoxic Marine-Sediments. *Geology* **4**(5), 297-300.

Barry J. P., Greene H. G., Orange D. L., Baxter C. H., Robison B. H., Kochevar R. E., Nybakken J. W., Reed D. L., and McHugh C. M. (1996) Biologic and geologic characteristics of cold seeps in Monterey bay, California. *Deep-Sea Research Part I-Oceanographic Research Papers* **43**(11-12), 1739-&.

Bian L. Q. (1994) Isotopic biogeochemistry of individual compounds in a modern coastal marine sediment (Kattegat, Denmark and Sweden). Master thesis, Indiana University.

Bian L. Q., Hinrichs K. U., Xie T. M., Brassell S. C., Iversen H., Fossing H., Jorgensen B. B., and Hayes J. M. (2001) Algal and archaeal polyisoprenoids in a recent marine sediment: Molecular isotopic evidence for anaerobic oxidation of methane. *Geochemistry Geophysics Geosystems* **2**, U1-U22.

Blumenberg M., Seifert R., Reitner J., Pape T., and Michaelis W. (2004) Membrane lipid patterns typify distinct anaerobic methanotrophic consortia. *Proceedings of the National Academy of Sciences of the United States of America* **101**(30).

Boetius A., Ravenschlag K., Schubert C., Rickert D., Widdel F., Gieseke A., Amann R., Jørgensen B. B., Witte U., and Pfannkuche O. (2000) A marine microbial consortium apparently mediating anaerobic methane of oxidation. *Nature* **407**, 623-626.

Boetius A. and Suess E. (2004) Hydrate Ridge: a natural laboratory for the study of microbial life fueled by methane from near-surface gas hydrates. *Chemical Geology* **205**(3-4), 291-310.

Boschker H. T. S., Nold S. C., Wellsbury P., Bos D., de Graaf W., Pel R., Parkes R. J., and Cappenberg T. E. (1998) Direct linking of microbial populations to specific biogeochemical processes by ^{13}C-labelling of biomarkers. *Nature* **392**, 801-805.

Brassell S. C., Wardroper A. M. K., Thomson I. D., Maxwell J. R., and Eglinton G. (1981) Specific acyclic isoprenoids as biological markers of methanogenic bacteria in marine sediments. *Nature* **290**, 693-696.

Brooks J. M., Field M. E., and Kennicutt M. C. (1991) Observations of Gas Hydrates in Marine-Sediments, Offshore Northern California. *Marine Geology* **96**(1-2), 103-109.

Cordes E. E., Arthur M. A., Shea K., Arvidson R. S., and Fisher C. R. (2005) Modeling the mutualistic interactions between tubeworms and microbial consortia. *Plos Biology* **3**(3), 497-506.

de Beer D., Sauter E., Niemann H., Witte U., and Boetius A. (submitted) In situ fluxes and zonation of microbial activity in surface sediments of the Håkon Mosby Mud Volcano. *Limnology and Oceanography*.

De Rosa M. and Gambacorta A. (1988) The lipids of archaebacteria. *Progress in Lipid Research* **27**, 153-175.

Egorov A. V. and Ivanov M. K. (1998) Hydrocarbon gases in sediments and mud breccia from the central and eastern part of the Mediterranean Ridge. *Geo-Marine Letters* **18**(2), 127-138.

Elvert M., Boetius A., Knittel K., and Jorgensen B. B. (2003) Characterization of specific membrane fatty acids as chemotaxonomic markers for sulfate-reducing bacteria involved in anaerobic oxidation of methane. *Geomicrobiology Journal* **20**(4), 403-419.

Elvert M., Hopmans E. C., Boetius A., and Hinrichs K.-U. (submitted) Spatial variatons of archaeal-bacterial assambladges in gas hydrate bearing sediments at a cold seep: Implications from a high resolution molecular and isotopic approach.

Elvert M., Suess E., and Whiticar M. J. (1999) Anaerobic methane oxidation associated with marine gas hydrates: superlight C-isotopes from saturated and unsaturated C_{20} and C_{25} irregular isoprenoids. *Naturwissenschaften* **86**(6), 295-300.

Fisher C. R. (1990) Chemoautotrophic and Methanotrophic Symbioses in Marine-Invertebrates. *Reviews in Aquatic Sciences* **2**(3-4), 399-436.

Gebruk A. V., Krylova E. M., Lein A. Y., Vinogradov G. M., Anderson E., Pimenov N. V., Cherkashev G. A., and Crane K. (2003) Methane seep community of the Hakon Mosby mud volcano (the Norwegian Sea): composition and trophic aspects. *Sarsia* **88**(6), 394-403.

Haese R. R., Meile C., Van Cappellen P., and De Lange G. J. (2003) Carbon geochemistry of cold seeps: Methane fluxes and transformation in sediments from Kazan mud volcano, eastern Mediterranean Sea. *Earth and Planetary Science Letters* **212**(3-4), 361-375.

Hanson R. S., Bratina B. J., and Brusseau G. A. (1993) Phylogeny and ecology of methylotrophic bacteria. In *Microbial Growth on C_1 Compounds* (ed. J. C. Murrell and D. P. Kelly), pp. 285-302. Intercept Limited.

Hanson R. S. and Hanson T. E. (1996) Methanotrophic bacteria. *Microbiological Reviews* **60**(2), 439-&.

Hensen C., Zabel M., Pfeifer K., Schwenk T., Kasten S., Riedinger N., Schulz H. D., and Boettius A. (2003) Control of sulfate pore-water profiles by sedimentary events and the significance of anaerobic oxidation of methane for the burial of sulfur in marine sediments. *Geochimica Et Cosmochimica Acta* **67**(14), 2631-2647.

Hinrichs K.-U. and Boetius A. (2002) The anaerobic oxidation of methane: New insights in microbial ecology and biogeochemistry. In *Ocean Margin Systems* (ed. G. Wefer, D. Billett, and D. Hebbeln), pp. 457-477. Springer-Verlag, Berlin.

Hinrichs K.-U., Hayes J. M., Sylva S. P., Brewer P. G., and DeLong E. F. (1999) Methane-consuming archaebacteria in marine sediments. *Nature* **398**, 802-805.

Hinrichs K. U., Summons R. E., Orphan V., Sylva S. P., and Hayes J. M. (2000) Molecular and isotopic analysis of anaerobic methane-oxidizing communities in marine sediments. *Organic Geochemistry* **31**(12), 1685-1701.

Hovland M. and Judd A. G. (1988) *Seabed Pockmarks and Seepages: Impact on Geology, Biology and the Marine Environment*. Graham & Trotman.

Huber R., Wilharm T., Huber D., Trincone A., Burggraf S., König H., Rachel R., Rockinger I., Fricke H., and Stetter K. O. (1992) *Aquifex pyrophilus* gen. nov. sp. nov., represents a novel group of marine hyperthermophilic hydrogen-oxidizing bacteria. *Systematic and Applied Microbiology* **15**, 340-351.

Iversen N. and Jørgensen B. B. (1985) Anaerobic methane oxidation rates at the sulfate-methane transition in marine sediments from Kattegat and Skagerrak (Denmark). *Limnology and Oceanography* **30**(5), 944-955.

Jensen P., Aagaard I., Burke R. A., Dando P. R., Jorgensen N. O., Kuijpers A., Laier T., Ohara S. C. M., and Schmaljohann R. (1992) Bubbling Reefs in the Kattegat - Submarine Landscapes of Carbonate-Cemented Rocks Support a Diverse Ecosystem at Methane Seeps. *Marine Ecology-Progress Series* **83**(2-3), 103-112.

Jørgensen B. B., Bottcher M. E., Luschen H., Neretin L. N., and Volkov, II. (2004) Anaerobic methane oxidation and a deep H2S sink generate isotopically heavy sulfides in Black Sea sediments. *Geochimica Et Cosmochimica Acta* **68**(9), 2095-2118.

Jørgensen B. B., Weber A., and Zopfi J. (2001) Sulfate reduction and anaerobic methane oxidation in Black Sea sediments. *Deep-Sea Research Part I-Oceanographic Research Papers* **48**(9), 2097-2120.

Joye S. B., Boetius A., Orcutt B. N., Montoya J. P., Schulz H. N., Erickson M. J., and Lugo S. K. (2004) The anaerobic oxidation of methane and sulfate reduction in sediments from Gulf of Mexico cold seeps. *Chemical Geology* **205**(3-4), 219-238.

Knittel K., Boetius A., Lemke A., Eilers H., Lochte K., Pfannkuche O., Linke P., and Amann R. (2003) Activity, distribution, and diversity of sulfate reducers and other bacteria in sediments above gas hydrate (Cascadia margin, Oregon). *Geomicrobiology Journal* **20**(4), 269-294.

Knittel K., Losekann T., Boetius A., Kort R., and Amann R. (2005) Diversity and distribution of methanotrophic archaea at cold seeps. *Applied and Environmental Microbiology* **71**(1), 467-479.

Koga Y., Morii H., Akagawa-Matsushita M., and Ohga I. (1998) Correlation of polar lipid composition with 16S rRNA phylogeny in methanogens. Further analysis of lipid component parts. *Bioscience Biotechnology and Biochemistry* **62**(2), 230-236.

Koga Y., Nishihara M., Morii H., and Akagawa-Matsushita M. (1993) Ether polar lipids of methanogenic bacteria: Structures, comparative aspects, and biosyntheses. *Microbiological Reviews* **57**(1), 164-182.

Kushwaha S. C. and Kates M. (1978) 2,3-Di-O-Phytanyl-Sn-Glycerol and Prenols from Extremely Halophilic Bacteria. *Phytochemistry* **17**(11), 2029-2030.

Langworthy T. A., Holzer G., Zeikus J. G., and Tornabene T. G. (1983) Iso- and anteiso-branched glycerol diethers of the thermophilic anaerobe *Thermodesulfotobacterium commune*. *Systematic and Applied Microbiology* **4**(1), 1-17.

Larock P. A., Hyun J. H., and Bennison B. W. (1994) Bacterioplankton Growth and Production at the Louisiana Hydrocarbon Seeps. *Geo-Marine Letters* **14**(2-3), 104-109.

Lein A., Vogt P., Crane K., Egorov A., and Ivanov M. (1999) Chemical and isotopic evidence for the nature of the fluid in CH4-containing sediments of the Hakon Mosby Mud Volcano. *Geo-Marine Letters* **19**(1-2), 76-83.

Levin L. A. and Michener R. H. (2002) Isotopic evidence for chemosynthesis-based nutrition of macrobenthos: The lightness of being at Pacific methane seeps. *Limnology and Oceanography* **47**(5), 1336-1345.

Levin L. A., Ziebis W., Mendoza G. F., Growney V. A., Tryon M. D., Brown K. M., Mahn C., Gieskes J. M., and Rathburn A. E. (2003) Spatial heterogeneity of macrofauna at northern California methane seeps: influence of sulfide concentration and fluid flow. *Marine Ecology-Progress Series* **265**, 123-139.

Lösekann T., Nadalig T., Niemann H., Knittel K., Boetius A., and Amann R. (unpubl.) Identification of a new cluster of anaerobic methane oxidizers at an Arctic mud volcano (Haakon Mosby Mud Volcano, Barents Sea).

Michaelis W., Seifert R., Nauhaus K., Treude T., Thiel V., Blumenberg M., Knittel K., Gieseke A., Peterknecht K., Pape T., Boetius A., Amann R., Jorgensen B. B., Widdel F., Peckmann J. R., Pimenov N. V., and Gulin M. B. (2002) Microbial reefs in the Black Sea fueled by anaerobic oxidation of methane. *Science* **297**(5583), 1013-1015.

Middelburg J. J., Nieuwenhuize J., Iversen N., Hogh N., De Wilde H., Helder W., Seifert R., and Christof O. (2002) Methane distribution in European tidal estuaries. *Biogeochemistry* **59**(1-2), 95-119.

Nauhaus K., Boetius A., Kruger M., and Widdel F. (2002) In vitro demonstration of anaerobic oxidation of methane coupled to sulphate reduction in sediment from a marine gas hydrate area. *Environmental Microbiology* **4**(5), 296-305.

Nauhaus K., Treude T., Boetius A., and Kruger M. (2005) Environmental regulation of the anaerobic oxidation of methane: a comparison of ANME-I and ANME-II communities. *Environmental Microbiology* **7**(1), 98-106.

Niewöhner C., Hensen C., Kasten S., Zabel M., and Schulz H. D. (1998) Deep sulfate reduction completely mediated by anaerobic methane oxidation in sediments of the upwelling area off Namibia. *Geochimica et Cosmochimica Acta* **62**(3), 455-464.

Nuzzo M., Hensen C., Hornibrook E., Brueckmann W., Magalhaes V. H., Parkes R. J., and Pinheiro L. M. (2005) Origin of Mud Volcano Fluids in the Gulf of Cadiz (E-Atlantic). *EGU General Assembly*.

Ollivier B., Hatchikian C. E., Prensier G., Guezennec J., and Garcia J. L. (1991) Desulfohalobium-Retbaense Gen-Nov, Sp-Nov, a Halophilic Sulfate-Reducing Bacterium from Sediments of a Hypersaline Lake in Senegal. *International Journal of Systematic Bacteriology* **41**(1), 74-81.

Olu K., Lance S., Sibuet M., Henry P., Fiala-Médioni A., and Dinet A. (1997) Cold seep communities as indicators of fluid expulsion patterns through mud volcanoes seaward of the Barbados accretionary prism. *Deep-Sea Research I* **44**(5), 811-841.

Orphan V. J., Hinrichs K. U., Ussler W., Paull C. K., Taylor L. T., Sylva S. P., Hayes J. M., and Delong E. F. (2001a) Comparative analysis of methane-oxidizing archaea and sulfate- reducing bacteria in anoxic marine sediments. *Applied and Environmental Microbiology* **67**(4), 1922-1934.

Orphan V. J., House C. H., Hinrichs K. U., McKeegan K. D., and DeLong E. F. (2001b) Methane-consuming archaea revealed by directly coupled isotopic and phylogenetic analysis. *Science* **293**(5529), 484-487.

Orphan V. J., House C. H., Hinrichs K. U., McKeegan K. D., and DeLong E. F. (2002) Multiple archaeal groups mediate methane oxidation in anoxic cold seep sediments. *Proceedings of the National Academy of Sciences of the United States of America* **99**(11), 7663-7668.

Orphan V. J., Ussler W., Naehr T. H., House C. H., Hinrichs K. U., and Paull C. K. (2004) Geological, geochemical, and microbiological heterogeneity of the seafloor around methane vents in the Eel River Basin, offshore California. *Chemical Geology* **205**(3-4), 265-289.

Pancost R. D., Bouloubassi I., Aloisi G., and Damste J. S. S. (2001) Three series of non-isoprenoidal dialkyl glycerol diethers in cold-seep carbonate crusts. *Organic Geochemistry* **32**(5), 695-707.

Peckmann J. and Thiel V. (2004) Carbon cycling at ancient methane-seeps. *Chemical Geology* **205**(3-4), 443-467.

Rütters H., Sass H., Cypionka H., and Rullkötter J. (2001) Monoalkylether phospholipids in the sulfate-reducing bacteria *Desulfosarcina variabilis* and *Desulforhabdus amnigenus*. *Archives of Microbiology* **176**(6), 435-442.

Sahling H., Rickert D., Lee R. W., Linke P., and Suess E. (2002) Macrofaunal community structure and sulfide flux at gas hydrate deposits from the Cascadia convergent margin, NE Pacific. *Marine Ecology-Progress Series* **231**, 121-138.

Schouten S., Hoefs M. J. L., Koopmans M. P., Bosch H.-J., and Sinninghe Damsté J. S. (1998) Structural characterization, occurrence and fate of archael ether-bound acyclic and cyclic biphytanes and corresponding diols in sediments. *Organic Geochemistry* **29**(5-7), 1305-1319.

Schouten S., Hopmans E. C., Pancost R. D., and Sinninghe Damsté J. S. (2000) Widespread occurrence of structurally diverse tetraether membrane lipids: Evidence for the ubiquitous presence of low-temperature relatives of hyperthermophiles. *Proceedings of the Natinonal Academy of Sciences* **97**(26), 14421-14426.

Schouten S., van der Maarel M. J. E. C., Huber R., and Sinninghe Damsté J. S. (1997) 2,6,10,15,19-pentamethylicosenes in *Methanolobus bombayensis*, a marine methanogenic archaeon, and in *Methanosarcina mazei*. *Organic Geochemistry* **26**(5/6), 409-414.

Schouten S., Wakeham S. G., Hopmans E. C., and Sinninghe Damste J. S. (2003) Biogeochemical Evidence that Thermophilic Archaea Mediate the Anaerobic Oxidation of Methane. *Appl. Environ. Microbiol.* **69**(3), 1680-1686.

Smirnov R. V. (2000) Two new species of Pogonophora from the arctic mud volcano off northwestern Norway. *Sarsia* **85**(2), 141-150.

Suess E., Torres M. E., Bohrmann G., Collier R. W., Greinert J., Linke P., Rehder G., Trehu A., Wallmann K., Winckler G., and Zuleger E. (1999) Gas hydrate destabilization: enhanced dewatering, benthic material turnover and large methane plumes at the Cascadia convergent margin. *Earth and Planetary Science Letters* **170**(1-2), 1-15.

Teske A., Hinrichs K. U., Edgcomb V., Gomez A. D., Kysela D., Sylva S. P., Sogin M. L., and Jannasch H. W. (2002) Microbial diversity of hydrothermal sediments in the Guaymas Basin: Evidence for anaerobic methanotrophic communities. *Applied and Environmental Microbiology* **68**(4), 1994-2007.

Thiel V., Peckmann J., Seifert R., Wehrung P., Reitner J., and Michaelis W. (1999) Highly isotopically depleted isoprenoids: molecular markers for ancient methane venting. *Geochimica et Cosmochimica Acta* **63**(23/24), 3959-3966.

Torres M. E., McManus J., Hammond D. E., de Angelis M. A., Heeschen K. U., Colbert S. L., Tryon M. D., Brown K. M., and Suess E. (2002) Fluid and chemical fluxes in and out of sediments hosting methane hydrate deposits on Hydrate Ridge, OR, I: Hydrological provinces. *Earth and Planetary Science Letters* **201**(3-4), 525-540.

Treude T. (2003) The anaerobic oxidation of methane in marine sediments, Unversity of Bremen.

Treude T., Boetius A., Knittel K., Wallmann K., and Jorgensen B. B. (2003) Anaerobic oxidation of methane above gas hydrates at Hydrate Ridge, NE Pacific Ocean. *Marine Ecology-Progress Series* **264**, 1-14.

Treude T., Niggemann J., Kallmeyer J., Wintersteller P., Schubert C. J., Boetius A., and Jørgensen B. B. (accepted) Anarobic oxidation of methane and sulfate reduction along the Chilean continetal margin. *Geochimica Et Cosmochimica Acta*.

Tryon M. D., Brown K. M., and Torres M. E. (2002) Fluid and chemical flux in and out of sediments hosting methane hydrate deposits on Hydrate Ridge, OR, II: Hydrological processes. *Earth and Planetary Science Letters* **201**(3-4), 541-557.

Werne J. P., Baas M., and Damste J. S. S. (2002) Molecular isotopic tracing of carbon flow and trophic relationships in a methane-supported benthic microbial community. *Limnology and Oceanography* **47**(6), 1694-1701.

Werne J. P. and Damste J. S. S. (2005) Mixed sources contribute to the molecular isotopic signature of methane-rich mud breccia sediments of Kazan mud volcano (eastern Mediterranean). *Organic Geochemistry* **36**(1), 13-27.

Werne J. P., Haese R. R., Zitter T., Aloisi G., Bouloubassi L., Heijs S., Fiala-Medioni A., Pancost R. D., Damste J. S. S., de Lange G., Forney L. J., Gottschal J. C., Foucher J. P., Mascle J., and Woodside J. (2004) Life at cold seeps: a synthesis of biogeochemical and ecological data from Kazan mud volcano, eastern Mediterranean Sea. *Chemical Geology* **205**(3-4), 367-390.

Whiticar M. J. (1999) Carbon and hydrogen isotope systematics of bacterial formation and oxidation of methane. *Chemical Geology* **161**(1-3), 291-314.

Zhang C. L. L., Li Y. L., Wall J. D., Larsen L., Sassen R., Huang Y. S., Wang Y., Peacock A., White D. C., Horita J., and Cole D. R. (2002) Lipid and carbon isotopic evidence of methane-oxidizing and sulfate-reducing bacteria in association with gas hydrates from the Gulf of Mexico. *Geology* **30**(3), 239-242.

Poster and oral presentations during my PhD study

(1) EGU General Assembly: H. Niemann, M. Elvert, B. Orcutt, M. Hovland, A. Judd, K. Finster, S. Joye, I. Suck, J. Gutt, E. Damm, J. Wunderlich, G. Wendt, A. Boetius (2005, **oral**): **Multiple Archaeal Groups Control Methane Emissions of a North Sea pockmark.**

(2) EGU General Assembly: G. Wegener, M.Shovitri, H. Niemann, M. Hovland, G. Wendt, A. Boetius (2005, **poster**): **Gullfaks Seep Area: Anaerobic Oxidation of Methane in sandy Sediments.**

(3) EGU General Assembly: S. Joye, A. Boetius, J. Montoya, H. Niemann, and B. Orcutt (2005, **oral**): **Water column methane oxidation in the vicinity of benthic methane seeps in the North Sea and Gulf of Mexico.**

(4) EGU General Assembly: H. Niemann, J. Duarte, C. Hensen, E. Omoregie, M. Elvert, V. H. M. Magalhães, A. Boetius, L. M. Pinheiro (2005, **oral**): **Diverse Microbial Communities Mediate Anaerobic Oxidation of Methane at Mud Volcanoes in the Gulf of Cadiz.**

(5) EGU General Assembly: J. Duarte, H. Niemann, C. Hensen, V. Magalhães, A. Boetius, L. M.Pinheiro (2005, **poster**): **Anaerobic methane oxidation reduces methane efflux in sub-surface sediments of mud volcanoes in the Gulf of Cadiz.**

(6) EGU General Assembly: E. Omoregie, H. Niemann, A. Boetius and the MEDIFLUX team (2005, **poster**): **Anaerobic oxidation of Methane and Sulfate reduction in the Nile Deep Sea Fan.**

(7) EGU General Assembly: D. de Beer, E. Sauter, H. Niemann, U. Witte, M. Schlüter, A. Boetius (2005, **oral**): **In situ measurements of microbial activities and transport phenomena on the Haakon Mosby Mud Vulcano (Barents Sea).**

(8) EGU General Assembly: H. Niemann, T. Lösekann, M. Elvert, J. Jakob, A. Robador T. Nadalig, E. Sauter, D. de Beer, A. Boetius (2005, **poster**): **Succession of novel methanotrophic guilds on mud flows at Håkon Mosby Mud Volcano, Barents Sea -evidence of biomarker and DNA analyses.**

(9) ESF Euromargins Workshop, Barcelona J. Duarte, H. Niemann, C. Hensen, L. Pinheiro, V. Magalhaes, M. Elvert, A. Boetius. (2004, **poster**): **Methane consumption in subsurface sediments of Mud Volcanoes in the Gulf of Cadiz.**

(10) 32nd IGC Florence: Niemann, H. Lösekann, T. Elvert, M. Nadalig, T. Foucher, J.P., Boetius, A. (2004, **oral**): **Mud Volcanoes – a Paradise for Methane Oxidizing Communities in the Deep Sea Desert.**

(11) EGS-AGU-EUG Joint Assembly: H. Niemann, B. Orcutt, I. Suck, J. Gutt, A. Damm, A. Judd, M. Hovland, G. Wnedt, A. Boetius (2004, **poster**): **Methane Seeps in the North Sea: Tommeliten Revisited.**

(12) International Workshop on Geomicrobiology “aresearch area in progress”: Niemann, H. Elvert, M. Lösekann, T. Nadalig, T. de Beer, D. Boetius, A. (2004, **oral**): **Håkon Mosby Mud Volcano, Barents Sea - a Paradise for Methanotrophic Communities in the Deep Sea Desert.**

(13) ESF Euromargins workshop, Amsterdam: German (Alfred Wegener and Max Planck Institut) Contribution to Mediflux Ocean Margins Research Centre, Bremen: A. Boetius, Niemann, H.*, Jørgensen, B. (2003, **oral**): **Projekt MEDIFLUX: Geosphären-Biosphären Interaktion an Schlammvulkanen und Pockmarks des Nilfächers, Östliches Mittelmeer.**

(14) University of Aarhus, Dept. for Ecology and Genetics; Invited Speaker: Niemann, H., Elvert, M. Lösekann, T., Nadalig, T., Boetius, A.(2003, **oral**): **A Novel AOM Community reduces Methane Efflux from Håkon Mosby Mud Volcano.**

(15) EGS-AGU-EUG Joint Assembly: Elvert, M., Niemann, H., Sauter, E., Nadalig, T., Lösekann, T., Krüger, M., Boetius, A., Schlüter, M., Jørgensen, B. (2003, **oral**): **Various microbial communities reduce methane efflux from Håkon Mosby Mud Volcano.**

(16) VAAM, Society for General and Applied Microbiology: Lösekann, T., Nadalig, T., Niemann, H., Knittel, K., Boetius, A., Amann, R. (2003, **oral**): **Microbial Diversity and Community Structure at the Håkon Mosby Mud Volcano.**

(17) ASLO Aquatic Science meeting: Niemann, H., Elvert, M., Nadalig, T., Boetius, A. (2003, **oral**): **Biomarker Evidence of Methane Oxidation in Sediments of Håkon Mosby Mud Volcano.**

(18) Goldschmidt Conference: Elvert, M., Niemann, H., Boetius, A., Treude, T., Knittel, K. (2002, **oral**): **Lipid Biomarkers as Tool for the Analysis of Anaerobic Methanotrophy in Marine Environments.**

(19) Gashydrates in the Geosystem Status Seminar, Kiel: Niemann, H., Elvert, M., Nadalig, T., Boetius, A. (2002, **poster**): **Biomarker Evidence of Methane Oxidation in Sediments of Håkon Mosby Mud Volcano.**

Further publications during my PhD study

(1) D. de Beer, E. Sauter, H. Niemann, U. Witte, M. Schlüter, A. Boetius (submitted to Limnol. Oceanogr.). **In situ fluxes and zonation of microbial activity in surface sediments of the Håkon Mosby Mud Volcano**

(2) T. Lösekann, Knittel, K., Nadalig, T, Niemann, H., Boetius, A, Amann, R. (in prep). **Identification of novel clusters of aerobic and anaerobic methane oxidizers at an Arctic mud volcano (Haakon Mosby Mud Volcano, Barents Sea)**

(3) Vandieken, V., Mußmann, M., Niemann, H., Jørgensen B. B. (submitted to IJSEM). **Psychrophilic Fe-reducing bacteria isolated from Arctic sediments, Svalbard: *Desulfuromonas svalbardensis* sp. nov. and *Desulfuromusa ferrireducens* sp. nov.**

(4) D. Shlimon, M. W. Friedrich, H. Niemann, N. B. Ramsing and K. Finster (2004). **Methanobacterium aarhusense sp.nov., a novel methanogen isolated from a marine sediment (Aarhus Bay, Denmark).** *IJSEM*, DOI 10.1099/ijs.0.02994-0

(5) Niemann, H., Richter, C., Jonkers, H. M., Badran, M. (2004). **Red Sea gravity currents cascade near-reef phytoplankton to the twilight zone.** *MEPS,* (269) 91-99

(6) Jonkers, H. M., Ludwig, R., De Wit, R., Pringault, O., Muyzer, G., Niemann, H., Finke, N., De Beer, D (2003). **Structural and functional analysis of a microbial mat ecosystem from a unique permanent hypersaline inland lake: 'La Salada de Chiprana' (NE Spain).** *FEMS Microbiol. Ecol., 44 (2), 175-189*

Participations on research cruises during my PhD study

(1) R/V Atlantis, Costa Rica subduction zone, June 7 – June 16, 2005

(2) R/V Sonne, cruise SO175, Gulf of Cadiz, Nov. 27 – Dec. 23, 2003

(3) R/V Atalante cruise Nautinil, Eastern Medditerranean Ridge and Nile Deep Sea Fan, Sep 5 – Sep 17, 2003

(4) R/V Polarstern cruise ARKXIX3b, Håkon Mosby Mud Volcano, June 26 - July 21, 2003

(5) R/V Meteor, cruise ME56-2, Congo Deep Sea Fan, Dec 4 - Dec. 31, 2002

(6) R/V Heinke, cruise HE180, central North Sea and Norwegian margin, Oct. 17 - Oct 27, 2002

(7) R/V Heinke, cruise HE169, central North Sea and Norwegian margin, May 27 - June 4, 2002

Courses during my PhD study

(1) Grundkurs im Strahlenschutz (basic course in radiation protection), Sep 2 - Sep 9, 2002

(2) International Geobiology Course at the USC Wrigley Institute for Environmental Studies, Agouron Institute, July 6 – Aug 16, 2002

Danksagung

Zuerst einmal möchte ich meinem Prüfungskomitee (Antje Boetius und Dieter Wolf-Gladrow, Willehelm Hagen, Marcus Elvert, Maxim Scheludchenko und Sybille Zitzmann) und meinem Thesis Committee (Antje Boetius, Marcus Elvert, Bo Barker Jørgensen und Dieter Wolf-Gladrow) für die Unterstützung bei meiner Dissertation danken. Ein weiterer, ganz herzlicher Dank gilt vor allem Antje Boetius und Marcus Elvert: für die freundliche Aufnahme am MPI, die intensive Einarbeitung in verschiedenste, analytische Methoden, insbesondere aber auch dafür, dass es mir ermöglicht wurde, an einem so spannenden Thema in "allen sieben Weltmeeren" arbeiten zu können. An dieser Stelle möchte ich auch erwähnen, dass mir die zwischenmenschliche Seite an unserem Team sehr gefallen hat - so konnte man dann doch auch mal das eine oder andere Bier zusammen trinken. Als "Doktoreltern" haben Antje und Marcus mir neue Bereiche der Wissenschaftswelt gezeigt.

Auch Tina Lösekann sei für unsere erfolgreiche Zusammenarbeit an den Håkon Mosby Proben gedankt. An dieser Stelle möchte ich auch ein großes Lob "meinen" Studenten, Joana Duarte, Alberto Robador und Jacob Jacob aussprechen.

Ein ebenso herzlicher Dank meinerseits geht an die Techniker der Biogeochemie und Habitat Gruppe für die tolle Unterstützung auf See und im Labor, vor allem Viola Beier, Imke Busse und Tomas Wilkop (in alphabetischer Reihenfolge). Ich bin mir ganz sicher, dass die wissenschaftlichen Ergebnisse ohne diese Drei - um es mal vorsichtig auszudrücken - eher mager wären. Meine volles Lob gilt in diesem Zusammenhang auch den Ingenieuren und Technikern der Länderhalle, Jens Langreder, Axel Nordhausen und Marc Viehweger sowie auch Michael Fitze für die ein oder andere Bastelstunde und logistische Hilfe bei den

Expeditionsvorbereitungen. Nicht unerwähnt dürfen Manfred Schlösser und Axel Krack bleiben, die sich um das Versenden von Radioisotopen gekümmert haben.

Ulrike Tietjen und Algrid Hillermann sei an dieser Stelle für die vielen Flug- und Hotelbuchungen gedankt, die sich im Laufe meiner Doktorandenzeit angesammelt haben. Der Verwaltung des MPI's möchte ich meinen Dank für die schnelle und unbürokratische Abwicklung "lästiger" Formalitäten aussprechen. Insbesondere sei hier Heike Wojack lobend erwähnt, die meine Reisekosten in "Lichtgeschwindigkeit" abgerechnet hat.

Ich möchte auch meinen anderen Kollegen aus dem MPI für das tolle Arbeitsklima hier am Institut danken, vor allem meinen Bürokollegen Verona Vandieken, Julie Leloup, Jochen Nüster und Lev Neritin.

Ich möchte an dieser Stelle auch meine Eltern und Großeltern erwähnen, die mich, vor allem während meiner Studienzeit unterstützt haben. Ein großes Dankeschön soll auch an meine Geschwister gehen, da mir unser Zusammenhalt im letzten Jahrzehnt viel geholfen hat. Auch meinem langjährigen Freund Simon Gielnick möchte ich noch danken. Er hat mir über die Jahre, direkt und indirekt, bei Entscheidungen geholfen, die mich letztendlich bis zum Abschluss dieser Doktorarbeit gebracht haben.

Abschließend möchte ich auch noch all jenen danken, die ich namentlich hier nicht erwähnt habe, die mich aber dennoch bei meiner Doktorarbeit unterstützt haben.

Erklärung

Hiermit versichere ich, dass ich die vorliegende Arbeit

1. Ohne unerlaubte, fremde Hilfe angefertigt habe

2. keine anderen, als die von mir im Text angegebenen Quellen und Hilfsmittel benutzt habe,

3. die den benutzten Werken wörtlich oder inhaltlich entnommenen Stellen als solche kenntlich gemacht habe

Bremen den 03.06.2005

Helge Niemann